Oxetane-Based Peptidomimetics

by

Jonathan Beadle

A thesis submitted in partial fulfilment of the requirements for the degree of Doctor of Philosophy in Chemistry

Department of Chemistry, University of Warwick

May 2018

Table of Contents

Acknowledgements

Firstly, I would like to thank Professor Mike Shipman for all of his guidance, encouragement and support throughout the course of my PhD, and for giving me the opportunity to work on such an interesting and enjoyable project. Secondly, I would like to thank Dr Piotr Raubo for all his help and assistance with the project and for looking after me during my placement at AstraZeneca. I would also like to thank Dr Nicola Powell for all her work on this project. Funding from the Warwick Collaborative Postgraduate Research Scholarship and AstraZeneca is gratefully acknowledged.

I would like to thank a number of people for their collaboration as part of this project. I am especially grateful to Dr Andrew Jamieson for all his help with the solid-phase and hydrogel projects, and for looking after me during my time at the University of Leicester. I would also like to thank Dr Astrid Knuhtsen and Dr Alex Hoose for their help with the solid-phase project and members of the Jamieson research group at the University of Leicester for helping me during my time there. Thanks also to Professor Dave Adams, Laura McDougall and Dr Emily Draper for their work on the hydrogel project. I am also grateful for the invaluable help provided by Dr Guy Clarkson with X-ray crystallography. I am also thankful to Dr Nikola Chmel and Marco Pinto for their help with the CD experiments, and to Dr Ann Dixon for her expertise regarding NMR and CD spectroscopy. I also thank Dr John Traynor for his studies on the enkephalin analogues. Thanks also to Lijiang Song, Phil Aston, Robert Perry and Ivan Prokes for their analytical expertise.

I would like to thank members of the Shipman and Chan groups for making my journey at Warwick enjoyable and productive: Alpa, Conor, Dave, George, Greg, Ina, Jo, Leo, Martin, Nastja, Nat, Paul, Raj, Stefan and Stuart. In particular, I am very grateful to Ina for all her help with the helix project and to Stefan for proofreading this thesis. Many thanks also to Anaïs and Lauren for being great students. Thanks also to members of the Chaplin group for invaluable discussions at the weekly Research Refresh meeting.

Finally, I would like to thank my parents, family and friends for their continued support and encouragement throughout my time at Warwick.

Declaration

This thesis is submitted to the University of Warwick in support of my application for the degree of Doctor of Philosophy. It has been composed by myself and has not been submitted in any previous application for any degree.

The work presented in this thesis is an account of my own work carried out at the University of Warwick, the University of Leicester and AstraZeneca, Cambridge, between October 2014 and May 2018, except in the cases outlined below:

Chapter 3: Peptides **225**-**233** were synthesised and analysed by Dr Astrid Knuhtsen, Dr Alex Hoose and Dr Andrew Jamieson at the University of Glasgow. Binding affinity studies of Met- and Leu-enkephalin analogues **231** and **232** were carried out in the laboratories of Dr John Traynor at the University of Michigan, USA. The preparation and analysis of hydrogels was carried out by Laura McDougall, Dr Emily Draper, Dr Andrew Jamieson and Professor Dave Adams at the University of Glasgow.

Chapter 4: Peptides **246**, **248**, **252** and **254** were synthesised by Dr Ina Wilkening at the University of Warwick.

At the time of submission, elements of this work have appeared in the scientific literature:

Beadle, J. D.; Powell, N. H.; Raubo, P.; Clarkson, G. J.; Shipman, M. Synthesis of Oxetane- and Azetidine-Containing Spirocycles Related to the 2,5-Diketopiperazine Framework. *Synlett* **2015**, *27*, 169–172.

Beadle, J. D.; Knuhtsen, A.; Hoose, A.; Raubo, P.; Jamieson, A. G.; Shipman, M. Solid-Phase Synthesis of Oxetane Modified Peptides. *Org. Lett.* **2017**, *19*, 3303–3306.

McDougall, L.; Draper, E. R.; Beadle, J. D.; Shipman, M.; Raubo, P.; Jamieson, A. G.; Adams, D. J.; Enzymatically-Stable Oxetane-Based Dipeptide Hydrogels. *Chem. Commun.* **2018**, *54*, 1793-1796.

Abstract

This thesis describes the synthesis, structural preferences and biological properties of oxetane-containing peptidomimetics in which one of the amide C=O bonds of a peptide backbone is replaced by an oxetane ring. Chapter 1 gives a brief introduction on peptidomimetics, oxetanes in medicinal chemistry and oxetane-containing peptidomimetics.

Chapter 2 describes the development of a simple two-step sequence to spirocyclic analogues of 2,5-diketopiperazines. Conjugate addition of α-amino methyl esters to nitroalkenes, generated from oxetan-3-one or *N*-Boc-azetidin-3-one, followed by reduction of the nitro group with Raney Ni under an atmosphere of hydrogen provides, after spontaneous cyclisation of the primary amine, the spirocycles in good overall yields. These novel spirocycles can be functionalised by selective *N*-alkylations as well as by carbonyl reduction to the corresponding piperazines.

Chapter 3 describes the development of a practical route to oxetane-modified peptides (OMPs) using solid-phase peptide synthesis (SPPS) techniques. Our approach involves the application of oxetane-containing dipeptide building blocks which are easily prepared in three steps in solution. The building blocks are then integrated into peptide chains using conventional Fmoc/^{t}Bu SPPS. This approach was used to prepare a range of OMPs in high purity including oxetane analogues of Met- and Leu-enkephalin and the nonapeptide bradykinin.

Chapter 4 explores the impact of oxetane-modification on the structure and stability of α-helices. Initially, an asymmetric route to a dipeptide building block in which the oxetane-residue is based on alanine is described. Following this, the SPPS methodology described in Chapter 3 was used to prepare oxetane-modified analogues of an alanine-based α-helical peptide in which a single alanine residue is replaced with an oxetane-modified residue. The structural preferences of the oxetane-modified analogues were then studied using circular-dichroism (CD) spectroscopy. These studies revealed that introduction of an oxetane-modification results in a helix-destabilising effect.

Chapter 5 gives a summary of the key findings and possible future work.

Chapter 6 provides detailed experimental procedures for the work carried out in Chapters 2-4.

Abbreviations

$[\alpha]_D$	Optical rotation
$[\theta]_{MRW}$	Mean residue ellipticity
1D	1 Dimensional
2D	2 Dimensional
Å	Angstrom
AA	Amino Acid
Ac	Acetyl
Alloc	Allyloxycarbonyl
A_{Ox}	Oxetane-modified alanine
APT	Attached proton test
aq.	Aqueous
Ar	Aryl
b	Broad
Bn	Benzyl
Boc	*tert*-Butyloxycarbonyl
Bt	Benzatriazole
Bu	Butyl
c	Concentration
Calcd.	Calculated
Cbz	Carboxybenzyl
CD	Circular Dichroism
COSY	Correlation Spectroscopy
d	Doublet
Da	Dalton
DCC	*N*,*N'*-Dicyclohexylcarbodiimide
DCE	1,2-Dichloroethane
de	Diastereomeric excess
deg	Degrees
DIAD	Diisopropyl azodicarboxylate
DIC	*N*,*N*′-Diisopropylcarbodiimide
DIPEA	*N*,*N*-Diisopropylethylamine
DKP	Diketopiperazine

DMAP	4-Dimethylaminopyridine
DMB	Dimethoxybenzyl
DMF	Dimethylformamide
DMSO	Dimethyl sulfoxide
dr	Diastereomeric ratio
EDC	*N*-(3-Dimethylaminopropyl)-*N'*-ethylcarbodiimide
eq	Equation
equiv	Equivalent
ESI	Electrospray Ionisation
Et	Ethyl
FDA	Food and Drug Administration
f_H	Mean helix content
Fmoc	Fluorenylmethyloxycarbonyl
F_{Ox}	Oxetane-modified phenylalanine
G_{Ox}	Oxetane-modified glycine
h	Hour
HATU	1-[Bis(dimethylamino)methylene]-1*H*-1,2,3-triazolo[4,5-b]pyridinium 3-oxide hexafluorophosphate
HBTU	3-[Bis(dimethylamino)methyliumyl]-3*H*-benzotriazol-1-oxide hexafluorophosphate
HCTU	*O*-(1*H*-6-Chlorobenzotriazole-1-yl)-1,1,3,3-tetramethyluronium hexafluorophosphate
HFP	Hexafluoroisopropanol
HPLC	High Performance Liquid Chromatography
HRMS	High Resolution Mass Spectroscopy
Hz	Hertz
^{i}Pr	*iso*-Propyl
IR	Infrared
J	Coupling constant
K	Kelvin
LC-MS	Liquid Chromatography Mass Spectrometry
lit.	Literature
m	Multiplet
m/z	Mass-to-charge ratio

MD	Molecular Dynamics
Me	Methyl
MHz	Megahertz
min	Minute
mp	Melting Point
Ms	Methanesulfonyl
MS	Mass Spectrometry
n	Normal
NMM	4-Methylmorpholine
NMR	Nuclear Magnetic Resonance
Nu	Nucleophile
OMP	Oxetane-modified peptide
Ox	Oxetane
Pbf	Pentamethyl-2,3-dihydrobenzofuran-5-sulfonyl
Pg	Protecting group
Ph	Phenyl
P_i	Phosphate
P_{Ox}	Oxetane-modified proline
ppm	Parts per million
PyBOP	(Benzotriazol-1-yloxy)tripyrrolidinophosphonium hexafluorophosphate
q	Quartet
quint	Quintet
Ref.	Reference
R_f	Retention factor
rt	Room temperature
s	Second, Singlet
sep	Septet
solv.	Solvent
SPPS	Solid-phase peptide synthesis
Su	Succinimide
t	Temperature
t	Time, Triplet
TBAI	Tetrabutylammonium iodide

TBTU	2-(1*H*-Benzotriazole-1-yl)-1,1,3,3-tetramethylaminium tetrafluoroborate
^{t}Bu	*tert*-Butyl
Tf	Trifluoromethanesulfonyl
TFA	Trifluoroacetic acid
THF	Tetrahydrofuran
TIS	Triisopropylsilane
TLC	Thin Layer Chromatography
t_R	Retention time
Tris	2-Amino-2-(hydroxymethyl)-1,3-propanediol
Trt	Triphenylmethyl
Ts	Tosyl
UPLC-MS	Ultra-Performance Liquid Chromatography Mass Spectrometry
UV	Ultraviolet
v	Volume
V_{Ox}	Oxetane-modified valine
Y_{Ox}	Oxetane-modified tyrosine
δ	Chemical shift
ε	Extinction coefficient
λ	Wavelength
μW	Microwave

Chapter 1: Introduction

1.1 Project Aims

This thesis builds upon previous research within our group and describes the synthesis, structural preferences and biological properties of novel oxetane-containing peptidomimetics, in which one of the amide C=O bonds of a peptide backbone is replaced by an oxetane ring (Figure 1.1).[1] Initially, the project will focus on the development of practical methods for the synthesis of oxetane-modified peptides (OMPs). Following this, the emergent chemical methods will be used to investigate the impact of oxetane-modification on the properties and structure of biologically interesting peptides. Through these investigations, we hope to gain the tools and knowledge to selectively modify peptides and learn how the changes induced by oxetane-modification influence the properties and secondary structure of peptides.

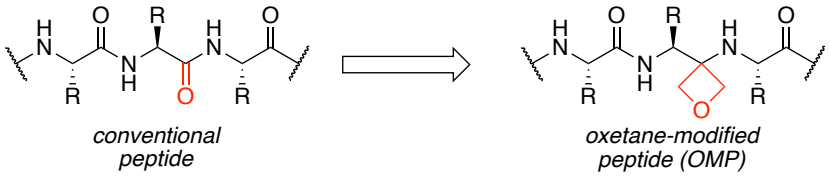

Figure 1.1 Oxetane-modified peptides (OMPs).[1]

1.2 Peptidomimetics

Peptides and their larger counterparts, proteins, are oligomers of amino acids covalently linked together by amide bonds (peptide bonds).[2] Although they are constructed from relatively simple building blocks, the resulting oligomeric structures form complex architectures that play vital roles in almost all biological processes, for example functioning as hormones, enzyme inhibitors or substrates, growth promoters or inhibitors and neurotransmitters.[3,4] Consequently, the therapeutic application of peptides and proteins is of great interest in biomedical research.[5–7] Despite this, the use of peptides as therapeutics is limited by their vulnerability to proteases, poor bioavailability and undesired effects due to interaction of flexible peptides with several receptors.[8,9] To tackle these problems, molecules called peptidomimetics have been designed to mimic the structure and/or action of a natural peptide and potentially improve the physicochemical and biochemical properties.

1.2.1 Peptidomimetics *via* Modification of the Peptide Backbone

There are a number of excellent reviews on the synthesis and medicinal chemistry of peptidomimetics.[4,8–12] This section does not aim to replicate these reports but to highlight some relevant examples.

A common method for preparing peptidomimetics is *via* modification of the amino acid backbone of native peptides.[4] Such modifications can create novel structures with increased bioavailability, enzymatic stability and increased activity and/or selectivity for a target receptor. Examples of backbone modifications include: isosteric replacement or alkylation of the amino functionality, substitution or replacement of the α-carbon, backbone extension and modification of the carbonyl group (Figure 1.2).

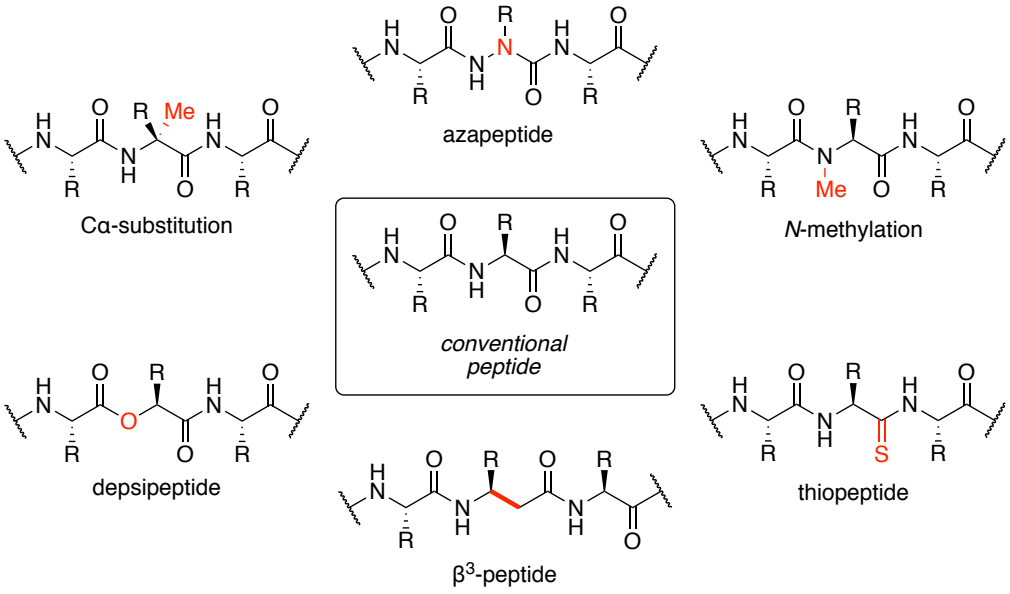

Figure 1.2 Peptidomimetics with modification of the peptide backbone.[4]

Azapeptides are peptide analogues in which the α-carbon of one or more of the amino acid residues is replaced with a nitrogen atom and can be easily prepared *via* acylation of hydrazines.[4,13,14] They exhibit a preference to adopt *β*-turn conformations and are more resistant to enzymatic hydrolysis. Azapeptides are attractive targets in drug discovery and have been used as inhibitors of hepatitis C virus NS3 serine protease and human immunodeficiency virus (HIV) protease.[15,16] Atazanavir **1** (Reyataz™), a highly active HIV protease inhibitor, is an example of an FDA-approved azapeptide drug (Figure 1.3).[17]

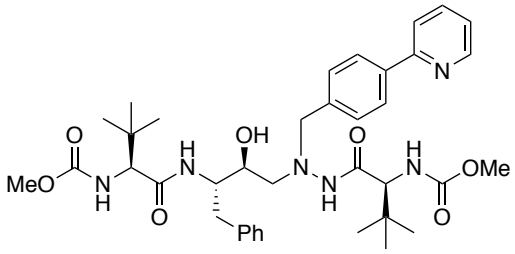

Atazanavir, **1**
HIV protease inhibitor

Figure 1.3 Atazanavir **1** an azapeptide inhibitor of HIV protease.[17]

Depsipeptides are peptidomimetics in which one or more amino groups in the peptide chain is replaced by an oxygen atom.[4] Replacement of the N-H group results in reduced H-bonding ability and a lower barrier of rotation for *cis-trans* isomerisation than native peptides, which has a significant effect on the secondary structure of depsipeptides.[18] Numerous depsipeptides, particularly cyclic structures, have been isolated from various microorganisms and exhibit a wide spectrum of biological activity including antimicrobial, antitumour and immunosuppressive activity.[19] Consequently, naturally occurring depsipeptides have emerged as promising lead structures for the development of novel synthetically derived drugs.[20] Romidepsin **2** (Istodax^{TM}) is an FDA-approved cyclic depsipeptide anticancer drug used for the treatment of cutaneous T-cell lymphoma. (Figure 1.4).[21]

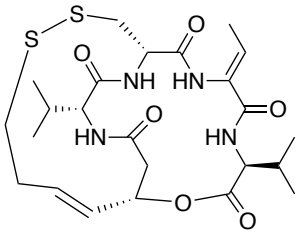

Romidepsin, **2**
Cutaneous T-cell lymphoma

Figure 1.4 Romidepsin **2**, a depsipeptide anticancer drug.[21]

Thiopeptides, perhaps one of the simplest modifications, are peptide analogues in which the oxygen atom of one or more of the amide bonds is replaced with a sulphur atom.[22] Despite their similarity, replacement of an amide bond with a thioamide has a significant impact on the structural and biological properties of a peptide. This is a result of the significantly longer C=S bond and change in H-bonding properties. These aspects have been utilised in the design and study of synthetic foldamers, such as β-sheets and α-

helices.[23,24] In addition, thiopeptides have displayed enhanced *in vivo* activity due to their increased resistance to enzymatic hydrolysis.[25] This has been demonstrated by Strømgaard and co-workers, who identified thiopeptide **3** as a potent and plasma-stable inhibitor of the postsynaptic density-95 (PSD-95) and *N*-methyl-*D*-aspartate (NMDA) receptor interaction, which is a potential target in the treatment of Alzheimer's disease (Figure 1.5).[26]

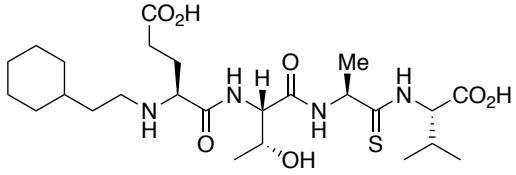

N-cyclohexylethyl-ETA$_S$V, **3**

Figure 1.5 Thiopeptide **3**, a potent and plasma-stable inhibitor of the PSD-95/NMDA receptor interaction.[26]

1.3 Oxetanes in Medicinal Chemistry

There are a number of excellent reviews on the synthesis, reactivity and medicinal chemistry of oxetanes.[27–31] This section does not aim to replicate these reports but to highlight the relevance of oxetanes in medicinal chemistry.

1.3.1 Oxetane

Oxetane **4** is a four-membered heterocyclic ring containing an oxygen atom that adopts an essentially planar conformation with a small puckering angle of ~9° at 140 K and ~11° at 90 K (Figure 1.6).[27,32] The oxetane ring is an excellent H-bond acceptor and is used as a stable motif in medicinal chemistry to influence the physicochemical properties of potential drug candidates.[27,29] In addition, the oxetane ring is a valuable synthetic intermediate due to its ability to undergo ring-opening reactions under acidic conditions.[27,28] These characteristics have led to the development of numerous synthetic approaches to novel oxetane derivatives.[27,29]

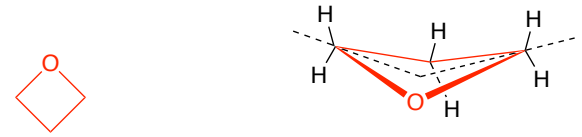

Figure 1.6 Structure and ring puckering of oxetane **4**.[32]

1.3.2 Oxetanes in Natural Products

There are relatively few natural products that contain the oxetane ring.[27] The structures of those that do range from simple β-peptides to highly functionalised fused ring systems (Figure 1.7). Perhaps, the most well-known example is paclitaxel, sold under the brand name Taxol **5**, which was first isolated in 1971 by McPhail and co-workers and is used as a chemotherapy drug.[33] Other examples include the β-amino acid oxetin **6**,[34] which displays antibacterial and herbicidal activity, the nucleoside analogue oxetanocin A **7**,[35] which is a potent antitumour, antiviral and antibacterial agent, and the marine diterpene dictyoxetane **8**,[36] whose biological properties are currently not well understood.

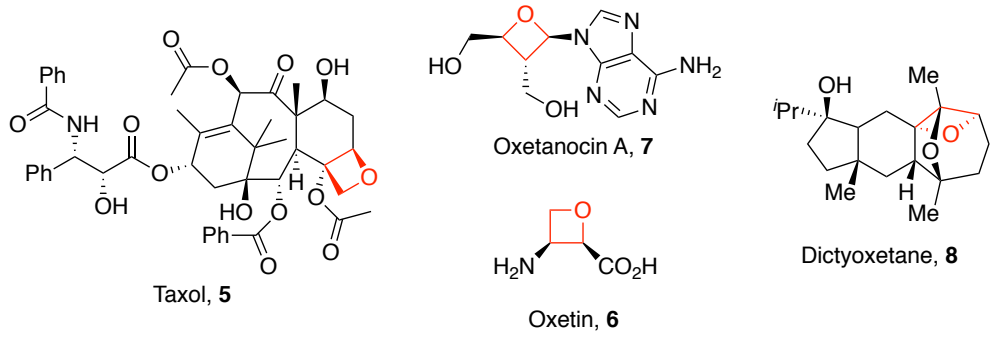

Figure 1.7 Oxetane-containing natural products.

1.3.3 Oxetanes as Replacement Groups in Medicinal Chemistry

Studies by Carreira, Roger-Evans, Müller and co-workers have demonstrated the benefits of the oxetane motif as an isosteric replacement for *gem*-dimethyl, carbonyl and morpholine groups in medicinal chemistry.[29,30,37,38]

1.3.3.1 Oxetane as a Replacement for *gem*-Dimethyl Groups

gem-Dimethyl groups have commonly been used in medicinal chemistry to block metabolic attack of methylene groups. However, replacement of the hydrogen atoms with methyl groups results in a significant increase in lipophilicity, which can have an adverse effect on the physicochemical and pharmacological properties.[37] In addition, the *gem*-dimethyl group itself can become a target of metabolic attack. Carreira and co-workers have proposed that the oxetane ring can be used as a polar equivalent of the *gem*-dimethyl group, as the oxetane ring is similar in molecular volume to the *gem*-dimethyl group and can provide a reduction in lipophilicity and metabolic vulnerability (Figure 1.8).[29,37]

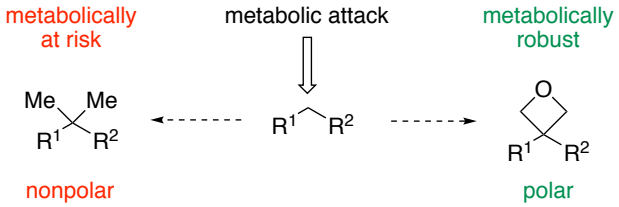

Figure 1.8 Comparison of *gem*-dimethyl and oxetane modules.[37]

The impact of replacing a *gem*-dimethyl unit with an oxetane ring was demonstrated by replacing the *tert*-butyl group in parent compound **9** with a methyl-substituted oxetane **10** (Table 1.1).[37] Comparison of the physicochemical and biochemical properties revealed that oxetane-modified **10** was significantly more polar and soluble than the parent compound **9**. In addition, oxetane-modified **10** had improved metabolic stability as indicated by reduced intrinsic clearance rates (CL_{int}) measured in human (h) and mouse (m) liver microsomes. Replacement of the *tert*-butyl group with a methyl-substituted oxetane also resulted in reduction of hERG (human ether-a-go-go-related gene) inhibition, as a result of the decrease in lipophilicity.

	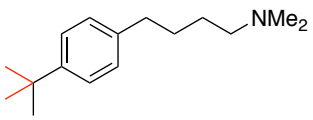 Parent compound, **9**	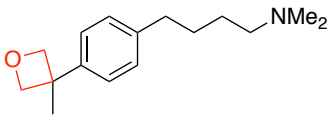 Oxetane-modified compound, **10**
logD (logP)	1.8 (4.3)	0.8 (3.3)
Solubility (μg mL^{-1})	<1	4,400
hCL_{int} (min^{-1} mg^{-1} μL)	16	0
mCL_{int} (min^{-1} mg^{-1} μL)	417	43
hERG IC_{50} (μM)	7.5	35

Table 1.1 Physicochemical and biochemical properties of parent compound **9** and oxetane-modified compound **10**.[37]

1.3.3.2 Oxetane as a Replacement for Carbonyl Groups

Carreira and co-workers have examined the benefits of oxetanes as replacements for carbonyl groups in medicinal chemistry.[29,30] Oxetane can be a valuable replacement for a carbonyl group due to their similar dipoles, H-bonding properties and spatial arrangement of lone pair electrons (Figure 1.9). In addition, carbonyl functional groups in drug-like structures are susceptible to enzymatic modification and to epimerisation at neighbouring stereogenic centres, whereas oxetane derivatives are stable to both of these concerns. One main difference between an oxetane and carbonyl group is the longer length and larger volume, which could potentially be beneficial or detrimental at a receptor pocket.

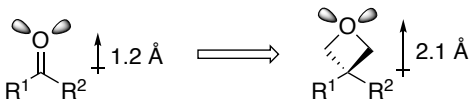

Figure 1.9 Comparison between carbonyl and oxetane.[29]

The impact of oxetane as a replacement for a carbonyl group was studied by comparison of the physicochemical and biochemical properties of carbonyl-containing heterocycle compounds (**11** and **13**) with their oxetane-containing spirocyclic derivatives (**12** and **14**, Table 1.2).[38] In both the piperidine and pyrrolidine series, replacement of the carbonyl group with an oxetane ring resulted in a decrease in solubility. No significant change in

lipophilicity was observed for the piperidine series, whilst a small increase was observed for oxetane-modified pyrrolidine **14**. However, both oxetane-modified analogues **12** and **14** had improved metabolic profiles as indicated by reduced intrinsic clearance rates (CL_{int}) measured in human (h) and mouse (m) liver microsomes.

R = 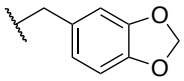	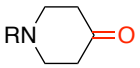 **11**	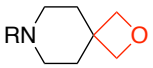 **12**	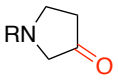 **13**	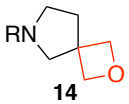 **14**
logD (logP)	1.2 (1.6)	1.0 (2.0)	−0.1 (−0.1)	0.7 (1.5)
Solubility (μg mL^{-1})	4,000	1,400	4,100	730
hCL_{int} (min^{-1} mg^{-1} μL)	120	6	100	2
mCL_{int} (min^{-1} mg^{-1} μL)	88	22	580	27

Table 1.2 Physicochemical and biochemical properties of **11-14**.[38]

In an additional study, Carreira and co-workers investigated the impact of carbonyl to oxetane substitution in the drugs thalidomide **15** and lenalidomide **16** (Figure 1.10).[39] The two enantiomers of thalidomide are known to rapidly interconvert *in vivo*, and each enantiomer causes a distinct effect, with (*R*)-**15** acting as a sedative and (*S*)-**15** as a teratogen. Substitution of the imide C=O with an oxetane ring produced analogues **17** and **18** which displayed similar physiochemical and *in vitro* properties to the parent drugs, but were significantly more stable in human plasma. Importantly, oxetane-modification of thalidomide prevents *in vivo* racemisation. This work did not include any studies into the biological activities of oxetane-modified analogues **17** and **18**.

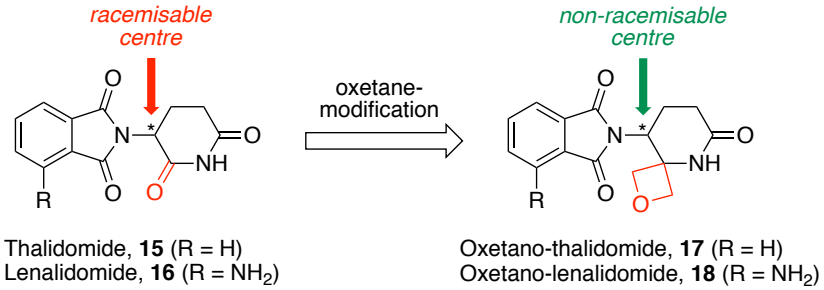

Figure 1.10 Oxetane analogues of thalidomide and lenalidomide.[39]

In addition to these reports, a recent study by Ballatore and co-workers has demonstrated that oxetan-3-ol may be considered as an alternative bioisostere to the carboxylic acid functional group (Figure 1.11).[40] The authors' investigation revealed that replacement of

the carboxylic acid group in model compound **19** with oxetan-3-ol causes a significant decrease in acidic character and an increase in permeability. These properties are desirable in context of central nervous system (CNS) drug design, when isosteric replacement of the carboxylic acid is often required to improve the brain penetration of a candidate compound.

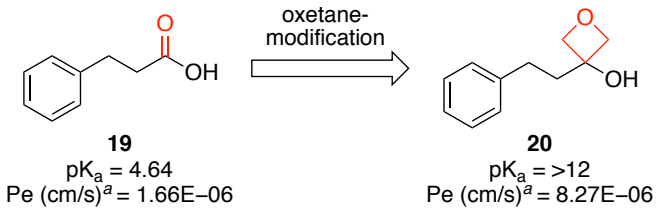

Figure 1.11 Oxetan-3-ol as a bioisostere of the carboxylic acid functional group.[40] ^{a} Effective permeability.

1.3.3.3 Spirocyclic Oxetanes as a Replacement for Morpholine

Morpholine units are often introduced into drug scaffolds to improve aqueous solubility. However, morpholine is known to be vulnerable to oxidative metabolism. Carreira and co-workers have proposed that spirocyclic oxetanes can be considered as structural analogues of morpholine, as they are able to increase solubility while remaining stable towards oxidative metabolism (Figure 1.12).[38]

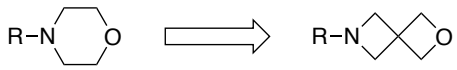

Figure 1.12 Spirocyclic oxetane as a replacement for morpholine.[38]

Following this publication, Carreira and co-workers reported the synthesis of 1,6-heteroatom-substituted spiro[3.3]heptanes **22** as alternatives to 1,3-heteroatom-substituted cyclohexanes **21** (Figure 1.13).[41] The instability of **21** has prevented their application in drug discovery. In contrast, spiro[3.3]heptanes **22** have no associated instability and are able to position the heteroatoms in a similar orientation to **21**, hence making them attractive replacements.

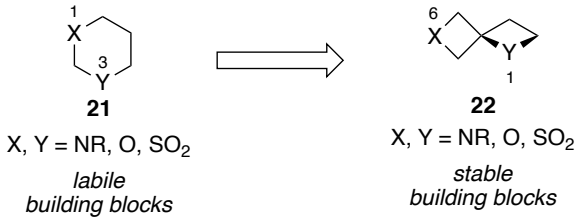

Figure 1.13 1,6-Heteroatom-substituted spiro[3.3]heptanes **22** as alternatives to 1,3-heteroatom-substituted cyclohexanes **21**.[41]

1.4 Oxetane-Containing Peptidomimetics

1.4.1 Homo-Oligomers of Oxetin

Aitken and co-workers have prepared homo-oligomers of oxetin **6** (Figure 1.7) and studied their conformational preferences in solution and solid state.[42] Analysis of the secondary structure using ^{1}H-NMR, CD and X-ray diffraction techniques indicate that *C*- and *N*-terminal protected oxetin-hexamer **23** adopts an uncommon left-handed 10-helix β-peptide manifold, wherein a network of 10-membered ring H-bonds is formed between the NH group at position *i* to the C=O at position *i* + 1. The 10-helix is further stabilised by a cooperative 5-membered ring H-bonding network between the NH at position *i* with the O(oxetane) at position *i* – 1 (Figure 1.14). Helical patterns of β-peptides have been shown to possess promising biological activity, hence the 10-helix architecture of oxetin homo-oligomers may have applications in medicinal chemistry. Similar studies have been reported by Fleet and co-workers, who have demonstrated that hexamers of C4-substituted oxetins also preferentially adopt 10-helix β-peptide architectures.[43,44]

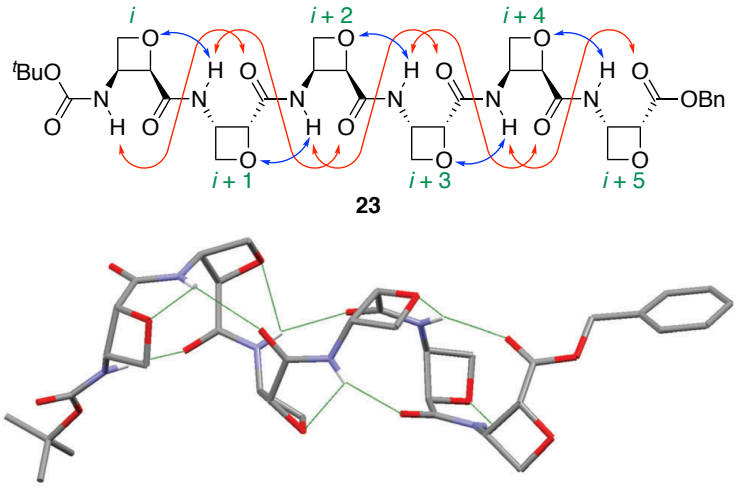

Figure 1.14 Cooperative 5- (blue arrows) and 10-membered (red arrows) ring interactions in the 10-helix folding of oxetin hexamer **23** and X-ray structure of **23**.[42] Figure of X-ray structure taken from *Chem. Commun.* **2018**, *54*, 1968-1971.[42]

1.4.2 Oxetane-Modified Peptides

In 2014, Shipman and co-workers reported the preparation of a new class of peptidomimetic in which one of the amide C=O bonds of a peptide backbone is replaced by an oxetane ring (Figure 1.1).[1] Several features of oxetane-modified peptides were expected to make them of interest as peptidomimetics. Firstly, substitution of an amide bond with the 3-aminooxetane unit was expected to produce peptidomimetics with greatly reduced vulnerability to proteases. Secondly, the 3-aminooxetane is able to participate in H-bonding, as both a donor and acceptor, therefore OMPs were expected to support conventional secondary structures. Finally, changes in the conformational preferences of OMPs, arising from removal of the double bond character of the peptide bond, might open up new areas of peptide structural space.

Initially, the authors' investigation focused on the preparation of oxetane-containing tripeptide analogues, in which the central C=O amide bond was substituted for an oxetane ring.[1] The general synthetic approach is given in Scheme 1.1. The first step involved conjugate addition of a chiral α-amino ester **25** to oxetane-substituted nitroalkene **24**. Following this, reduction of the nitro group in **26**, and coupling of the resulting amine **27** with an *N*-protected amino acid gave the protected peptidomimetic with the oxetane residue centrally located. Deprotection of the *N*- and *C*- terminal protecting groups provided the desired oxetane-modified tripeptide **28**.

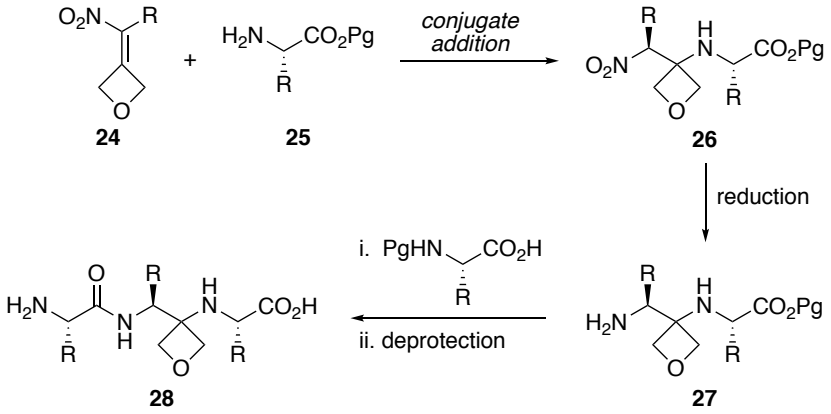

Scheme 1.1 Synthetic strategy to oxetane-based peptidomimetics developed by Shipman and co-workers.[1]

Two oxetane-substituted nitroalkenes **30** (R^1 = H) and **31** (R^2 = Bn) were used in this study to produce peptidomimetics of glycine (G_{Ox}) and phenylalanine (F_{Ox}), respectively (Scheme 1.2).[1] The nitroalkenes were prepared *via* nitro-aldol reaction of commercially available oxetan-3-one **29** with the appropriate nitroalkane and elimination of the resulting alcohol with methanesulfonyl chloride. In the case of nitroalkene **30** (R = H), it proved more convenient to generate **30** *in situ* and react it directly without work-up. Following this, conjugate addition of an amino ester to nitroalkene **30** or **31** generally gave the addition products **32** in good overall yields. A wide selection of polar and hydrophobic amino esters, as well as dipeptide based nucleophiles, were demonstrated in the addition step. Interestingly, addition of *L*-valine methyl ester to trisubstituted nitroalkene **31** (R = Bn) gave the addition product **36** as a mixture of diastereoisomers, with the inherent chirality of *L*-valine exerting little influence on the resulting stereochemistry. The diastereoisomers were inseparable by column chromatography.

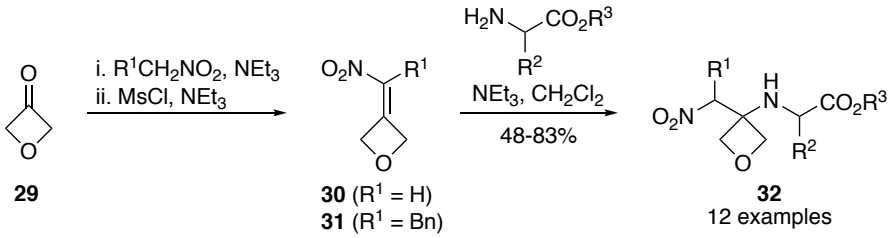

Examples include:

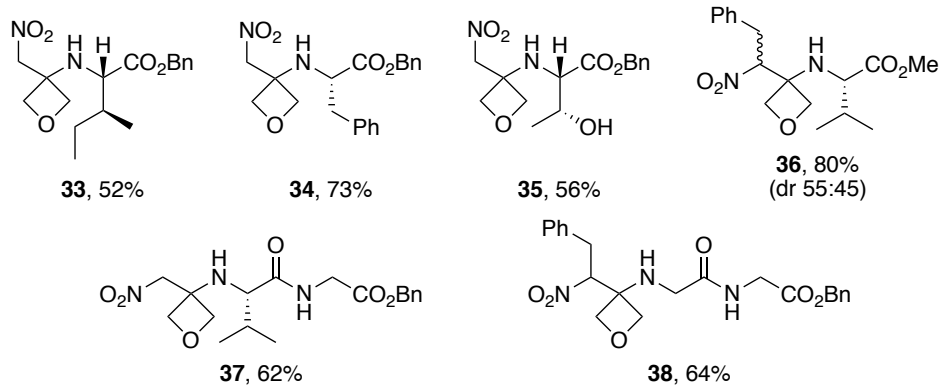

Scheme 1.2 Conjugate addition of a variety of amino esters and dipeptides to oxetane-substituted nitroalkenes.[1,45]

Next, reduction of the nitro group and coupling of the resulting amine with a *N*-terminal protected amino acid was demonstrated.[1] The most reliable conditions for reduction proved to be indium in aq. HCl-THF followed by immediate coupling of the resulting amine with EDC and the appropriate *N*-Cbz protected amino acid (Scheme 1.3). Finally, concomitant removal of the Cbz and benzyl ester groups by hydrogenolysis gave the oxetane-modified tripeptides **41**-**46** in high purity and good overall yields.

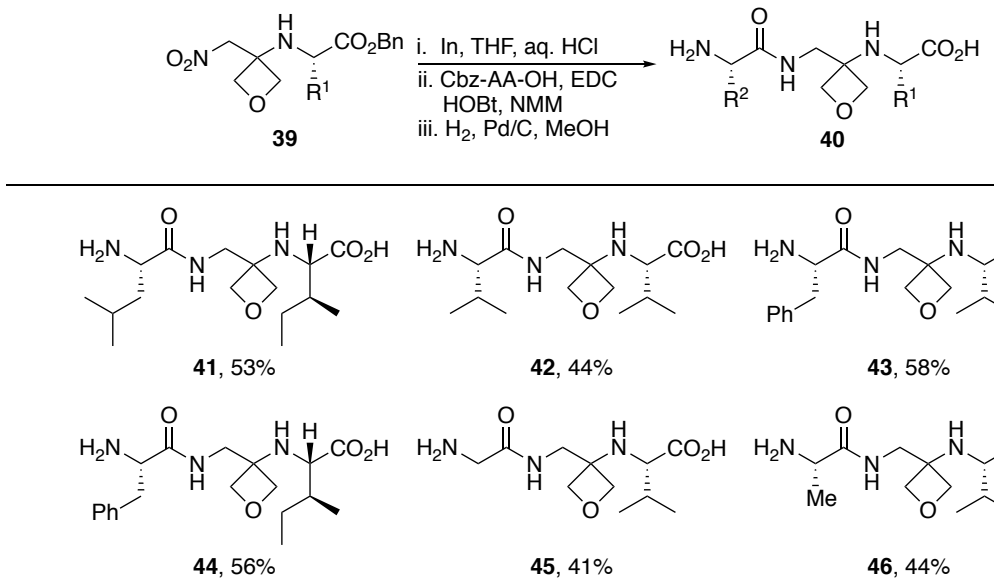

Schemes 1.3 Synthesis of oxetane-containing tripeptide motifs.[1]

In addition to mid-chain oxetane-containing tripeptides, the authors also prepared *N*- and *C*-terminal oxetane-modified tripeptides (**47** and **49**) using variations of the chemistry described above (Scheme 1.4).[45]

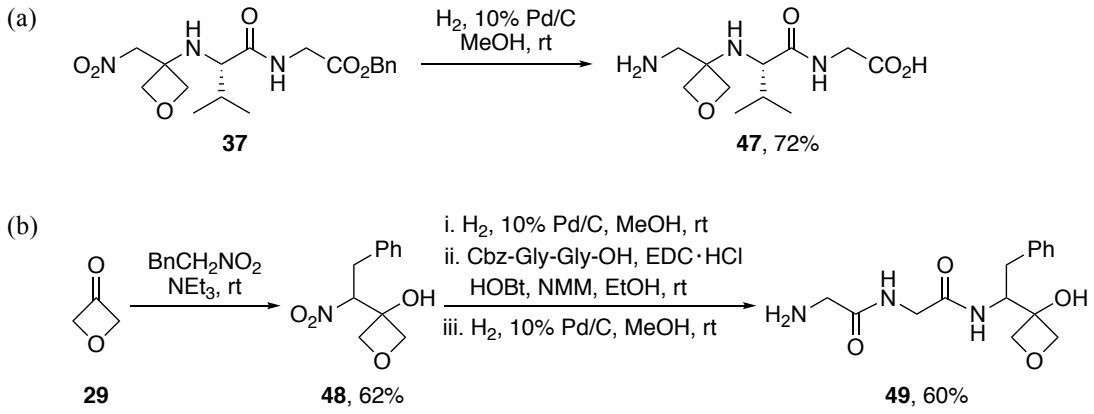

Scheme 1.4 Synthesis and structure of (a) *N*-terminal **47** and (b) *C*-terminal **49** oxetane peptidomimetics.[45]

Following the synthesis of oxetane-modified tripeptides, the authors investigated the structural preferences of these novel peptidomimetics.[1] In the solid state, oxetane-modified tripeptide **41** was shown to be zwitterionic with the terminal amine protonated, not the secondary amine of the 3-aminooxetane unit, and displayed antiparallel sheet-like arrangements (Figure 1.15). Both the secondary amine and the oxygen of the 3-aminooxetane unit were involved in the hydrogen bonding network, with the oxygen of the oxetane hydrogen bonding outside the plane of the sheet. Further analysis of the X-

ray crystal structure revealed that the nitrogen atom adjacent to the oxetane is pyramidal and the averaged C-N-C_{Ox}-C torsional angle (ω) was 60.2°. This is compared to a conventional sp^2-hybridised peptide bond where the nitrogen atom is trigonal and ω = ~180° (Figure 1.15).

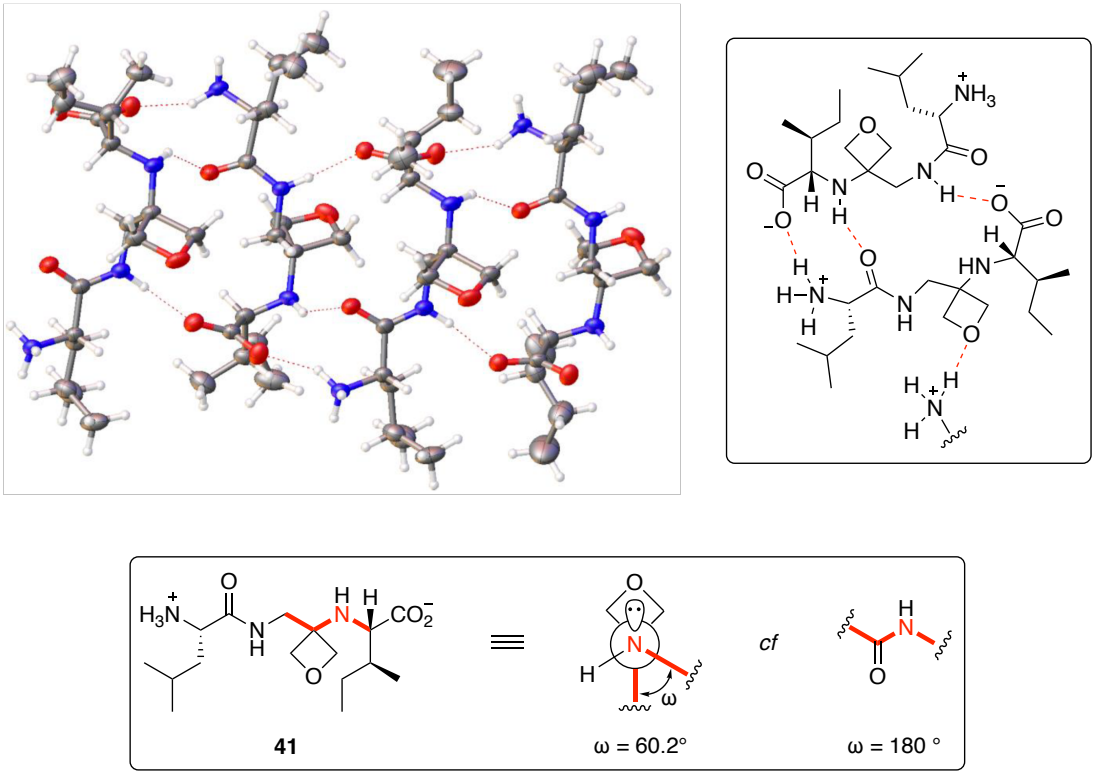

Figure 1.15 Antiparallel sheet-like arrangement of **41** in the solid state.[1] Figure of X-ray structure taken from *Chem. Commun.* **2014**, *50*, 8797-8800.[1]

Molecular dynamic (MD) simulations indicate that oxetane-modified tripeptide **41** has greater conformational flexibility compared to the native tripeptide **50**.[1] Snapshots of the two most populated clusters for **50** and **41** are shown in Figure 1.16. The native tripeptide **50** adopts extended conformations in which the *C*- and *N*-termini are separated by >7 Å. In contrast, oxetane-modified tripeptide **41** adopts folded conformations in which the *C*- and *N*- termini distance is 3-4 Å. The preference for **41** to adopt folded conformations likely arises from the change in hybridisation (sp^2 to sp^3) and dihedral angle at the 3-aminooxetane unit. These observations suggest that oxetane-modification could give rise to turn-like conformations in longer chain peptidomimetics.

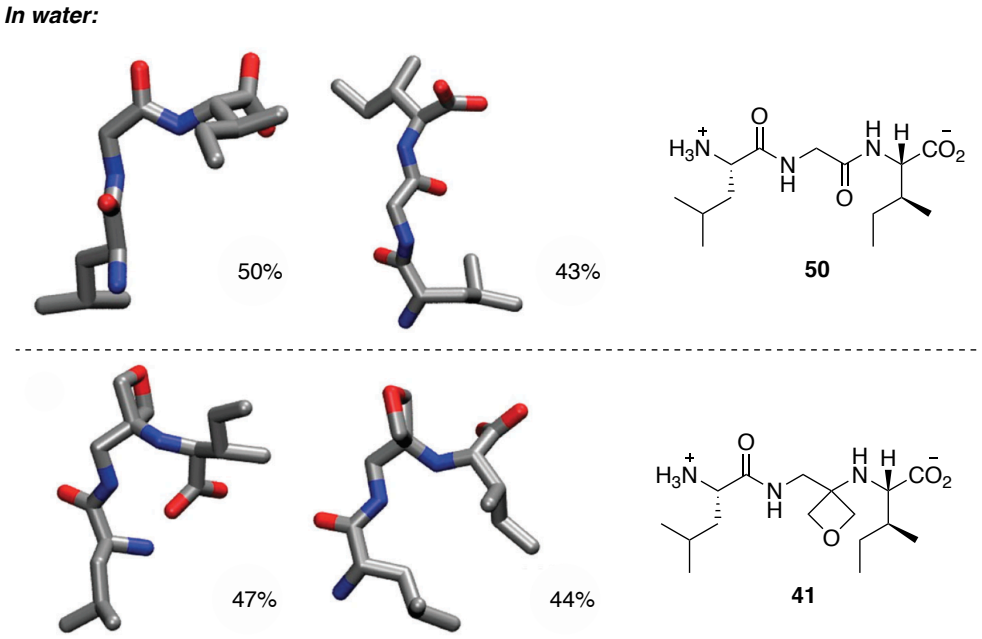

Figure 1.16 Snapshots of the two most populated clusters of **50** and **41** derived from MD simulations, along with the percentages of total structures accounted for by each cluster.[1] Figure of MD derived snapshots taken from *Chem. Commun.* **2014**, *50*, 8797-8800.[1]

Shortly after the publication of this work, Carreira and co-workers independently reported on the chemical synthesis of oxetane-modified peptides.[46] The authors developed a similar approach to oxetane-containing dipeptides **52** *via* conjugate addition of α-amino *n*-propyl esters to nitroalkene **24** followed by nitro reduction with Raney Ni and *in situ* protection of the resulting amine (Scheme 1.5). Similar to observations reported by Shipman and co-workers, addition of chiral amino esters to trisubstituted nitroalkenes **24** ($R^1 \neq H$) gave the addition products as a mixture of diastereoisomers which were inseparable by column chromatography. Subsequent deprotection of the *N*- or *C*-terminal protecting group, followed by standard amide coupling conditions gave longer chain peptidomimetics. This work did not include any structural insights into the folding of oxetane-modified peptides.

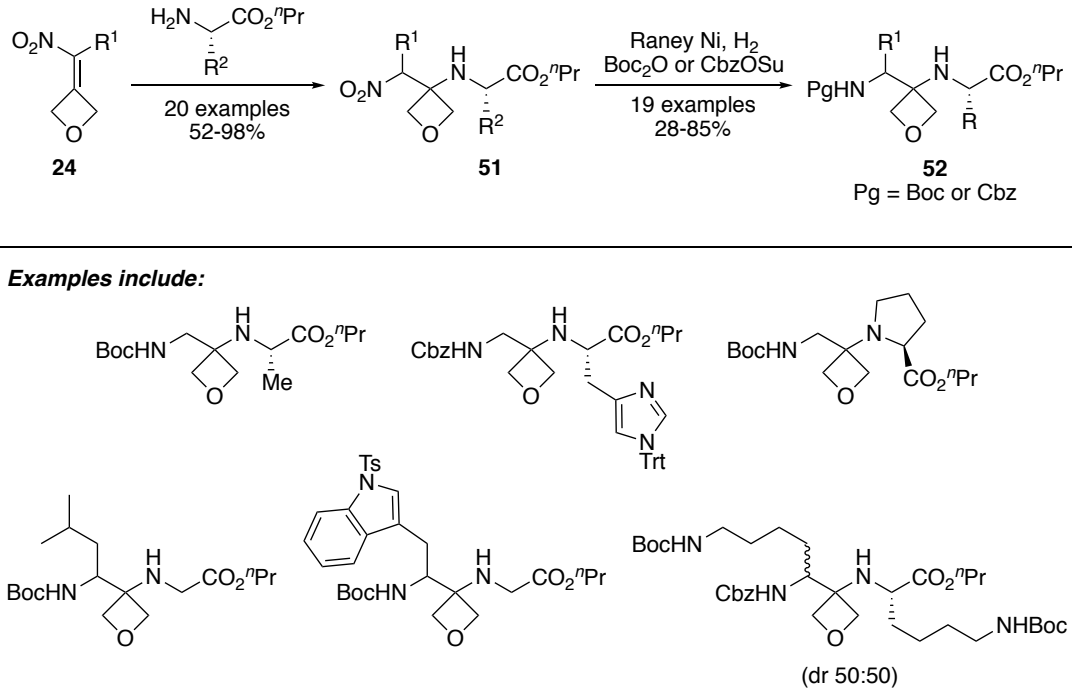

Scheme 1.5 Synthetic route to oxetane-containing dipeptides developed by Carreira and co-workers.[46]

The synthetic approach to oxetane-modified peptides, developed independently by Shipman[1] and Carreira,[46] is highly efficient for the preparation of oxetane-containing peptides in which the oxetane residue is based on glycine (G_{Ox}). However, this route is currently not suitable for the preparation of oxetane-containing peptides in which the oxetane residue is based on residues other than glycine as a mixture of inseparable diastereoisomers is obtained.

In 2017, during the course of the authors' research described in this thesis, Carreira and co-workers published an asymmetric route to oxetane-containing dipeptide building blocks **53**.[47] Their expeditious route involved substitution of activated (*i.e.* X = OTf) enantiopure hydroxyesters **55** with enantiopure 3-aminooxetanes **54** (Scheme 1.6). The enantiopure amines **54** were prepared *via* addition of an organometallic reagent to chiral imine **56**, which in turn, was accessed from commercially available Tris hydrochloride **58**. Enantiopure hydroxyesters **55** were derived from *D*-amino acids.

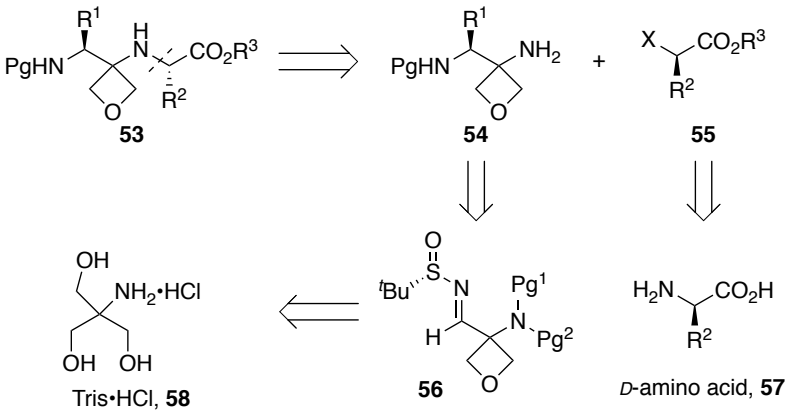

Scheme 1.6 Carreira and co-workers' synthetic approach to oxetane-containing dipeptide building blocks.[47]

Chiral imine **63** was prepared in 7 steps from Tris·HCl **58** (Scheme 1.7).[47] Tris·HCl **58** was first converted to hydroxy-oxetane **61** using a route that involved protection of the amine and formation of the oxetane ring. Following this, Swern oxidation and condensation of the resulting aldehyde with Ellman's auxiliary **62** gave the desired chiral imine **63**.

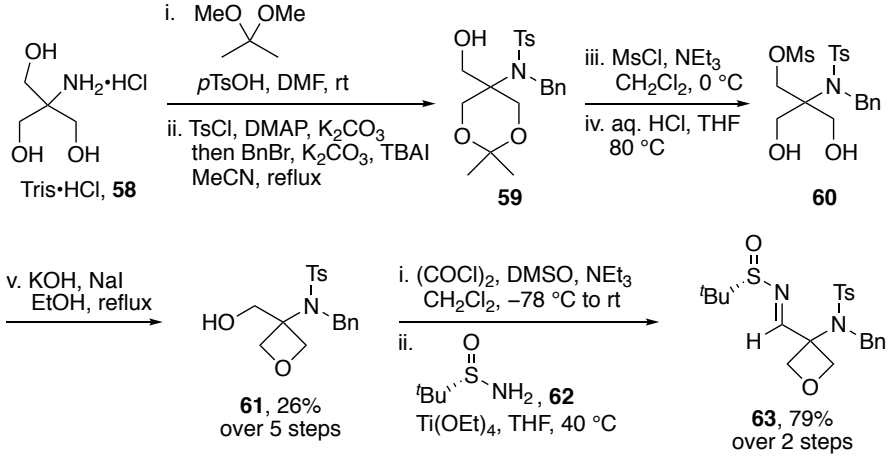

Scheme 1.7 Carreira and co-workers' synthesis of chiral imine **63**.[47]

Chiral imine **63** served as a crucial intermediate for the synthesis of enantiopure 3-aminooxetane building blocks **54**. For example, the synthetic route to an oxetane-modified alanine (A_{Ox}) building block **66** is detailed below (Scheme 1.8).[47] Addition of methyllithium to chiral imine **63** gave the addition product **64** as a single diastereoisomer (dr >95:5). Following this, cleavage of Ellman's auxiliary and Boc-protection of the resulting amine gave intermediate **65**. Finally, tosyl and benzyl deprotection gave the desired A_{Ox} residue **66** as a single enantiomer. Using variations of this route, Carreira and

co-workers were able to prepare several enantiopure 3-aminooxetane building blocks **54**, including analogues of phenylalanine (F_{Ox}), tyrosine (Y_{Ox}), valine (V_{Ox}) and proline (P_{Ox}).

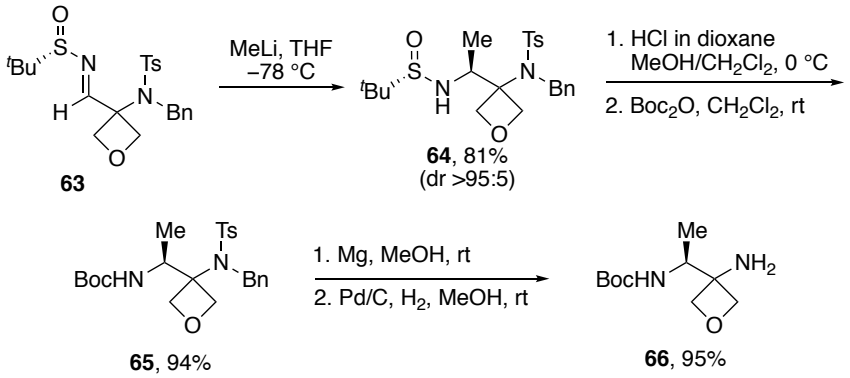

Scheme 1.8 Carreira and co-workers' synthesis of enantiopure 3-aminooxetane **66**.[47]

Effenberger and co-workers have demonstrated that displacement of triflates with an amine proceeds exclusively in an S_N2 fashion to produce a single enantiomer.[48] On this basis, Carreira and co-workers prepared a number of triflates **69** from the corresponding hydroxyesters **68**, which in turn, were prepared from *D*-amino acids **57** (Scheme 1.9).[47]

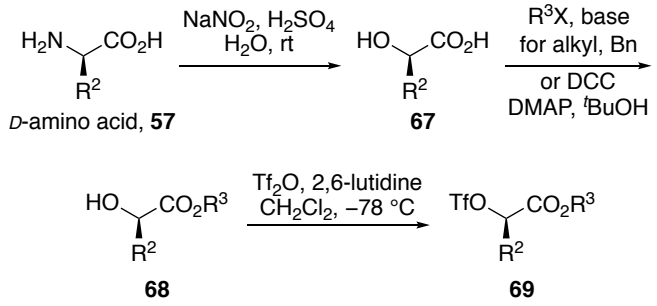

Scheme 1.9 Synthesis of triflates from *D*-amino acids.[47]

With access to a variety of enantiopure 3-aminooxetanes **54** and activated hydroxyesters **55**, a collection of oxetane-containing dipeptide building blocks **53** were prepared (Scheme, 1.10).[47] Alkylation of enantiopure 3-aminooxetanes **54** with triflates **55** proceeded exclusively in an S_N2 fashion to provide the building blocks **53** as single diastereoisomers. In the case of dipeptides incorporating a glycine residue, commercially available bromo acetates were used.

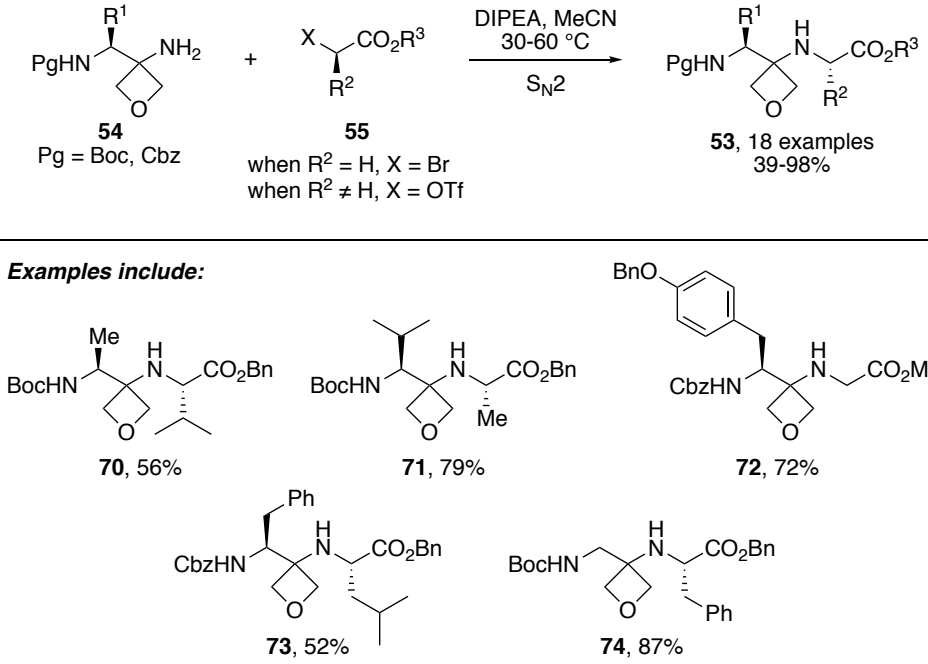

Scheme 1.10 Carreira and co-workers' synthesis of oxetane-containing dipeptide building blocks.[47]

Although the approach developed by Carreira provided access to dipeptide building blocks containing a variety of oxetane-modified residues, the route to prepare enantiopure 3-aminooxetanes **54** was not particularly practical. The route involved a significant number of steps, requiring the use of a number of protecting groups and chromatographic purifications. Therefore, shorter routes to enantiopure 3-aminooxetanes **54** would be of advantage.

The authors demonstrated the application of these building blocks by preparing analogues of Leu-enkephalin **75**, an opioid peptide that modulates the reception of pain,[3] wherein each amide bond was sequentially replaced by the 3-aminooxetane unit (Figure 1.17).[47] Investigations on the impact of oxetane-modification on the biological activity of Leu-enkephalin revealed that the oxetane-modified analogues showed largely improved hydrolytic stability in human serum and two of the analogues retained affinity towards the δ-opioid receptor comparable to the native system. These results provide proof of concept that oxetane-modification of an amide bond can be used to increase the stability of a peptide towards proteases while retaining bioactivity. A more detailed discussion on the stability and biological activity of oxetane-modified Leu-enkephalin analogues is included in Chapter 3.

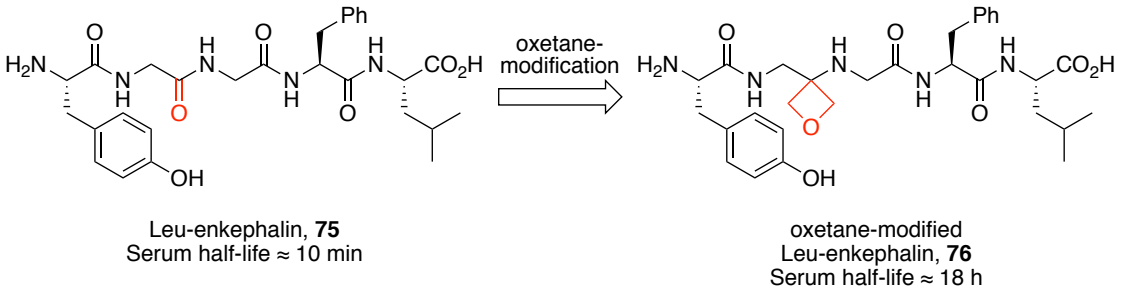

Figure 1.17 Example of an oxetane-modified analogue **76** of Leu-enkephalin **75** with improved hydrolytic stability in human serum.[47]

1.4.3 Oxetane-Modification of Proteins

Recently, Bernardes and co-workers have reported a method for the chemoselective introduction of oxetane moieties into proteins through alkylation of cysteine residues under mild conditions.[49] Initially, the authors demonstrated the site-selective incorporation of the 3-*S*-oxetane motif into proteins *via* S_N2 reaction of 3-bromooxetane **79** with single-Cys mutants of the C2A domain of Synaptotagmin-I Cys95 (C2Am, **77**) and Annexin-V (AnxV, **78**) to afford Cys-to-oxetane alkylation products **80** and **81** in >95% conversion (Scheme 1.11). Stability studies revealed that the 3-*S*-oxetane motif was stable upon incubation with human plasma, reduced glutathione (GSH), and other *S*- and *N*-nucleophiles. Importantly, C2Am-3-*S*-Ox **80** retained its inherent binding activity against phosphatidylserine (PS), an internal membrane lipid externalised during apoptosis.

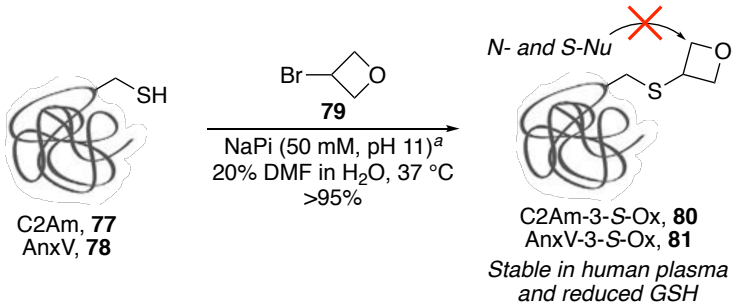

Scheme 1.11 Site-selective modification of proteins with oxetanes.[49] [a] P_i = phosphate.

Next, the authors reported an extension of this chemistry to include other oxetanes. Reaction of C2Am **77** with 3,3-bis(bromomethyl)oxetane **82** afforded C2Am-*S*-Ox-CH_2Br **83** in >95% conversion (Scheme 1.12).[49] The resulting modified protein **83**

contained an electrophilic handle (*S*-Ox-CH_2Br) amenable to a second round of chemical modification after incubation with an appropriate nucleophile (*e.g.* post-translational modifications, cytotoxics and spectroscopic tags). Subsequently, incubation of **83** with 2-mercaptoethanol, βGalSNa, thiophenol and benzylamine gave substitution products **84a-d** in >95% conversion. Interestingly, the oxetane linker (*S*-CH_2-Ox-CH_2-*S/N*) proved to be a more rigid scaffold compared to a common aliphatic linker (*S*-CH_2-CH_2-CH_2-*S/N*) containing the same number of carbons. Hence, this rigid and soluble oxetane linker may find application in the development of vaccine conjugates.

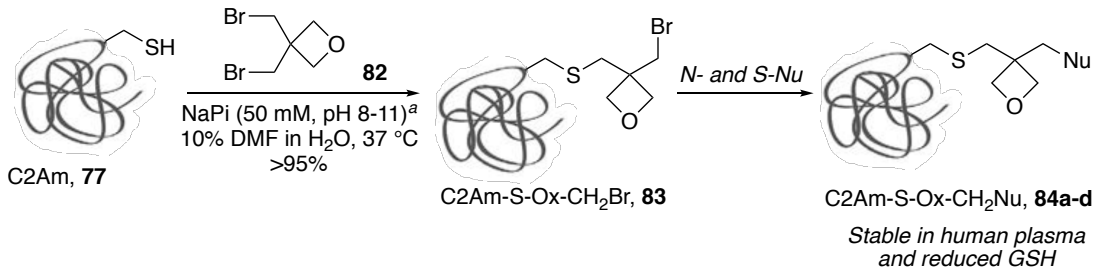

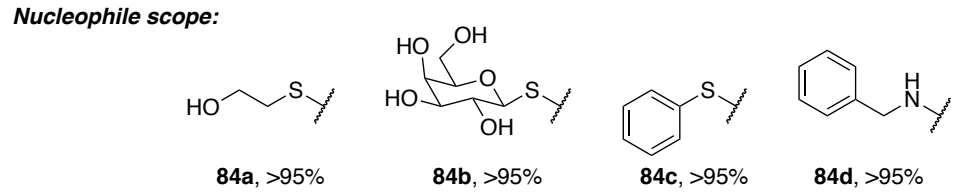

Scheme 1.12 Selective incorporation of an S-to-S/N oxetane linker on proteins.[49] [a] P_i = phosphate.

Following this study, Bernardes and co-workers reported an efficient method for the site-selective installation of an oxetane-containing constraint for disulphide containing peptides and proteins under mild and biocompatible aqueous conditions (Figure 1.13).[50] Somatostatin **85** and octreotide **87**, which can be used for imaging and treating neuroendocrine tumours, were reacted simultaneously with tris(2-carboxyethyl)-phosphine (TCEP) and **82** in 10% DMF in water to give, after HPLC purification, the grafted cyclic peptides **86** and **88** in 76% and 81% yield, respectively. Investigations into the binding properties of these derivatives to the somatostatin receptor 2 (SSTR2) revealed that octreotide **87** and oxetane-grafted surrogate **88** had similar affinity against this receptor, while oxetane-grafted **86** showed a 4-fold enhancement in binding affinity compared to somatostatin **85**. MD simulations suggested that oxetane-grafted somatostatin **86** was more rigid and displayed a more defined conformation in solution than **85**, which is ideal for a more efficient binding to the receptor. Both oxetane-grafted peptides **86** and **88** were stable in human plasma and in the presence of GSH.

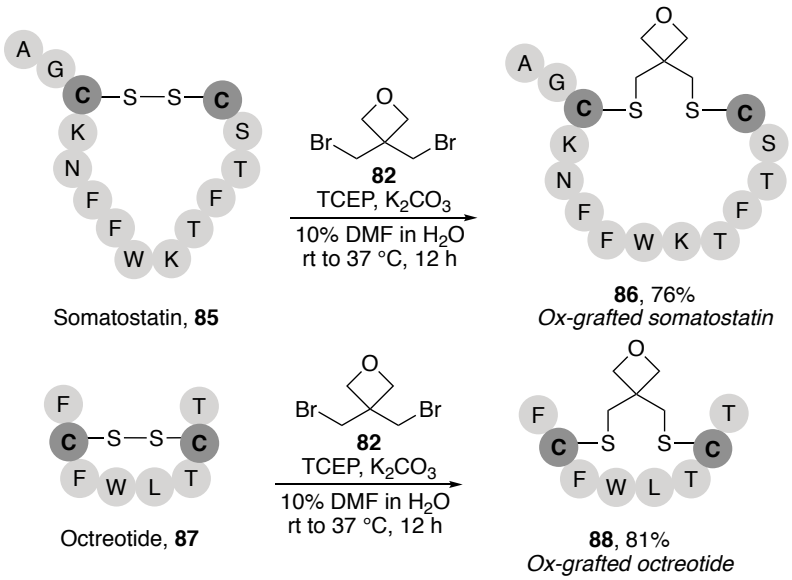

Scheme 1.13 Installation of an oxetane-containing constraint for disulphide-containing cyclic peptides.[50]

Next, the authors demonstrated the utility of this chemistry to prepare oxetane-grafted antibodies (Scheme 1.14).[50] The exposed disulphide bond of a Fab fragment of Herceptin (Fab-Her, **89**), an antibody currently used to treat Her2+ breast cancer patients, was reacted with **82** under aqueous buffered conditions in the presence of TCEP to give oxetane-grafted Fab-Her **90** in >95% conversion. Unlike the native antibody **89**, oxetane-grafted **90** was stable under reducing conditions and in human plasma, which is a key aspect in antibody therapeutics design as thiol-exchange reactions in plasma lowers efficacy and adds side-toxicity. Importantly, oxetane-grafted **90** showed a small increase in binding affinity (K_D) to the Her2 receptor compared with the native antibody **89**. Taken together, these results demonstrate that installation of an oxetane-graft in disulphides present in peptides and proteins enables stabilisation of folded structures and results in disulphide-grafted products with improved bioactivity that are stable under biological conditions.

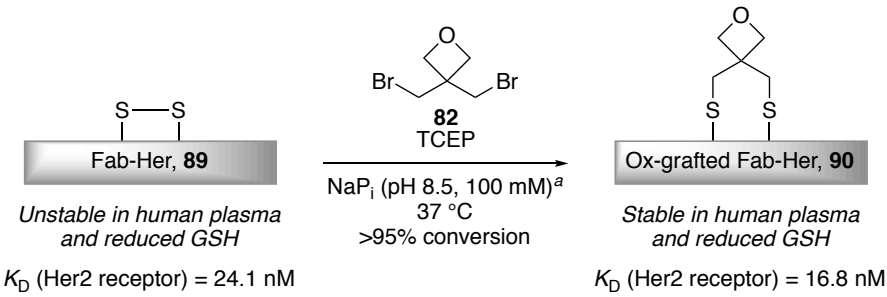

Scheme 1.14 Representation of a disulphide constraint in native antibody sequences using an oxetane graft.[50] [a] P_i = phosphate.

1.5 Conclusions

This chapter has discussed the relevance of peptidomimetics and oxetanes in medicinal chemistry. Recently, these exciting areas of research have led to the development of a novel class of peptidomimetic in which one of the amide C=O bonds of a peptide backbone is replaced by an oxetane ring. Independent publications by Shipman[1] and Carreira[46,47] have begun to explore the properties and structure of these novel peptidomimetics, and have demonstrated that oxetane-modification within a peptide sequence can promote turn-like conformations and improve stability towards proteases. In order to establish the full potential of oxetane-modified peptides, it is important to further develop methods for their synthesis and to investigate the impact of oxetane-modification on the properties and structure of biologically interesting peptides.

Chapter 2: Synthesis of Oxetane- and Azetidine-Containing Spirocycles Related to the 2,5-Diketopiperazine Framework

2.1 Previous Work and Project Aims

Previous research in our group explored conditions for the reduction of the nitro group in nitro amino esters to the corresponding amine for the synthesis of oxetane-containing peptides. During this investigation, reduction of the nitro group in **91** using samarium (II) iodide failed to give the desired primary amine **92** but instead gave oxetane-containing spirocycle **93**, as a result of reduction followed by spontaneous cyclisation. This novel spirocyclic scaffold is similar in structure to the 2,5-diketopiperazine framework (2,5-DKP **94**, Scheme 2.1).[45]

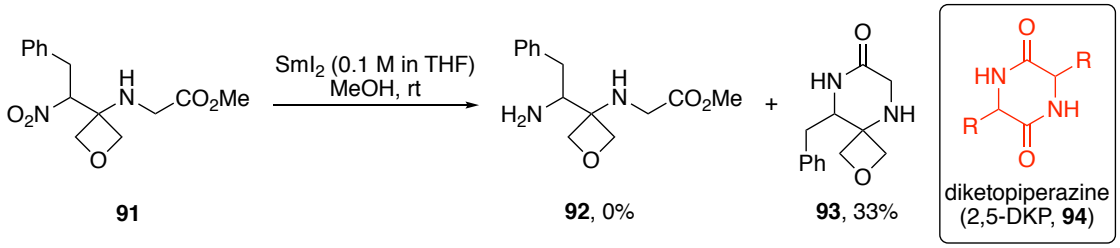

91 **92**, 0% **93**, 33%

Scheme 2.1 Synthesis of **93** *via* reduction of the nitro group of **91**.

As part of an ongoing interest in the preparation of spirocyclic heterocycles, oxetane-containing frameworks and 2,5-DKP templates in drug discovery projects,[31,51–53] we thought it would be worthwhile to examine the feasibility of optimising this process and preparing a series of novel spirocyclic scaffolds related to the 2,5-DKP framework. Additionally, this investigation would allow us to further examine the scope of the conjugate addition chemistry developed in earlier publications by us[1,45] and by Carreira.[46] Furthermore, this project would serve as a good starting point for the author to familiarise himself with the chemistry previously developed.

2.2 Introduction

There are a number of excellent reviews written on 2,5-DKPs[53,54] and spirocyclic heterocycles.[31,51,52] This short introduction does not aim to replicate these reports but to highlight the relevance of 2,5-DKPs and spirocyclic heterocycles in drug discovery.

2.2.1 2,5-Diketopiperazines

2,5-Diketopiperazines (2,5-DKPs, Scheme 2.1) are the smallest possible cyclic peptides derived from the condensation of two α-amino acids and are found in numerous natural products and biologically active compounds. These small, conformationally constrained, chiral scaffolds contain multiple H-bond donors and acceptors, are stable to proteolysis and have the potential for derivatisation at up to four positions. These properties make them attractive motifs in drug discovery.[53]

The structures of bioactive natural products containing the 2,5-DKP framework range from simple cyclic dipeptides to highly functionalised fused ring systems. Examples include, the naturally occurring peptide antibiotic brevianamide F **95**[55] and bicyclomycin **96**,[56] as well as the indolic alkaloid spirotryprostatin A **97**,[57] a promising antimitotic arrest agent (Figure 2.1). Due to their therapeutic potential, the total syntheses of natural products containing the 2,5-DKP framework is a major pursuit of organic chemists.

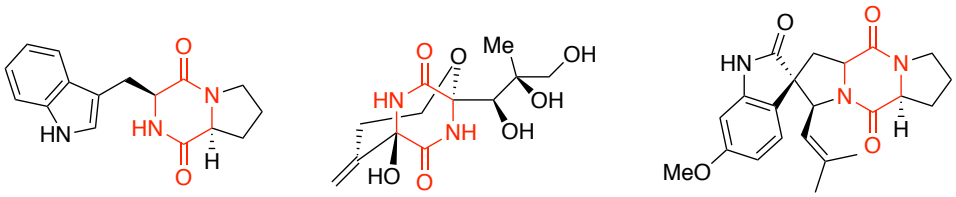

Figure 2.1 Bioactive natural products containing the 2,5-DKP framework.

Chirally enriched 2,5-DKPs are easily prepared from readily available α-amino acids using robust chemistry and have been used as core templates from which to construct libraries of compounds in medicinal chemistry projects. Structure-activity relationship (SAR) has been investigated for many of these compounds, and has led to the development of several clinical drugs. Examples include the marketed drug Tadalafil **98**[58,59] and Retosiban **99**,[60,61] as well as Plinabulin **100**, which is currently in phase 3 clinical trials for non-small cell lung cancer (Figure 2.2).[62,63]

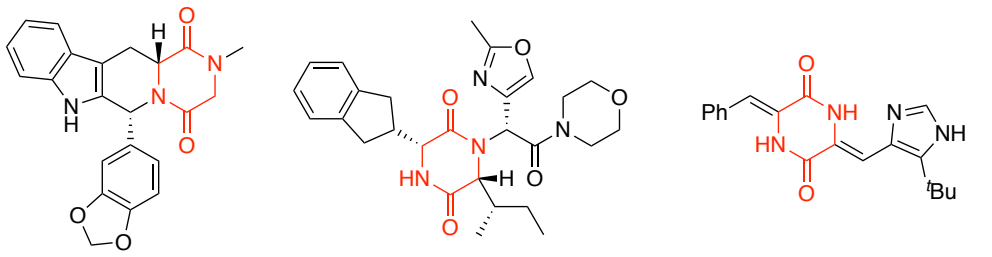

Figure 2.2 Therapeutic agents containing the 2,5-DKP framework.

In addition to this, peptidomimetics containing 2,5-DKPs have been used to construct conformational mimics of linear peptides. For example, 2,5-DKP **101**, containing a carboxylic acid and amino functionality in a *cis*-relationship, has been used to prepare peptide sequences that result in the formation of *β*-hairpin mimic **101** containing 10- and 18-membered H-bonded rings (Scheme 2.2).[64]

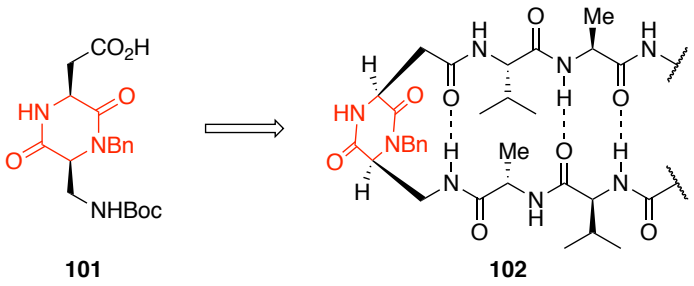

Scheme 2.2 Bifunctional 2,5-DKP **101** acting as a *β*-hairpin inducer.[64]

2.2.2 Spirocycles in Drug Discovery

Spiro compounds (spirocycles) are molecules containing two rings linked together by the same atom, referred to as the spiroatom. Recent progress towards the synthesis of spirocyclic systems has seen a significant increase in the incorporation of spirocycles into pharmaceutically active molecules. Properties of spirocycles that make them of benefit in medicinal chemistry projects include their inherent rigidity, ability to place functional groups precisely in three-dimensional space, and structural novelty for patentability.[31,51,52]

Recent examples of spirocyclic compounds in drug development projects include Zoliflodacin (ETX0914) **103**,[65] a novel oral antibiotic currently in clinical trials for the treatment of gonorrhoea, and AMG-8718 **104**, a BACE1 (*β*-site APP cleaving enzyme)

inhibitor which is a potential target for the development of an Alzheimer's disease therapy.[66] Irbesartan **105**, which is widely used to treat high blood pressure, is an example of a marketed drug containing a spirocyclic moiety (Figure 2.3).[51,67]

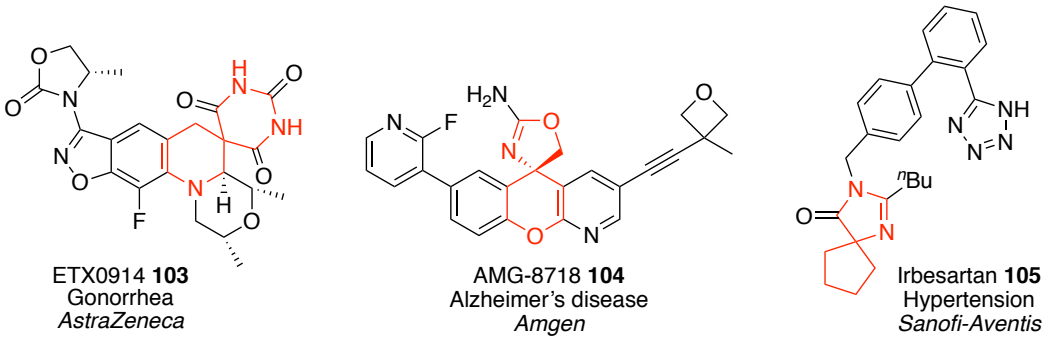

Figure 2.3 Therapeutic agents containing spirocyclic scaffolds.

More recently, as part of an ongoing interest in four-membered rings and the need to access novel structures, there has been a significant increase in the number of oxetane- and azetidine-containing spirocycles in drug discovery programmes (Figure 2.4).[31,52] Examples include spiro-oxetane **106** as a potential anti-hepatitis C virus (HCV) agent,[68] spiro-oxetane **107** a potent inhibitor of respiratory syncytial virus (RSV) RNA polymerase,[69] and spiro-oxetane-azetidine **108** a clinical candidate for weight loss.[70]

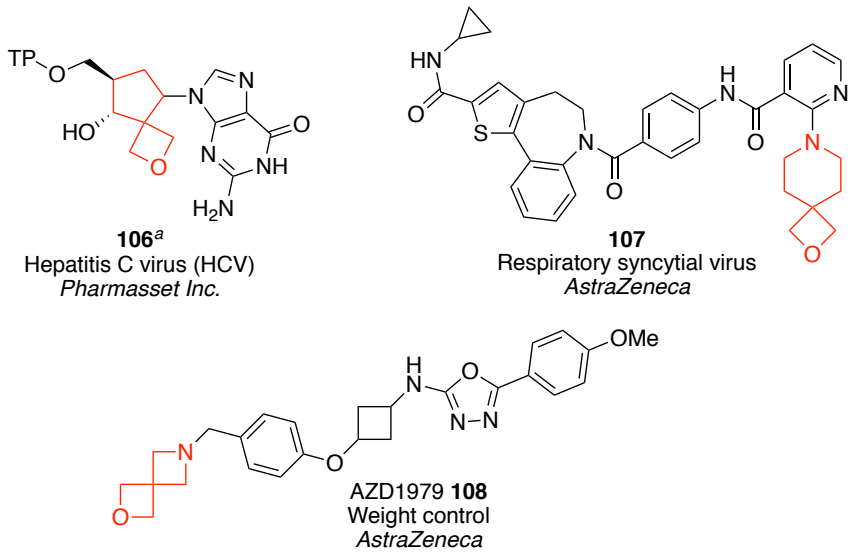

Figure 2.4 Spirocyclic compounds incorporating oxetane and azetidine rings. [a] TP = triphosphate

It is worth noting that it is often difficult to determine whether a spirocycle has been introduced to improve the pharmaceutical properties of a compound or to create novel scaffolds that do not impede on existing intellectual property space.[52]

2.3 Results and Discussion

2.3.1 Optimisation of Reduction and Cyclisation Conditions

The first task was to make suitable substrates to optimise the reduction-cyclisation sequence presented in Scheme 2.1. Methyl ester (*S*)-**109**, benzyl ester **110** and *tert*-butyl ester **111**, all possessing the same valine backbone substitution, were selected as test substrates and were prepared following a previously described literature procedure (Scheme 2.3).[1] Conjugate addition of the appropriate valine ester (2.0 equiv) to 3-(nitromethylene)oxetane **30** (1.0 equiv), which was prepared *in situ* from oxetane-3-one **29** (1.0 equiv) and nitromethane (1.4 equiv), gave the desired oxetane-modified DKP precursors.

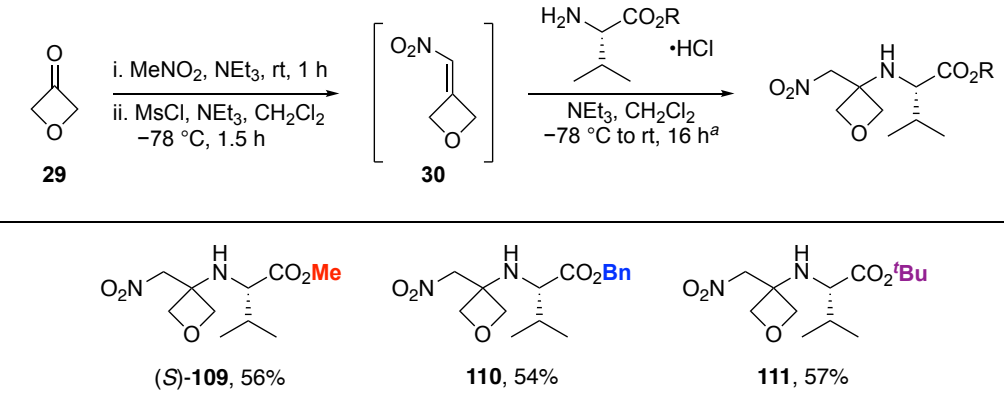

Scheme 2.3 Synthesis of test substrates. [a] Method: $MeNO_2$ (1.4 equiv), oxetan-3-one (1.0 equiv), NEt_3 (0.2 equiv); NEt_3 (2.0 equiv), MsCl (1.0 equiv); amino ester hydrochloride (2.0 equiv), NEt_3 (2.0 equiv).

With these test-substrates in hand, a variety of conditions for the controlled reduction of the nitro group in methyl ester (*S*)-**109** were explored (Table 3.1, entries 1-6). In each case, the DKP analogue **112** was isolated as a result of spontaneous cyclisation of the reduced primary amine. Reduction using zinc[71,72] and indium[73] under acidic conditions gave **112** in poor yields. Catalytic hydrogenation using Pd/C gave **112** in a slightly improved yield of 50%, whereas Pt/C gave a lower yield of 21%. The use of Raney Ni under an atmosphere of hydrogen proved to be most effective. Under these conditions, which were adapted from chemistry previously reported by Carreira and co-workers (see Scheme 1.5),[46] **112** was isolated in 81% yield after chromatography. Following this result, the impact of the *C*-terminal ester group on the cyclisation was investigated (Table 3.1, entries 7-8). When benzyl ester **110** was subjected to the optimised conditions, **112** was isolated in a significantly lower yield. The *tert*-butyl group of **111** prevented cyclisation

after reduction of the nitro group and only the corresponding primary amine was observed in the crude product.

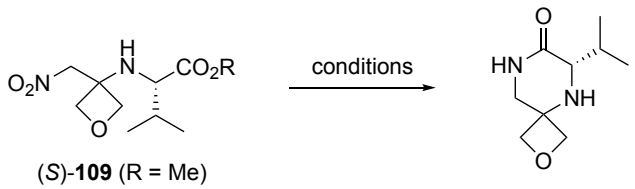

(*S*)-**109** (R = Me)
110 (R = Bn)
111 (R = ^{t}Bu)

112

Entry	Substrate	R	Conditions[a]	Yield (%)[b]
1	(*S*)-**109**	Me	Zn, AcOH, THF[71]	22
2	(*S*)-**109**	Me	Zn, aq. NH_4Cl, EtOH[72, c]	26
3	(*S*)-**109**	Me	In, HCl, THF/H_2O (1:3)[73]	25
4	(*S*)-**109**	Me	10% Pd/C, H_2, MeOH	50
5	(*S*)-**109**	Me	10% Pt/C, H_2, MeOH	23
6	(*S*)-**109**	Me	Raney Ni, H_2, MeOH	81
7	**110**	Bn	Raney Ni, H_2, MeOH	17
8	**111**	^{t}Bu	Raney Ni, H_2, MeOH	0[d]

Table 2.1 Optimisation of cyclisation conditions to **112**. [a] Conducted at room temperature unless otherwise stated. [b] Isolated yield after chromatography. [c] Reduction at 30 °C, then heated at reflux for 24 h. [d] Major product was the primary amine from reduction of nitro group without concomitant cyclisation.

2.3.2 Synthesis of Oxetane-Modified Diketopiperazine Precursors

With conditions for the reduction-cyclisation optimised, we next wanted to explore the substrate scope of this chemistry. We began by preparing a set of oxetane-modified DKP precursors. Using the previously described conditions, conjugate addition of commercially available α-amino methyl esters (2.0 equiv) to nitroalkene **30** (1.0 equiv) gave access to a variety of oxetane-modified DKP precursors (Scheme 2.4). Whilst this methodology is based on earlier publications by us[1] and by Carreira,[46] it should be noted that all the examples contained within Scheme 2.4, with the exception of **109** and **115**,

are novel. The new examples include those involving non-polar (Gly **113**, Ala **114**), aromatic (Phe **116**), acidic (Asp **117**) and basic (Lys **118**) residues. In addition to this, secondary amines (Pro **119**) and non-proteinogenic (phenyl glycine **120**) examples have been demonstrated in the conjugate addition step for the first time.

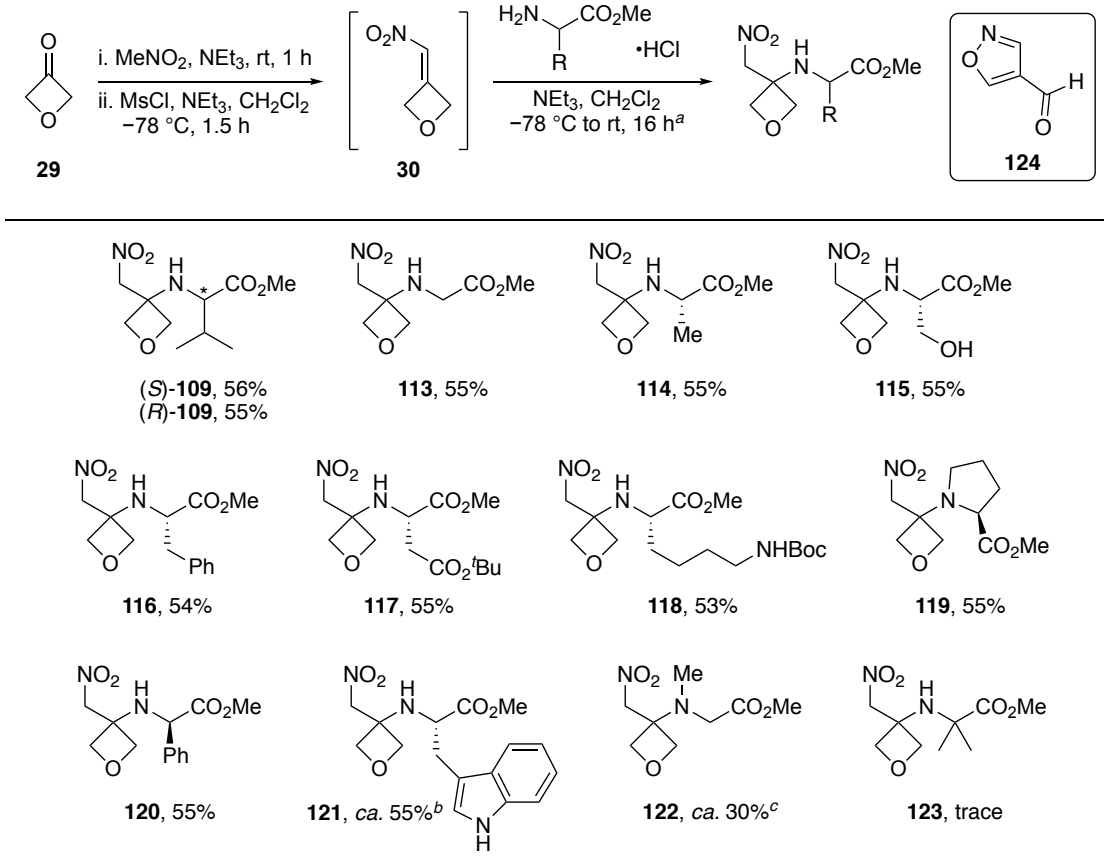

Scheme 2.4 Synthesis of oxetane-modified DKP precursors. [a] Method: $MeNO_2$ (1.4 equiv), oxetan-3-one (1.0 equiv), NEt_3 (0.2 equiv); NEt_3 (2.0 equiv), MsCl (1.0 equiv); amino methyl ester hydrochloride (2.0 equiv), NEt_3 (2.0 equiv). [b] Isolated as an inseparable mixture with the nitro-aldol intermediate. [c] Isolated as an inseparable mixture with nitroalkene **30**.

Although addition of *L*-tryptophan methyl ester to nitroalkene **30** was successful, the product **121** co-eluted with the nitro-aldol intermediate and attempts to purify the material by chromatography were unsuccessful (Scheme 2.4). When sarcosine methyl ester was used, some conversion to product **122** was observed. However, attempts to purify the material by chromatography resulted in retro-aza-Michael reaction and gave the product as an inseparable mixture with nitroalkene **30**. Achiral quaternary α-aminoisobutyric acid (Aib) methyl ester only gave traces of product **123** when used in the conjugate addition. As the Aib residue is sterically hindered, it is possible that the rate of addition to nitroalkene **30** is significantly reduced and instead rearrangement to isoxazole **124** is

favoured, although only traces of **124** were observed in the ^{1}H-NMR spectrum of the crude reaction mixture. This rearrangement is known to be promoted by secondary and tertiary amines, and has been used to prepare a series of substituted isoxazoles from oxetane-substituted nitroalkenes (Scheme 2.5).[74]

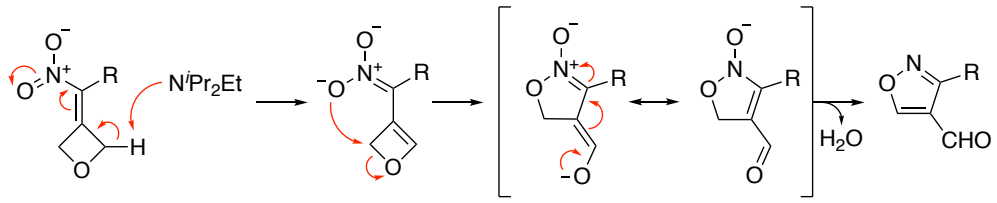

Scheme 2.5 Proposed mechanism for the rearrangement of oxetane-substituted nitroalkenes to isoxazoles.[74]

Next, we examined the preparation of oxetane-modified DKP precursors with variation at the α-carbon of the nitroalkane. This had previously been studied by Dr Nicola Powell in the group by conjugate addition of amino esters to trisubstituted nitroalkenes.[1] On this basis, we first prepared trisubstituted nitroalkenes **31** and **128** following modified procedures previously reported by Carreira[74] and Ellman,[75] respectively. (Scheme 2.6). Henry reaction using either 2-phenylnitroethane **126** or nitroethane with oxetan-3-one, followed by elimination with methanesulfonyl chloride, gave nitroalkenes **31** and **128** in good isolated yields. As nitroalkane **126** was not commercially available, it was first prepared by reduction of *trans*-β-nitrostyrene following a literature method.[76]

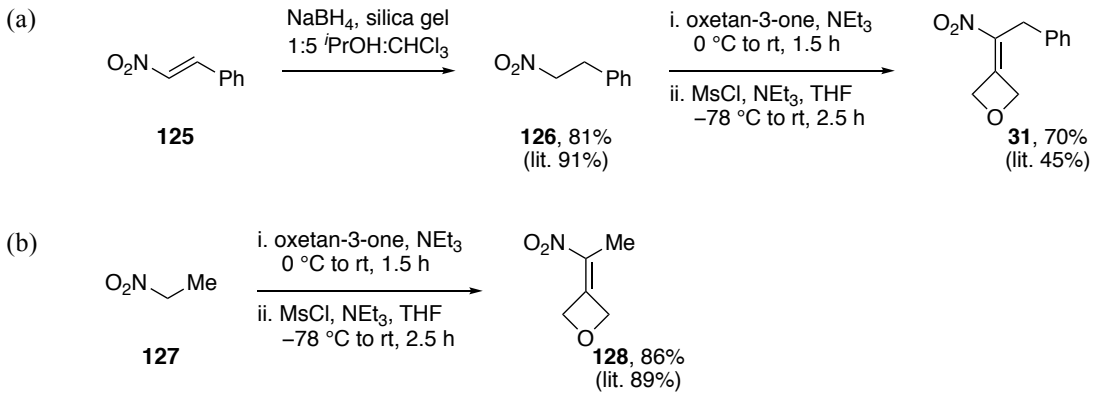

Scheme 2.6. Synthesis of trisubstituted nitroalkenes **31** and **128**.

Having obtained nitroalkenes **31** and **128**, the conjugate addition of α-amino methyl esters was studied (Scheme 2.7). Initially, conjugate addition of glycine methyl ester was investigated to avoid the complication of diastereoisomers. Glycine methyl ester was first prepared from the corresponding hydrochloride salt following a literature procedure and

used immediately in the addition step due to its tendency to polymerise.[77] Using this route, methyl esters **91** and **131** were prepared in excellent yields from nitroalkenes **31** and **128** respectively. We next investigated the conjugate addition of *L*-valine methyl ester to trisubstituted nitroalkenes. *L*-Valine methyl ester was first prepared from the corresponding hydrochloride salt and then added to **128** to give methyl ester **132** in excellent yield. The inherent chirality of *L*-valine had no influence on the resulting stereochemistry, providing **132** as a 50:50 mixture of diastereoisomers that could not be separated by column chromatography. A more detailed discussion on the conjugate addition of chiral amine nucleophiles to trisubstituted nitroalkenes is included in Chapter 4.

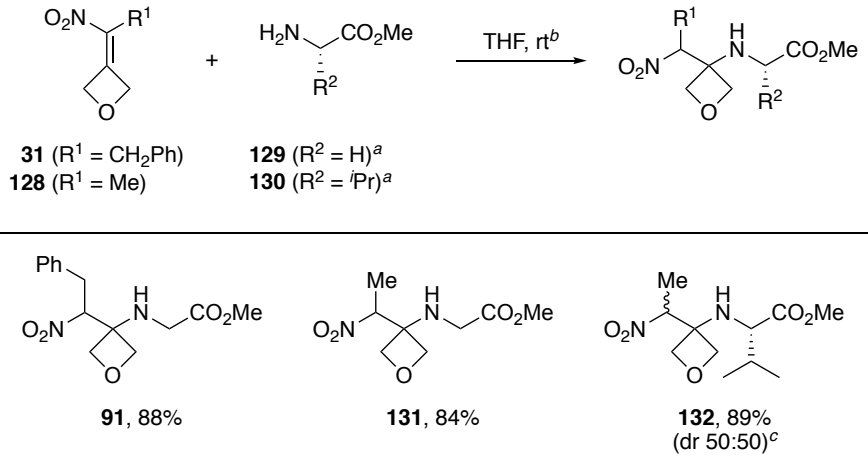

Scheme 2.7. Synthesis of oxetane-modified precursors. [a] Prepared from the corresponding hydrochloride salt and used immediately.[77] [b] Method: Nitroalkene (1.0 equiv), amino methyl ester (2.0 equiv). [c] Formed and isolated as a 50:50 mixture of diastereoisomers determined by ^{1}H-NMR analysis (see Section 6.7).

2.3.3 Synthesis of Oxetane-Containing Spirocycles

With a variety of oxetane-modified DKP precursors in hand the scope of the optimised reduction-cyclisation conditions was explored. Using Raney Ni under an atmosphere of hydrogen, a variety of 2,5-DKP analogues bearing different side chains and substitution patterns were produced in good yields (Scheme 2.8). All of the substrates used were tolerant of the reaction conditions. Both enantiomers of **112** were made, and we were able to confirm by ^{1}H-NMR analysis in the presence of Pirkle's reagent that no detectable racemisation occurs during the reduction-cyclisation sequence (Section 6.4). Disubstituted derivatives such as **142** can be produced in high yield as a mixture of

diastereoisomers. Unfortunately, attempts to separate the diastereoisomers using column chromatography were unsuccessful and **142** was isolated as a 50:50 mixture.

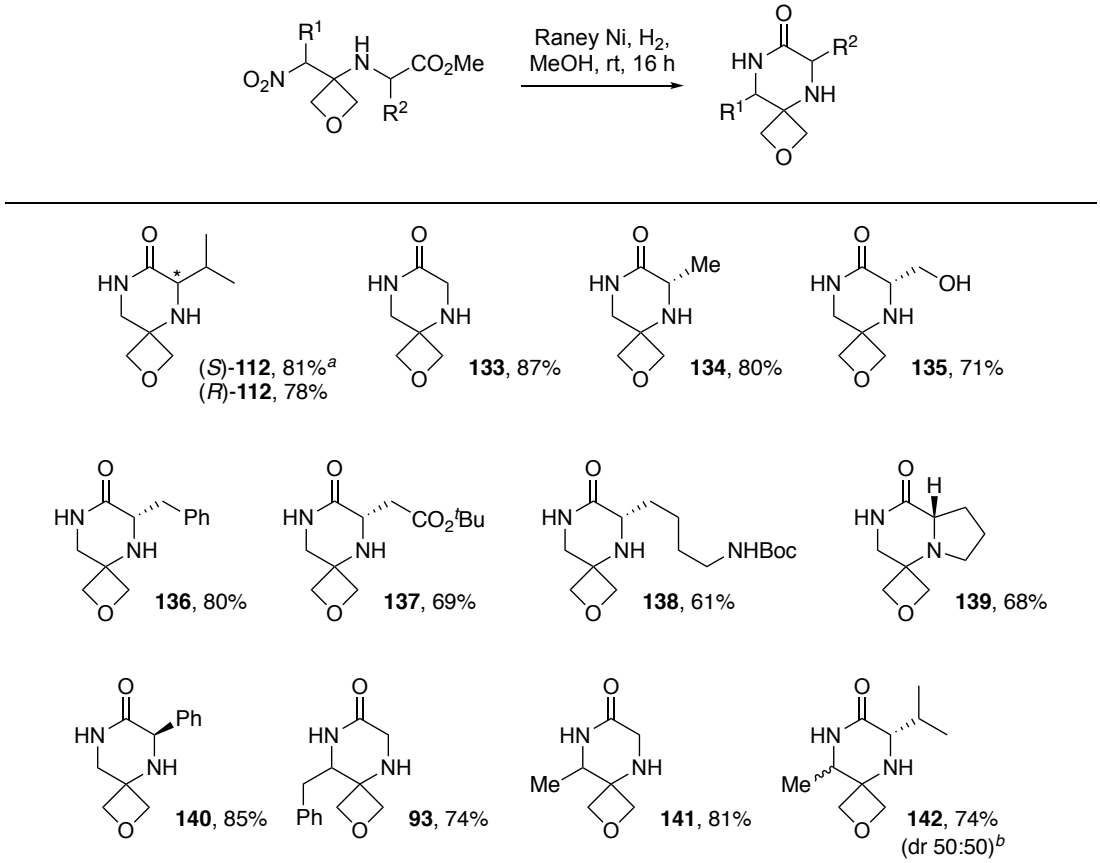

Scheme 2.8 Synthesis of oxetane containing spirocycles. [a] >95% ee as determined by 700 MHz ^{1}H-NMR analysis in the presence of Pirkle's reagent (see Section 6.4). [b] Obtained as a 50:50 mixture of diastereoisomers determined by ^{1}H-NMR analysis (see Section 6.7).

2.3.4 Synthesis of Azetidine-Containing Spirocycles

Having successfully developed conditions for the reduction-cyclisation chemistry and synthesised a library of novel oxetane-containing DKP analogues, we were interested to know if the scope of the chemistry could be expanded to prepare novel spirocycles containing other four-membered rings such as azetidines or cyclobutanes.

We began by investigating whether azetidine-modified DKP precursors could be synthesised. We proposed that azetidine-containing nitroalkene **144** could be prepared using commercially available *N*-Boc-azetidin-3-one **143** and nitromethane using the same conditions as for the oxetane chemistry. Starting from **143**, Henry reaction with nitromethane followed by elimination with methanesulfonyl chloride generated

nitroalkene **144** *in situ*. In this case, nitromethane was used as a solvent in the nitro-aldol step as *N*-Boc-azetidin-3-one **143** is a solid. Following this, conjugate addition of glycine and *L*-valine methyl ester gave the desired azetidine-modified DKP precursors **145** and **146** (Scheme 2.9). To our knowledge, these are the first examples of the conjugate addition of amine nucleophiles to azetidine-substituted nitroalkenes.

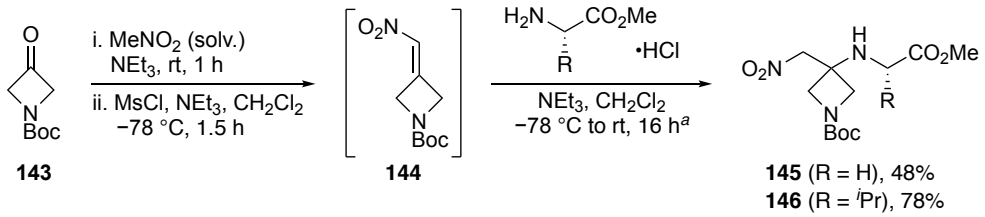

Scheme 2.9 Synthesis of azetidine-modified DKP precursors. [a] Method: $MeNO_2$ (1.0 M), *N*-Boc-azetidin-3-one (1.0 equiv), NEt_3 (0.2 equiv); NEt_3 (2.0 equiv), MsCl (1.0 equiv); amino methyl ester hydrochloride (2.0 equiv), NEt_3 (2.0 equiv).

With azetidine-modified DKP precursors in hand, the reduction-cyclisation to azetidine-containing DKP analogues was attempted. When **145** and **146** were treated with Raney Ni under an atmosphere of hydrogen the corresponding DKP analogues **147** and **149** were produced in good yields (Scheme 2.10).

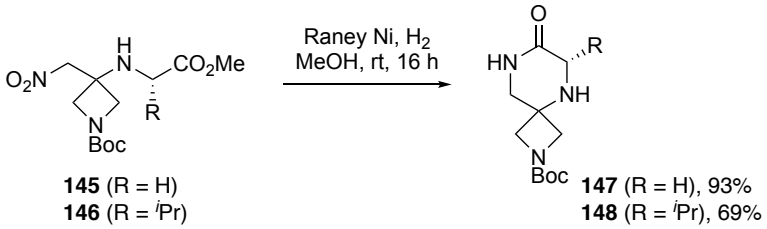

Scheme 2.10 Synthesis of azetidine-containing spirocycles.

Following the successful synthesis of azetidine-containing DKP analogues, we turned our attention to whether the synthesis of cyclobutane-containing analogues was possible. Again, we proposed that cyclobutane-containing nitroalkene **150** could be prepared from cyclobutanone **149**. Addition of an α-amino methyl ester would then provide the desired cyclobutane-modified DKP precursor. Unfortunately, attempts to access the cyclobutane precursor **141** using our standard reaction conditions were unsuccessful (Scheme 2.11).

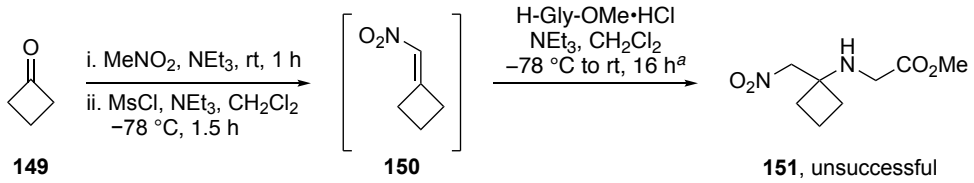

Scheme 2.11 Attempted synthesis of cyclobutane-modified DKP precursor **151**. [a] Method: $MeNO_2$ (1.4 equiv), cyclobutane (1.0 equiv), NEt_3 (0.2 equiv); NEt_3 (2.0 equiv), MsCl (1.0 equiv); H-Gly-OMe·HCl (2.0 equiv), NEt_3 (2.0 equiv).

The reaction was analysed in more detail to determine why the synthesis had been unsuccessful. ^{1}H-NMR analysis of the initial nitro-aldol reaction between cyclobutanone **149** and nitromethane showed that no reaction had taken place (Scheme 2.12).

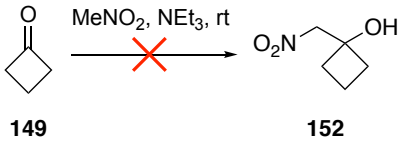

Scheme 2.12 Attempted nitro-aldol reaction between cyclobutanone **149** and nitromethane.

A literature search for nitro-aldol reactions involving cyclobutanone **149** gave limited results but suggested that a stronger base than triethylamine may be required for this reaction to proceed. For example, Stoermer and co-workers have previously prepared **152** in 45% yield from cyclobutanone **149** and nitromethane using sodium ethoxide as the base.[78] In addition to this, Jørgensen and co-workers have prepared trisubstituted-nitroalkene **155** from cyclobutanone **149** and nitroethane using Verkade's base **153** (conjugate acid, pK_a [MeCN] = 33.63)[79] and magnesium sulfate in the nitro-aldol step (Scheme 2.13).[80] At this stage, further attempts to prepare cyclobutane-containing DKP precursors were abandoned as any synthetic route appeared difficult and low yielding.

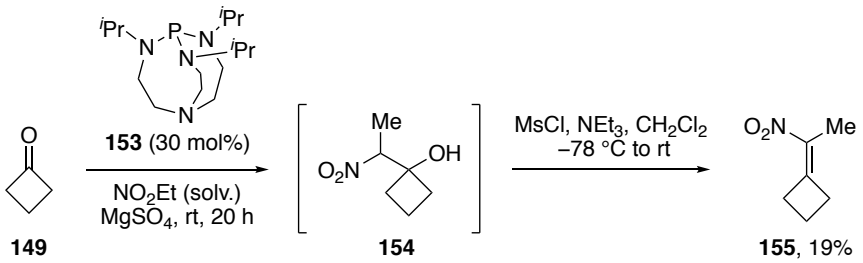

Scheme 2.13 Jørgensen's synthesis of nitroalkene **155** using Verkade's base **153**.[80]

2.3.5 X-Ray Crystal Structures of Oxetane-Containing Spirocycles

Crystals of (*S*)-**112** and **93** were grown and their structures confirmed by X-ray crystallography (Figure 2.5).† In the solid-state, both oxetane-containing spirocycles adopt an envelope-type structure with the spiroatom projecting out of the ring and the neighbouring nitrogen sp^3-hybridised. Unfortunately, crystal structures of the parent 2,5-DKP systems were not available for direct comparisons between the conformations. However, it is known that 2,5-DKPs typically adopt planar or puckered boat conformations in the solid-state (Figure 2.5).[53]

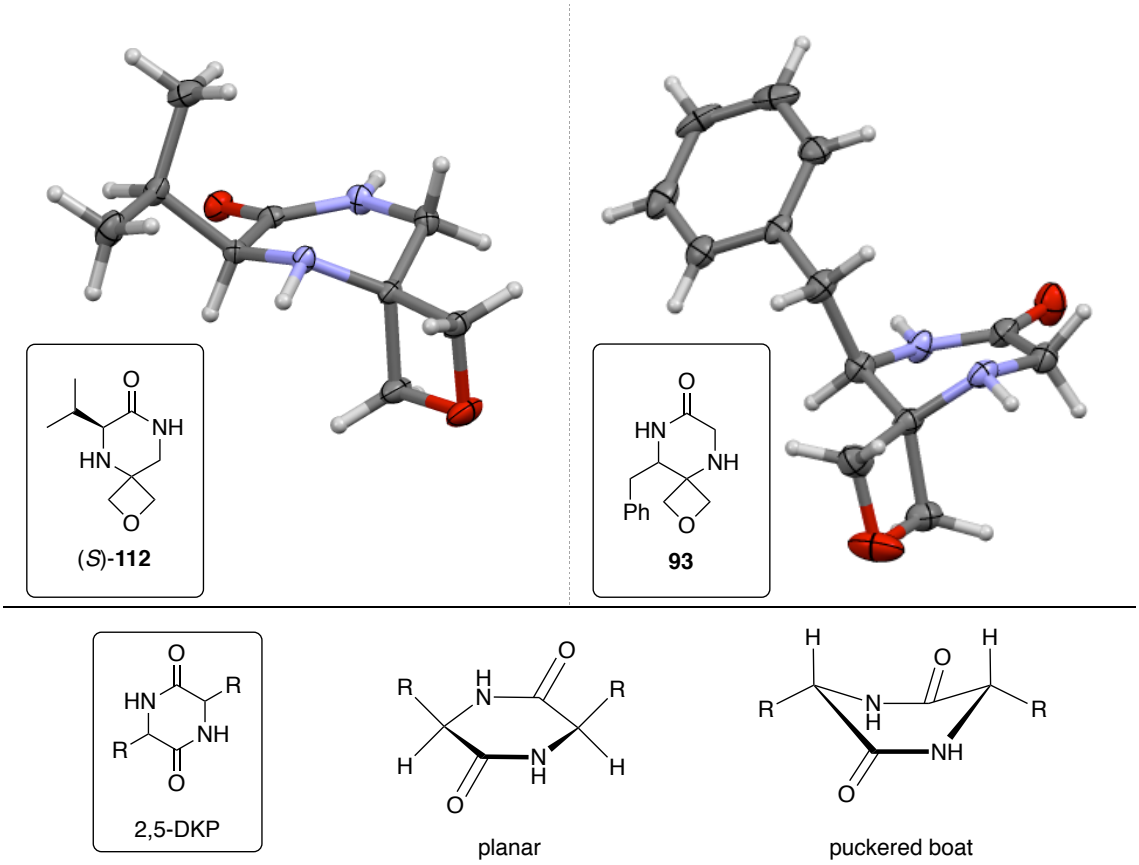

Figure 2.5 X-ray crystal structures of oxetane-containing spirocycles (*S*)-**112** and **93** with thermal ellipsoids drawn at 50% probability level and typical confirmations of 2,5-DKPs.[53]

† Crystals of **93** were grown by Dr Nicola Powell.

2.3.6 Further Modifications of Oxetane-Containing Spirocycles

With a simple and efficient route to oxetane- and azetidine-containing spirocycles developed, we next explored the synthetic value of these novel spirocyclic scaffolds by investigating what additional modifications could be made to them.

Our initial investigations focused on whether selective alkylation of the amine and amide nitrogens was possible. The differences in the nucleophilicity and basicity of these nitrogens should allow us to selectively alkylate one centre over the other. Selective amine benzylation was achieved when oxetane-analogue **134** was treated with benzyl bromide in the presence of sodium iodide in acetonitrile at reflux, providing benzyl amine **156** in good yield (Scheme 2.14). Following this, selective amide benzylation of **134** was realised. Deprotonation of the amide with sodium hydride in DMF followed by addition of benzyl bromide gave benzyl amide **157** in good yield (Scheme 2.14).

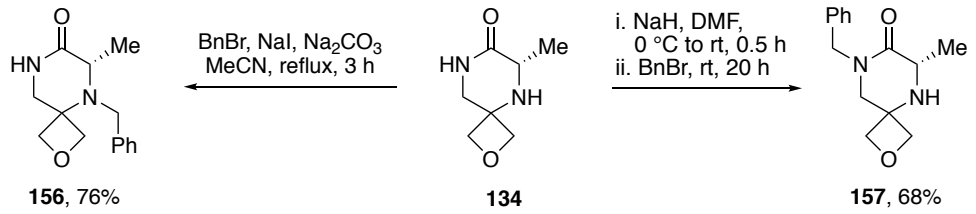

Scheme 2.14 Selective benzylation of the amine and amide nitrogens in spirocycle **134**.

Next, we turned our attention to the reduction of the amide carbonyl to furnish the corresponding piperazine framework as substituted piperazines are valuable structural motifs in biologically active compounds.[81] Recently, Bode and co-workers have developed routes to spirocyclic-piperazines using stannyl amine protocol (SnAP) reagents (Scheme 2.15).[82] However, SnAP reagents are expensive and potentially toxic, therefore additional routes to these structures would be of benefit.

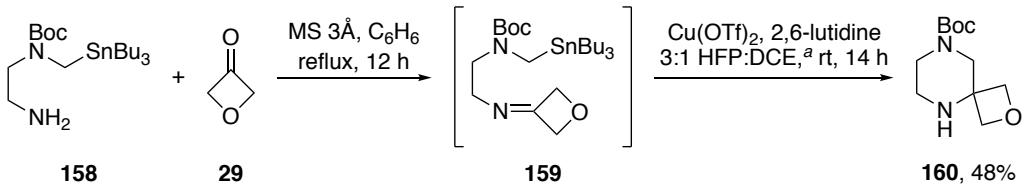

Scheme 2.15 Bode and co-workers' synthesis of spirocycle **160** from oxetan-3-one **29** and SnAP reagent **158**.[82] [a] HFP = hexafluoroisopropanol

A literature search for the reduction of DKPs to piperazines indicated that lithium aluminium hydride was the most common reagent for this transformation. With this

knowledge in hand, we attempted the reduction of oxetane-containing DKP analogues (*S*)-**112** and **134** to the corresponding piperazine **161** and **162**, respectively (Scheme 2.16). Unfortunately, when lithium aluminium hydride was used for the reduction significant opening of the oxetane ring was observed in addition to reduction of the amide carbonyl. This observation was confirmed by ^{1}H-NMR and ESI-MS (**163**, *m/z* = 173 $[M+H]^+$; **164**, *m/z* = 145 $[M+H]^+$) analysis of the crude reaction mixtures. Attempts using alternative reducing agents, such as borane tetrahydrofuran complex, also resulted in opening of the oxetane ring.

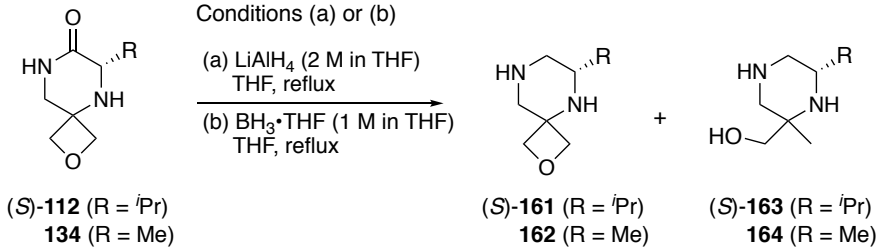

Scheme 2.16 Reduction of oxetane-containing DKP analogues with $LiAlH_4$ or $BH_3 \cdot THF$.

As direct reduction of the amide carbonyl to the corresponding piperazine appeared problematic we explored alternative routes. We decided to investigate a two-step sequence that involved converting the amide to the corresponding thioamide which could then be reduced under milder conditions to give the desired piperazine. This route therefore might prevent opening of the oxetane ring and would also provide novel sprirocyclic-thioamides that could also be of interest to medicinal chemistry.

Using Lawesson's reagent, we were first able to convert the amide of **156** to the corresponding thioamide **165** which was isolated in good yield. Following this, reductive desulfurisation of thioamide **165** using Raney Ni gave piperazine **166** in good yield with the oxetane ring still intact (Scheme 2.17).

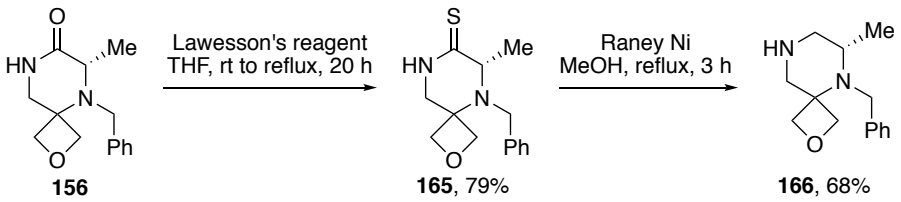

Scheme 2.17 Synthesis of piperazine **166** *via* synthesis and reduction of thioamide **165**.

2.4 Conclusions

In conclusion, this chapter describes the development of a simple and efficient synthesis of novel oxetane- and azetidine-containing spirocycles related to the 2,5-diketopiperazine framework. Conjugate addition of α-amino methyl esters to nitroalkenes prepared from oxetan-3-one or *N*-Boc-azetidin-3-one provides the spirocyclic precursors. Subsequent reduction of the nitro group with Raney Ni under an atmosphere of hydrogen gives, after spontaneous cyclisation, the spirocycles in good overall yield (Scheme 2.18).

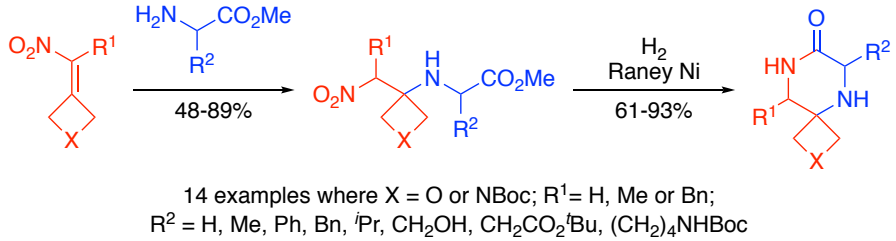

Scheme 2.18 Synthesis of oxetane- and azetidine-containing spirocycles.

Further manipulations of compound **134** have demonstrated the utility of these novel scaffolds. Selective alkylation of the amide and amine nitrogens has been shown along with reduction of the amide carbonyl to the corresponding piperazine (Scheme 2.19). Thus, these building blocks may have potential for library generation in medicinal chemistry.

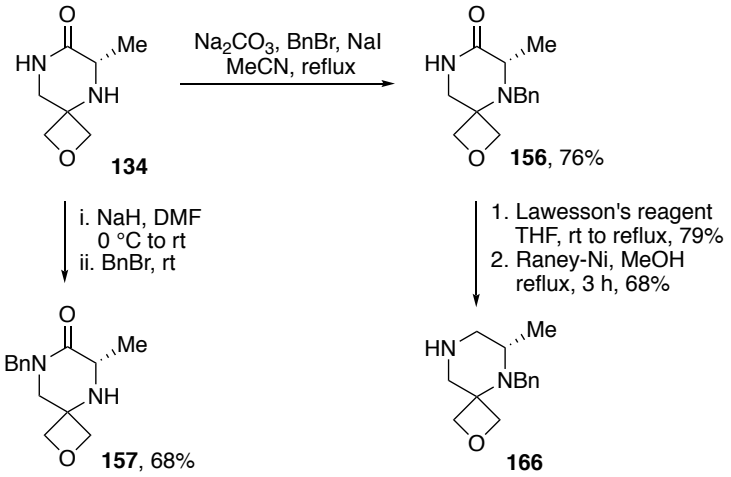

Scheme 2.19 Illustrative manipulations of oxetane spirocycles.

Currently, the known limitations to this work include: (i) acyclic secondary and quaternary amino esters are not compatible with the conjugate addition chemistry; (ii) addition of chiral amino esters to trisubstituted nitroalkenes exerts little stereochemical

bias providing the addition product as a mixture of diastereoisomers; (iii) the approach is not readily extendable to the synthesis of cyclobutane-containing spirocycles as there is no reaction between nitromethane and cyclobutanone using our standard reaction conditions.

The work discussed in this chapter was published in Synlett in 2016.[83]

Chapter 3: Solid-Phase Synthesis of Oxetane-Modified Peptides

3.1 Project Aims

To date, oxetane-modified peptides (OMPs) have been prepared using solution-based methods.[1,46,47] However, in order to study the impact of oxetane-modification on the properties and structures of larger peptides of biological interest, more practical and general methods for the synthesis of OMPs were required. Solid-phase peptide synthesis (SPPS) seemed an ideal route to OMPs as SPPS is largely automated and the products can be readily purified.[84]

Thus, we set ourselves the goal of developing general methodology to introduce oxetane-modification into larger peptides using SPPS techniques. This work was done in collaboration with Dr Andrew Jamieson of the University of Leicester, and since 2016, the University of Glasgow.

3.2 Introduction

3.2.1 Solid-Phase Peptide Synthesis

The preparation of peptides using solid support techniques was first reported by Merrifield in 1963.[85] This work revolutionised peptide synthesis and earned Merrifield the Nobel Prize for Chemistry in 1986.[86] Since then, SPPS has become the standard technique for the preparation of peptides.

The main principle of SPPS involves the stepwise coupling of the *C*-terminal carboxylic acid of an amino acid with the *N*-terminal amine of a growing peptide chain covalently bound to an insoluble polymer support, also referred to as the resin. After each coupling or deprotection step, the unreacted reagents and by-products can be easily removed by filtration leaving behind the resin bound peptide chain. Once the desired peptide sequence has been prepared, the peptide is cleaved from the resin and purified typically by reverse-phase HPLC (Scheme 3.1).[2] A major advantage of SPPS is that peptides of various length and complexity can be rapidly prepared, without the need to perform time-consuming isolation and purification procedures of the intermediates, as would be necessary for solution-phase synthesis.[87]

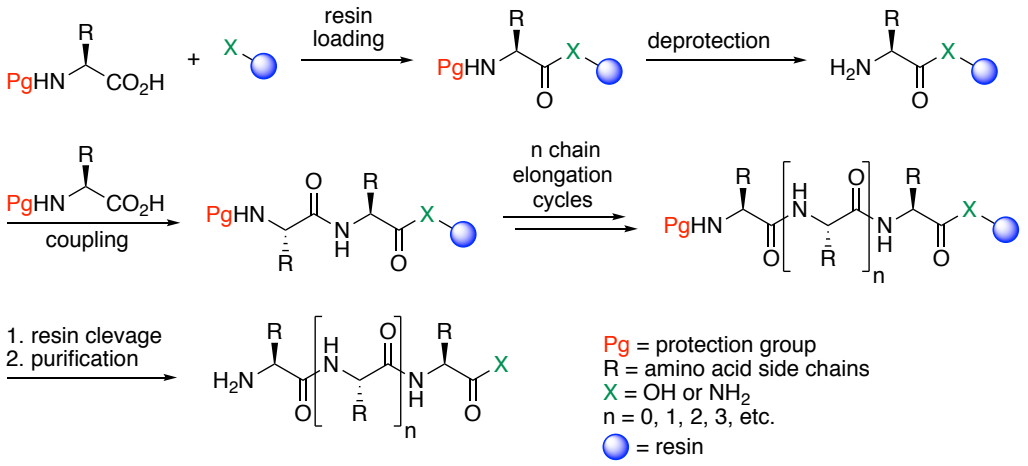

Scheme 3.1 Generalised depiction of solid-phase peptide synthesis.

Resins used in SPPS consist of polymeric beads functionalised with reactive linker groups, such as an amine or alcohol, which can be used to covalently attach the *C*-terminus of the peptide (Figure 3.1). The linker group also dictates the functionality of the *C*-terminus of the peptide once it is cleaved from the resin. Conditions required for cleavage of the peptide from the resin depend on the nature of the resin used.[87]

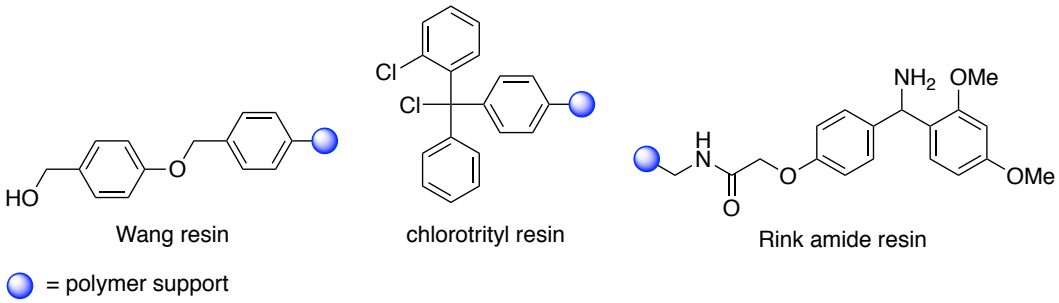

Figure 3.1 Examples of resins used for SPPS.

High yields are required in each coupling step to produce the peptide sequence in good overall yield and to minimise the formation of difficult to separate peptides with one or more deleted residues. Typically, this is achieved by using a large excess of the incoming *N*-terminal protected amino acid along with highly efficient coupling reagents that have been optimised to minimise racemisation and other side reactions.[87] There are many different examples of coupling reagents that are widely used in SPPS. Uronium-based coupling reagents, such as HATU, HBTU and HCTU, are particularly suited for SPPS, as they are exceptionally stable in solutions of DMF (Figure 3.2).[88]

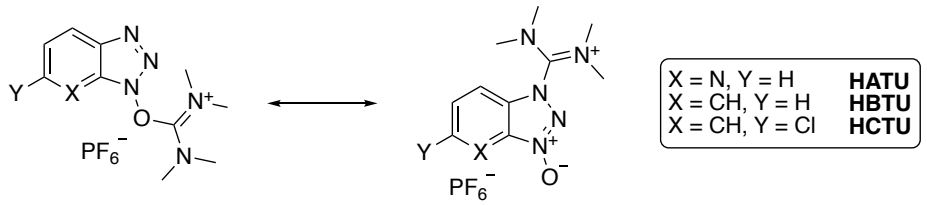

Figure 3.2 Uronium-based peptide coupling reagents used in SPPS.

As with solution-phase synthesis, SPPS requires protection of amino acid side-chains that contain potentially reactive functional groups to avoid unwanted reactions during the synthesis. The protecting groups used must be stable to the conditions required for the removal of the *N*-terminal protecting group. A common protecting group strategy used in SPPS is the Fmoc/^{t}Bu approach. The *N*-terminal Fmoc protecting group is removed using mild conditions, typically 20-50% piperidine in DMF, which does not disturb the acid labile linker or side-chain protecting groups. A major advantage with the Fmoc strategy is that the fulvene-piperidine group **167** generated during the deprotection is highly UV active, allowing the progress of the reaction to be monitored by UV spectroscopy (Scheme 3.2). On completion of the peptide sequence, the Boc/^{t}Bu side-chain protecting groups are removed concomitantly with cleavage of the peptide from the resin using high concentrations of TFA in the presence of cation scavengers.[89]

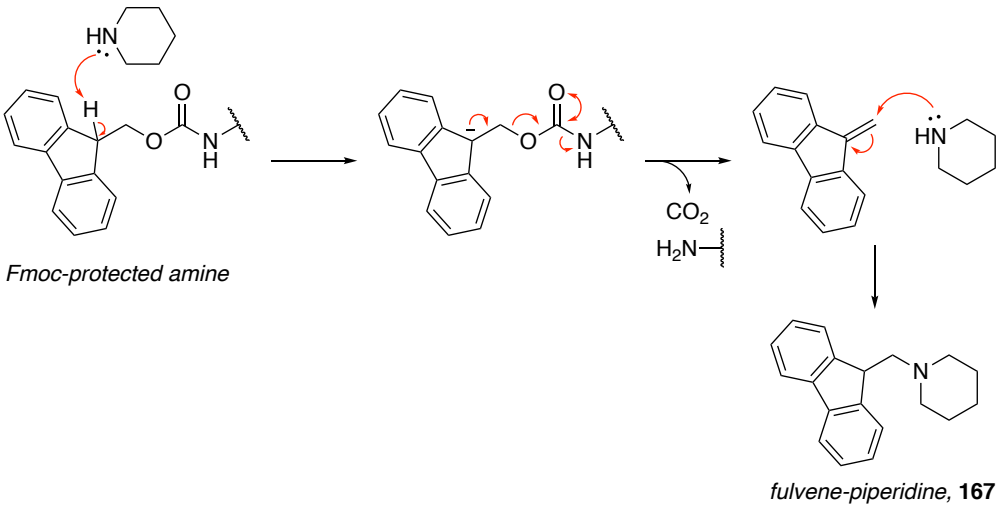

Scheme 3.2 Mechanism of Fmoc deprotection with piperidine.

Recently, microwave-assisted peptide synthesis has become a popular tool for the synthesis of both routine and difficult peptide sequences. Microwave energy allows the majority of amino acid couplings to be completed within 5 min and for Fmoc deprotection steps to be complete within 3 min. This significantly reduces the overall synthesis time

of the peptides produced. In addition, microwave-assisted peptide synthesis generally gives higher crude yields and purities of the peptides produced.[90]

3.2.2 Solid-Phase Synthesis of Peptidomimetics

There are numerous examples of solid-phase peptide synthesis (SPPS) strategies that have been used to prepare analogues of biologically or structurally interesting peptides that contain a peptidomimetic modification.[91–95] Some relevant examples are summarised below.

Lubell and co-workers reported a general protocol for the synthesis of azapeptides on the solid-phase by introducing the aza-modified residue as an aza-containing dipeptide.[13] Aza-containing dipeptides **171** were first prepared in solution by reaction of *N*-Boc-*N*'-alkyl hydrazines **169** with isocyanates **168** derived from *α*-amino acids (Scheme 3.3-A). These building blocks were then incorporated on the solid-phase using a Boc/Bn protection strategy on an oxime resin (Scheme 3.3-B). This approach was used to prepare aza-modified analogues, up to 11 residues in length, of the *C*-terminal peptide fragment of the human calcitonin gene-related peptide (hCGRP).[13]

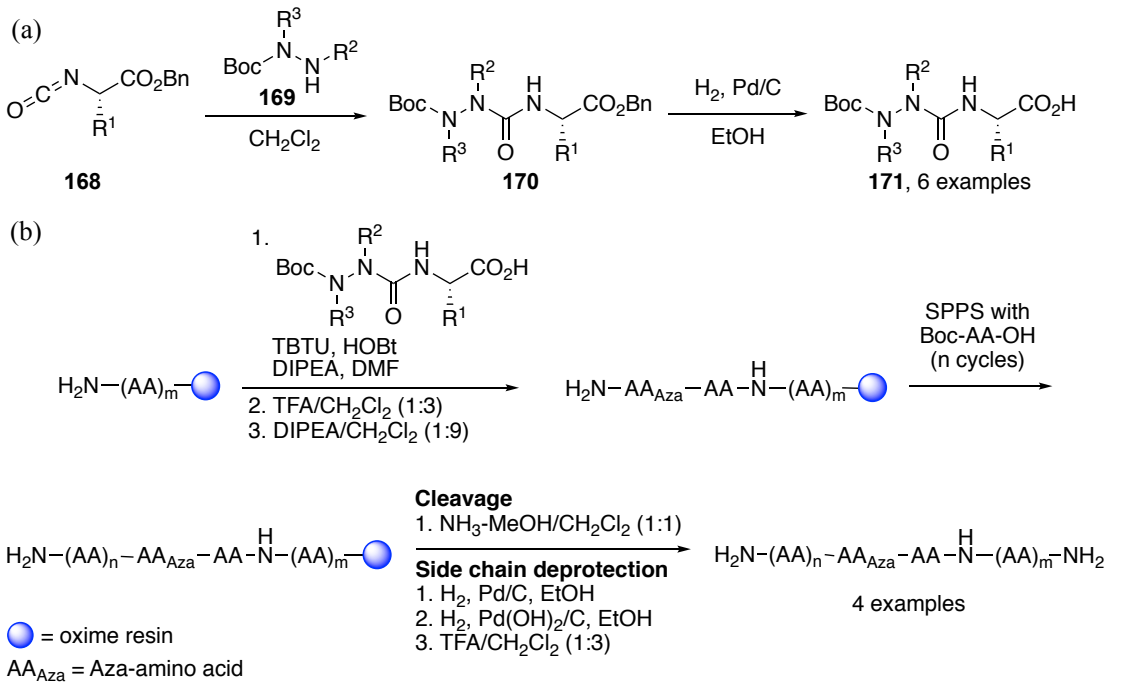

Scheme 3.3 Solid-phase synthesis of azapeptides. (a) Synthesis of aza-dipeptides. (b) Application of aza-dipeptides in solid-phase peptide synthesis.[13]

Cai and co-workers, reported an efficient synthesis of oligomers of γ-substituted-*N*-acylated-*N*-aminoethyl amino acids (γ-AApeptides) using SPPS techniques.[96] The method makes use of common *N*-alloc γ-AApeptide building blocks **172** that are prepared in solution using the chemistry described in Route 1 or Route 2 (Scheme 3.4-a). These building blocks are then integrated onto the solid-phase. The key step of this work involves the removal of the alloc-protecting group on the solid phase, using $Pd(PPh_3)_4$ and borane dimethylamine complex, to reveal the secondary amine. Following this, a variety of carboxylic acids and acyl chlorides were used to acylate the backbone nitrogen of the γ-AApeptides (Scheme 3.4-b). This methodology was used to prepare a diverse library of γ-AApeptide sequences and their application as peptidomimetics is currently being explored.[96]

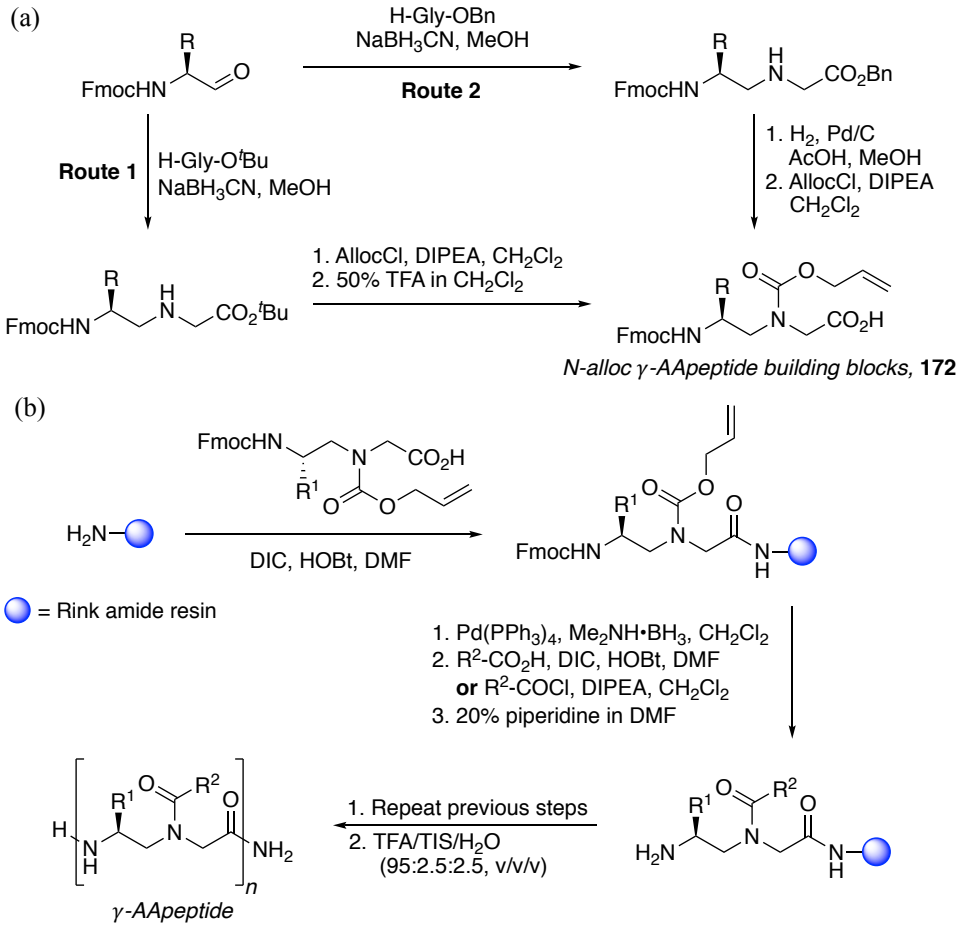

Scheme 3.4 Synthesis of γ-AApeptides. (a) Synthesis of *N*-alloc γ-AApeptide building blocks. (b) Solid-phase synthesis of γ-AApeptide sequences.[96]

3.3 Results and Discussion

3.3.1 SPPS Route to Oxetane-Modified Peptides

Our approach to introduce oxetane-modification into larger peptides by use of SPPS was to prepare oxetane-containing Fmoc-protected dipeptides such as **173** in solution and then integrate them into a growing peptide chain using conventional Fmoc/^{t}Bu SPPS techniques (Scheme 3.5). Initially, we focused our attention on the preparation of Fmoc-protected dipeptide building blocks in which the oxetane residue is based on glycine. Efforts towards Fmoc-protected dipeptide building blocks in which the oxetane residue is based on other amino acid residues is discussed in Chapter 4.

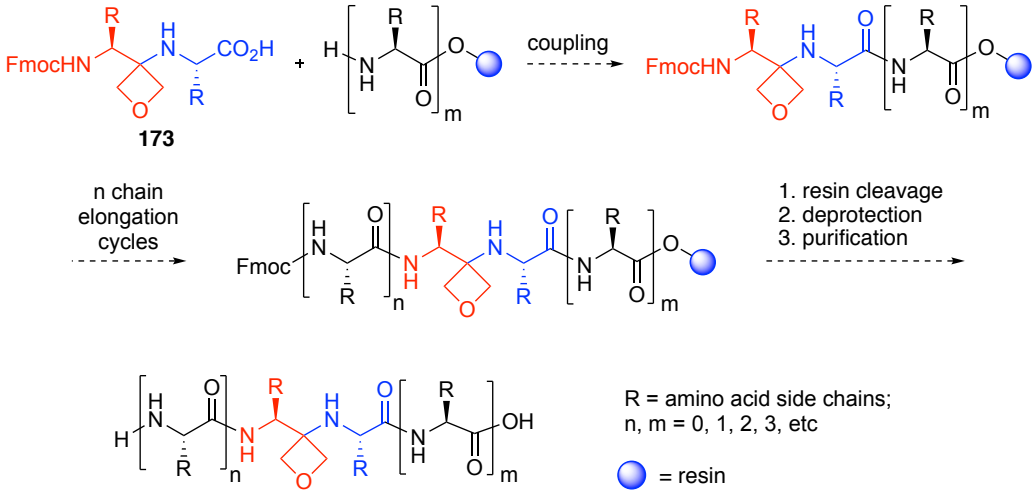

Scheme 3.5 Proposed SPPS route to oxetane-modified peptides.

3.3.2 Initial Synthesis of an Oxetane-Containing Dipeptide Building Block

Our initial route to oxetane-containing dipeptide building block **175** is detailed below (Scheme 3.6). Previously described nitroalkane **34** was prepared by conjugate addition of *L*-phenylalanine benzyl ester (2.0 equiv) to nitroalkene **30** (1.0 equiv).[1] Reduction of the nitro group with Raney Ni in the presence of Fmoc *N*-hydroxysuccinimide ester (FmocOSu, 1.2 equiv) provided the *N*- and *C*-terminal protected dipeptide **174**. This approach builds upon chemistry previously reported by Carreira and co-workers (see Scheme 1.5).[46] Following this, deprotection of the *C*-terminal ester was examined. Hydrogenation of the benzyl ester appeared to proceed to full conversion. However, poor solubility of the product **175** in methanol made separation from the palladium catalyst difficult. In order to isolate the product, the reaction mixture was diluted with EtOAc and

heated to 60 °C. The mixture was then filtered through a plug of Celite® and the eluent concentrated under reduced pressure to give the desired building block **175** in 50% isolated yield.

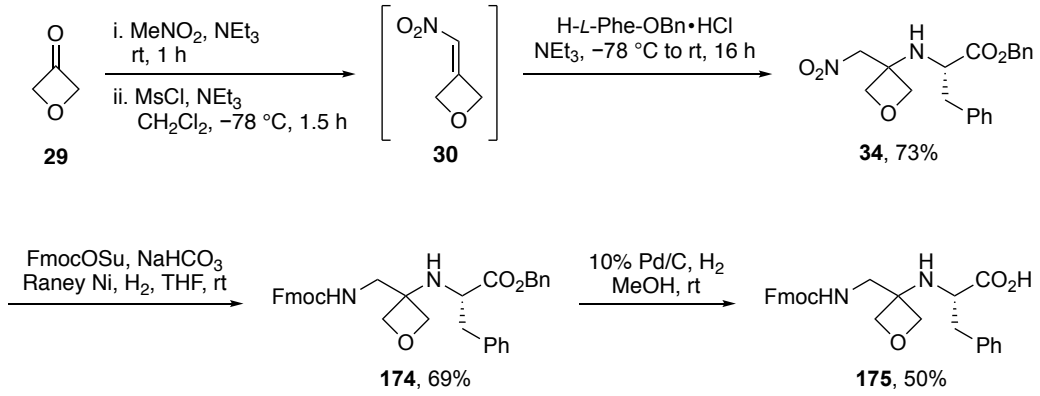

Scheme 3.6 Initial synthesis of Fmoc-G_{Ox}-Phe-OH **175**.

3.3.3 Initial Solid-Phase Synthesis of an Oxetane-Modified Peptide

With an oxetane-containing dipeptide building block in hand, we examined its application in solid-phase peptide synthesis (SPPS). This portion of work was carried out in the laboratories of Dr Andrew Jamieson at the University of Leicester, where the author spent two weeks developing the skills to conduct SPPS.

Using building block **175**, we set out to prepare a simple oxetane-containing tetrapeptide **176** on a CEM microwave peptide synthesiser on a 0.1 mmol scale using Rink amide resin (Scheme 3.7). Rink amide resin was first preloaded with Fmoc-alanine using standard coupling conditions [HCTU, DIPEA, DMF], followed by Fmoc removal [20% piperidine/DMF]. Oxetane-containing building block **175** was then coupled in a similar fashion using HCTU activation. Standard conditions for Fmoc removal [20% piperidine/DMF] and coupling [Fmoc-Ala-OH, HCTU, DIPEA, DMF] gave the resin-bound tetrapeptide. Finally, *N*-terminal acetylation [Ac_2O, DIPEA, DMF] and resin cleavage [TFA/TIS/H_2O, 95:2.5:2.5, v/v/v] gave crude tetrapeptide **176**. After reverse-phase HPLC purification, oxetane-modified tetrapeptide **176** was isolated in high purity as confirmed by HPLC, HRMS and ^{1}H-NMR. For full details, see Section 6.6.

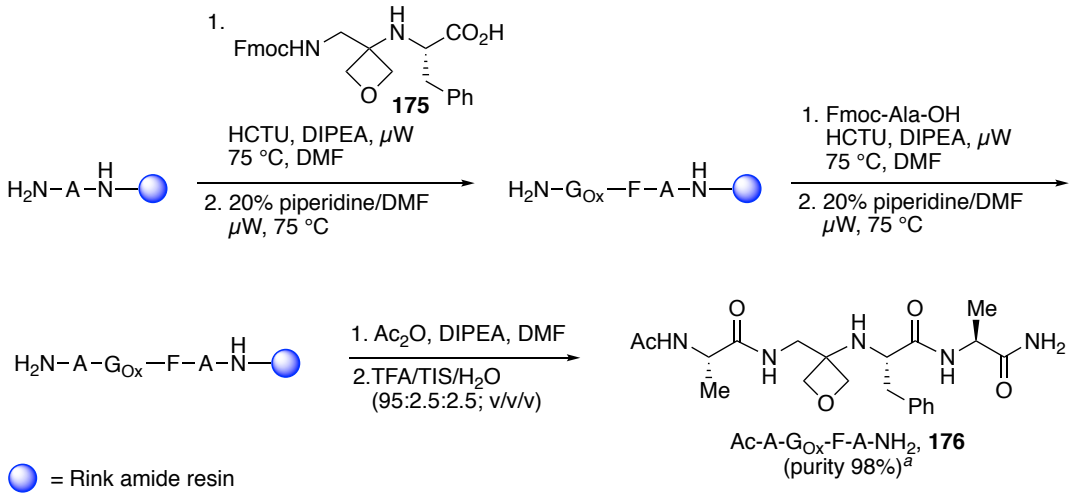

Scheme 3.7 Solid-phase synthesis of **176**. [a] By reverse-phase HPLC (at 214 nm). [b] G_{Ox} = oxetane-modified glycine.

LC-MS analysis of the crude material also showed the presence of a small amount of impurity with a molecular mass of 18 Da more than the tetrapeptide. This observation suggests that opening of the oxetane ring with water to give diol **177** is happening during the synthesis, possibly when the peptide is cleaved from the resin using high concentrations of TFA in the presence of water (Scheme 3.8). Unfortunately, we were not able to isolate this material to confirm whether opening of the oxetane ring had occurred.

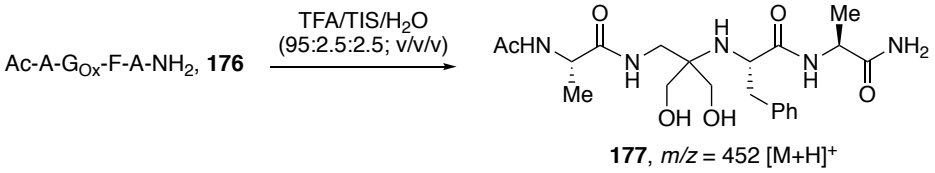

Scheme 3.8 Possible ring-opening of **176** to give diol **177**.

3.3.4 Synthesis of Oxetane-Containing Dipeptide Building Blocks

Encouraged by these preliminary results, we set out to optimise the synthesis of oxetane-containing dipeptide building blocks and further explore their use in SPPS.

As previously discussed, hydrogenolysis of benzyl ester **174** appeared to proceed to full conversion but poor solubility of the corresponding carboxylic acid **175** made isolation difficult. Following this observation, we investigated alternative solvents in the hydrogenolysis reaction. A small solvent screen gave no improvement in the isolated yield of acid **175** (Table 3.1, entries 1-4). When EtOAc or THF was used the reaction

appeared to proceed quantitatively by TLC and ESI-MS analysis, however, problems with solubility made isolation of **175** difficult. When DMF was used as reaction solvent, the product **175** was soluble. However, an EtOAc/brine work-up was required to remove the DMF which resulted in a poor isolated yield of **175**.

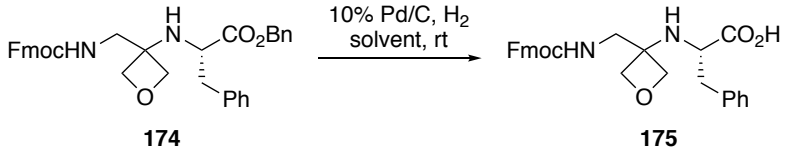

174 **175**

Entry	Solvent	Yield (%)	Comments
1	MeOH	50[a]	Product insoluble in reaction solvent
2	EtOAc	-	Product insoluble in reaction solvent
3	THF	-	Product insoluble in reaction solvent
4	DMF	42[b]	

Table 3.1 Solvent screen for the hydrogenation of **174**. [a] Isolated yield after hot filtration with EtOAc through Celite®. [b] Isolated yield after DMF removed with an EtOAc and brine work-up.

As poor solubility of carboxylic acid **175** was making isolation difficult, we were interested to see if building blocks containing alternative amino acid residues could be prepared using this route. We began by preparing dipeptide building blocks containing a glycine and valine residue. Using the same route as before, benzyl protected building blocks **179** and **180** were readily prepared from the corresponding α-amino benzyl esters (Scheme 3.9).

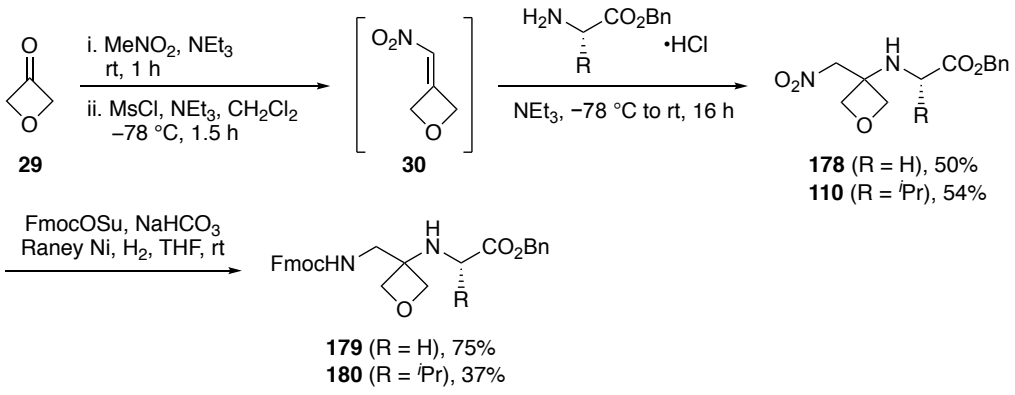

29 **30**

178 (R = H), 50%
110 (R = ^{i}Pr), 54%

179 (R = H), 75%
180 (R = ^{i}Pr), 37%

Scheme 3.9 Synthesis of benzyl ester building blocks **179** and **180**.

With the building blocks in hand, removal of the benzyl group was explored (Scheme 3.10). When **179** and **180** were subjected to catalytic hydrogenation conditions complete consumption of the starting material was observed. However, no desired product was isolated after work-up. ^{1}H-NMR analysis of the crude material showed the presence of 9-methyl-9*H*-fluorene **183** and the corresponding unprotected oxetane-containing dipeptide **184** and **185**. This observation indicated that the Fmoc group of the building blocks was susceptible to cleavage under the hydrogenolysis conditions. Similar observations for the cleavage of Fmoc groups under hydrogenation conditions have previously been reported in the literature.[97] We propose that the success observed for **175** was a result of its poor solubility. During hydrogenolysis, the product **175** rapidly precipitates preventing further Fmoc cleavage. At this point, routes involving benzyl esters for the synthesis of oxetane-containing dipeptide building blocks were abandoned.

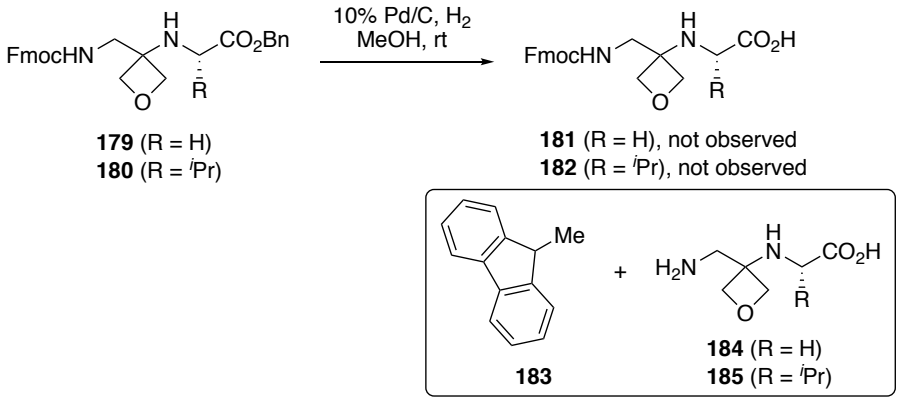

Scheme 3.10 *N*-Fmoc cleavage during hydrogenolysis of benzyl esters **179** and **180**.

We next explored other *C*-terminal protecting groups for the synthesis of oxetane-containing building blocks. We began with methyl esters which are typically removed by hydrolysis with LiOH or NaOH.[98] Starting from previously prepared nitro alkane **116**, *N*-Fmoc protected methyl ester **186** was synthesised in excellent yield (Scheme 3.11).

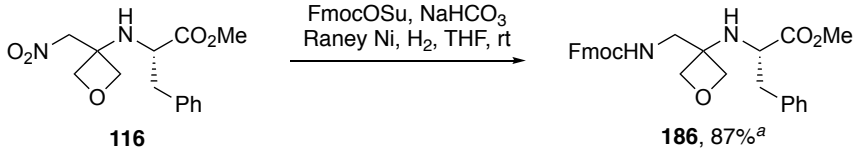

116 **186**, 87%[a]

Scheme 3.11 Synthesis of oxetane-containing dipeptide building block **186**.

With methyl ester **186** in hand, conditions for the hydrolysis to carboxylic acid **187** were explored (Table 3.2, entries 1-4). Using LiOH-THF/H_2O resulted in unwanted Fmoc

cleavage and no desired product was isolated after work-up. Other conditions that reported to leave Fmoc groups intact, such as Me_3SnOH[99] and $NaOH/CaCl_2$,[100] also caused Fmoc cleavage which results in poor yields. LiI, which has been used as a mild reagent for the cleavage of methyl esters,[101] resulted in the formation of unknown products and poor mass recovery. As hydrolysis conditions resulted in Fmoc cleavage, routes involving methyl esters for the synthesis of oxetane-containing dipeptide building blocks were abandoned.

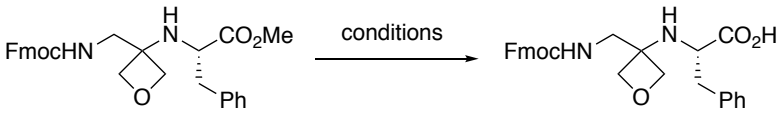

186 **175**

Entry	Conditions	Yield (%)	Comments
1	LiOH-THF/H_2O	0	Fmoc cleavage observed
2	Me_3SnOH, DCE, 80 °C	40[a]	Fmoc cleavage observed
3	1 M NaOH, 0.8 M $CaCl_2$, ^{i}PrOH	20[a]	Fmoc cleavage observed
4	LiI, EtOAc, reflux	0	Poor mass recovery, unknown products

Table 3.2 Attempted hydrolysis of methyl ester **186**. [a] Isolated yield after acid-base extraction.

Following the investigation of *C*-terminal benzyl and methyl esters, we next explored the use of acid labile protecting groups. As our strategy involved using amino acid residues containing ^{t}Bu or Boc protected side chains, which are typically removed using high concentrations of TFA,[98] we focused our attention on the use of ester protecting groups that can be removed under mildly acidic conditions. This led us to investigate 2,4-dimethoxybenzyl (2,4-DMB)[102] and 2-phenyl-2-propyl (cumyl) esters[103,104] which are typically hydrolysed using 1-4% TFA in CH_2Cl_2.

The first step in the preparation of dipeptide building blocks containing *C*-terminal acid labile protecting groups required the synthesis of the 2,4-DMB and cumyl esters. Using Steglich esterification conditions, Fmoc-*L*-phenylalanine was protected as 2,4-DMB ester **189** using 2,4-dimethoxybenzyl alcohol **188** (Scheme 3.12-a). Following a modified procedure,[103] cumyl ester **192** was prepared by reaction of Fmoc-Phe-OH with imidate **191**, which was derived from the condensation of 2-phenyl-2-propanol **190** with trichloroacetonitrile (Scheme 3.12-b).

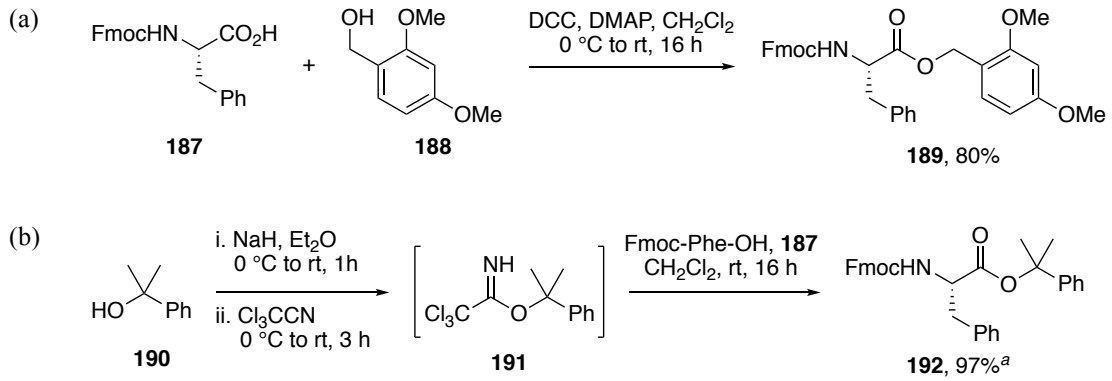

Scheme 3.12 Synthesis of acid-labile ester protecting groups **189** and **192**. [a] Contaminated with 2-phenyl-2-propanol **190** (~19:1 by ^{1}H-NMR).

Next, conjugate addition of 2 equivalents of the amino esters to nitroalkene **30** was explored. The Fmoc groups of **189** and **192** were first removed using diethylamine. Upon completion, the diethylamine was removed under reduced pressure to give the crude amine which was used in the conjugate addition step without further purification. This gave the addition products **193** and **194** in good isolated yields. Following this, nitro reduction and Fmoc protection furnished the desired oxetane-containing dipeptide building blocks **195** and **196** (Scheme 3.13).

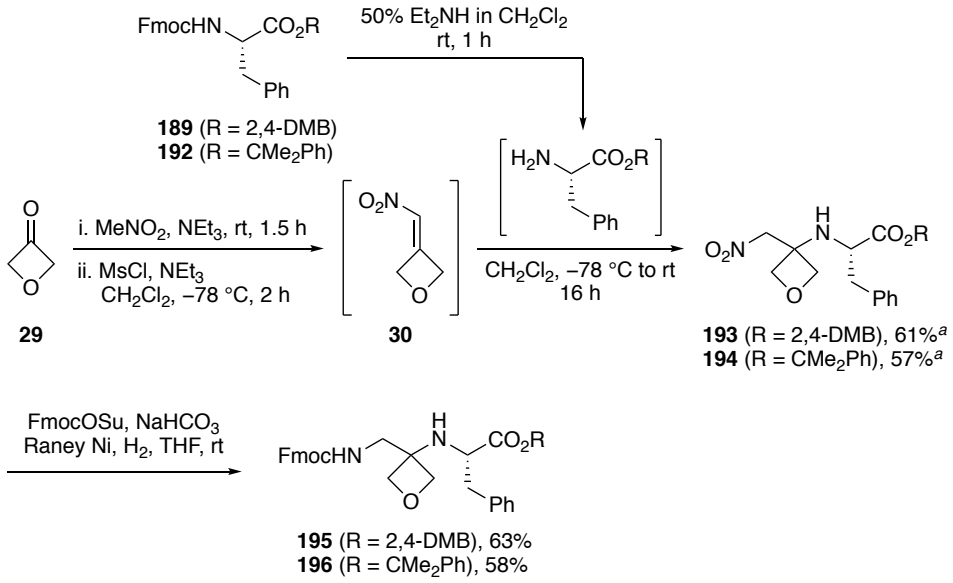

Scheme 3.13 Synthesis of oxetane-containing dipeptide building blocks **195** and **196**. [a] Method: $MeNO_2$ (1.4 equiv), oxetan-3-one (1.0 equiv), NEt_3 (0.2 equiv); NEt_3 (2.0 equiv), MsCl (1.0 equiv); *N*-Fmoc amino ester (2.0 equiv), 50% Et_2NH in CH_2Cl_2 (0.5 M).

With acid-labile protected building blocks **195** and **196** in hand, deprotection to carboxylic acid **175** was investigated (Table 3.3, entries 1-3). Removal of the 2,4-

dimethoxybenzyl group in **195** using 1% TFA in CH_2Cl_2 with anisole as a scavenger gave **175** along with significant amounts of an insoluble by-product that could not be identified. Poor results were also observed when 1% HCl in CH_2Cl_2 was used. Much better outcomes were achieved with the cumyl ester **196**. When **196** was treated with 2% TFA in CH_2Cl_2 quantitative conversion to **175** was observed after 1.5 h, which was isolated in 61% yield after precipitation with Et_2O.

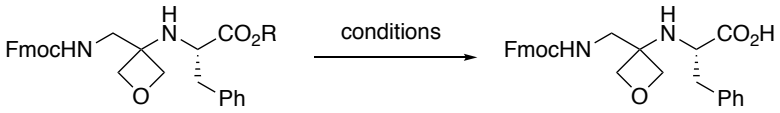

195 (R = 2,4-DMB)
196 (R = CMe_2Ph)

175

Entry	Substrate	Conditions	Yield (%)	Comments
1	**195**	1% TFA in CH_2Cl_2, anisole	n.d.[a]	Unknown products
2	**195**	1% HCl in CH_2Cl_2	0	Unknown products
3	**196**	2% TFA in CH_2Cl_2	61[b]	

Table 3.3 Deprotection of acid-labile esters **195** and **196**. [a] Product isolated with significant amounts of an insoluble impurity. [b] Isolated yield after precipitation with Et_2O.

With cumyl ester identified as an optimal *C*-terminal protecting group in the synthesis of oxetane-containing dipeptide building blocks, we next focused our efforts on preparing a series of building blocks containing other amino acid residues.

Following a modified procedure of Potier,[103] the *C*-terminus of commercially available Fmoc-amino acids, containing a range of protected side chain types, were protected to give the corresponding cumyl esters (Scheme 3.14). Residues containing potentially reactive side chains **198-200** were purchased with their functional groups either ^{t}Bu or Boc protected to prevent reaction of the functional groups with imidate **191** and ready for SPPS. Cumyl esters **192**, **198** and **199** were isolated with traces of 2-phenyl-2-propanol **190**, which was later removed during purification of the conjugate addition products using column chromatography (Scheme 3.16).

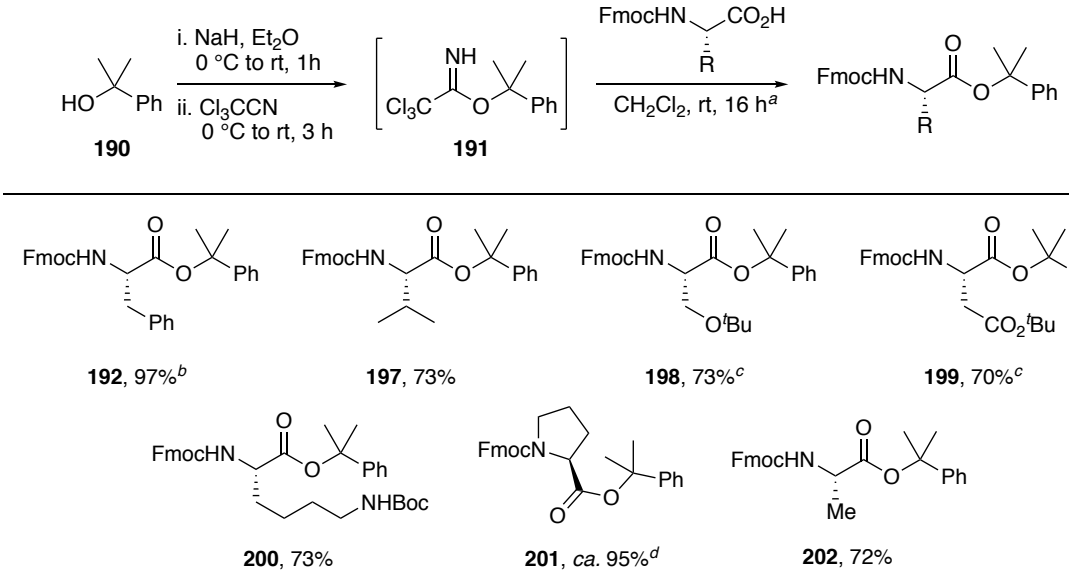

Scheme 3.14 Synthesis of *N*-Fmoc amino cumyl esters. [a] Method: **190** (2.2 equiv), NaH (60% dispersion in mineral oil, 0.5 equiv); Cl_3CCN (2.0 equiv); *N*-Fmoc amino acid (1.0 equiv). [b] Contaminated with 2-phenyl-2-propanol **190** (~19:1 by ^{1}H-NMR). [c] Contaminated with 2-phenyl-2-propanol **190** (~9:1 by ^{1}H-NMR). [d] Isolated as an inseparable mixture with trichloroacetamide and 2-phenyl-2-propanol **190**.

Although cumyl protection of Fmoc-*L*-proline was successful, the desired product **201** co-eluted with significant amounts of trichloroacetamide and 2-phenyl-2-propanol **190**, and attempts to purify the material by chromatography were unsuccessful. It proved more convenient to remove the Fmoc group of the crude material and purify the product using column chromatography to give secondary amine **203** in good overall yield (Scheme 3.15).

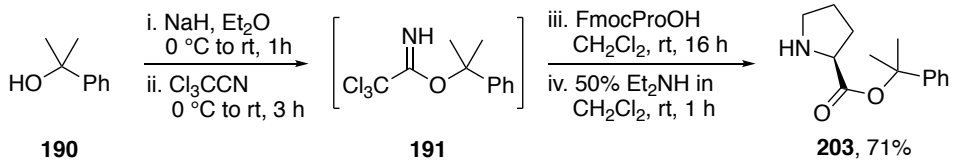

Scheme 3.15 Synthesis of H-Pro-OCumyl **203**.

Following this, the *N*-Fmoc amino cumyl esters were investigated in the conjugate addition step (Scheme 3.16). At this stage, the cumyl esters were considered more synthetically valuable than nitroalkene **30**. Consequently, the cumyl esters were used as the limiting reagent in the addition step along with 2 equivalents of nitroalkene **30**, which was generated *in situ* from oxetan-3-one **29** (2.0 equiv) and nitromethane (2.8 equiv). Using these conditions, removal of the Fmoc group and addition of the resulting crude

amine to nitroalkene **30** gave the addition products in moderate to good yields. Secondary amine **203** was used directly in the conjugate addition, to give proline **208** in good yield.

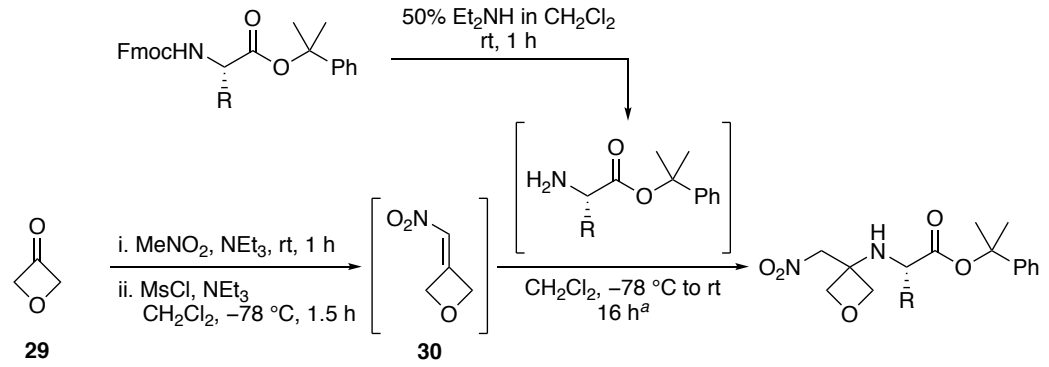

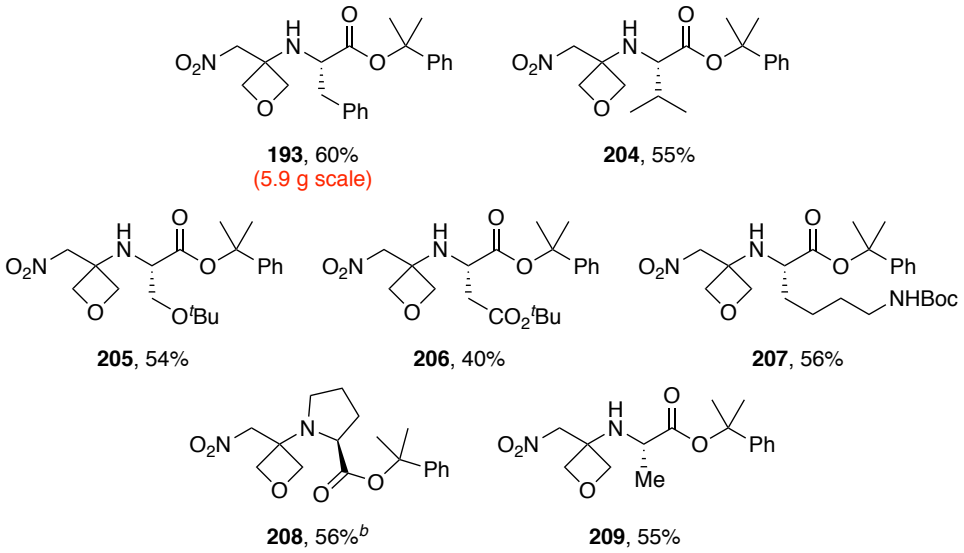

Scheme 3.16 Synthesis of nitro amino cumyl esters. [a] Method: $MeNO_2$ (2.8 equiv), oxetan-3-one (2.0 equiv), NEt_3 (0.4 equiv); NEt_3 (4.0 equiv), MsCl (2.0 equiv); *N*-Fmoc amino cumyl ester (1.0 equiv), 50% Et_2NH in CH_2Cl_2 (0.5 M). [b] Made directly from isolated H-Pro-OCumyl **203**.

The penultimate step in the synthesis required reduction of the nitro group and *in situ* Fmoc protection of the resulting amine. Reduction with Raney Ni under an atmosphere of hydrogen in the presence of FmocOSu generally gave the *N*-Fmoc protected cumyl esters in good yields (Scheme 3.17). Using this route, seven representative dipeptide building blocks with a variety of protected side chains were produced.

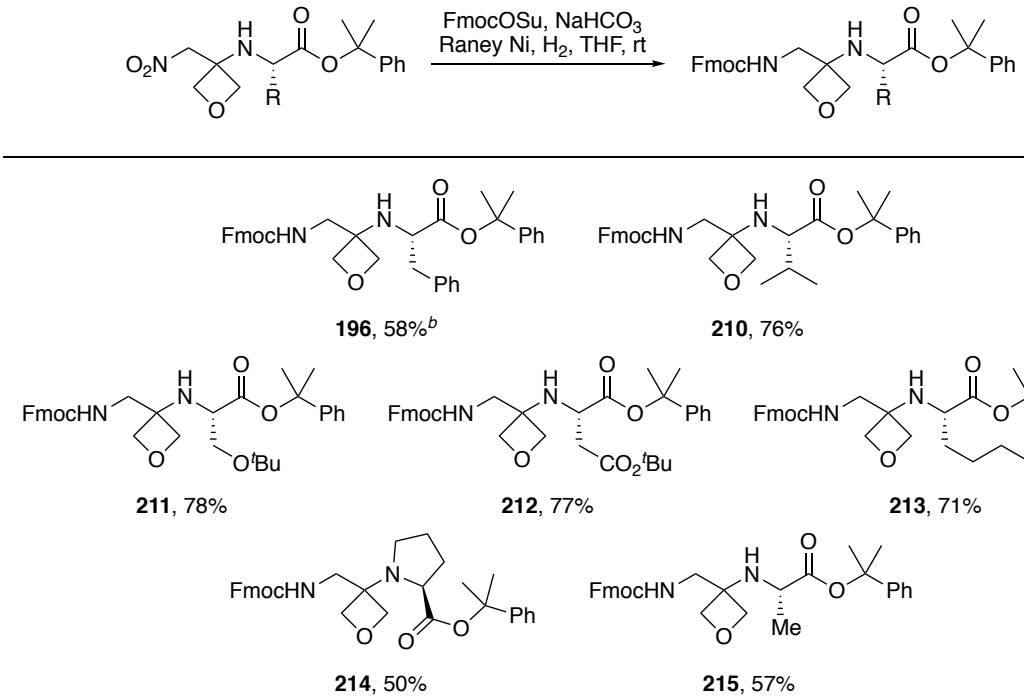

Scheme 3.17 Synthesis of oxetane-containing dipeptide building blocks. [a] Method: Nitroalkane (1.0 equiv), FmocOSu (2.0 equiv), $NaHCO_3$ (4.0 equiv), Raney Ni (slurry in H_2O, 1 mL/mmol), H_2 (balloon). [b] 52% yield on a larger 2.3 g scale.

With a variety of *N*- and *C*-terminal protected dipeptide building blocks in hand, cleavage of the cumyl ester to the carboxylic acid was investigated. The dipeptide building blocks were treated with 2% TFA in CH_2Cl_2 to give the corresponding carboxylic acid (Scheme 3.18). UPLC-MS analysis of the crude reaction mixtures demonstrated full conversion to the carboxylic acids along with a common by-product, assumed to be α-methylstyrene. However, not all attempts to purify the crude products were successful. As previously discussed, phenylalanine analogue **175** was isolated in 61% yield after precipitation with diethyl ether. Valine **182** and ^{t}Bu-serine **216** analogues were isolated in excellent yields, as improved solubility meant that they could be purified using column chromatography. Unfortunately, attempts to purify the aspartic acid **217** and lysine **218** analogues using column chromatography resulted in decomposition.

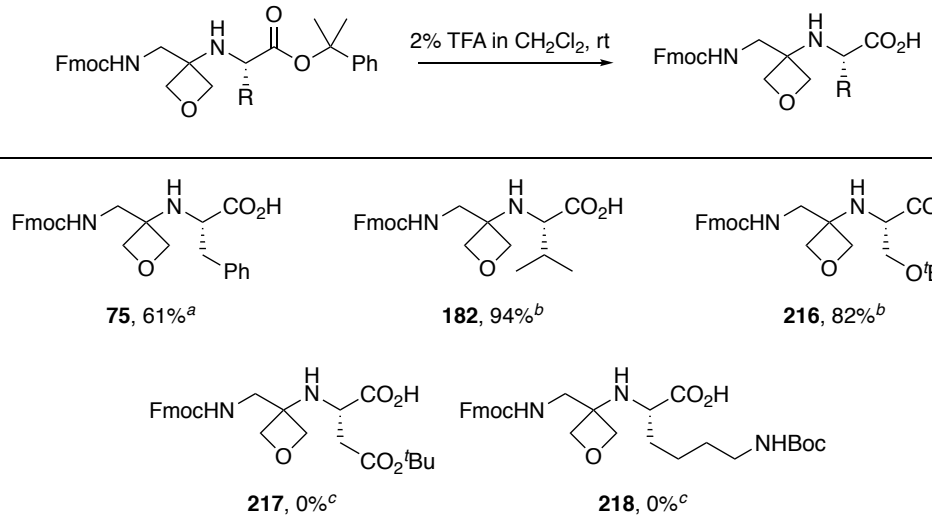

Scheme 3.18 Cumyl ester deprotection scope. [a] Isolated yield after precipitation with Et_2O. [b] Isolated yield after column chromatography. [c] Product decomposed during column chromatography.

Following these observations, it was decided that it was more convenient to store the building blocks as the cumyl esters and, after *C*-terminal deprotection with 2% TFA in CH_2Cl_2, use the crude acids directly on SPPS without purification. Furthermore, the majority of the cumyl ester building blocks were easy to handle crystalline solids.

3.3.5 Solution-Phase Chemistry of Oxetane-Containing Building Blocks

Before examining the use of the dipeptide building-blocks in SPPS, we decided to further study their chemistry in solution. We began by investigating couplings of these oxetane-containing building blocks at the *C*-terminus. Cleavage of the cumyl ester from **210**, using 2% TFA in CH_2Cl_2, followed by coupling of the crude acid with *L*-phenylalanine *tert*-butyl ester with HCTU gave (*S*,*S*)-**219** in excellent yield (Scheme 3.19). Following this, the configurational integrity of the *C*-terminal amino acid residue of the dipeptide building block during the coupling was determined by preparing the corresponding diastereoisomer (*S*,*R*)-**219**. Using *D*-phenylalanine *tert*-butyl ester, the procedure was repeated to give (*S*,*R*)-**219**. The diastereotopic purity of (*S*,*S*)-**219** and (*S*,*R*)-**219** was determined by comparison of the diastereotopic CH_3-Val signals in the ^{1}H-NMR spectra of the crude reaction mixtures. Spectral analysis confirmed that (*S*,*S*)-**219** and (*S*,*R*)-**219** was of dr >95:5 indicating that no detectable epimerisation arose during these couplings. (see Section 6.5).

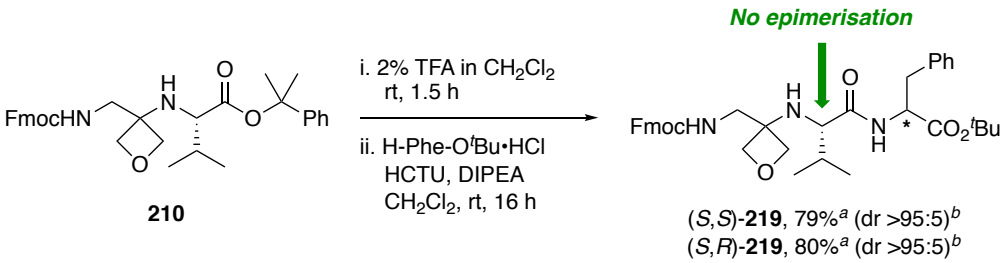

Scheme 3.19 *C*-Terminal couplings of oxetane-containing dipeptides proceed with no detectable epimerisation. [a] Determined by ^{1}H-NMR analysis of the crude reaction mixture (see Section 6.5). [b] Coupling conditions: H-Phe-O^{t}Bu·HCl (2.0 equiv), HCTU (1.0 equiv), DIPEA (4.0 equiv).

Next, we examined whether the cumyl ester group could selectively be removed in the presence of other acid labile protecting groups. Building block **213**, containing an acid-sensitive Boc protected lysine residue, was treated with 2% TFA in CH_2Cl_2, then coupled with *L*-phenylalanine *tert*-butyl ester to give tripeptide **220** in excellent yield (Scheme 3.20). No products resulting from Boc-deprotection and reaction of the resulting amine were observed by ^{1}H-NMR or ESI-MS, indicating that the cumyl ester can be selectively cleaved with 2% TFA in CH_2Cl_2 in the presence of other acid labile protecting groups.

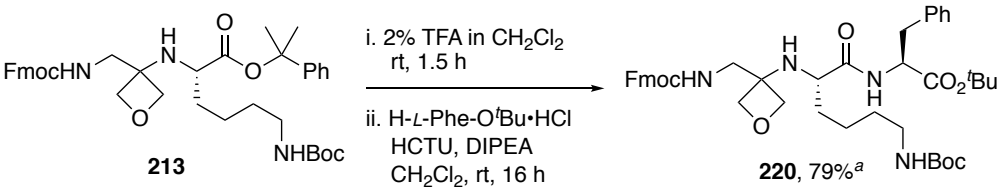

Scheme 3.20 Selective cumyl ester deprotection of oxetane-containing dipeptide building block **213**. [a] Coupling conditions: H-*L*-Phe-O^{t}Bu·HCl (2.0 equiv), HCTU (1.0 equiv), DIPEA (4.0 equiv).

We then focused our attention on *N*-terminal couplings of oxetane-containing building blocks. As solid-phase peptide synthesis typically uses *N*-protected amino acids and coupling reagents in large excess to drive reactions to completion,[87] there was some concern that unwanted acylation of the unprotected 3-aminooxetane unit may take place. We investigated *N*-terminal solution-phase couplings with the building blocks mimicking conditions typically used for solid-phase synthesis. The Fmoc group of **196** was removed using diethylamine and the resulting crude amine coupled with 4 equivalents of both Boc-glycine and HCTU (Scheme 3.21). Using these conditions, tripeptide **221** was isolated in good yield, and no products resulting from acylation of the 3-aminooxetane unit were observed by ^{1}H-NMR or ESI-MS.

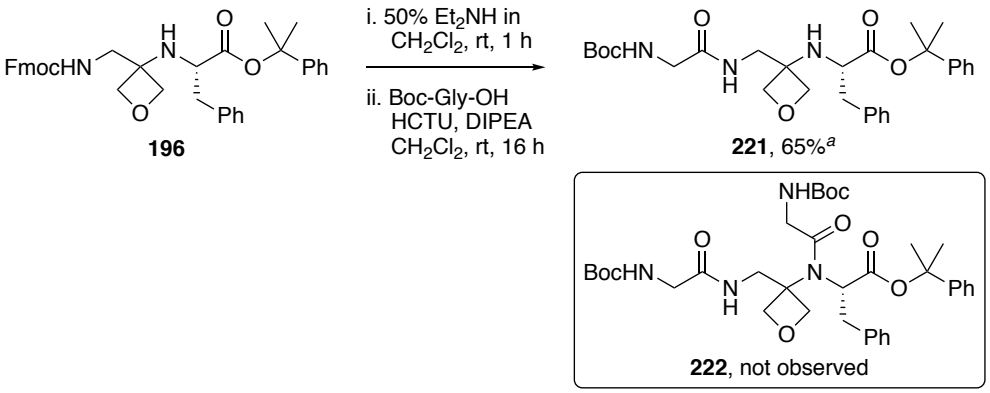

Scheme 3.21 *N*-Terminal coupling of oxetane-containing dipeptide building block **196**. [a] Coupling conditions: Boc-Gly-OH (4.0 equiv), HCTU (4.0 equiv), DIPEA (8.0 equiv).

In addition to this, further studies have demonstrated that Boc protection of the nitrogen of the 3-aminooxetane unit is not only difficult but also results in opening of the oxetane ring. For example, attempts to protect the 3-aminooxetane unit when the *N*- and *C*-terminals were both protected were unsuccessful (Scheme 3.22). It was possible to protect this nitrogen when the carboxylic acid was unprotected with the reaction presumably proceeding *via* a mixed anhydride intermediate. However, the resulting Boc protected 3-aminooxetane unit underwent spontaneous ring expansion to give the corresponding oxazolidinone **224**, as indicated by ESI-MS analysis (*m/z* = 469 $[M+H]^+$). Similar ring expansions of Boc protected 3-aminooxetanes under acidic conditions have previously been reported in the literature.[105]

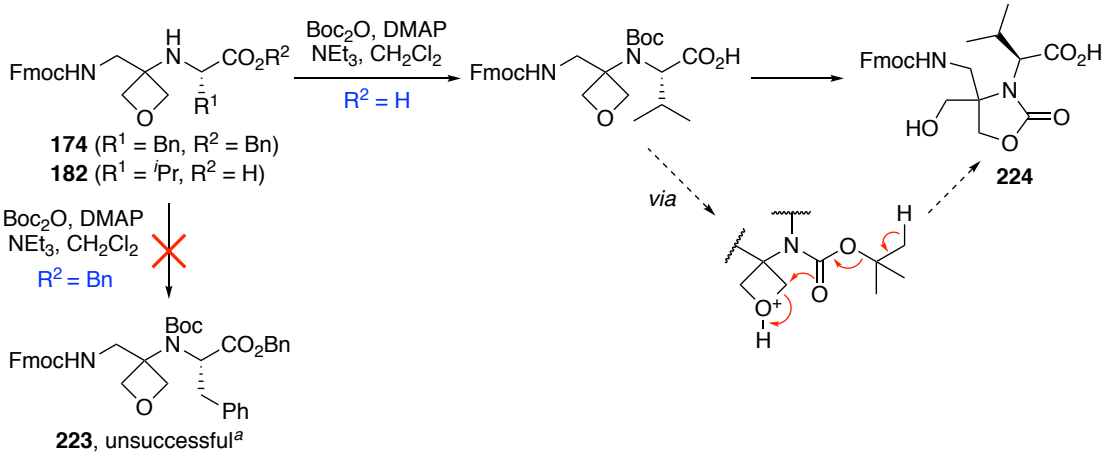

Scheme 3.22 Boc protection of the 3-aminooxetane unit undergoes ring expansion to oxazolidinone **224**. [a] Experiment carried out by Lauren Chapman.

Taken together, these findings encouraged us to explore the use of our building blocks on the solid-phase without protection of the 3-aminooxetane unit.

3.3.6 Solid-Phase Synthesis of Oxetane-Modified Peptides

With oxetane-containing building blocks in hand and their chemistry established in the solution-phase, we set out to examine their use in SPPS.

During the course of this project our collaborator Dr Andrew Jamieson, and his research group, moved from the University of Leicester to the University of Glasgow. This meant that it was no longer convenient for the author to examine the use of the building blocks in SPPS under the supervision of Dr Andrew Jamieson. Instead, it was decided that the building blocks would be delivered to the University of Glasgow and our collaborators would explore their use on SPPS. Therefore, the work reported in this section was carried out by Dr Andrew Jamieson, Dr Astrid Knuhtsen and Dr Alex Hoose at the University of Glasgow.

Experiments for the preparation of oxetane-modified peptides were conducted on a Biotage Initiator + Alsta microwave assisted peptide synthesiser on a 0.1 mmol scale using preloaded chlorotrityl resin. Fmoc deprotection was carried out using 20% piperidine in DMF + 0.1 M Oxyma Pure at 75 °C.[106] Couplings were performed with four equivalents of Fmoc-protected amino acids using HCTU activation with DIPEA in DMF at 75 °C. Peptide cleavage and concomitant side chain deprotection was performed using a cleavage cocktail of TFA/CH_2Cl_2/TIS (70:20:10, v/v/v). For full details, see Section 6.6.

To begin with, six oxetane-modified tetrapeptides **225-230** were prepared using each of the building blocks (Table 3.4, entries 1-6).[‡] Two equivalents of the oxetane-containing building blocks were first deprotected using 2% TFA in CH_2Cl_2 to give the crude acid which was dissolved in DMF and coupled with resin bound alanine using HCTU activation. Following this, standard conditions for Fmoc deprotection, coupling of Fmoc-Trp(Boc)-OH and resin cleavage/deprotection gave the crude tetrapeptides. Purification by reverse phase HPLC gave the oxetane-modified tetrapeptides **225-230** in high purity and acceptable yields. Lower purities were initially observed for tetrapeptides **227** and **228** but could be improved to ≥90% after a second purification. No ring opening of the oxetane was observed under the harsh acidic conditions required for resin cleavage and concomitant side chain deprotection. However, traces of ring opening were observed during reverse phase HPLC purification which was performed using solvent systems

[‡] Building block **215**, containing an alanine residue, was later used to prepare an oxetane-modified peptide described in Chapter 4.

consisting of H_2O in MeCN + 0.1% TFA. This problem was overcome by immediately combining and freeze-drying fractions containing the desired peptide to avoid prolonged exposure to the acidic aqueous solvent.

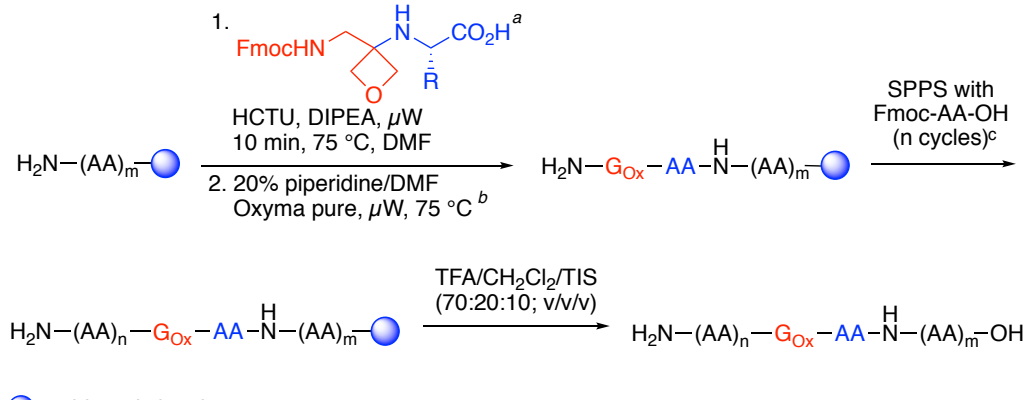

Entry	Building Block[a]	Peptide sequence	Purity (%)[d]	Mass, mg (yield, %)	Peptide Content (%)[e]
1	**196**	W-G_{Ox}-F-A, **225**	89	10.7 (21)	75
2	**210**	W-G_{Ox}-V-A, **226**	93	8.4 (18)	55
3	**211**	W-G_{Ox}-S-A, **227**	81 (90)[f]	12.0 (27)	73
4	**212**	W-G_{Ox}-D-A, **228**	81 (91)[f]	13.7 (29)	75
5	**213**	W-G_{Ox}-K-A, **229**	93	5.0 (10)	48
6	**214**	W-G_{Ox}-P-A, **230**	94	14.6 (32)	62
7	**196**	Y-G-G_{Ox}-F-M, **231**	91	17.0 (28)	81
8	**196**	Y-G-G_{Ox}-F-L, **232**	91	16.4 (28)	79
9	**196**	R-P-P-G_{Ox}-F-S-P-F-R, **233**	94	25.3 (46)	63

Table 3.4 Solid-phase synthesis of oxetane-modified peptides. [a] Treated with 2% TFA in CH_2Cl_2 for 2 h to reveal the free carboxylic acid from **196** and **210-214** prior to coupling with the resin-bound peptide. [b] 30 s, then 3 min with fresh reagents. [c] All couplings preformed at 75 °C for 10 min except arginine (60 min at rt, then 5 min at 75 °C, repeated with fresh reagents). [d] By reverse-phase HPLC (at 214 nm). [e] Determined by UV spectroscopy (at 280 nm) except **233** (at 214 nm). [f] Improved to ≥90% by second purification.

Encouraged by these results, we next examined the use of our building blocks to prepare oxetane-modified analogues of biologically important peptides. We began with analogues of the endogenous opioid peptides Met- and Leu-enkephalin, in which the central glycine was replaced. Using the same conditions as before, pentapeptides **231** and **232** were prepared from phenylalanine-containing building block **196** in good yield and high purity (Table 3.4, entries 7 and 8).

Finally, this methodology was further extended to include nonapeptide **233** as an analogue of the blood vessel dilator bradykinin, which was produced in good yield and excellent purity (Table 3.4, entry 9). No loss in peptide yield and purity was observed during the synthesis of the oxetane-modified bradykinin analogue **233** indicating that the 3-aminooxetane unit tolerates repetitive rounds of coupling and Fmoc deprotection. The benefits of our SPPS methodology for the synthesis of oxetane-modified peptides is demonstrated by comparison of our synthesis of Leu-enkephalin analogue **232** with the previously reported solution-phase synthesis reported by Carreira and co-workers, that required multiple steps and chromatographic purifications (Scheme 3.23).[47]

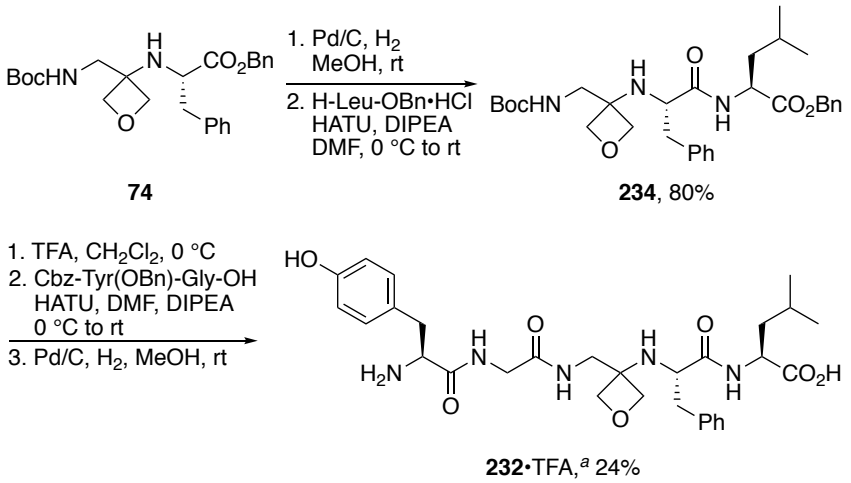

Scheme 3.23 Carreira's solution-phase synthesis of oxetane-modified Leu-enkephalin **232** using dipeptide building block **74**.[47] [a] Isolated as the TFA salt after reverse-phase HPLC.

3.3.6 Further Synthesis of Oxetane-Containing Dipeptide Building Blocks

Following the successful development of a methodology for the synthesis of oxetane-modified peptides using SPPS techniques, the scope of the oxetane-containing dipeptide building blocks has been further explored by other members of the group (Scheme 3.24). Five additional building blocks have been prepared in generally good overall yield using

the chemistry described in this chapter. A modified route towards methionine-analogue **236** was used, as reduction of the nitro group in the precursor using Raney Ni under an atmosphere of hydrogen resulted in cleavage of the S−C bond. Consequently, this analogue was prepared *via* reduction of the nitro group using Zn-AcOH followed by protection of the crude primary amine with FmocOSu to give **236** in 37% yield. The application of these building blocks in solution and on the solid-phase is currently being further explored by our group.

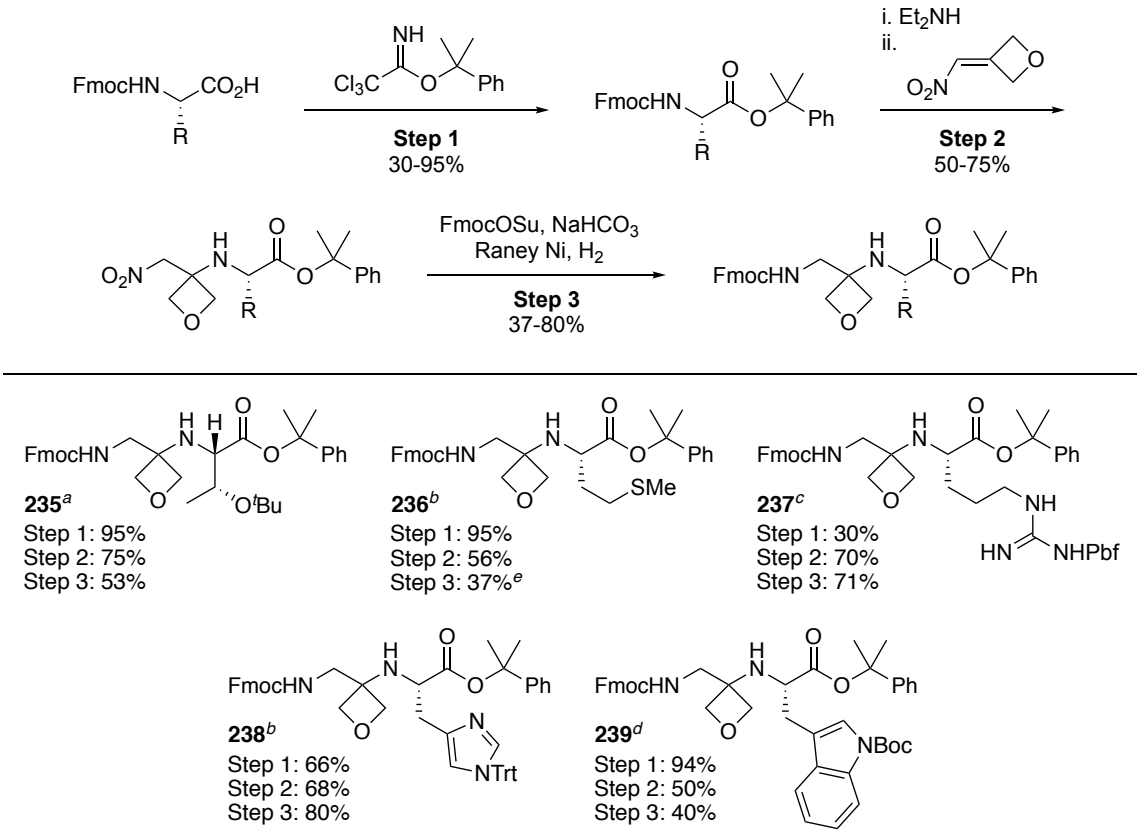

Scheme 3.24 Further examples of oxetane-containing dipeptide building blocks prepared by the Shipman group. [a] Prepared by George Saunders. [b] Prepared by Leo Tam. [c] Prepared by Dr Stefan Roesner. [d] Prepared by Dr Ina Wilkening. [e] Reaction conditions: i) Zn, AcOH; ii) FmocOSu, $NaHCO_3$.

3.3.7 Binding Affinity Studies of Oxetane-Modified Analogues of Met- and Leu-Enkephalin

With a practical route to oxetane-modified analogues of biologically interesting peptides developed, the impact of oxetane-modification on the biological properties of Met- and Leu-enkephalin was investigated. In collaboration with Dr John Traynor at the University

of Michigan, the binding affinities of oxetane-modified Met- **231** and Leu-enkephalin **232** to the δ- and μ-opioid receptors was examined.

Opioid receptor binding affinities of oxetane-modified Met- **231** and Leu-enkephalin **232** analogues were determined by displacement of the radioligand [^{3}H]-diprenorphine **241** from the δ- and μ-opioid receptors. The binding affinities (K_i) of the parent Met- **240** and Leu-enkephalin **75** peptides were found to be 1.5 nM and 4.1 nM for the δ-opioid receptor and 4.0 nM and 25 nM for the μ-opioid receptor (Table 3.5 entries 1 and 2). These values were comparable to those previously reported.[107] Oxetane-modified Met-enkephalin **231** showed weak affinity towards the δ- and μ-opioid receptors with binding affinities of 6.4 μM and 18.9 μM (Table 3.5, entry 3). Oxetane-modified Leu-enkephalin **232** also showed weak affinity towards δ- and μ-opioid receptors with binding affinities of 5.0 μM and 12.9 μM (Table 3.5, entry 4).

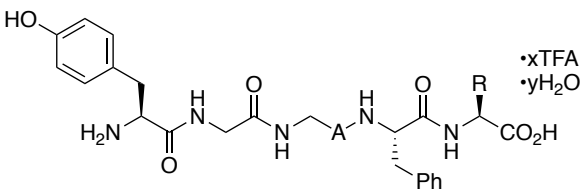

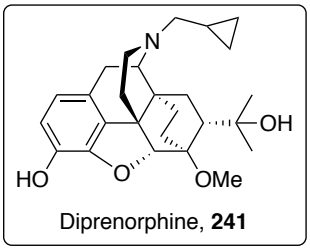

Diprenorphine, **241**

Entry	Peptide Sequence[a]	A	R	δ-Affinity K_i (nM)[b,c]	μ-Affinity K_i (nM)[b,c]
1	Y-G-G-F-M, **240** Met-enkephalin		CH_2CH_2SMe	1.5	4.0
2	Y-G-G-F-L, **75** Leu-enkephalin		$CH_2{}^iPr$	4.1	25
3	Y-G-G_{Ox}-F-M, **231**		CH_2CH_2SMe	6,400	18,900
4	Y-G-G_{Ox}-F-L, **232**		$CH_2{}^iPr$	5,000	12,900

Table 3.5 Binding affinities of Met- **240** and Leu-enkephalin **75** and their oxetane analogues **231** and **232** to δ- and μ-opioid receptors. [a] G_{Ox} = oxetane-modified glycine. [b] Displacement of [^{3}H]-diprenorphine **241** from opioid receptors. [c] Affinity values are given as a mean (n = 3).

Our investigations indicate that oxetane-modification of the central glycine residue in Met- and Leu-enkephalin has a detrimental impact on the binding affinities towards the δ- and μ-opioid receptors. Although the bioactive conformation of the enkephalins has not yet been confirmed, it has been proposed that they adopt a β-turn in their bioactive conformations, stabilised *via* a H-bond between the tyrosine C=O (*i*) and the phenylalanine NH (*i* + 3).[108,109] It is possible that substitution of the amide group with the 3-aminooxetane unit reduces the strength of this intramolecular H-bond,[110] potentially destabilising the β-turn conformation relative to competing γ-turn or linear conformations (Scheme 3.25). This consequently disrupts binding with the opioid receptors. However, further structural investigations would be required to confirm this.

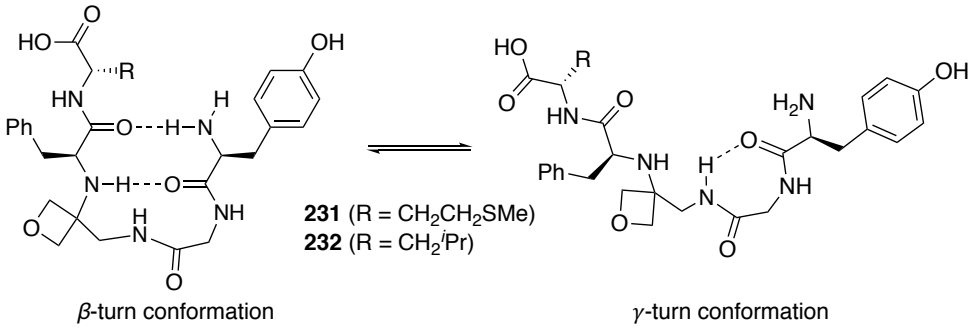

Scheme 3.25 Potential β-turn and γ-turn conformations of oxetane-modified enkephalin analogues.

During our investigation into the impact oxetane-modification had on the biological properties of Met- and Leu-enkephalin, Carreira and co-workers published a complete study on the binding affinities of oxetane-modified analogues of Leu-enkephalin towards the δ-receptor.[47] This study used oxetane-modified dipeptide building blocks to prepare four analogues of Leu-enkephalin, wherein each amide bond was sequentially replaced by the 3-aminooxetane unit (Table 3.6).

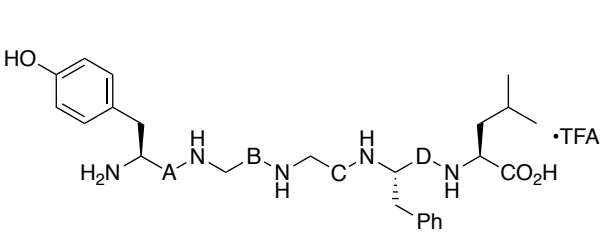

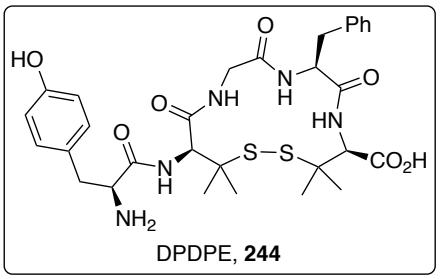

Entry	Peptide sequence[a]	A	B	C	D	δ-affinity K_i (nM)[b,c]	Serum half-life[d]
1	Y-G-G-F-L, **75** (Leu-enkephalin)					9.2	≈10 min
2	Y_{Ox}-G-G-F-L, **242**					>1000	≈3.2 h
3	Y-G_{Ox}-G-F-L, **76**					>1000	≈18 h
4	Y-G-G_{Ox}-F-L, **232**					157	≈15 min
5	Y-G-G-F_{Ox}-L, **243**					43	≈26 min

Table 3.6 Stability and binding affinities of oxetane-modified analogues of Leu-enkephalin **75** prepared by Carreira and co-workers.[47] [a] Y_{Ox} = oxetane-modified tyrosine, G_{Ox} = oxetane-modified glycine, F_{Ox} = oxetane-modified phenylalanine. [b] Displacement of [^{3}H]-DPDPE **244** from δ-opioid receptor. [c] Affinity values are given as a mean (n = 3). [d] Half-life in human serum.

Binding affinities of oxetane-modified Leu-enkephalin analogues were determined by displacement of the radio ligand [^{3}H]-DPDPE **244** from the *δ*-opioid receptor (Table 3.6). In this assay, the binding affinity for natural Leu-enkephalin **75** was 9.2 nM, which is comparable to the value reported by us and in the literature.[107] Analogue **232**, in which the central glycine residue has been modified, showed significant nanomolar affinity towards the *δ*-opioid receptor with a binding affinity of 157 nM. This is in contrast to results from our assay, that found **232** had a binding affinity of 5,000 nM. Analogue **243** showed affinity comparable to the parent Leu-enkephalin **75** with a binding affinity of 43 nM. Analogues **242** and **76** did not show any affinity towards the *δ*-opioid receptor up to

a concentration of 1 μM. The reason for the large difference in the binding affinity values for analogue **232**, obtained independently by us and Carreira, is unclear. One possible explanation is that the material prepared by us decomposed en route to the University of Michigan for testing.

In addition to examining the binding affinities to the *δ*-opioid receptor, Carreira and co-workers also investigated the degradation of oxetane-modified Leu-enkephalin analogues in human serum (Table 3.6 and Figure 3.3). Leu-enkephalin **75** is known to readily degrade in human serum with a half-life of 10-12 min.[111] The mechanism of hydrolysis has been extensively studied and has identified that the Tyr-Gly bond is the most susceptible to proteolytic cleavage.[112,113] Analogue **232**, in which the central glycine has been replaced, shows a slightly increased half-life of ~15 min compared to the native system. Phenylalanine-modified analogue **243** is even more stable to hydrolysis (half-life ~26 min). Analogue **242**, in which the Tyr-Gly connection has been modified, shows a significant increase in proteolytic stability with a half-life of ~3.2 h. Finally, analogue **76** has the highest half-life in human serum with a half-life of ~18 h. It is likely that in this substrate, the oxetane-modification inhibits the hydrolysis of both the Tyr-Gly and the Gly-Gly bond by interfering with the substrate recognition process of proteases.

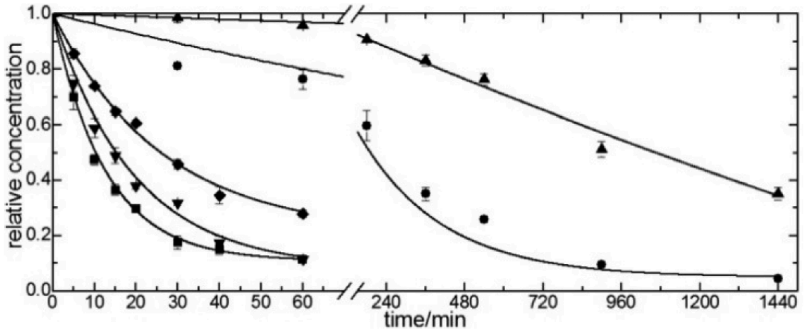

Figure 3.3 Stability of Leu-enkephalin (**75**, ■) and its analogues (**242**, ●), (**76**, ▲), (**232**, ▼) and (**243**, ◆) in human serum. Figure taken from *Org. Lett.* **2017**, 19, 2510-2513.[47]

Carreira and co-workers' investigation has demonstrated that oxetane-modification of the central glycine **232** and phenylalanine residue **243** can produce analogues of Leu-enkephalin that display affinity towards the *δ*-opioid receptor comparable to natural Leu-enkephalin **75**. Furthermore, all oxetane-modified analogues showed greater hydrolytic stability in human serum compared to the parent system **75**. These results provide proof of concept that oxetane-modification of an amide bond can be used to increase the stability of a peptide towards proteases while retaining bioactivity.[47] No further efforts to

study this system were undertaken in light of the thorough published investigation by Carreira and co-workers.

3.4 Enzymatically-Stable Oxetane-Based Dipeptide Hydrogels

In addition to the work described in this chapter, a further collaborative project with Professor Dave Adams and Dr Andrew Jamieson at the University of Glasgow has demonstrated that oxetane-modified dipeptides can be used to form hydrogels. This section aims to provide a brief summary of this work.

Low molecular weight hydrogels arise from the self-assembly of small molecules (gelators) in water to form three-dimensional supramolecular structures that trap large amounts of water.[114] These supramolecular structures are currently being investigated for a number of applications such as imaging, tissue engineering, drug delivery and wound healing.[114–116] For some of these applications it is desirable that the self-assembled network is not easily degraded by enzymes. Since Fmoc-dipeptides are a well-known, effective class of gelator,[114,117–119] we proposed that oxetane-based Fmoc-dipeptides could be used to prepare gels with increased resistance to enzymatic cleavage (Figure 3.4).

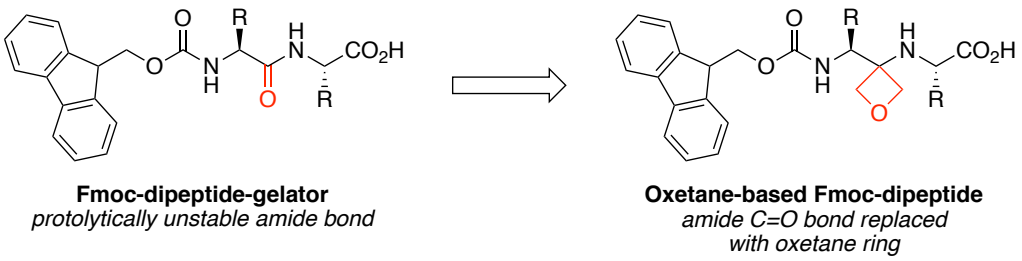

Figure 3.4 Concept of oxetane modification of Fmoc dipeptide gelators.

A pH-triggered approach was used to investigate the ability of oxetane-based dipeptides as gelators. The dipeptides were first suspended in water and a molar equivalent of sodium carbonate added. Following this, the pH of the solution was decreased *via* the addition of glucono-δ-lactone (GdL).[120] GdL slowly hydrolyses in water to give gluconic acid, which controllably lowers the pH (Scheme 3.28). As the pH decreases the molecules begin to self-assemble into fibrous structures that then entangle to form supra-molecular networks that trap water.

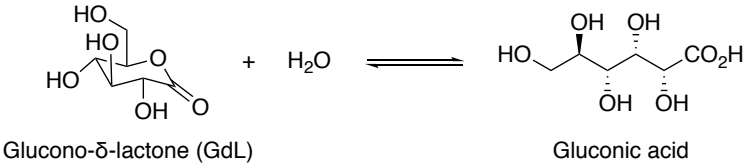

Scheme 3.28 Hydrolysis of GdL to gluconic acid.[120]

Using this approach, oxetane-containing dipeptide **175** was found to be an effective gelator, forming a self-supporting material at a concentration of 3 mg mL^{-1} after standing overnight (Figure 3.5). Remarkably, the impact of oxetane-modification is immediately apparent as the corresponding parent analogue, Fmoc-Gly-Phe-OH **245**, is known to not be able to form gels.[121,122]

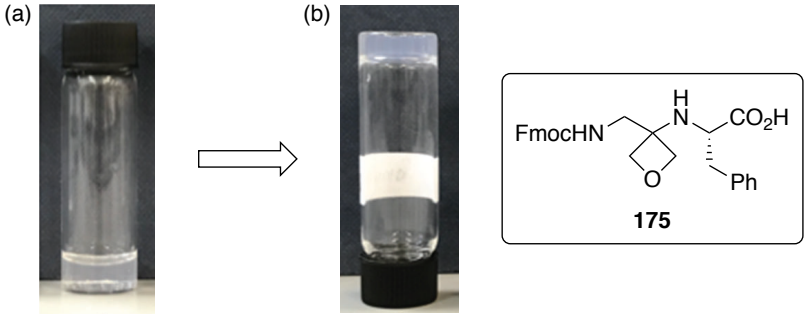

Figure 3.5 (a) Photograph of a solution of **175** at a concentration of 3 mg mL^{-1} at high pH. (b) Photograph of the sample shown in (a) after the pH has been lowered *via* the hydrolysis of GdL. The white bands in (b) are labels on the sample tubes. Photographs taken from *Chem. Commun.* **2018**, *54*, 1793-1796.[123]

Next, the stability of oxetane-modified dipeptide **175** to proteolysis, relative to Fmoc-Gly-Phe-OH **245**, was examined. Carboxypeptidase A, an exopeptidase that hydrolyses peptide bonds of *C*-terminal residues with aromatic side chains, was added to solutions of **175** and Fmoc-Gly-Phe-OH **245** in Tris buffer at pH 7.9 and the products probed by HPLC. Under these conditions, Fmoc-Gly-Phe-OH **245** rapidly degraded, with 98% conversion to Fmoc-Gly-OH after 1 minute and complete conversion after 5 mins (Figure 3.6-a). In comparison, **175** showed significant stability with no enzymatic conversion after 24 hours (Figure 3.6-b).

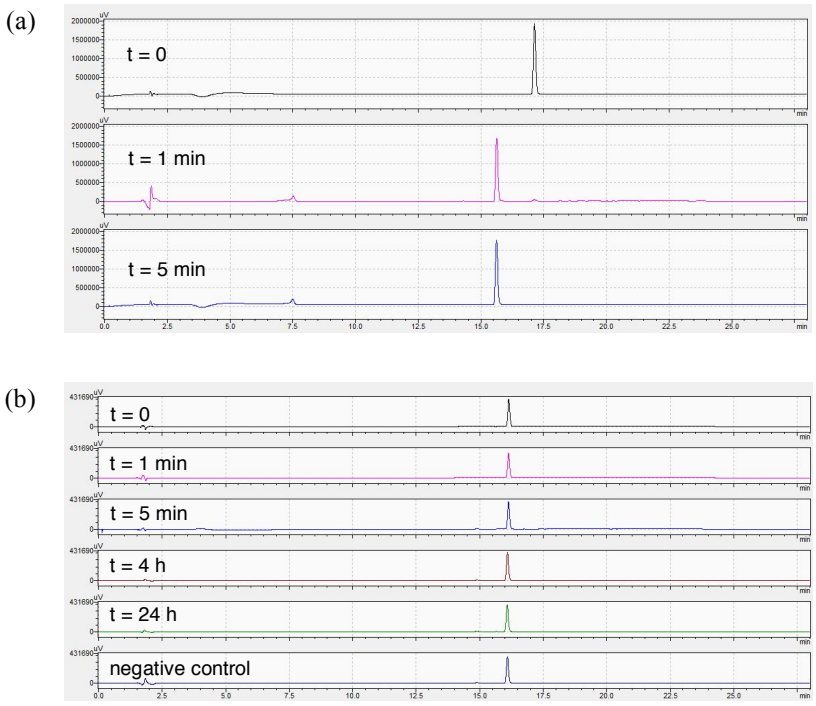

Figure 3.6 (a) Degradation of Fmoc-Gly-Phe-OH **245** over 5 min to Fmoc-Gly-OH. (b) **175** was sampled at t = 0, 1 min, 5 min, 4 h and 24 h. No degradation was observed over this timescale. Negative control containing no enzyme was conducted in parallel.

Taken together, these results demonstrate that gels can be formed from oxetane-based dipeptides that are significantly more stable to proteolysis compared to native dipeptides (Figure 3.7). Consequently, this class of material may have applications *in vivo*.

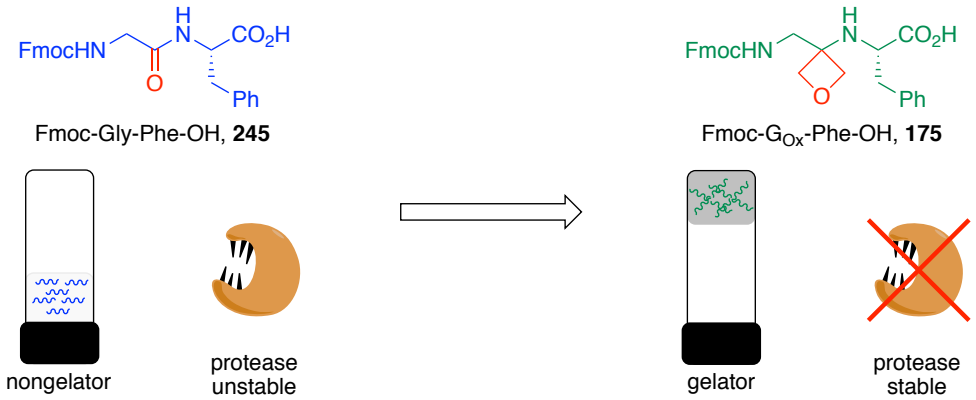

Scheme 3.7 Enzymatically-stable oxetane-based dipeptide hydrogels.[123]

The work described in this section was published in Chemical Communications in 2018.[123]

3.5 Conclusions

In conclusion, this chapter has described the development of a practical route to oxetane-modified peptides (OMPs) using conventional Fmoc/^{t}Bu solid-phase peptide synthesis (SPPS) techniques. Our strategy involves using cumyl protected dipeptide building blocks that are readily prepared in three steps in solution-phase (Scheme 3.26). The cumyl ester is then selectively cleaved with 2% TFA in CH_2Cl_2 to reveal the terminal carboxylic acid immediately prior to coupling. Since the work described in this chapter has been carried out, additional examples of oxetane-containing dipeptide building blocks have been prepared and used by other members of the group.

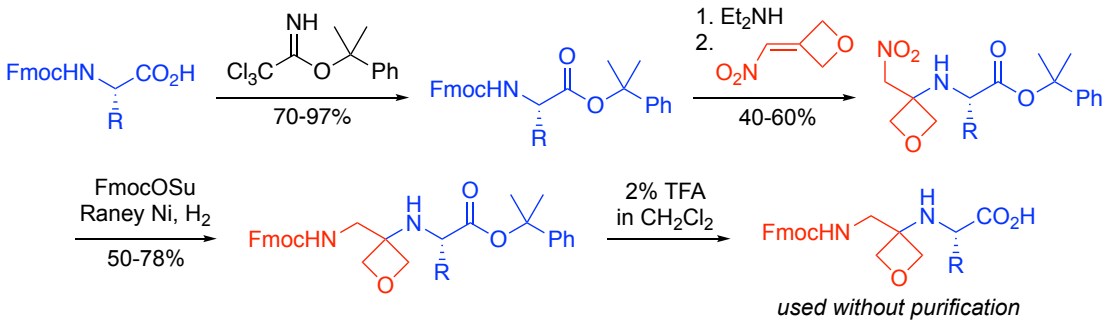

Scheme 3.26 Solution-phase synthesis of oxetane-containing dipeptide building blocks.

Solution and solid-phase experiments demonstrated that amide couplings using these building blocks can proceed in high yield, without racemisation, and without the need to protect the secondary amine of the 3-aminooxetane unit. Hence, oxetane-modified peptides can be produced in high purities and acceptable yields using conventional SPPS methods for coupling, deprotection, resin cleavage and purification (Scheme 3.27). This methodology has been used to prepare oxetane-modified analogues of enkephalin and bradykinin.

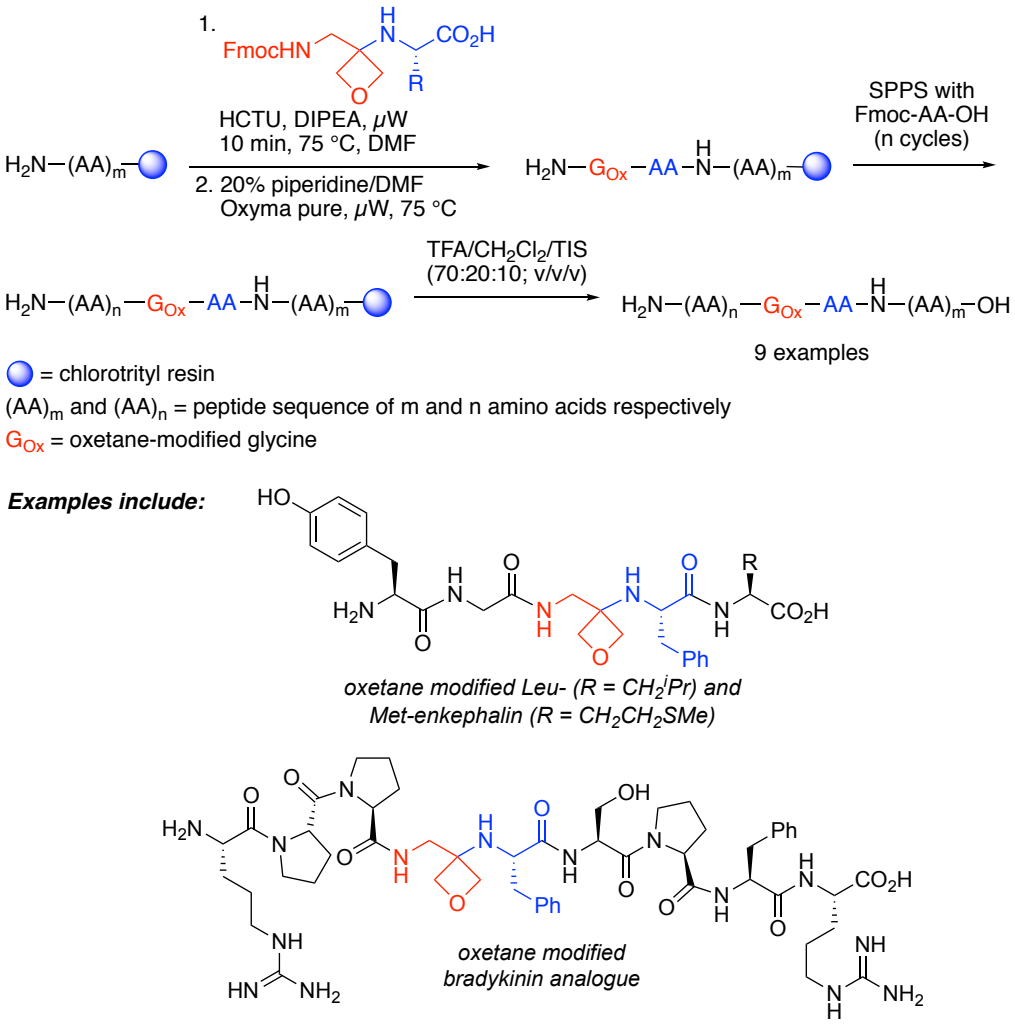

Scheme 3.27 Solid-phase synthesis of oxetane-modified peptides.

Preliminary studies towards the impact of oxetane-modification on the biological properties of native peptides by investigating the binding affinities of oxetane-modified enkephalin analogues towards the δ- and μ-opioid receptors were conducted. However, a more complete study by Carreira and co-workers was reported during our own investigations which demonstrated that oxetane-modified analogues of Leu-enkephalin have improved hydrolytic stability in human serum, and that two of four analogues retain appreciable affinity towards the δ-opioid receptor.[47]

This methodology is currently being used to produce a variety of OMPs in order to further explore the impact of oxetane-modification on the secondary structure and biological properties of these peptides.

Much of the work described in this chapter was published in Organic Letters in 2017.[124]

Chapter 4: Incorporation of Oxetanes into α-Helices

4.1 Project Aims

Following the development of a practical route to oxetane-modified peptides (OMPs) using solid-phase peptide synthesis (SPPS) techniques, we were interested to explore the impact of oxetane-modification on common types of secondary structures (*e.g.* turns, α-helices and β-sheets). Here, we begin by investigating the impact on α-helices.

The α-helix is one of the most common types of secondary structure in proteins and polypeptide chains.[125] Therefore, it would be of great interest to explore the impact of oxetane-modification on the structure and stability of known α-helices. Alanine-based model peptides have been well-studied and are known to form α-helices.[24,126–128] Hence, these alanine-rich sequences are ideal systems to investigate the impact of oxetane-modification on the structure and stability of α-helices (Figure 4.1).

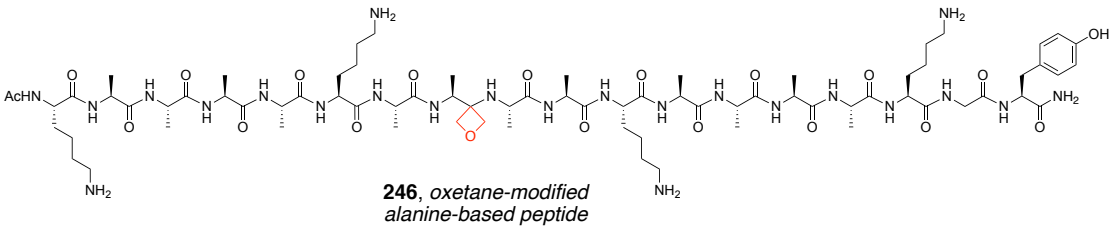

Figure 4.1 Proposed structure of an oxetane-modified alanine-based model peptide required for this study.

To study the impact of oxetane-modification on the structure and stability of α-helices, this project is focused in three parts:

1. The asymmetric synthesis of an oxetane-modified alanine (A_{Ox}) containing dipeptide building block, suitable for solid-phase peptide synthesis (SPPS).
2. The preparation of oxetane-modified analogues of alanine-based model peptides using the SPPS methodology described in Chapter 3.
3. Study the secondary structure of these oxetane-modified peptides using circular dichroism (CD) and NMR spectroscopy.

4.2 Introduction

4.2.1 The α-Helix

The α-helix was first characterised by Pauling in 1951 and is one of the most common secondary structure conformations in natural proteins, with ~40% of all residues adopting helical conformations.[125,129] A typical α-helix, also known as a 3.6_{13}-helix, consists of amino acids arranged in a helical structure where the C=O group at the *i* position is hydrogen-bonded to the NH group at the *i* + 4 position (Figure 4.2). Each residue is related to the next one by a translation of 1.5 Å along the helix axis and a 100° rotation, which gives 3.6 residues per turn of the helix. The pitch of the helix, the vertical distance between consecutive turns of the helix, is 5.4 Å and is equal to the product of the translation (1.5 Å) and the number of residues per turn (3.6). Although the screw-sense of an α-helix can be right- or left-handed, an α-helix composed of *L*-amino acids typically adopts a right-handed conformation as the corresponding left-handed conformation is destabilised due to steric crowding of the side chains and the carbonyl groups. Virtually all α-helices found in proteins are right-handed.[3,130]

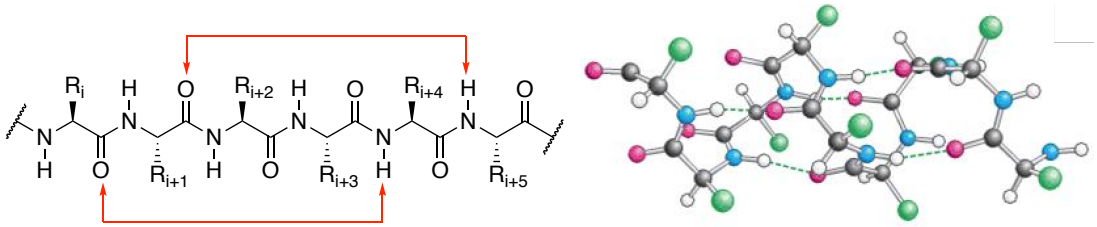

Figure 4.2 Hydrogen bonding scheme and a ball-and-stick depiction of an α-helix. Ball-and-stick image from *Biochemistry 6th Edition,* W. H. Freeman and Company, New York, 2006.[3]

4.2.2 Alanine-Based Helical Peptides

Baldwin and co-workers have demonstrated that short alanine-based peptides form highly stable α-helices in water.[24,126–128] For example, under optimal helix-forming conditions alanine-based peptide **247**, containing three lysines and thirteen alanines, can display up to 80% helix content (Figure 4.3).[126] These model systems have been used in amino acid substitution experiments to measure the helix forming propensities of various amino acids.[127,128]

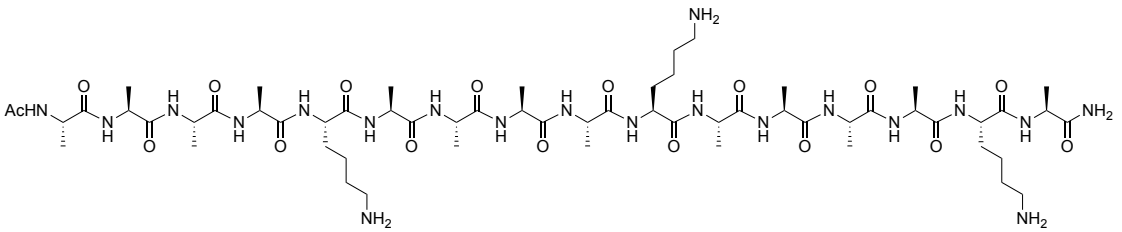

Ac-AAAAK-AAAAK-AAAAK-A-NH_2, **247**

f_H = 80%[a]

Figure 4.3 Structure of alanine-based peptide **247** displaying 80% helix content.[126] [a] Mean helix content measured in 1.0 M NaCl, pH 7.0 at 1 °C.

Alanine-based model peptides have also been used to investigate the influence of peptidomimetic modifications on α-helix structure and stability. For example, Kiefhaber and co-workers determined the impact of single thioamide bonds on α-helix structure and stability by preparing thioamide-analogues of alanine-based peptides **248** and **250** in which a single amide to thioamide substitution was introduced at a central **249** and *N*-terminal position **251** (Table 4.1). Circular dichroism (CD) studies revealed that introducing a thioamide group at these two positions results in a highly helix-destabilising effect, with the decrease in helical content more prominent in the central region compared with the *N*-terminal substitution. Comparison of the helical content values with other reference peptides confirmed that the effect of an amide to thioamide substitution is of similar magnitude as an alanine to glycine substitution. Despite this, ^{1}H-NMR characterisation of *N*-terminal analogue **251** demonstrated that the thioamide group was engaged in an $i \rightarrow i + 4$ hydrogen bond, indicating that thioamides can be tolerated in α-helical structures.[24]

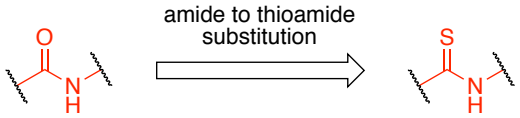

Entry	Peptide Sequence[a]	f_H (%)[b]
1	Ac-KAAAA-KAAAA-KAAAA-KGY-NH_2, **248**	68
2	Ac-KAAAA-KAAΨAA-KAAAA-KGY-NH_2, **249**	24
3	Ac-DFAAA-KAAAA-KAAAA-K-NH_2, **250**	69
4	Ac-DFΨAAA-KAAAA-KAAAA-K-NH_2, **251**	48

Table 4.1 Effect of thioamide bonds on helix content.[24] [a] Ψ denotes the substitution of the amide bond [CO−NH] by a thioamide bond [CS−NH]. [b] Mean helix content measured in 10 mM potassium phosphate, pH 7.0 at 0 °C, with the addition of 1.0 M NaCl.

4.3 Results and Discussion

4.3.1 Design of Alanine-Based Model Peptides

Alanine-rich peptide **248** was chosen as a model system to investigate the impact of oxetane-modification on α-helix structure and stability and has been shown to have a helical content of ~68% at 0 °C (Figure 4.4).[24] The peptide **248** contains lysine residues at every fifth position to increase solubility and the *N*- and *C*-termini have been capped to prevent unfavourable electrostatic interactions with the helix dipole. **248** also contains a *C*-terminal Tyr residue that is separated from the Ala-Lys sequence by a Gly residue. Addition of a Tyr residue enables accurate determination of the peptide concentration by Tyr absorbance (ε_{275} = 1450 M^{-1}) and does not significantly affect the far-UV CD spectrum when separated by a Gly residue.[24,128]

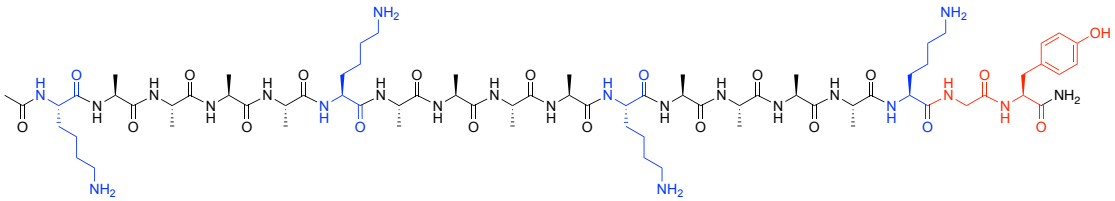

Ac-KAAAA-KAAAA-KAAAA-KGY-NH_2, **248**

f_H = 68%[a]

Figure 4.4 Structure of alanine-based model peptide **248**.[24] [a] Mean helix content measured in 10 mM phosphate buffer, pH 7.0 at 0 °C with the addition of 1.0 M NaCl.

Helical content is expected to reach a maximum at the centre of peptide making this section particularly sensitive to modifications. In comparison, the terminal regions exhibit significantly less helical content, hence modifications to these regions are expected to have less effect on helix content.[24,127] To investigate the impact of oxetane-modification on α-helix structure and stability, we proposed to prepare oxetane-modified analogues of **248** in which a single central and *N*-terminal alanine residue is replaced by an oxetane-modified alanine (A_{Ox}) residue (Table 4.2, entries 1 and 2). In addition, we also proposed to prepare analogues containing an oxetane-modified glycine (G_{Ox}) residue as deletion of the methyl side-chain might make it easier to accommodate the oxetane-modified residue into the α-helix (Table 4.2, entries 3 and 4). Following this, analysis of secondary structure content of the oxetane-modified analogues using circular dichroism (CD) and NMR spectroscopy was expected to enable us to assess the impact of oxetane-modification on α-helix structure and stability.

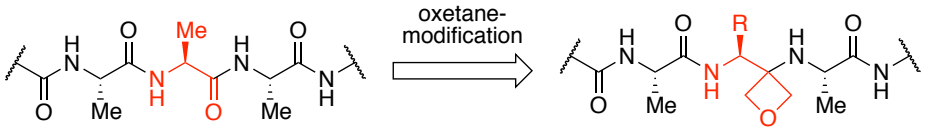

Entry	Peptide[a]	Peptide Sequence[a]	R
1	Central A_{Ox}, **246**	Ac-KAAAA-KA**A_{Ox}**AA-KAAAA-KGY-NH_2	Me
2	*N*-Terminal A_{Ox}, **252**	Ac-KA**A_{Ox}**AA-KAAAA-KAAAA-KGY-NH_2	Me
3	Central G_{Ox}, **253**	Ac-KAAAA-KA**G_{Ox}**AA-KAAAA-KGY-NH_2	H
4	*N*-Terminal G_{Ox}, **254**	Ac-KA**G_{Ox}**AA-KAAAA-KAAAA-KGY-NH_2	H

Table 4.2 Sequences of oxetane-modified peptides required for this study. [a] A_{Ox} = oxetane-modified alanine, G_{Ox} = oxetane-modified glycine.

4.3.2 Towards the Stereocontrolled Synthesis of Oxetane-Containing Dipeptide Building Blocks

The oxetane-modified peptides required for this study could be prepared using the methodology described in Chapter 3. However, this required the preparation of an Fmoc-protected dipeptide building block in which the oxetane residue is based on alanine. Therefore, our initial efforts focused on routes towards A_{Ox}-containing dipeptide building block **255** (Scheme 4.1). The synthesis of the required G_{Ox}-containing dipeptide building block **215** has previously been reported in Chapter 3.

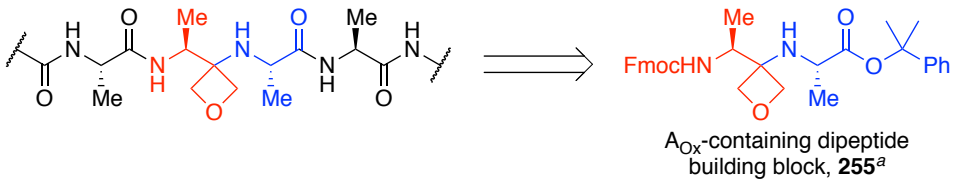

Scheme 4.1 Structure of the oxetane-containing building block required for this study. [a] A_{Ox} = oxetane-modified alanine.

4.3.2.1 Addition of Chiral Amines to Trisubstituted Nitroalkenes

To begin with, we focused our efforts on the synthesis of A_{Ox}-containing dipeptide building block **255** using the route described in Chapter 3. Although previous work by us

and Carreira suggested that this route would produce the building block as a mixture of diastereoisomers,[45,46] we envisaged that it might be possible to separate these diastereoisomers after the conjugate addition step or after the nitro reduction-Fmoc protection step. Starting from alanine cumyl ester **202**, the Fmoc group was first removed using diethylamine and the resulting crude amine **256** added to nitroalkene **128** to give the addition product as a 50:50 mixture of diastereoisomers (Scheme 4.2). Attempts to separate the diastereoisomers using column chromatography were unsuccessful and **257** was isolated in excellent yield as a 55:45 mixture of diastereoisomers. Following this, nitro reduction with Raney Ni under an atmosphere of hydrogen and *in situ* Fmoc protection gave the crude Fmoc-protected dipeptide building block **255**. Attempts to separate the diastereoisomers at this stage were also unsuccessful and A_{Ox}-containing building block **255** was isolated as a 58:42 mixture of diastereoisomers as determined by chiral HPLC analysis (see Section 6.8).

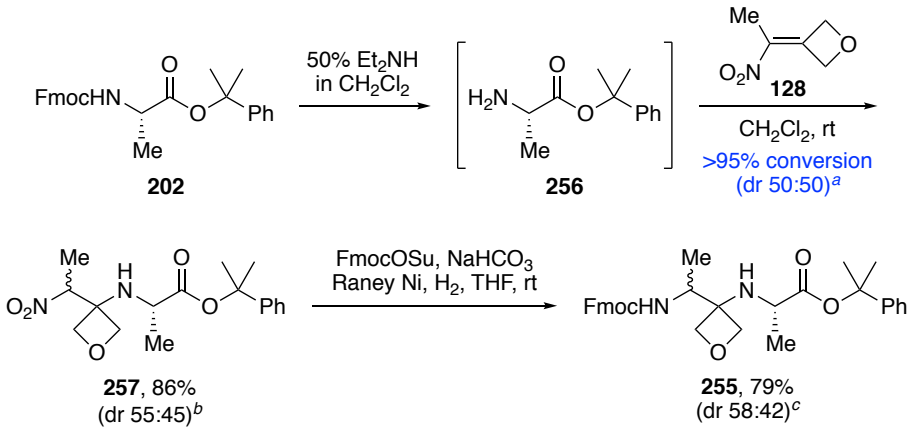

Scheme 4.2 Synthesis of A_{Ox} containing dipeptide building block **255** *via* conjugate addition of **256** to trisubstituted nitroalkene **128**. [a] Determined by ^{1}H-NMR analysis of the crude reaction mixture (see Section 6.7). [b] Determined by ^{1}H-NMR analysis. [c] Determined by chiral HPLC analysis (see Section 6.8).

Following this result, we investigated the addition of other chiral α-amino esters to nitroalkene **128** to determine if any diastereoselectivity could be obtained and whether the resulting diastereoisomers could be separated. A series of α-amino esters, containing various side chains and ester protecting groups, were added to trisubstituted nitroalkene **128** (Table 4.3). Alanine methyl ester gave no diastereoselectivity and the resulting addition product **263** was formed as a 50:50 mixture of diastereoisomers, which were not separable using column chromatography (Table 4.3, entry 2). More sterically hindered valine cumyl ester gave a small amount of selectivity to provide the addition product **264**

as a 55:45 mixture of diastereoisomers which were not separable using column chromatography (Table 4.3 entry 3). Valine, serine and phenylglycine methyl esters gave no diastereoselectivity and the corresponding addition products (**132**, **265**-**266**) were produced as 50:50 mixtures of diastereoisomers; none of which were separable using column chromatography (Table 4.3, entries 4-6). The addition of proline methyl ester to nitroalkene **128** gave a significant increase in diastereoselectivity to provide tertiary amine **267** as a 70:30 mixture of diastereoisomers (Table 4.3, entry 7). However, similar to the previous examples, the diastereoisomers were not separable using column chromatography.

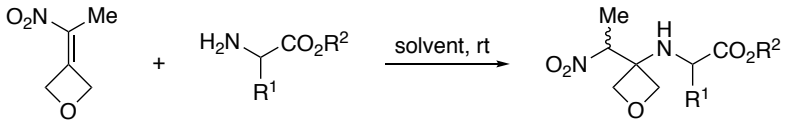

Entry[a]	Amino ester	Solvent	Product	Conversion (%)[b]	dr[b]
1[c]	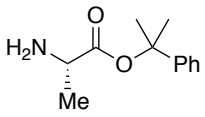 **256**	CH_2Cl_2	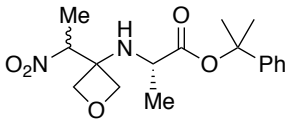 **257**	>95	50:50
2[d]	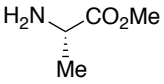 **258**	THF	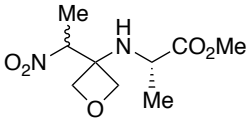 **263**	>95	50:50
3[c]	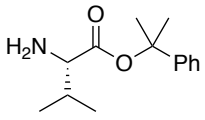 **259**	CH_2Cl_2	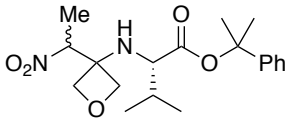 **264**	>95	55:45
4[d]	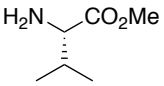 **130**	THF	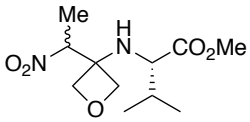 **132**	>95	50:50
5[d]	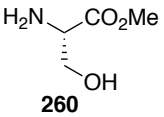 **260**	THF	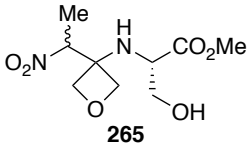 **265**	>95	50:50
6[d]	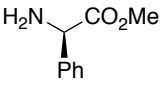 **261**	CH_2Cl_2	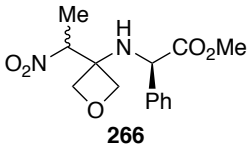 **266**	>95	50:50
7[d]	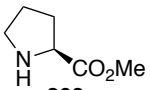 **262**	THF	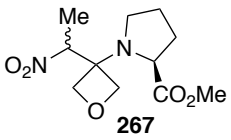 **267**	>95	70:30

Table 4.3 Conjugate addition of chiral amino esters to trisubstituted nitroalkene **128**. [a] Method: **128** (1.0 equiv), amino ester (1.2-2.0 equiv), solvent (0.1 M). [b] Determined by ^{1}H-NMR analysis of the crude reaction mixture (see Section 6.7). [c] Prepared by deprotection of the corresponding Fmoc-protected amino ester and used without purification. [d] Prepared from the corresponding hydrochloride salt.

Our screening results for the addition of various α-amino esters to nitroalkene **128** indicate that chiral primary amino esters exert little stereochemical bias on the reaction providing the addition products as a mixture of diastereoisomers. Furthermore, none of the resulting diastereoisomers could be readily separated using column chromatography. A possible explanation for the lack of diastereoselectivity in the conjugate addition-protonation reaction is the conformational freedom of the primary amino esters and the remoteness of R^1 and R^2 from the site of protonation. Assuming the addition of an amino ester **268** to nitroalkene **128** proceeds in a stepwise manner, the first step corresponds to the formation of the C_β–N bond in a reaction leading to a 6-membered nitronate transition state **269** (Scheme 4.3). In this transition state, there is a low energy barrier for rotation around the $X(R^1)C_\alpha$–N bond resulting in a conformational equilibrium between **269a** and **269b**. Consequently, in the following protonation step, there is little preference between protonation of the *Si* face **270a** or *Re* face **270b** of the nitronate intermediate, resulting in formation of the addition product **271** as a mixture of diastereoisomers.

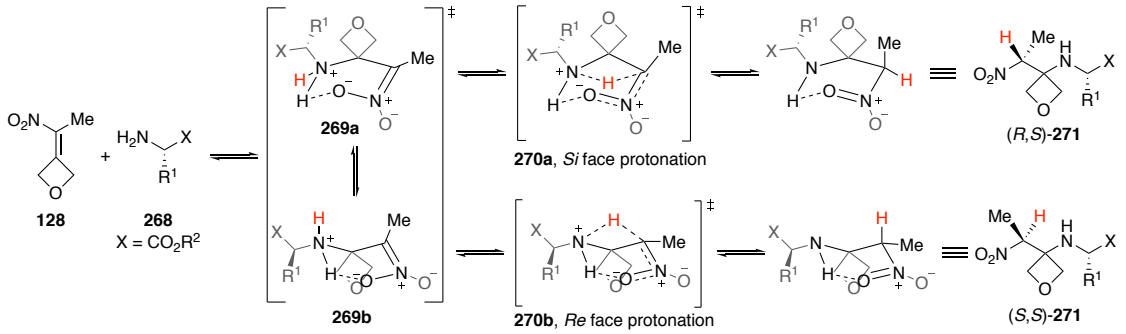

Scheme 4.3 Proposed reaction pathway for the conjugate addition of primary amino esters **268** to nitroalkene **128**.

In comparison, modest diastereoselectivity was obtained using proline methyl ester in the conjugate addition. A possible explanation for the selectivity, is that proline is significantly more conformationally restricted compared to primary α-amino acid residues.[131] This could cause the conjugate addition reaction to proceed *via* a lower energy transition state **272** which leads to preferential protonation of one face of the nitronate intermediate in **272** over the other (Scheme 4.4). As this project did not require the preparation of building blocks containing a proline residue, the conjugate addition of proline to trisubstituted nitroalkenes was not investigated any further. It may be of interest to revisit this reaction in the future.

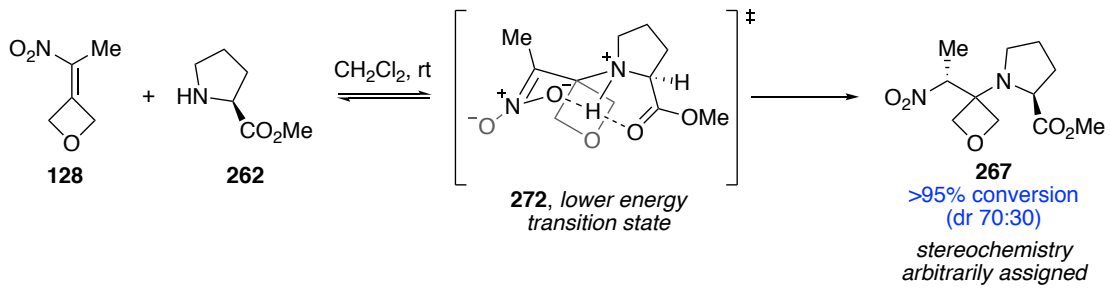

Scheme 4.4 Proposed transition state for the conjugate addition of **262** to nitroalkene **128**.

Following the screening of chiral α-amino esters, additional chiral nitrogen nucleophiles were investigated in the conjugate addition reaction (Table 4.4). Both enantiomers of α-methylbenzylamine **273**, which has previously been used in stereoselective aza-Michael additions,[132] were used and gave the addition products **277** as a 60:40 mixture of diastereoisomers. Encouragingly, the major diastereoisomers could be isolated (dr >95:5) using column chromatography (Table 4.4, entries 1 and 2). No improvement in diastereoselectivity was observed using amine **274**, containing a sterically bulky *tert*-butyl group. The addition product **278** was produced as 60:40 mixture of diastereoisomers which were not separable using column chromatography (Table 4.4, entry 3). Formation of isoxazole **281** was observed when chiral acyclic secondary amine **275** was used in the conjugate addition with no formation of the addition product **279** (Table 4.4, entry 4). This observation is in agreement with reports by Carreira and co-workers.[74] Following the observation with proline, oxazolidinone **276** was used in the conjugate addition. Deprotonation of **276** using potassium *tert*-butoxide followed by addition to nitroalkene **128** gave the addition product **280** as a 70:30 mixture of diastereoisomers (Table 4.4, entry 5). However, the resulting diastereoisomers were not separable using column chromatography.

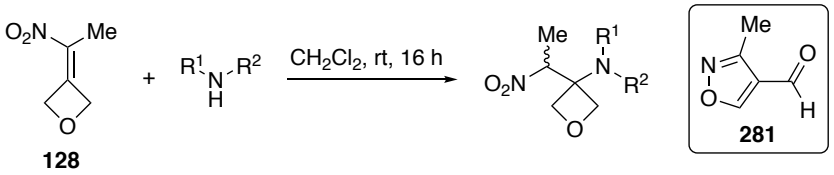

Entry[a]	Nucleophile	Product	Conversion (%)[b]	dr[b]
1	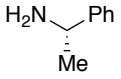 (*S*)-**273**	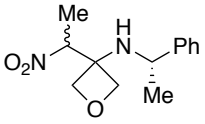 **277a**	>95 (56)[d]	60:40
2	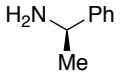 (*R*)-**273**	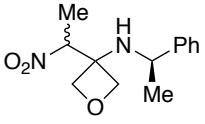 **277b**	>95 (50)[d]	60:40
3	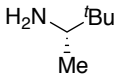 **274**	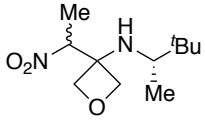 **278**	>95	60:40
4	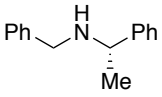 **275**	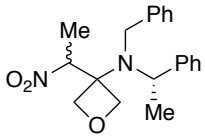 **279**	0[b]	–
5[e]	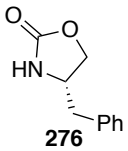 **276**	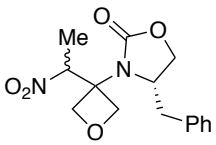 **280**	>95	70:30

Table 4.4 Conjugate addition of chiral nitrogen nucleophiles to trisubstituted nitroalkene **128**. [a] Method: **128** (1.0 equiv), nucleophile (1.2 equiv), CH_2Cl_2 (0.1 M). [b] Determined by ^{1}H-NMR analysis of the crude reaction mixture (see Section 6.7). [c] Major product was rearrangement product **281**. [d] Isolated yield of the major diastereoisomer (dr >95:5, see Section 6.7). [e] Reaction conditions: **128** (1.0 equiv), **276** (1.0 equiv), KO^{t}Bu, (1.0 equiv), 18-crown-6, (1.0 equiv), THF, 0 °C to rt, 16 h.

Following these observations, we were encouraged by the result for the addition of α-methylbenzylamine **273** to nitroalkene **128** (Table 4.4, entries 1 and 2). We proposed that the major diastereoisomer **277** isolated from the reaction could be used to access the required A_{Ox}-containing building block **255** *via* modification of the synthetic approach developed by Carreira and co-workers in a much more expedient fashion (Scheme 4.5).[47]

Enantiopure 3-aminooxetane **282** could be prepared from **277** *via* reduction of the nitro group, cleavage of the α-methylbenzyl group and Fmoc protection of the less sterically hindered amine. Alkylation of enantiopure amine **282** with triflate **283** could then provide A_{Ox}-containing building block **255** (Scheme 4.5). Both enantiomers of **255** would be accessible using this route, which in turn could be used to prepare both enantiomers of an A_{Ox} residue.

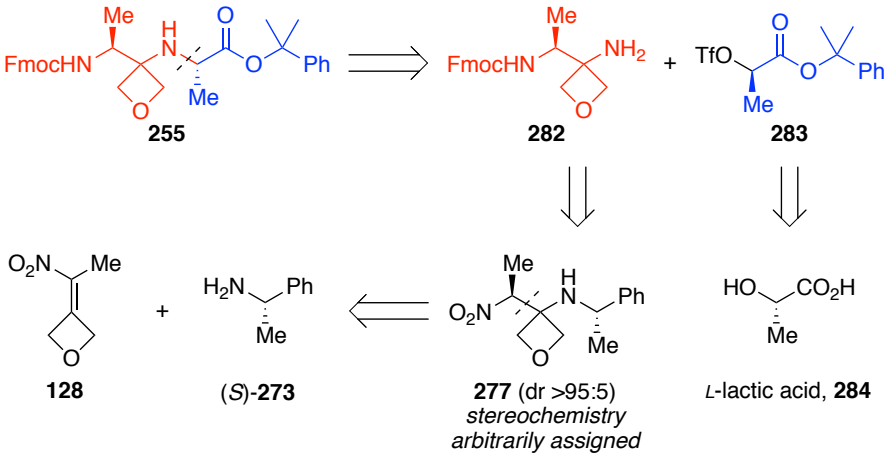

Scheme 4.5 Synthetic approach to A_{Ox}-containing dipeptide building block **255**.

4.3.2.2 Optimisation Studies for the Addition of (*S*)-273 to Nitroalkene 128

Before investigating routes towards enantiopure 3-aminooxetane **282**, we attempted to maximise the diastereoselectivity in the addition reaction of (*S*)-**273** to nitroalkene **128**.

We began by investigating the influence of reaction solvent on the diastereoselectivity (Table 4.5). The majority of solvents investigated gave no improvement. Toluene and *n*-hexane gave a small improvement producing the addition product **277** as 65:35 mixture of diastereoisomers (Table 4.5, entries 4-5). No change in diastereoselectivity was observed using the protic solvents ethanol or nitromethane (Table 4.5, entries 9-10). Hexafluoroisopropanol (HFP) resulted in a decrease in the conversion and diastereoselectivity, and produced the addition product **277** as 55:45 mixture of diastereoisomers (Table 4.5, entry 11). The decrease in conversion is likely a result of acidic hexafluoroisopropanol (pK_a = 9.3)[133] promoting the retro-aza-Michael reaction. Performing the reaction using (*S*)-(+)-α-methylbenzylamine **273** as the solvent gave no improvement in the diastereoselectivity (Table 4.5, entry 12).

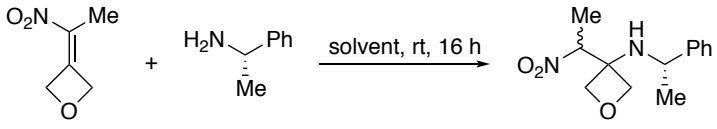

128 (*S*)-**273** **277**

Entry	Solvent	Conversion (%)[a]	dr[a]	Entry	Solvent	Conversion (%)[b]	dr[b]
1	CH_2Cl_2	>95	60:40	7	dioxane	>95	60:40
2	DCE	>95	60:40	8	EtOAc	>95	60:40
3	MeCN	>95	60:40	9	EtOH	>95	60:40
4	toluene	>95	65:35	10	NO_2Me	>95	60:40
5	*n*-hexane	>95	65:35	11	HFP[c]	80	55:45
6	THF	>95	60:40	12[d]	-	>95	60:40

Table 4.5 Solvent screen for the conjugate addition-protonation reaction of (*S*)-**273** with **128**. [a] Method: **128** (1.0 equiv), (*S*)-**273** (1.2 equiv), solvent (0.1 M). [b] Determined by ^{1}H-NMR analysis of the crude reaction mixture (see Section 6.7). [c] HFP = hexafluoroisopropanol. [d] Reaction conditions: **128** (1.0 equiv), (*S*)-**273** (1.0 M), rt, 16 h.

Following the solvent screen, we examined the effect of temperature (*t*) on the diastereoselectivity. The addition of (*S*)-**273** to nitroalkene **128** was performed in toluene, *n*-hexane and dichloromethane at either −20 or −78 °C (Table 4.6). In all cases, performing the reaction at lower temperature gave no improvement to the diastereoselectivity.

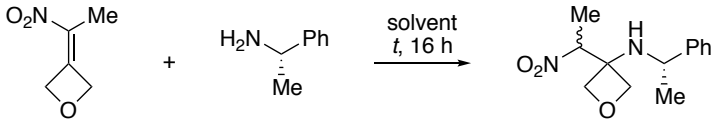

128 (*S*)-**273** **277**

Entry[a]	Solvent	*t*	Conversion (%)[b]	dr[b]
1	PhMe	−20 °C to rt	>95	65:35
2	*n*-hexane	−20 °C to rt	>95	65:35
3	CH_2Cl_2	−78 °C to rt	>95	60:40
4	PhMe	−78 °C to rt	>95	65:35
5	*n*-hexane	−78 °C to rt	>95	65:35

Table 4.6 Temperature screen for the conjugate addition of (*S*)-**273** to **128**. [a] Method: **128** (1.0 equiv), (*S*)-**273** (1.2 equiv), solvent (0.1 M). [b] Determined by ^{1}H-NMR analysis of the crude reaction mixture (see Section 6.7).

Following the results of the solvent and temperature screen, we explored the application of additives in the conjugate addition reaction (Table 4.7). The addition of a suitable reagent has been shown to enhance the reactivity and selectivity in certain reactions.[134] To begin with, the reaction was carried out in the presence of 10 mol% acetic acid, phenol and triethylamine hydrochloride as an additional proton source. The introduction of these additives had no impact on the diastereoselectivity and addition product **277** was isolated as a 60:40 mixture of diastereoisomers (Table 4.7, entries 2-4). Next, the addition of basic additives was investigated. Addition of 10 mol% triethylamine had no impact on the diastereoselective and promoted rearrangement of nitroalkene **128** to isoxazole **281** (Table 4.7, entry 5). Addition of 10 mol% (−)-sparteine **285**, which has been used as a chiral base,[135] had no impact on the diastereoselectivity (Table 4.7, entry 6). Addition of 120 mol% acetic acid gave no improvement in the diastereoselectivity and resulted in a decrease in conversion (Table 4.7, entry 7). No change in diastereoselectivity was observed with the addition of 120 mol% triethylamine hydrochloride (Table 4.7, entry 8). Finally, addition of 120 mol% triethylamine gave no improvement in the diastereoselectivity and resulted in significant amounts of isoxazole **281** formation (Table 4.7, entry 9).

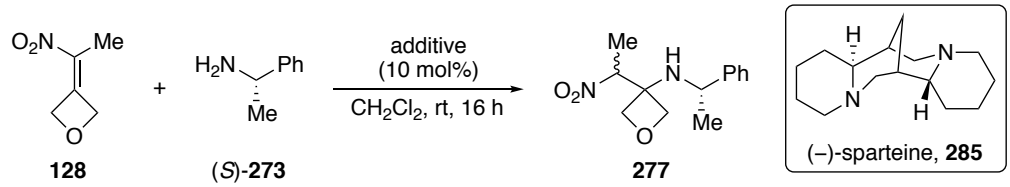

Entry[a]	Additive	Conversion (%)[b]	dr[b]
1	–	>95	60:40
2	AcOH	>95	60:40
3	phenol	>95	60:40
4	$NEt_3 \cdot HCl$	>95	60:40
5	NEt_3	85 (+15% **281**)	60:40
6	(−)-sparteine, **285**	>95	60:40
7[c]	AcOH (120 mol%)	80	60:40
8[c]	$NEt_3 \cdot HCl$ (120 mol%)	>95	60:40
9[c]	NEt_3 (120 mol%)	65 (+35% **281**)	60:40

Table 4.7 Additive screen for the addition reaction of (*S*)-**273** to **128**. [a] Method: **128** (1.0 equiv), (*S*)-**273** (1.2 equiv), additive (10 mol%), CH_2Cl_2 (0.1 M). [b] Determined by ^{1}H-NMR analysis of the crude reaction mixture (see Section 6.7). [c] Method: **128** (1.0 equiv), (*S*)-**273** (1.2 equiv), additive (120 mol%), CH_2Cl_2 (0.1 M).

Recently, Ellman and co-workers have developed a catalytic enantioselective addition of thioacids to azetidine- and oxetane-containing trisubstituted nitroalkenes using bifunctional thiourea catalysts **286** and **287** (Scheme 4.6).[75] Conjugate addition into the nitroalkenes and subsequent enantioselective protonation led to 1,2-nitrothioacetates in high yields and enantioselectivities. This methodology has been extended to include the enantioselective addition of pyrazol-5-ones.[136] Encouraged by these reports, we investigated the application of bifunctional thiourea catalysts in the conjugate addition reaction.

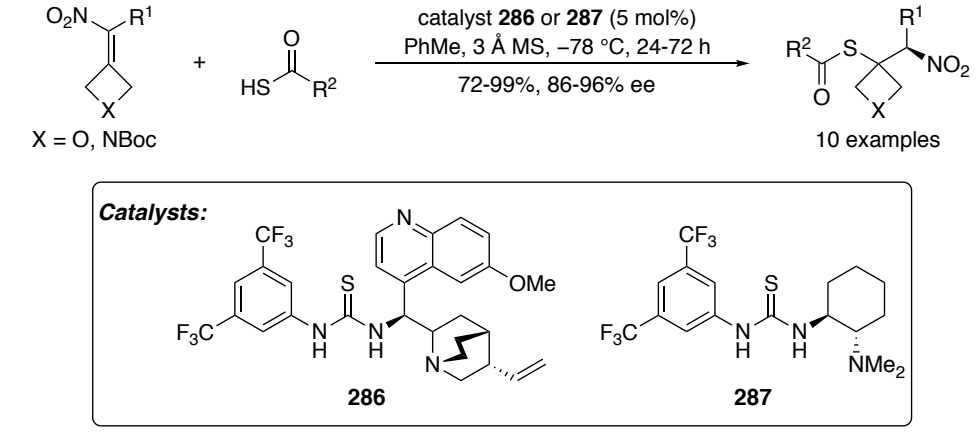

Scheme 4.6 Catalytic enantioselective addition of thioacids to trisubstituted nitroalkenes developed by Ellman and co-workers.[75]

The application of bifunctional thiourea catalyst **287** was investigated in the addition reaction. (*S*)-**273** was added to a mixture of **128** and 10 mol% **287** in dichloromethane at −78 °C. After 24 h, ^{1}H-NMR analysis indicated that addition of catalyst **287** gave no improvement in the diastereoselectivity and addition product **277** was formed as 60:40 mixture of diastereoisomers (Table 4.8, entry 1). Following this, the (*R*)-**273** enantiomer was used in the addition reaction to determine if unfavourable interactions between the chiral catalyst **287** and the (*S*)-enantiomer **273** had prevented control in the protonation step. Under identical conditions, addition of (*R*)-**273** gave the addition product as a 60:40 mixture of diastereoisomers, indicating that the lack of control in the protonation step was not a result of unfavourable interactions between chiral catalyst **287** and the (*S*)- or (*R*)-enantiomer **273** (Table 4.8, entry 2). Although far from exhaustive, attempts to use bifunctional thiourea **287** to influence the diastereoselectivity in the addition of **273** to nitroalkene **128** were unsuccessful. Further investigations into the application of chiral bifunctional thiourea catalysts in the conjugate addition reaction were not carried out.

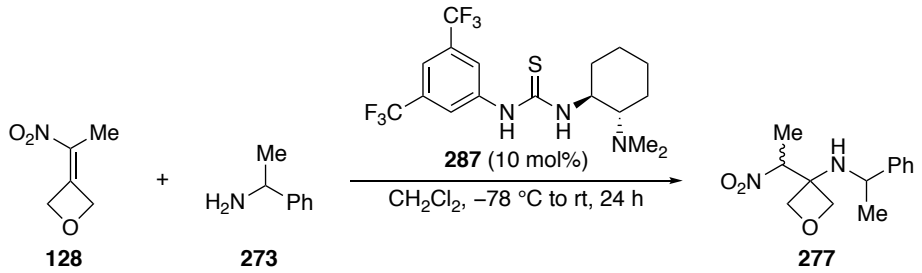

Entry[a]	Amine	Product	Conversion (%)[b]	dr[b]
1	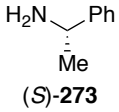 (*S*)-**273**	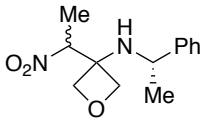 **277a**	>95	60:40
2	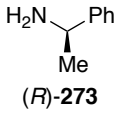 (*R*)-**273**	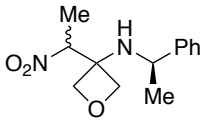 **277b**	>95	60:40

Table 4.8 Application of bifunctional thiourea catalyst **287** in the addition reaction. [a] Method: **128** (1.0 equiv), **273** (1.0 equiv), **287** (10 mol%), CH_2Cl_2 (0.1 M). [b] Determined by ^{1}H-NMR analysis of the crude reaction mixture (see Section 6.7).

Attempts to maximise the diastereoselectivity in the addition of (*S*)-**273** to nitroalkene **128** were unsuccessful. Varying the reaction solvent and temperature gave no significant improvement to the diastereoselectivity and, under the majority of conditions, the addition product **277** was formed as a 60:40 mixture of diastereoisomers. Introduction of basic and acidic additives to the reaction gave no observable improvement to the diastereoselectivity and, in some cases, promoted rearrangement to isoxazole **281** or retro-aza-Michael reaction. Attempts to influence the diastereoselectivity using bifunctional thiourea catalyst **287** also proved unsuccessful. At this point, no further attempts to improve the diastereoselectivity were investigated.

4.3.2.3 Addition of (*S*)-273 to Trisubstituted Nitroalkenes

We next explored the addition of (*S*)-**273** to a variety of other oxetane-substituted nitroalkenes to determine the influence of the α-substituent of the nitroalkene on the diastereoselectivity in the conjugate reaction and to see if the resulting diastereoisomers were separable. This investigation would also provide insight into whether additional oxetane-modified residues could be prepared *via* this route.

We began by preparing trisubstituted nitroalkene **289**, containing an ethyl substituent, which was prepared following a modified procedure previously reported by Ellman and co-workers (Scheme 4.7).[75] Henry reaction of nitropropane with oxetan-3-one, followed by elimination with methanesulfonyl chloride, gave **289** in moderate yield.

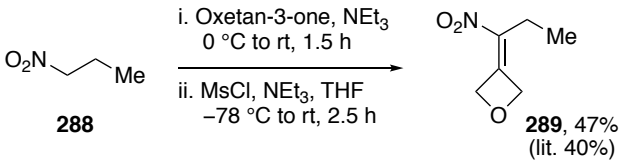

Scheme 4.7 Synthesis of trisubstituted nitroalkene **289**.[75]

Trisubstituted nitroalkene **293**, containing an isopropyl substitution, had previously been accessed from 2-methyl-1-nitropropane **291**.[75] However, no commercial supplies of **191** were available. On this basis, nitroalkene **293** was prepared using a modified route (Scheme 4.8). Nucleophilic substitution of 1-iodo-2-methylpropane **291** with silver nitrite gave crude nitroalkane **291**. Nitro-aldol reaction of **291** with oxetane-3-one at 60 °C gave alcohol **292**, which was isolated in low yield. Elimination with methanesulfonyl chloride yielded trisubstituted nitroalkene **293** in 36% yield.

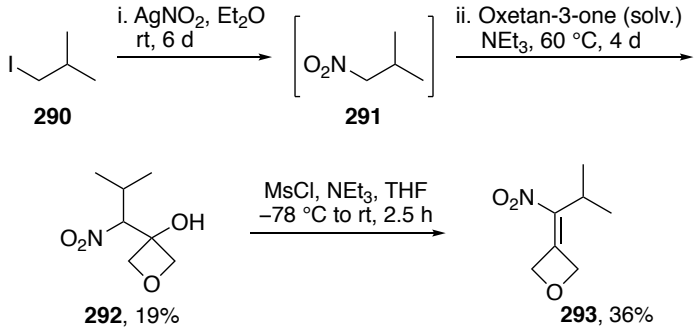

Scheme 4.8 Synthesis of trisubstituted nitroalkene **293**.

Attempts to isolate phenyl-substituted nitroalkene **295** were unsuccessful (Scheme 4.9). Reaction of (nitromethyl)benzene **294** with oxetan-3-one, followed by elimination with methanesulfonyl chloride gave **295** along with significant amounts of isoxazole **296**. Purification using column chromatography resulted in further rearrangement of phenyl-substituted nitroalkene **295** to isoxazole **296**.

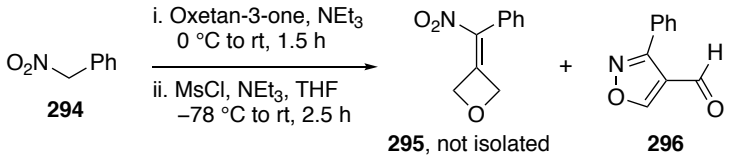

Scheme 4.9 Attempted synthesis of trisubstituted nitroalkene **295**.

With a collection of trisubstituted nitroalkenes in hand, the relationship between the α-substituent and diastereoselectivity in the addition reaction was explored (Table 4.9). The addition of (*S*)-**273** to trisubstituted nitroalkenes was performed in dichloromethane at room temperature and in *n*-hexane at −20 °C. As previously discussed, addition of (*S*)-**273** to methyl-substituted nitroalkene **128** gave a 60:40 mixture of diastereoisomers in dichloromethane and a 65:35 mixture in *n*-hexane at −20 °C (Table 4.9, entries 1 and 2). Addition of (*S*)-**273** to ethyl-substituted nitroalkene **289** resulted in a small increase in the diastereoselectivity producing the addition product **297** as a 65:35 mixture of diastereoisomers in dichloromethane and a 70:30 mixture in *n*-hexane at −20 °C (Table 4.9, entries 3 and 4). Attempts to separate the diastereoisomers of **297** using column chromatography were unsuccessful. Similarly, addition of (*S*)-**273** to benzyl-substituted nitroalkene **31** gave a 65:35 and 70:30 mixture of diastereoisomers in dichloromethane and *n*-hexane respectively (Table 4.9, entries 5 and 6). Attempts to separate the diastereoisomers of **298** using column chromatography were unsuccessful. Isopropyl-substituted nitroalkene **293** gave the highest observed diastereoselectivity. Addition of (*S*)-**273** to nitroalkene **293** gave the addition product **299** as an 80:20 mixture of diastereoisomers in dichloromethane and an 85:15 mixture in *n*-hexane (Table 4.9, entries 7 and 8). Encouragingly, the major diastereoisomer **299** could be isolated in 71% yield using column chromatography (Table 4.9, entry 8).

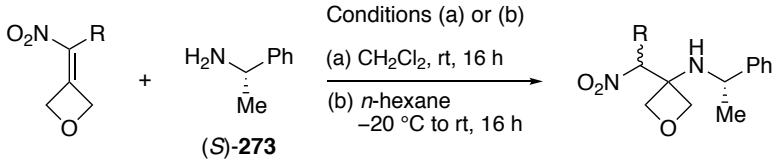

Entry[a]	Nitroalkene	A-value (substituent)[b]	Conditions	Product	Conversion (%)[c]	dr[c]
1	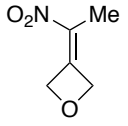 **128**	1.74 (Me)[137]	(a)	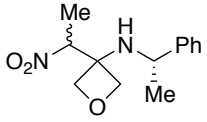 **277**	>95	60:40
2			(b)		>95	65:35
3	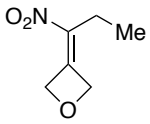 **289**	1.79[137] (CH2CH3)[137]	(a)	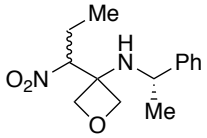 **297**	>95	65:35
4			(b)		>95	70:30
5	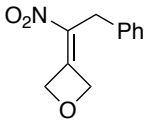 **31**	1.81 (CH2Ph)[138]	(a)	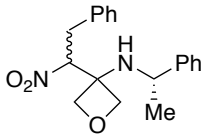 **298**	>95	65:35
6			(b)		>95	70:30
7	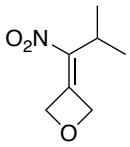 **293**	2.21 (iPr)[137]	(a)	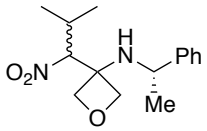 **299**	>95	80:20
8			(b)		>95 (71)[d]	85:15

Table 4.9 Conjugate addition of (*S*)-**273** to trisubstituted nitroalkenes. [a] Method: Nitroalkene (1.0 equiv), (*S*)-**273** (1.2 equiv), solvent (0.1 M). [b] Derived from equilibrium measurements of monsubstituted cyclohexanes. [c] Determined by ^{1}H-NMR analysis of the crude reaction mixture (see Section 6.7). [d] Isolated yield of the major diastereoisomer (dr >95:5).

The relationship between the nitroalkene α-substituent and the diastereoselectivity was studied by plotting the A-value of the α-substituents against the diastereomeric excess (de) of the addition products (Table 4.9 and Figure 4.5). A-values are numerical measurements of steric bulk and are derived from equilibrium measurements of monosubstituted cyclohexanes.[139]

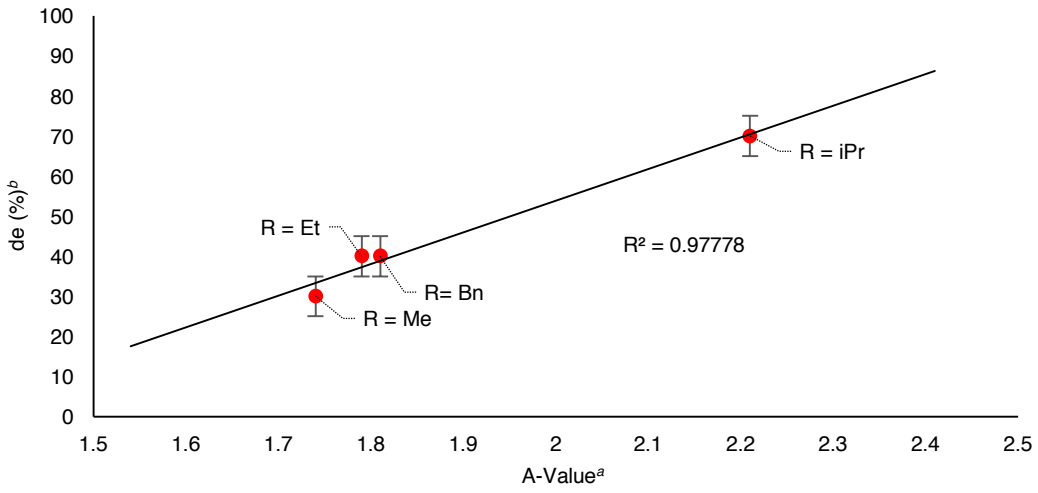

Figure 4.5 A value vs. de for the addition of (*S*)-**273** to trisubstituted nitroalkenes in *n*-hexane, −20 °C to rt. [a] Derived from equilibrium measurements of monsubstituted cyclohexanes. [b] Determined by ^{1}H-NMR analysis of the crude reaction mixture.

Analysis of the plot indicates that there is a strong relationship between the steric bulk of the nitroalkene α-substituent and the diastereoselectivity, although additional data points are required to confirm this trend. As steric bulk increases the diastereoselectivity of the addition reaction increases. It would be of interest to prepare *tert*-butyl-substituted nitroalkene **300** (A-value [^{t}Bu] = >4)[137] to determine if the addition product **301** can be produced as a single diastereoisomer (Scheme 4.10). However, due to time constraints we were unable to investigate additional trisubstituted nitroalkenes in the addition reaction.

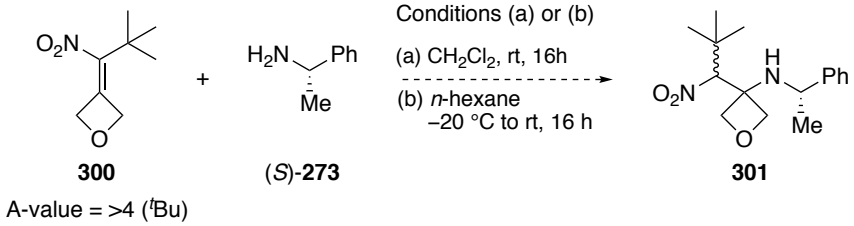

Scheme 4.10 Proposed addition of (*S*)-**273** to *tert*-butyl-substituted nitroalkene **300**.

Following this, the diastereoselectivity of the conjugate addition reaction was monitored over the course of the reaction to determine if reversibility of the reaction (retro-aza-Michael reaction) or epimerisation of the newly generated chiral centre was having an impact on the final ratio of diastereomers of the addition products. As a preliminary investigation, the reaction of (*S*)-**273** to ethyl-substituted nitroalkene **289** was carried out in CD_2Cl_2 at 25 °C and monitored by ^{1}H-NMR spectroscopy. Figure 4.6 shows the

conversion and diastereoselectivity of the addition reaction plotted against time. Although the reaction was not monitored to completion, analysis of the plot shows that conversion to addition product **297** increases at a constant rate over the first 5 hours of the reaction, whilst the de remains constant at 30%. Taken together, these results indicate that reversibility and epimerisation of the chiral centre is not having an impact on the diastereoselectivity of the addition reaction. At this stage, no further studies on the addition of chiral amines to trisubstituted nitroalkenes were carried out.

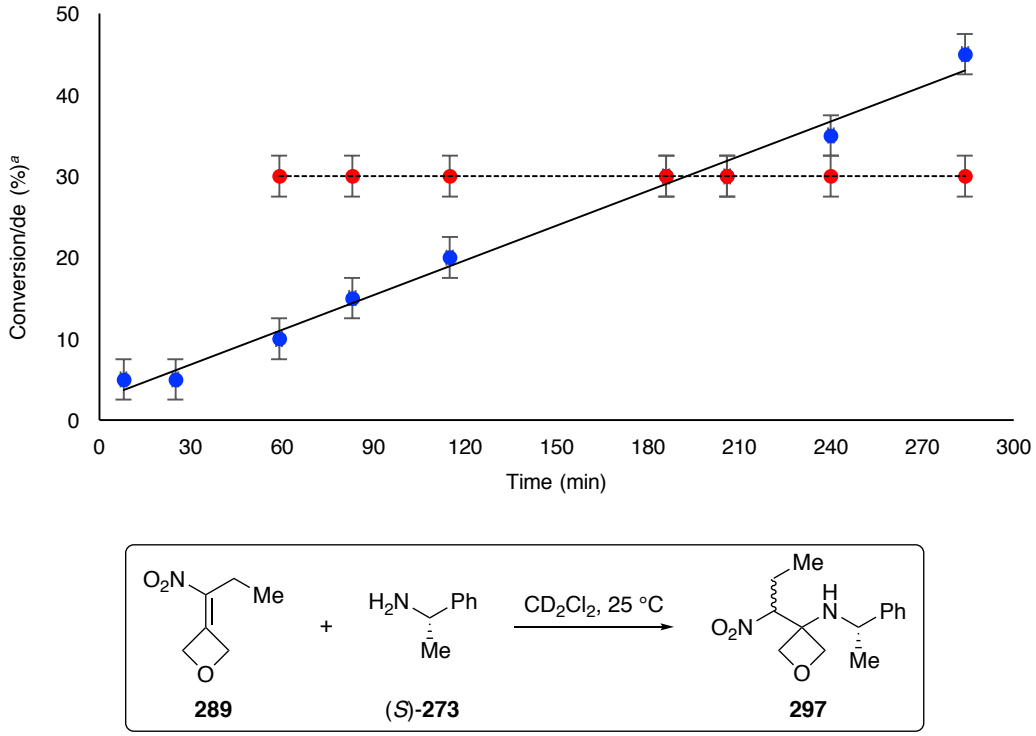

Figure 4.6 Conversion (blue dots) and de (red dots) vs. time for the addition of (*S*)-**273** to nitroalkene **289**. [a] Determined by ^{1}H-NMR analysis of the reaction mixture.

4.3.2.4 Modified Route to Oxetane-Containing Dipeptide Building Blocks

We next explored routes to enantiopure 3-aminooxetane **282** from addition product **277**. Concomitant reduction of the nitro group and cleavage of the α-methylbenzyl group using catalytic hydrogenation conditions gave unprotected 1,2-diamine **302** (Scheme 4.11). Treatment of crude **302** with one equivalent of FmocOSu resulted in protection of the less sterically hindered amine to yield enantiopure 3-aminooxetane **282** with the regiochemistry confirmed using 2D ^{1}H-NMR experiments.

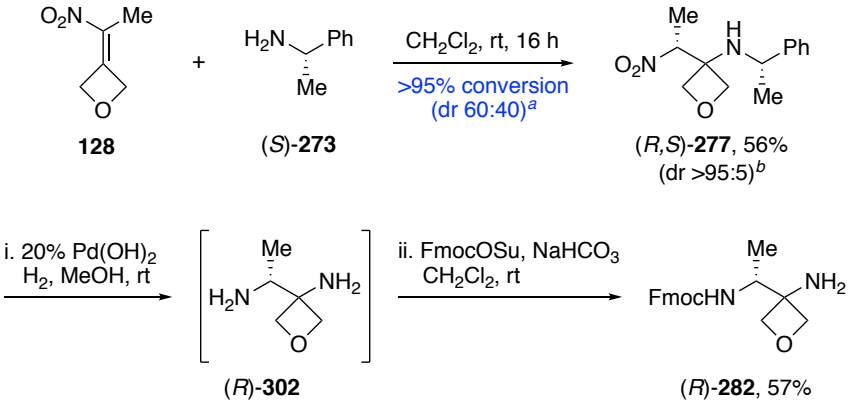

Scheme 4.11 Synthesis of enantiopure amino oxetane (*R*)-**282**. [a] Determined by ^{1}H-NMR analysis of the crude reaction mixture. [b] Major diastereoisomer isolated in dr >95:5 as determined by ^{1}H-NMR (see Section 6.8).

The absolute configuration at the newly created centre in **282** was confirmed as (*R*) by X-ray crystal structure analysis of 4-bromobenzamide derivative **304** (Scheme 4.12). Acylation of **282** with 4-bromobenzoyl chloride **303** gave **304** in excellent yield with crystals suitable for X-ray analysis grown from toluene.

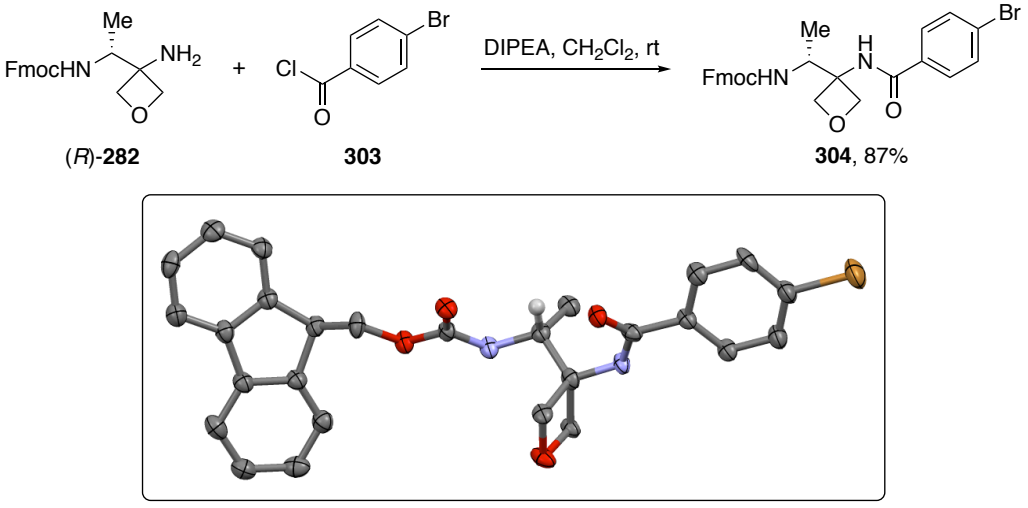

Scheme 4.12 Synthesis of amide **304** and X-ray structure. Hydrogen atoms, except at the C-stereocenter, are omitted for clarity.

Following this, the desired (*S*)-enantiomer **282** was prepared (Scheme 4.13). Addition of (*R*)-**273** to nitroalkene **128** produced a 60:40 mixture of diastereoisomers. Isolation of the major diastereoisomer using column chromatography gave the addition product (*S*,*R*)-**277** in moderate yield. Nitro reduction and cleavage of benzylamine gave 1,2-diamine (*S*)-**302** which was Fmoc protected to yield enantiopure 3-aminooxetane (*S*)-**282**.

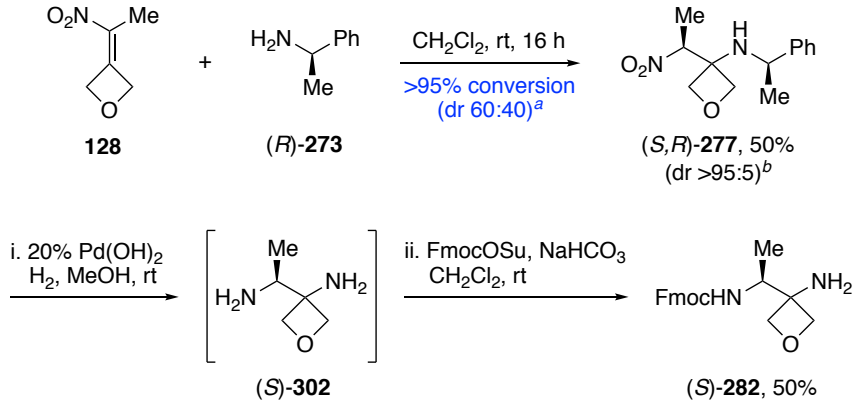

Scheme 4.13 Synthesis of enantiopure amino oxetane (*S*)-**282**. [a] Determined by ^{1}H-NMR analysis of the crude reaction mixture. [b] Major diastereoisomer isolated in dr >95:5 as determined by ^{1}H-NMR (see Section 6.7).

With access to both enantiomers of 3-aminooxetane **282**, we turned our attention to the synthesis of the activated hydroxyester fragment. Initially, we attempted the diazotisation of *D*-alanine to give the corresponding hydroxyacid **306** following a literature procedure (Scheme 4.14).[140] However, after work-up, no desired product was isolated.

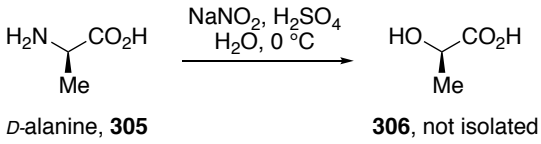

Scheme 4.14 Attempted synthesis of hydroxyacid **306**.[140]

Following this result, the required hydroxyester fragment was prepared using an alternative approach (Scheme 4.15). Cumyl ester (*S*)-**307** was prepared by reaction of *L*-lactic acid with imidate **191**. Next, inversion of the stereochemistry using Mitsunobu reaction conditions yielded diester **308** with (*R*)-stereochemistry. Hydrolysis of the benzoate ester using potassium carbonate in methanol provided the activated hydroxyester precursor (*R*)-**307**.

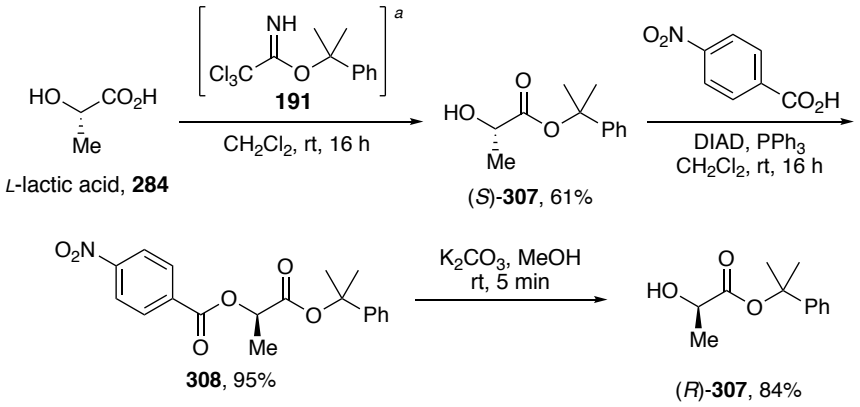

Scheme 4.15 Synthesis of (*R*)-**307** from *L*-lactic acid. [a] Prepared from 2-phenyl-2-propanol **190** and trichloroacetonitrile.

With hydroxyester (*R*)-**307** in hand, we explored the synthesis of triflate **283**. Since alkyl triflates are extremely reactive electrophiles, it was decided that **283** would be prepared immediately prior to the substitution reaction. Hydroxyester (*R*)-**307** was treated with triflic anhydride and DIPEA to provide crude triflate **283** which was used immediately (Scheme 4.16). An excess of DIPEA was required in the reaction to prevent traces of triflic acid promoting cleavage of the cumyl ester. Adopting the conditions developed by Carreira and co-workers,[47] nucleophilic substitution of triflate **283** with both enantiomers of 3-aminooxetane **282** gave the A_{Ox}-containing dipeptide blocks (*R,S*)-**255** and (*S,S*)-**255** in moderate yields. Chiral HPLC analysis confirmed that (*R,S*)-**255** and (*S,S*)-**255** were isolated as single diastereoisomers (see Section 6.8), indicating that the substitution reaction proceeds exclusively in an S_N2 fashion and that no epimerisation arises during the synthesis of enantiopure 3-aminooxetanes (*R*)-**282** and (*S*)-**282**.

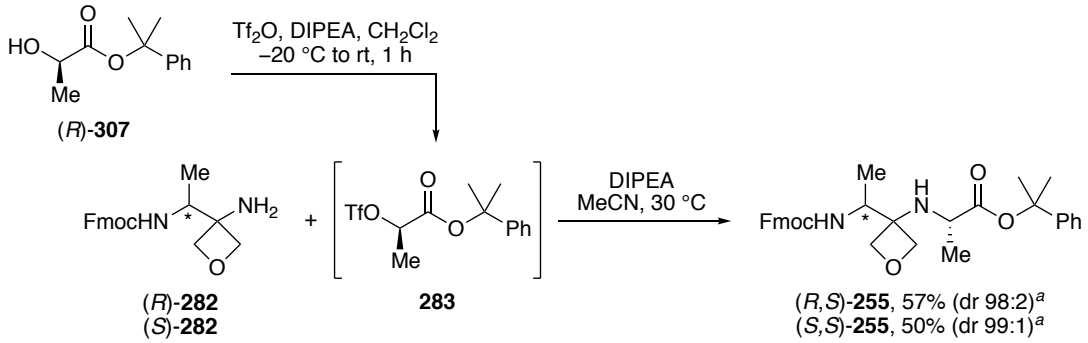

Scheme 4.16 Synthesis of A_{Ox}-containing dipeptide building blocks (*R,S*)-**255** and (*S,S*)-**255**. [a] Determined by chiral HPLC analysis (see Section 6.8).

Following the synthesis of A_{Ox}-containing dipeptide blocks (*R*,*S*)-**255** and (*S*,*S*)-**255**, we proposed addition product **299** could be used to prepare enantiopure 3-aminooxetane **308**, which in turn, could be used to prepare an oxetane-modified valine (V_{Ox}) dipeptide building block **309** (Scheme 4.17). Due to time constraints and the lower yielding synthesis of nitroalkene **293**, we did not attempt this chemistry.

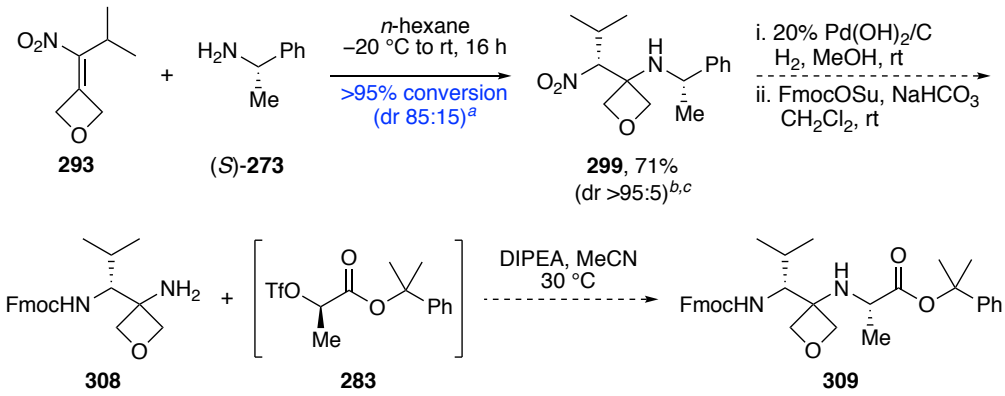

Scheme 4.17 Proposed route to V_{Ox}-containing dipeptide building block **309**. [a] Determined by ^{1}H-NMR analysis of the crude reaction mixture. [b] Major diastereoisomer isolated in dr >95:5 as determined by ^{1}H-NMR. [c] Stereochemistry assigned on the basis of (*R*,*S*)-**277**.

The results of this investigation have demonstrated that the addition products of α-methylbenzylamine **273** to oxetane-substituted nitroalkenes can be used to prepare enantiopure 3-aminooxetanes. Using this approach, Fmoc-protected enantiopure 3-aminooxetane (*S*)-**282** was prepared in three steps from oxetan-3-one in an overall yield of 22%. This is significantly shorter than the route reported by Carreira and co-workers, who prepared Boc-protected enantiopure 3-aminooxetane **66** in twelve steps from Tris hydrochloride, in an overall yield of 15% (Chapter 1, Schemes 1.7 and 1.8).[47] In addition, reaction of enantiopure amines with hydroxyl-cumyl esters can provide oxetane-containing dipeptide building blocks suitable for solid-phase peptide synthesis (SPPS).

4.3.3 Solid-Phase Synthesis of Oxetane-Modified Peptides

With access to A_{Ox}-containing building block (*S*,*S*)-**255** established, the required oxetane-modified pepetides were prepared using the solid-phase methodology described in Chapter 3. This portion of work was carried out by Dr Ina Wilkening at the University of Warwick.

Oxetane-modified peptides were prepared on a Prelude peptide synthesiser (Protein Technologies Inc.) using NovaSyn® TGR R resin that had been preloaded with Fmoc-Tyr(O^{t}Bu)-OH using PyBOP, HOBt and DIPEA in DMF. Fmoc deprotection was carried out using 20% piperidine in DMF. Couplings were performed with Fmoc-protected amino acids using HATU activation with DIPEA in DMF. Two equivalents of oxetane-containing building blocks **255** and **215** were first deprotected using 2% TFA in CH_2Cl_2 to give the crude acid which was dissolved in DMF and manually coupled with resin bound peptide using HATU activation with DIPEA in DMF. This process was repeated using fresh reagents. *N*-Terminal acetylation was carried out manually using Ac_2O:NMM:DMF (5:5:95; v/v/v) at room temperature. Peptide cleavage and concomitant side chain deprotection was performed using a cleavage cocktail of TFA/H_2O/TIS (95:2.5:2.5, v/v/v). For full details, see Section 6.9.

Using these conditions, parent peptide **248** and three oxetane-modified analogues were isolated after purification by reverse-phase HPLC (Table 4.10). Parent peptide **248** was isolated in high purity using standard Fmoc/^{t}Bu SPPS conditions (Table 4.10, entry 1). A_{Ox}-containing building block **255** was used to access central A_{Ox}-modified analogue **246** in high purity (Table 4.10, entry 2). The synthesis of *N*-terminal A_{Ox}-modified analogue **252**, using building block **255**, gave the oxetane-modified peptide **252** in 76% purity along with 16% of an impurity identified as the peptide sequence with deletion of an alanine residue (Table 4.10, entry 3). *N*-Terminal G_{Ox}-analogue **254** was prepared in high purity using G_{Ox}-containing dipeptide building block **215** (Table 4.10, entry 4). During the synthesis of the oxetane-modified peptides, no by-products resulting from acetylation of the 3-aminooxetane unit were observed during the conditions used for *N*-terminal capping with acetic anhydride. Due to time and material constraints, the central G_{Ox}-modified analogue **253** proposed at the outset of this study was not prepared.

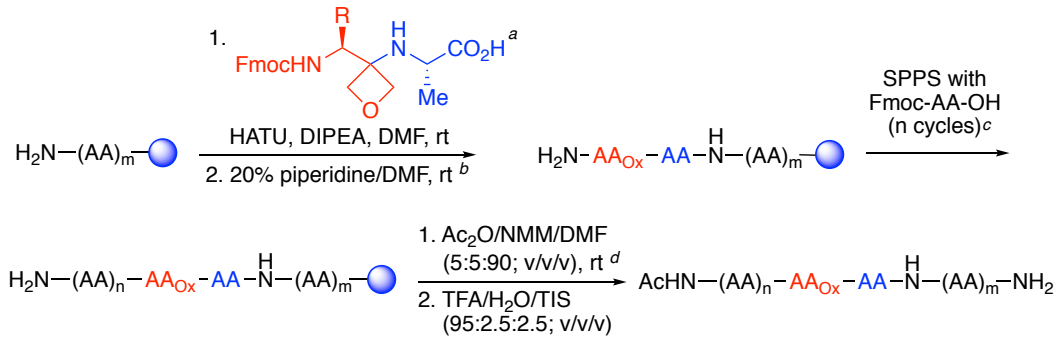

Entry	Building Block	Peptide Sequence	Purity (%)[e]
1	-	Ac-KAAAA-KAAAA-KAAAA-KGY-NH_2, **248** Parent	92
2	(*S,S*)-**255**	Ac-KAAAA-KA$\mathbf{A_{Ox}}$AA-KAAAA-KGY-NH_2, **246** Central A_{Ox}	90
3	(*S,S*)-**255**	Ac-KA$\mathbf{A_{Ox}}$AA-KAAAA-KAAAA-KGY-NH_2, **252** *N*-Terminal A_{Ox}	76
4	**215**	Ac-KA$\mathbf{G_{Ox}}$AA-KAAAA-KAAAA-KGY-NH_2, **254** *N*-Terminal G_{Ox}	90

Table 4.10 Solid-phase synthesis of peptides. [a] Treated with 2% TFA in CH_2Cl_2 for 2 h to reveal the free carboxylic acid from **255** and **215** prior to manual coupling with the resin-bound peptide and repeated using fresh reagents. [b] All deprotections performed at rt for 20 min. [c] All couplings performed at rt for 45 min. [d] Performed at rt for 20 min and repeated using fresh reagents. [e] By reverse-phase HPLC (at 214 nm).

Although *N*-terminal A_{Ox} **252** was isolated in 76% purity, LC-MS analysis confirmed the impurity was the desired peptide sequence with deletion of an alanine residue indicating that the oxetane-containing building block **215** had successfully been incorporated. This observation led us to still investigate the secondary structure content of *N*-terminal A_{Ox} **252** using CD spectroscopy. Attempts to re-synthesise and purify *N*-terminal A_{Ox} **252** to a higher level of purity are ongoing.

These results nicely demonstrate the power of the solid-phase methodology developed in Chapter 3. Oxetane-modified peptides, up to 18 residues in length, were rapidly prepared using standard Fmoc/^{t}Bu SPPS conditions in high purity after purification by reverse-phase HPLC.

4.3.4 Conformational Analysis of Oxetane-Modified Peptides

Following the synthesis of the required peptides, the impact of oxetane-modification on helix structure and stability was determined using circular dichroism (CD) spectroscopy.

4.3.4.1 Methods for Estimating Secondary Structure Content

There are a number of methods used to estimate the secondary structure content of a peptide or protein from analysis of the CD spectrum. The methods used in this study are detailed below.

Method 1 involves analysis of the residual ellipticity at 222 nm ($[\theta]_{222}$) to estimate the helical content. Assuming that the mean helix content (f_H) is linearly related to the observed ellipticity at 222 nm ($[\theta]_{obs222}$) the equation for calculating helical content is:

$$f_H = ([\theta]_{obs222} - [\theta]_C)/([\theta]_{\infty 222} - [\theta]_C) \quad \text{(eq 1)}$$

where the random coil ($[\theta]_C$) and infinite helix ($[\theta]_{\infty 222}$) molar ellipticities are temperature dependent based on the equations:

$$[\theta]_C = 2220 - 53T \quad \text{(eq 2)}$$

$$[\theta]_{\infty 222} = (-44000 + 250T)(1 - k/N_p) \quad \text{(eq 3)}$$

where T is the temperature in degrees Celcius, k is the number of non-hydrogen-bonded peptide C=O groups in a carboxyamidated peptide and N_p is the number of peptide units. For this study, a value of $k = 3.0$ is used. As oxetane-modification involves deletion of an amide bond, the value of N_p used for the oxetane-modified peptides is 18 compared with a value of 19 for the parent peptide system **248**.[24,141]

Method 2 uses DichroWeb, an online interface to several algorithms that perform analysis of the CD data. These algorithms are used to provide a total estimate of all secondary structure content. Estimated secondary structure content is determined by comparison of the CD data of the sample with a set of reference proteins and peptides with known secondary structure content. For this study, DichroWeb analysis was performed using Selcon3 algorithms (Ref. set 4) to estimate secondary structure content.[142,143]

4.3.4.2 CD Analysis of Oxetane-Modified Peptides

To begin with, far-UV (250-185 nm) CD spectra were recorded in 10 mM potassium phosphate, pH 7.0 at 5 °C. This buffer system ensures that the peptides are soluble and stable in solution, and has previously been used in CD analysis of parent peptide **248**. Figure 4.7 compares the spectra of the oxetane-modified peptides to the spectrum of parent peptide **248**. Parent peptide **248** shows a characteristic α-helix spectrum with minima at ~222 and ~208 nm and a strong positive peak at ~190 nm. The oxetane-modified peptides are significantly less structured and display typical random coil spectra with a maximum at ~217 nm and minimum at ~197 nm. These results suggest that oxetane-modification of the central and *N*-terminal region of an α-helix has a strongly helix-destabilising effect under aqueous conditions.

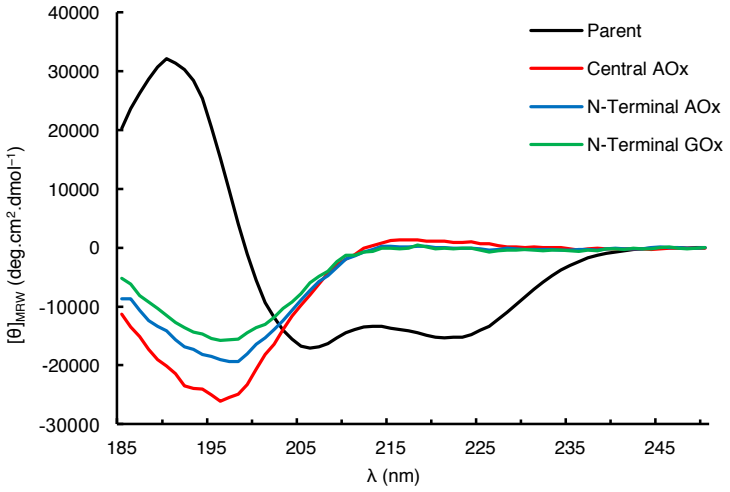

Figure 4.7 Far-UV CD spectra of parent peptide **248** (black line) and the oxetane-modified peptides **246** (red line), **252** (blue line) and **254** (green line) in 10 mM potassium phosphate, pH 7.0 at 5 °C.

To quantify the destabilising effect of oxetane-modification, CD spectra of the peptides were recorded in 10 mM potassium phosphate buffer, pH 7.0 at 0 °C, with the addition of 1.0 M NaCl. The addition of NaCl has been shown to allow a more reliable determination of helical content for alanine-based model peptides and is often used for quantitative analysis. In addition, the helical value obtained for parent peptide **248** using these conditions would allow direct comparison with the value previously reported.[24] It should be noted that NaCl absorbs strongly below 200 nm which means that this region of the spectrum cannot be used for analysis. CD spectra of the peptides in 10 mM potassium phosphate buffer, pH 7.0 at 0 °C, with the addition of 1.0 M NaCl are shown in Figure 4.8. Under these conditions, parent peptide **248** displays more pronounced α-

helical character with deep minima at ~222 and ~207 nm. The oxetane-modified peptides displayed characteristic random coil spectra.

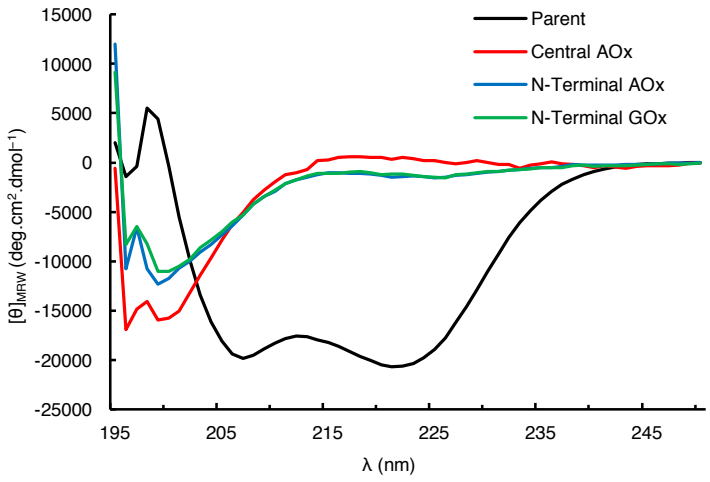

Figure 4.8 Far-UV CD spectra of parent peptide **248** (black line) and the oxetane-modified peptides **246** (red line), **252** (blue line) and **254** (green line) in 10 mM potassium phosphate, pH 7.0 at 0 °C, with the addition of 1.0 M NaCl.

The helical contents of the peptides were calculated using **Method 1**. For parent peptide **248** this results in a helix content of 58%, which is slightly lower than the reported value of 68% (Table 4.11, entry 1).[24] Central A_{Ox} **246** was calculated to have a helix content of 4% (Table 4.11, entry 2). The *N*-terminal A_{Ox} **252** and G_{Ox} **254** peptides were both calculated to have a slightly higher helix content value of 9% (Table 4.11, entries 3 and 4). Absorption of NaCl below 200 nm prevented analysis of the CD data using DichroWeb (**Method 2**).

Entry	Peptide	$[\theta]_{222}$ (deg.cm^2.dmol^{-1})^a	f_H (%) **Method 1**^{b}
1	Parent, **248**	−20655	58
2	Central A_{Ox}, **246**	+487	4
3	*N*-Terminal A_{Ox}, **252**	−1443	9
4	*N*-Terminal G_{Ox}, **254**	−1170	9

Table 4.11 Estimated helical content of the peptides in 10 mM potassium phosphate, pH 7.0 at 0 °C, with the addition of 1.0 M NaCl. [a] $[\theta]_{MRW}$ at 222 nm. [b] Mean helix content calculated using equations 1-3 described in **Method 1**.

These results indicate that oxetane-modification has a strongly helix-destabilising effect under aqueous conditions. Oxetane-modification in the central region of an α-helix results in essentially complete loss of helicity and favours the formation of random-coil conformations. Oxetane-modification of the *N*-terminal region retained a small amount of helical structure but predominantly favoured random coil conformations.

Following these observations, CD spectra of the peptides were recorded in methanol at 0 °C. Methanol, along with trifluoroethanol, is known to induce helicity in peptides and proteins.[144] Hence, the oxetane-modified peptides were expected to show an increase in helical content. Figure 4.9 compares the spectra of the oxetane-modified peptides to the spectra of parent peptide **248**. All of the oxetane-modified peptides show a significant increase in helical character compared to the spectra recorded in aqueous solution. Comparison with parent peptide **248** reveals a destabilising effect of oxetane-modification in methanol. However, the decrease in helical content caused by oxetane-modification is more prominent in central A_{Ox} **246** than the *N*-terminal analogues **252** and **254**. Central A_{Ox} **246** displays a minimum at ~207 nm accompanied by a shoulder at ~222 nm with intensities in a ratio $R = [\theta]_{222}/[\theta]_{208}$ of ~0.45, in addition to a positive band at ~195 nm of reduced intensity. These characteristics are suggestive of a 3_{10}-helix,[145] which has been proposed as an intermediate in the folding/unfolding mechanism of α-helices.[146,147] *N*-Terminal modified analogues **252** and **254** display identical spectra and indicate a significant fraction of α-helix.

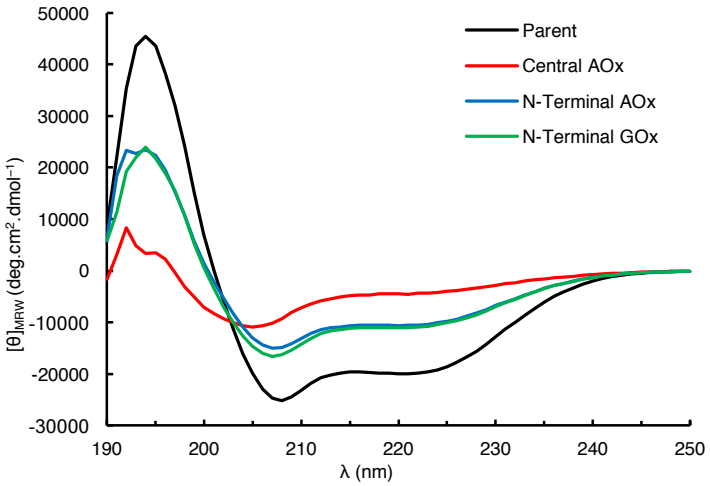

Figure 4.9 Far-UV CD spectra of parent peptide **248** (black line) and the oxetane-modified peptides **246** (red line), **252** (blue line) and **254** (green line) MeOH at 0 °C.

The helical content of the peptides were calculated using **Method 1** and **Method 2**. The values were in good agreement for all peptides and are shown in Table 4.12. Parent peptide **248** had a helix content of 56-57% in methanol, which was comparable to the value of 58% under aqueous conditions (Table 4.12, entry 1). The helix content of central A_{Ox} **246** was significantly lower (15-17%) confirming that oxetane-modification in the central region results in a strongly helix-destabilising effect (Table 4.12, entry 2). Helix content values for *N*-terminal analogues **252** (33-34%) and **254** (34-37%) confirmed that oxetane-modification of the *N*-terminal region also results in a helix-destabilising effect, although to a lesser extent (Table 4.12, entries 3-4). In addition, these values are very similar indicating that the α-substituent of the oxetane-modified residue has little impact on helix stability when located at the *N*-terminus in methanol. Further analysis using **Method 2** indicates that the oxetane-modified peptides show a significant increase in β-sheet content compared to parent peptide **248**, with central A_{Ox} **246** displaying a β-sheet content of ~30% (Table 4.12). The CD spectrum of a β-sheet is typically characterised by a minimum at ~215 nm and a maximum between 190-200 nm. As previous work in our group has suggested that oxetane-modification could give rise to turn-like conformations,[1] it is possible that introduction of an oxetane-modified residue into these sequences is promoting turn-like features which result in formation of β-hairpin conformations.

Entry	Peptide	$[\theta]_{222}$ (deg.cm^2.dmol^{-1})^a	f_H (%) **Method 1**^{b}	f_H (%) **Method 2**^{c}
1	Parent, **248**	−19861	56	57
2	Central A_{Ox}, **246**	−4394	17	15
3	*N*-Terminal A_{Ox}, **252**	−10496	33	34
4	*N*-Terminal G_{Ox}, **254**	−10902	34	37

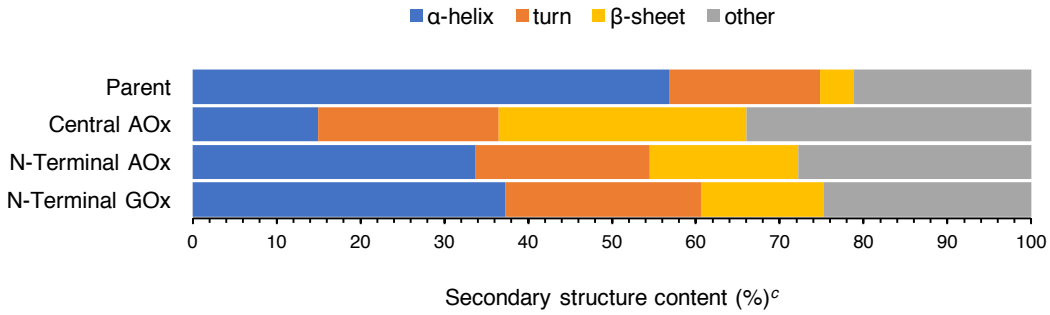

Table 4.12 Estimated secondary structure content of the peptides in MeOH at 0 °C. [a] $[\theta]_{MRW}$ at 222 nm. [b] Calculated using equations 1-3 described in **Method 1**. [c] Calculated using DichroWeb algorithms (Selcon3, Ref. set 4) as described in **Method 2**.[142,143]

These observations suggest that the oxetane-modified analogues can retain an appreciable amount of helical content in methanol. However, comparison with parent peptide **248** reveals again a helix-destabilising effect of the oxetane-modification, although the decrease in helical content is less pronounced than in aqueous solution. Oxetane-modification in the central region of an α-helix results in significant loss of helicity and only a small amount of helix content is retained. In comparison, oxetane-modification of the *N*-terminal region retains a significant fraction of helix content. Additionally, DichroWeb analysis (**Method 2**) indicates an increased preference for the oxetane-modified peptides to adopt β-sheet conformations in methanol compared to parent peptide **248**, with central A_{Ox} **246** displaying a β-sheet content of ~30%.

Encouraged by these observations, we were interested to further probe the impact of oxetane-modification on the secondary structure using 1D and 2D ^{1}H-NMR experiments. However, the conditions used to record the CD spectra were not suitable for the desired ^{1}H-NMR experiments. Therefore, CD spectra of the peptides were recorded in 80% methanol in water at 5 °C to confirm the secondary structure content under the conditions required for the ^{1}H-NMR experiments (80% MeOD in H_2O at 5 °C). CD spectra of the

peptides are shown in Figure 4.10. Under these conditions central A_{Ox} **246** is significantly less structured but still displays a small amount of helical structure. Both *N*-terminal analogues **252** and **254** retain helical structure with A_{Ox} analogue **252** displaying a larger amount of helical content. Again, parent peptide **248** shows a typical α-helix spectrum.

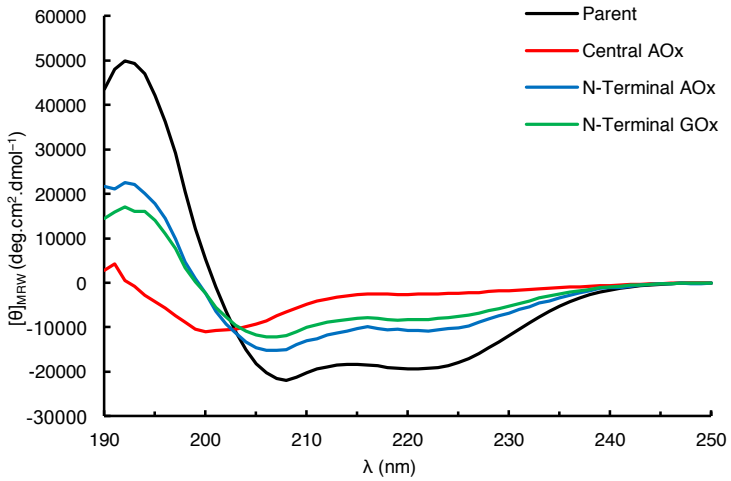

Figure 4.10 Far-UV CD spectra of parent peptide **248** (black line) and the oxetane-modified peptides **246** (red line), **252** (blue line) and **254** (green line) in 80% MeOH in H_2O at 5 °C.

Calculated values for helix content using **Method 1** and **Method 2** were in good agreement for the oxetane-modified peptides (Table 4.13, entries 2-4). The helix content of central A_{Ox} **246** is ~12%, further demonstrating that oxetane-modification in the central region has a strongly helix-destabilising effect (Table 4.13, entry 2). *N*-Terminal A_{Ox} **252** was calculated to have a helix content of 32-34%, compared with a value of 27% for G_{Ox} analogue **254**. In contrast to the results in 100% methanol, there is an appreciable difference between the helix content values of *N*-terminal analogues **252** (32-34%) and **254** (27%) indicating that the α-substituent of the oxetane-modified residue can have an impact on helix stability when located at the *N*-terminus. There was a significant difference between the helix content values calculated for parent peptide **248** (Table 4.13, entry 1). However, both values confirmed parent peptide **248** contained a substantial amount of helical character (46-56%). In addition, analysis using **Method 2** showed again that the oxetane-modified peptides have a preference to form β-sheet conformations compared to parent peptide **248**, with central A_{Ox} **246** displaying a β-sheet content of ~26%.

Entry	Peptide	$[\theta]_{222}$ (deg.cm^2.dmol^{-1})^a	f_H (%) **Method 1**^{b}	f_H (%) **Method 2**^{c}
1	Parent, **248**	−19239	56	46
2	Central A_{Ox}, **246**	−2483	12	12
3	*N*-Terminal A_{Ox}, **252**	−10813	34	32
4	*N*-Terminal G_{Ox}, **254**	−8262	27	27

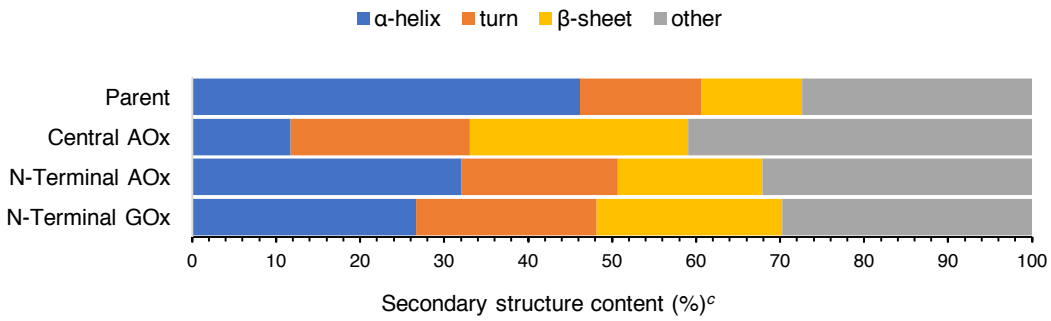

Table 4.13 Estimated secondary structure content of the peptides in 80% MeOH in H_2O at 5 °C. [a] $[\theta]_{MRW}$ at 222 nm. [b] Calculated using equations 1-3 described in **Method 1**. [c] Calculated using DichroWeb algorithms (Selcon3, Ref. set 4) as described in **Method 2**.[142,143]

Comparison of the helix content values obtained in 80% methanol in water at 5 °C with those obtained in 100% methanol at 0 °C indicate that no loss of helix content is observed for parent peptide **248** and *N*-terminal A_{Ox} **252**, and only a small decrease is detected for central A_{Ox} **246** and *N*-terminal G_{Ox} **254**. Based on these observations, it would be of interest to record CD in various concentrations of methanol in water, along with other helix inducing solvents such as trifluroethanol, in an attempt to maximise the helix content of the oxetane-modified peptides. Due to time constraints, further CD analysis of the peptides has not been performed.

^{1}H-NMR analysis and molecular dynamic (MD) simulations are being used to further understand the impact of oxetane-modification on the secondary structure content and stability of α-helices. This work is being conducted in collaboration with Eleanor Jayawant, Dr Ann Dixon and Dr Becky Notman at the University of Warwick, and is currently ongoing.

4.3.4.3 Conclusions from Circular Dichroism Analysis

Circular dichroism (CD) analysis of the oxetane-modified peptides in 10 mM potassium phosphate gave only random coil structures. In contrast, CD analysis of the oxetane-modified peptides in methanol all showed some helical character. Quantification of the CD data revealed that introduction of an oxetane-modification at two different positions within an alanine-based α-helical peptide has a helix-destabilising effect. There are three likely explanations for this:

1. The oxetane moiety is significantly bulkier in comparison to a carbonyl group, which makes it difficult to integrate into the densely packed α-helix.
2. The change in hybridisation (sp^2 to sp^3) of the oxetane-modified residue results in a higher degree of rotational freedom, which is unfavourable in an α-helix.
3. Both the hydrogen-bonding acceptor ability of an oxetane and the hydrogen-bonding donor ability of an amine are weaker than an amide,[38,110] which could further contribute to the helix-destabilising effect.

Despite their strong helix-destabilising effect, our results indicate that it is possible to incorporate oxetane-modification into the *N*-terminal region of α-helical structures and still retain an appreciable amount of helical content. In addition, the destabilising effect of oxetane-modification may be different in α-helices that are already stabilised by side-chain interactions, or by application of stapling techniques. Therefore, it would be worthwhile investigating the impact of oxetane-modification on stabilised α-helices.

Further analysis of the secondary structure content using DichroWeb revealed a preference for the oxetane-modified peptides to adopt β-sheet like conformations. It is possible that the higher degree of rotational freedom of the oxetane-modified residue is promoting turn-like features which result in formation of β-hairpin conformations. It would be of great interest to investigate this observation further by preparing oxetane-modified analogues of known β-hairpin motifs and determining the impact of oxetane-modification on the structure and stability of these important types of secondary structure.[148,149]

4.4 Conclusions

In conclusion, this chapter has described the synthesis and structural analysis of oxetane-modified analogues of an alanine-based α-helical peptide. The first part of this chapter

described efforts towards the synthesis of dipeptide building blocks containing oxetane-modified residues beyond glycine. These efforts have led to the development of a novel route to enantiopure 3-aminooxetane (*S*)-**282** which was used to prepare an A_{Ox}-containing dipeptide building block (*S,S*)-**255** (Scheme 4.18). This route is significantly shorter than the approach previously developed by Carreira and co-workers.[47]

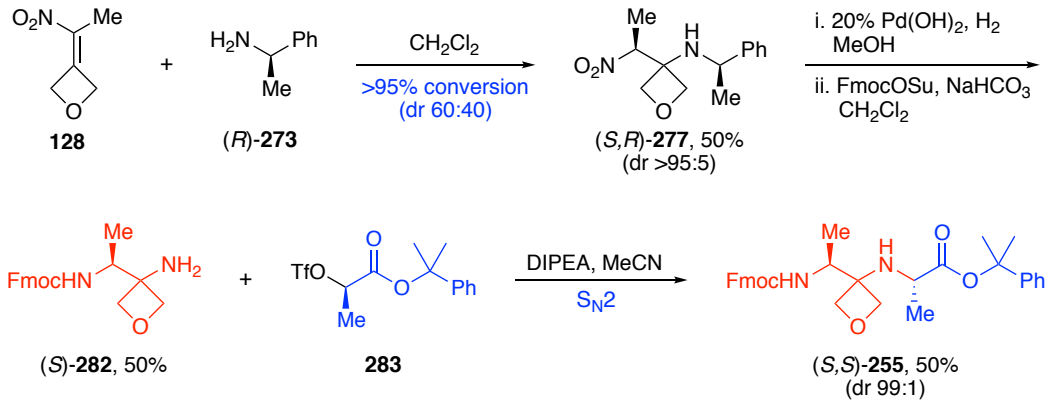

Scheme 4.18 Synthesis of oxetane-modified alanine (A_{Ox}) dipeptide building block (*S,S*)-**255**.

Using the solid-phase peptide synthesis (SPPS) methodology described in Chapter 3, oxetane-containing dipeptide building blocks **255** and **215** were used to prepare analogues of an alanine-based α-helical peptide in which a single alanine residue located in the central or *N*-terminal region was replaced with an oxetane-modified residue. The synthesis of these analogues further demonstrates the benefit of the solid-phase methodology as oxetane-modified peptides, up to 18 residues in length, can be rapidly prepared using standard Fmoc/^{t}Bu SPPS conditions in high purity after purification by reverse-phase HPLC.

Circular-dichroism (CD) studies of these peptides revealed that introduction of an oxetane-modification at a central and *N*-terminal position has a helix-destabilising effect. Despite this, *N*-terminal oxetane-modified analogues **252** and **254** retain a considerable amount of helical content in methanol. Further analysis of the secondary structure content of the oxetane-modified analogues reveals an increase in β-sheet content compared to the parent peptide **248**. ^{1}H-NMR experiments and molecular dynamic (MD) simulations are currently being conducted to further understand the structural basis of the helix-destabilising effect of oxetane-introduction.

Chapter 5: Key Findings and Future Work

5.1 Key Findings

This section provides a summary of the key findings reported in Chapters 2-4.

An efficient two-step sequence to spirocyclic scaffolds related to 2,5-diketopiperazines (DKPs) wherein one of the C=O bonds is replaced with an oxetane or azetidine ring has been developed. Conjugate addition of α-amino methyl esters to nitroalkenes generated from oxetan-3-one or *N*-Boc-azetidin-3-one gives the spirocyclic precursors. Subsequent, reduction of the nitro group with Raney Ni under an atmosphere of hydrogen generates, after spontaneous cyclisation of the primary amine, the spirocycles in good overall yield (Scheme 5.1).

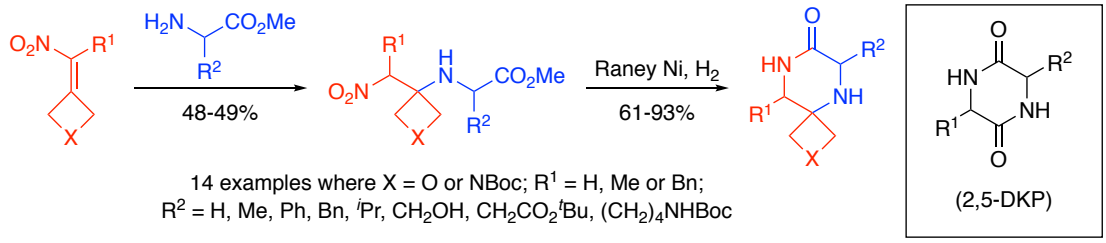

Scheme 5.1 Synthesis of oxetane- and azetidine-containing spirocycles related to the 2,5-diketopiperazine framework.

These rigid scaffolds could be further functionalised by selective alkylation of the amide and amine nitrogens as well as by carbonyl reduction to the corresponding piperazine (Scheme 5.2).

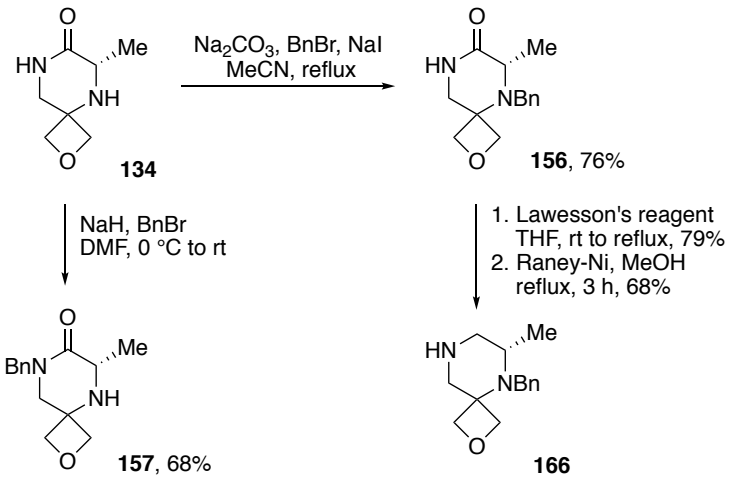

Scheme 5.2 Further functionalisation of oxetane-containing spirocycles.

In collaboration with Dr Andrew Jamieson, methodology for the synthesis of oxetane-modified peptides (OMPs) using conventional Fmoc/^{t}Bu solid-phase peptide synthesis (SPPS) techniques has been developed. The approach involves using cumyl-protected dipeptide building blocks where the ester can be selectively cleaved with 2% TFA in CH_2Cl_2 to reveal the terminal carboxylic acid. Initially, Fmoc-protected dipeptide building blocks in which the oxetane residue is based on glycine were prepared in three steps in solution (Scheme 5.3).

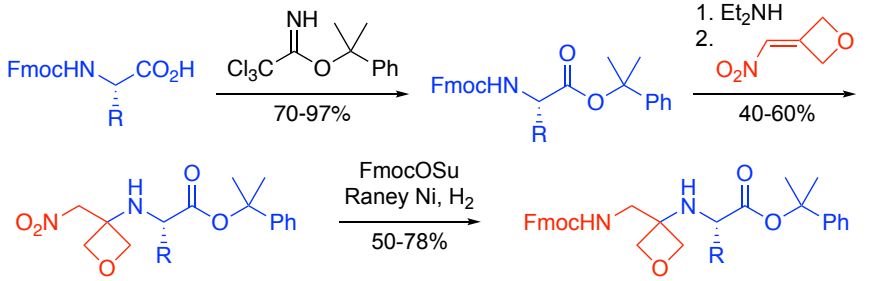

Scheme 5.3 Synthesis of dipeptide building blocks containing an oxetane-modified glycine residue.

A route to enantiopure 3-aminooxetane (*S*)-**282** was developed to access Fmoc-protected dipeptide building block (*S,S*)-**255** containing an oxetane-modified alanine residue. The key step involves addition of (*R*)-(+)-α-methylbenzylamine **273** to trisubstituted-nitroalkene **128** to give a mixture of diastereoisomers, from which the major diastereoisomer (*S,R*)-**277** was isolated in dr >95:5 (Scheme 5.4). The key limitation being the need to be able to efficiently separate the diastereoisomers as high levels of diastereocontrol could not be realised in the conjugate addition step. Although the full scope has yet to be explored, preliminary results indicate that dipeptide building blocks in which the oxetane residue is based on valine could be prepared using this approach.

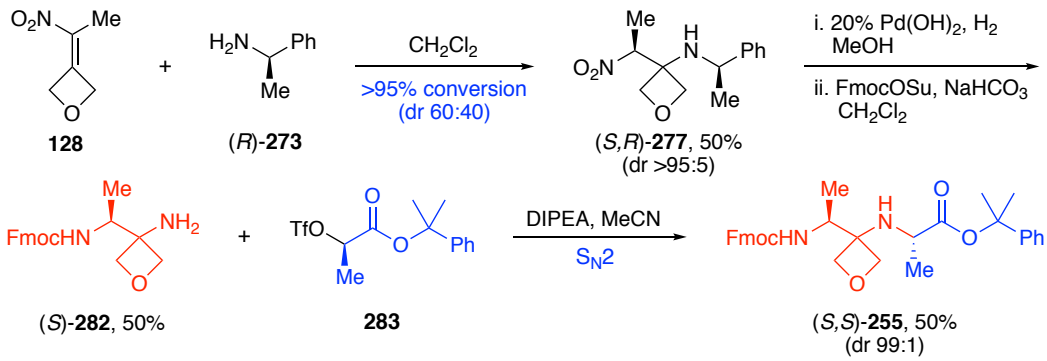

Scheme 5.4 Synthesis of dipeptide building block (*S,S*)-**255**.

Solution-phase chemistry using oxetane-containing dipeptide building blocks has demonstrated that amide couplings can proceed in high yield, without racemisation, and without the need to protect the secondary amine of the 3-aminooxetane unit. Hence, oxetane-modified peptides can be produced in high purities and acceptable yields using conventional Fmoc/^{t}Bu SPPS methods. This methodology has been used to prepare oxetane-modified peptides up to 18 residues in length, including analogues of Leu- and Met-enkephalin**,** bradykinin, and alanine-based model peptides (Figure 5.1).

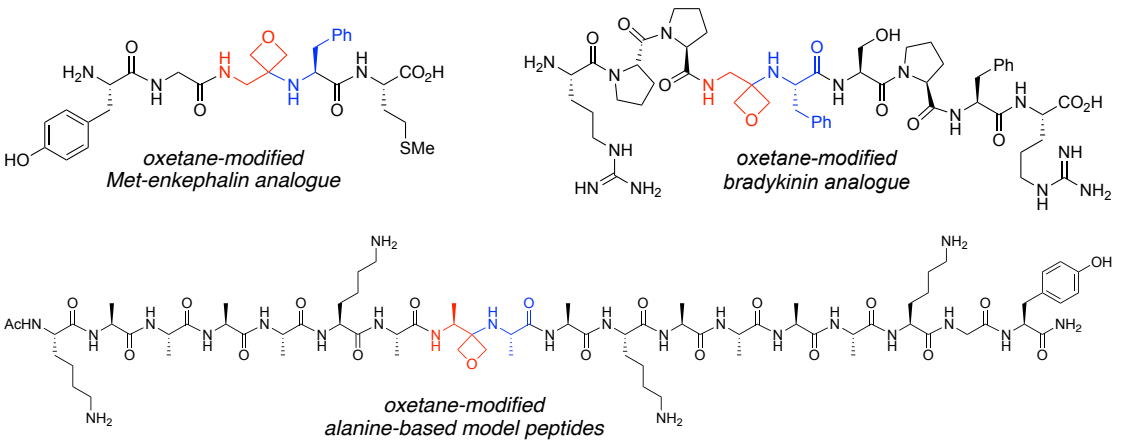

Figure 5.1 Solid-Phase Synthesis of Oxetane-Modified Peptides

Preliminary studies regarding the biological properties of oxetane-modified Met- **231** and Leu-enkephalin **232** analogues indicate that oxetane modification of the central glycine residue has a detrimental impact on the binding affinities towards the δ- and μ-opioid receptors. However, a more complete study by Carreira and co-workers has demonstrated that oxetane-modified analogues of Leu-enkephalin have improved hydrolytic stability in human serum and that two of four analogues retain reasonable affinity towards the δ-opioid receptor.[47]

Circular-dichroism (CD) studies on oxetane-modified alanine-based α-helices have revealed that introduction of an oxetane-modification at a central and *N*-terminal position results in a significantly helix-destabilising effect. Despite this, *N*-terminal oxetane-modified analogues **252** and **254** retain a considerable amount of helical content in methanol at 0 °C (Table 5.1). Further analysis of the secondary structure content revealed an increased preference for the oxetane-modified analogues to adopt β-sheet conformations compared to the parent peptide **248**.

Entry	Peptide Sequence	f_H (%)[a]
1	Ac-KAAAA-KAAAA-KAAAA-KGY-NH_2, **248** Parent	57
2	Ac-KAAAA-KA**A_{Ox}**AA-KAAAA-KGY-NH_2, **246** Central A_{Ox}	15
3	Ac-KA**A_{Ox}**AA-KAAAA-KAAAA-KGY-NH_2, **252** *N*-Terminal A_{Ox}	34
4	Ac-KA**G_{Ox}**AA-KAAAA-KAAAA-KGY-NH_2, **254** *N*-Terminal G_{Ox}	37

Table 5.1 Estimated helix content of the peptides in MeOH at 0 °C. [a] Calculated using DichroWeb algorithms (Selcon3, Ref. set 4).[142,143]

An additional collaboration, with Professor Dave Adams and Dr Andrew Jamieson, has also demonstrated that Fmoc-protected oxetane-dipeptides can be used to prepare hydrogels. For example, oxetane-based dipeptide **175** is an effective gelator, forming hydrogels at a concentration of 3 mg mL^{-1}. Furthermore, **175** is significantly more resistant to proteolysis compared to the parent dipeptide **245** (Scheme 5.5).

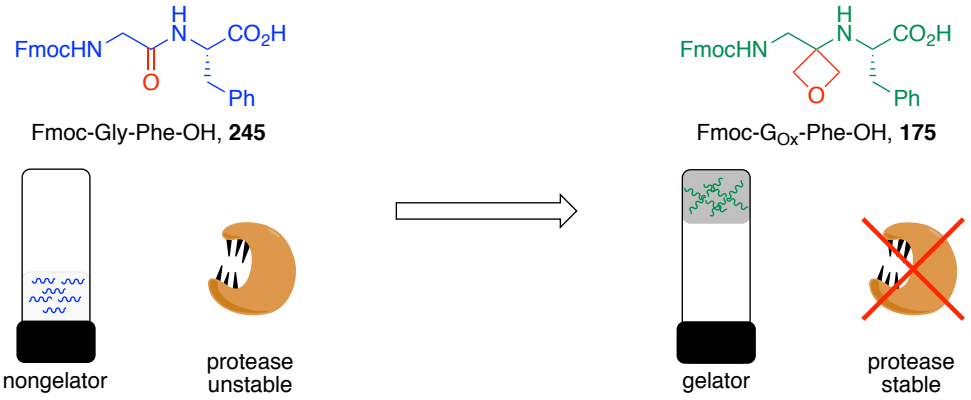

Scheme 5.5 Enzymatically-stable oxetane-based dipeptide hydrogels.

5.2 Future Work

It would be of interest to further explore modifications of the oxetane- and azetidine-containing spirocycles prepared in Chapter 1. For example, routes towards 2-substituted oxetan-3-ones and azetidine-3-ones **311** *via* metalated SAMP/RAMP hydrazones have

previously been prepared within our research group.[150,151] These substituted-analogues could be used to access nitroalkene **312**, which in turn could be used to prepare 2-substituted oxetane- and azetidine-containing spirocycles **314** (Scheme 5.6).

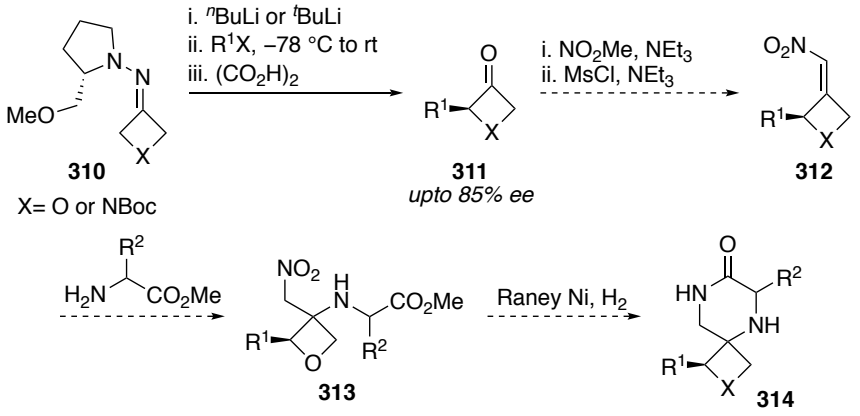

Scheme 5.6 Synthesis of 2-substituted oxetane- and azetidine-containing spirocycles **314**.

Furthermore, the application of β- and γ-amino methyl esters in the conjugate addition step could provide access to 7- and 8-membered oxetane- and azetidine-containing spirocycles **317** (Scheme 5.7). These additional modifications would further demonstrate the utility of these novel scaffolds.

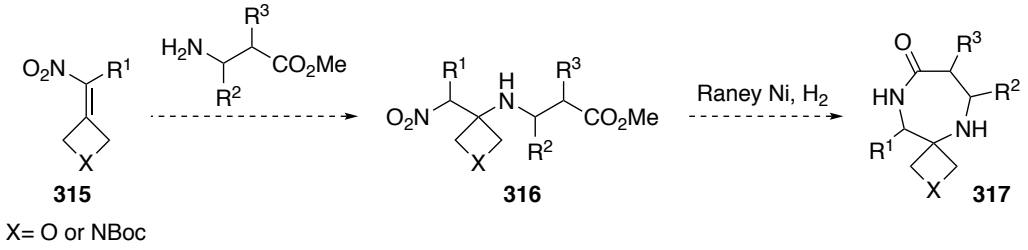

Figure 5.7 Synthesis of 7-membered oxetane- and azetidine-containing spirocycles **317**.

Due to time constraints, we were unable to explore the full potential of the approach towards enantiopure 3-aminooxetanes **319**. It would be of great interest to further investigate the addition of α-methylbenzylamine **273** to a variety of other trisubstituted nitroalkenes **24** to determine if additional oxetane-modified residues can be prepared using this approach (Scheme 5.8).

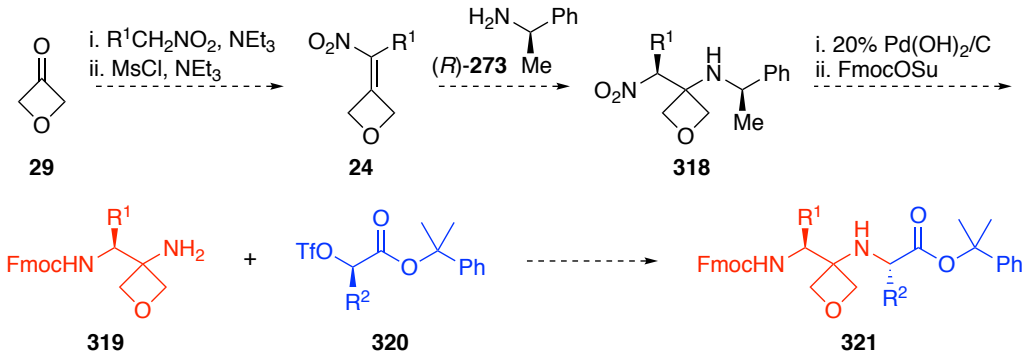

Scheme 5.8 Route towards oxetane-containing dipeptide building blocks **321** *via* enantiopure 3-aminooxetanes **319**.

Alternative routes to enantiopure 3-aminooxetanes **321**, such as nitro-Mannich reactions also merit investigation. For example, an auxiliary controlled reaction of nitroalkanes with imine **322**, derived from the condensation of oxetan-3-one and Ellmans's auxillary **62**,[152] could be developed as a novel route towards enantiopure 3-aminooxetanes **319** (Scheme 5.9). Similar base-promoted diastereoselective additions of nitroalkanes to *N*-*tert*-butylsulfinyl imines have previously been reported in the literature.[153,154]

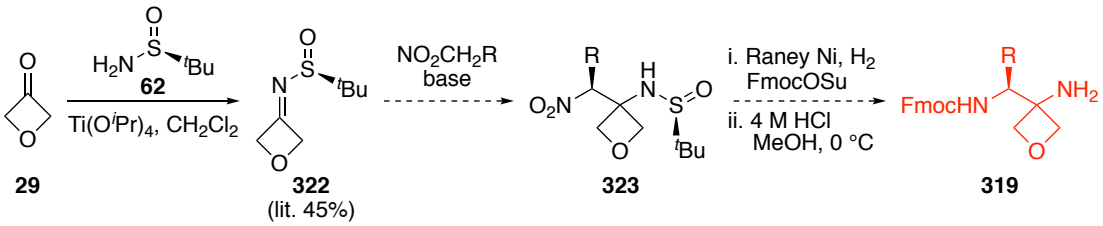

Scheme 5.9 Nitro-Mannich approach to enantiopure 3-aminooxetanes **319**.

Having established that introduction of oxetane-modification into α-helices results in helix-destabilisation, the impact of oxetane-modification on the structure and stability of other secondary structure types warrants investigation. Gellman and co-workers have demonstrated that tetrapeptide **324**, possessing a *D*-Pro-*D*-Ala sequence, readily forms a β-hairpin conformation with two intramolecular H-bonds in CD_2Cl_2 (Scheme 5.10).[155] This sequence offers an excellent experimental template to study the impact of oxetane-modification on the structure and stability of turn regions. Oxetane-modified analogues **325** and **326**, in which the *D*-alanine or *D*-proline residue is substituted for either a G_{Ox}, *D*-A_{Ox} or *L*-A_{Ox} residue, could be prepared using chemistry described in this thesis (Scheme 5.10). The structure and stability of these analogues relative to the native system

could then be studied using CD and NMR spectroscopy. These experiments would help determine the impact of oxetane-modification within turn regions.

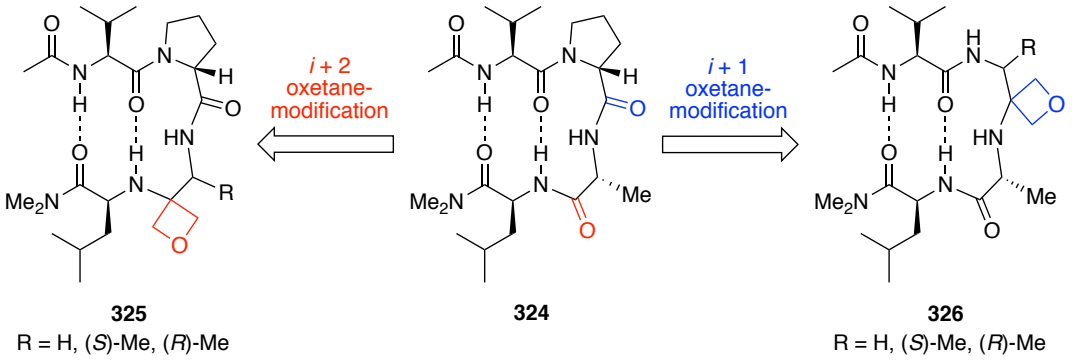

325
R = H, (*S*)-Me, (*R*)-Me

324

326
R = H, (*S*)-Me, (*R*)-Me

Scheme 5.10 Study of oxetane-modified *β*-hairpin motifs.[155]

Furthermore, it would be of interest to explore the impact of oxetane-modification within the strand region of a *β*-hairpin. Searle and co-workers have demonstrated that 16-mer **327** is ~50% folded in water and adopts a *β*-hairpin structure stabilised by the H-bonding network depicted in Figure 5.2.[156] This sequence is an excellent experimental platform to investigate the impact of oxetane-modification on the structure and stability within strand regions. Initially, if access to a dipeptide building block in which the oxetane residue is based on valine is realised, oxetane-modified analogues **328** and **329**, in which the valine residues at the *i* + 4 and *i* + 13 positions are substituted for a V_{Ox} residue, could be prepared using the solid-phase methodology described in this thesis. Additional oxetane-modified analogues could be prepared if access to other oxetane-modified residues is realised. The impact of oxetane-modification within the strand region could then be explored using CD and NMR spectroscopy. In addition, oxetane-modified analogue **330**, in which the glycine residue at the *i* + 8 position is substituted for a G_{Ox} residue could be prepared to further examine the impact of oxetane-modification within turn regions.

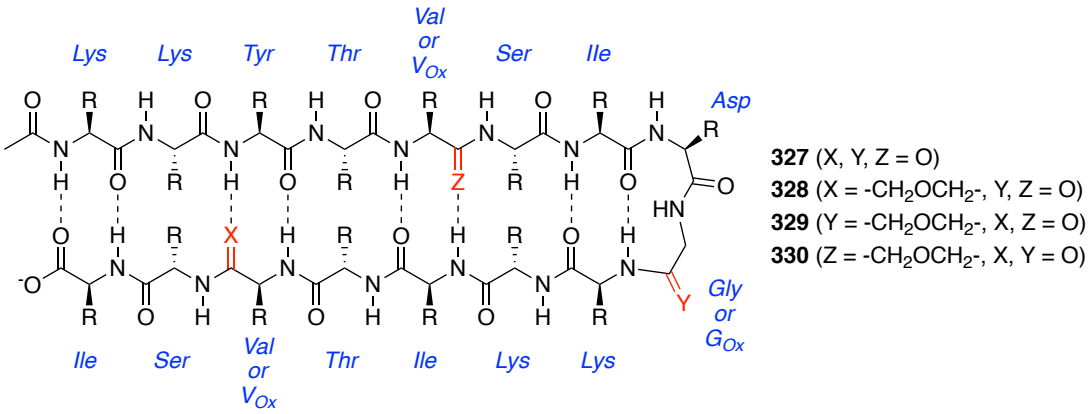

Figure 5.2 Study of oxetane-modification within the β-strand region of a hairpin.[156]

Chapter 6: Experimental Section

6.1 General Details

Anhydrous solvents were purchased from Sigma-Aldrich or Acros Organics in Sure-Seal™ bottles for use as reaction solvents. All other solvents were reagent grade and used as received. Petroleum ether refers to the fraction that boils in the range 40-60 °C. Commercially available starting materials were used without purification unless otherwise stated. All amino acids are of *L*-configuration unless otherwise stated. Compounds (*S*)-**109**,[1] (*R*)-**109**,[1] **110**,[1] **126**,[76] **34**[1] and **178**[1] were prepared following previously described literature procedures. Amino methyl esters were free based from the corresponding hydrochloride salt following a literature procedure and used immediately.[77]

Thin layer chromatography was performed on pre-coated aluminium-backed plates (Merck Silicagel 60 F254), visualised by UV 254 nm and then stained with phosphomolybdic acid (PMA) dip and heated. Flash column chromatography was performed using Aldrich 40-63 μm silica gel.

Nuclear magnetic resonance (NMR) spectra were recorded on Bruker DPX (300 or 400 MHz), or AV (500 MHz) spectrometers. Chemical shifts (δ) are reported in parts per million (ppm) relative to the solvent residual peaks ($CDCl_3$ δ_H: 7.26 ppm, δ_C: 77.16 ppm; CD_3OD δ_H: 3.31, δ_C 49.00; C_6D_6 δ_H: 7.16, δ_C: 128.06; DMSO-d_6 δ_H: 2.50 ppm, δ_C 39.52 ppm). Coupling constants (*J*) are reported in hertz (Hz). Splitting patterns are abbreviated as follows: singlet (s), doublet (d), triplet (t), quartet (q), quintet (quint), septet (sep), multiplet (m), broad (b), or combination of these. NMR assignments were deduced using 1D ^{13}C experiments (APT) and 2D experiments (COSY, HSQC and HMBC).

Low-resolution mass spectra were recorded on an Agilent Technologies 6130 Quadrupole LC-MS instrument. High-resolution mass spectra were recorded using a Bruker MaXis Impact. Infrared spectra were recorded with a Bruker ALPHA Platinum ATR apparatus and are reported as observed. Optical rotations $[\alpha]_D^T$ were measured using an AA-1000 polarimeter and reported as observed.

6.2 General Procedures

General procedure 1: *Synthesis of oxetane containing nitro amino esters*

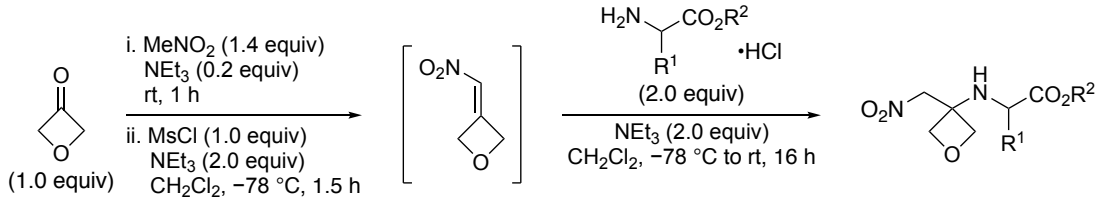

Oxetan-3-one (1.0 equiv), nitromethane (1.4 equiv) and triethylamine (0.2 equiv) were stirred at room temperature for 60 min. CH_2Cl_2 (0.25 M) was added and the reaction mixture cooled to –78 ˚C. Triethylamine (2.0 equiv) was added followed by the dropwise addition of a solution of methanesulfonyl chloride (1.0 equiv) in CH_2Cl_2 (1.0 M). The reaction mixture was left to stir at –78 ˚C for 90 min. Meanwhile, to a solution of amino ester hydrochloride (2.0 equiv) in CH_2Cl_2 (0.25 M) was added triethylamine (2.0 equiv) and this mixture was stirred at room temperature for 10 min. This solution was added to the oxetane mixture *via* syringe at –78 ˚C. The reaction mixture was allowed to warm to room temperature and stirred for 16 h. A saturated solution of NH_4Cl (8 mL/mmol) was added to the reaction mixture and stirred for 10 min. The layers were separated and the aqueous extracted with CH_2Cl_2 (2 x 10 mL/mmol) and EtOAc (2 x 10 mL/mmol). The combined organics were washed with saturated $NaHCO_3$ (2 x 8 mL/mmol) then brine (4 mL/mmol), dried ($MgSO_4$), filtered and concentrated under reduced pressure, and the products purified by column chromatography.

General Procedure 2: *Synthesis of oxetane nitroalkenes*

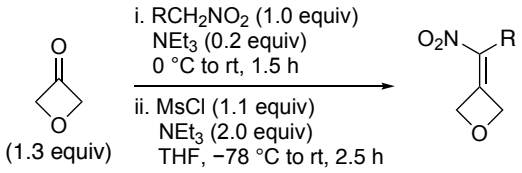

The synthesis of oxetane nitroalkenes were adapted from procedures originally published by Carreira[74] and Ellman.[75]

Oxetan-3-one (1.3 equiv) and nitroalkane (1.0 equiv) were cooled to 0 °C. Triethylamine (0.2 equiv) was added and the reaction mixture stirred at 0 °C for 30 min and then at room temperature for 90 min. THF (0.1 M) was added and the reaction cooled to −78 °C. Triethylamine (2.0 equiv) was added followed by the dropwise addition of

methanesulfonyl chloride (1.1 equiv). The reaction mixture was left to stir at −78 °C for 90 min, after which the dry-ice bath was removed, and the reaction mixture stirred for 60 min. The reaction mixture was filtered through a plug of silica gel eluting with 25% EtOAc in petroleum ether. The eluent was concentrated under reduced pressure and the products purified by column chromatography.

General procedure 3: *Synthesis of nitro amino esters from trisubstituted nitroalkenes*

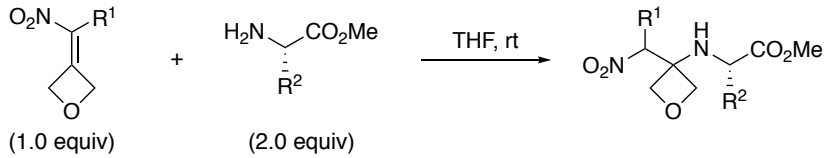

The nitroalkene (1.0 equiv) was dissolved in THF (0.1 M). Free amino ester (2.0 equiv) in THF (0.25 M) was added and the reaction mixture stirred at room temperature for the time stated. The reaction mixture was concentrated under reduced pressure to give a crude product which was purified by column chromatography or recrystallization.

General procedure 4: *Nitro reduction and cyclisation*

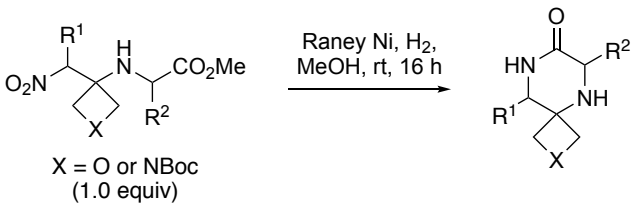

The substrate (1.0 equiv) and Raney Ni (1.0 mL/mmol, slurry in H_2O) in MeOH (0.1 M) were stirred at room temperature under an atmosphere of H_2 (balloon) for 16 h. The reaction mixture was filtered through a plug of Celite® eluting with EtOAc. The eluent was concentrated under reduced pressure and the crude product purified by column chromatography.

General procedure 5: *Synthesis of azetidine containing nitro amino esters*

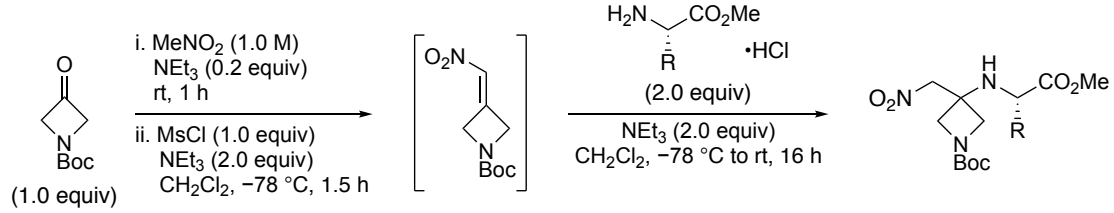

N-Boc-azetidin-3-one (1.0 equiv) and triethylamine (0.2 equiv) in nitromethane (1.0 M) were stirred at room temperature for 60 min. The reaction mixture was concentrated under reduced pressure and the resulting material dissolved in CH_2Cl_2 (0.25 M). The reaction mixture was cooled to –78 °C and triethylamine (2.0 equiv) added followed by the dropwise addition of methanesulfonyl chloride (1.0 equiv) in CH_2Cl_2 (1.0 M). The reaction mixture was left to stir at –78 °C for 90 min. Meanwhile, to a solution of amino ester hydrochloride (2.0 equiv) in CH_2Cl_2 (0.25 M) was added triethylamine (2.0 equiv) and stirred at room temperature for 10 min. This solution was added to the azetidine mixture *via* syringe at –78 °C. The reaction mixture was allowed to reach room temperature and left to stir for 16 h. A saturated solution of NH_4Cl (8 mL/mmol) was added to the reaction mixture and stirred for 10 min. The layers were separated and the aqueous extracted with CH_2Cl_2 (2 x 10 mL/mmol) and EtOAc (2 x 10 mL/mmol). The combined organics were washed with saturated $NaHCO_3$ (2 x 8 mL/mmol) and brine (4 mL/mmol), dried ($MgSO_4$), filtered and concentrated under reduced pressure to give a crude product that was purified by flash column chromatography.

General procedure 6: *Nitro reduction and Fmoc protection using 1.2 equivalents of FmocOSu*

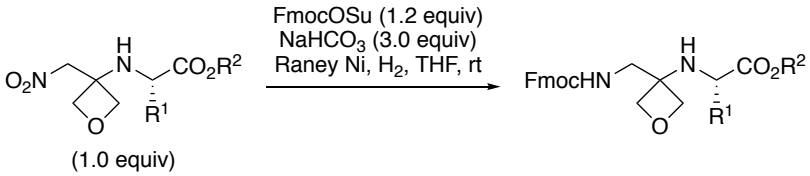

To substrate (1.0 equiv) in THF (0.1 M) was added Fmoc *N*-hydroxysuccinimide ester (1.2 equiv), $NaHCO_3$ (3.0 equiv) and Raney Ni (1 mL/mmol, slurry in H_2O). The reaction mixture was stirred at room temperature under an atmosphere of H_2 (balloon) until consumption of starting material (MS monitoring). The reaction mixture was filtered through a plug of Celite® eluting with EtOAc. The eluent was washed with saturated Na_2CO_3 (3 x 8 mL/mmol) and brine (4 mL/mmol), dried ($MgSO_4$), filtered and

concentrated under reduced pressure, and the products purified by column chromatography.

General procedure 7: *Synthesis of cumyl esters*

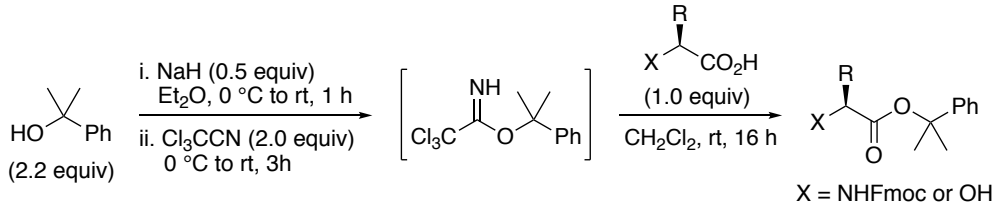

Cumyl esters were prepared following a modified method of Potier and co-workers.[103] To sodium hydride (60% dispersion in mineral oil, 0.5 equiv) in Et_2O (0.5 M) at 0 °C was added freshly distilled 2-phenyl-2-propanol (2.2 equiv) in Et_2O (2.0 M) and the reaction mixture was stirred at room temperature for 1 h. The reaction mixture was cooled to 0 °C. Trichloroacetonitrile (2.0 equiv) was added, the reaction mixture was stirred at room temperature for 3 h and then concentrated under reduced pressure. Petroleum ether (4.0 M) and MeOH (0.5 equiv) were added and this mixture was stirred at room temperature for 10 min. The reaction mixture was filtered through a plug of Celite® eluting with petroleum ether. The eluent was concentrated under reduced pressure to give the crude imidate. To the crude imidate in CH_2Cl_2 (1.0 M) was added carboxylic acid (1.0 equiv) and the reaction mixture was stirred at room temperature for 16 h. The mixture was filtered through a plug of Celite® to remove precipitated trichloroacetamide. The crude product was concentrated under reduced pressure and purified by column chromatography.

General procedure 8: *Synthesis of oxetane containing nitro amino cumyl esters*

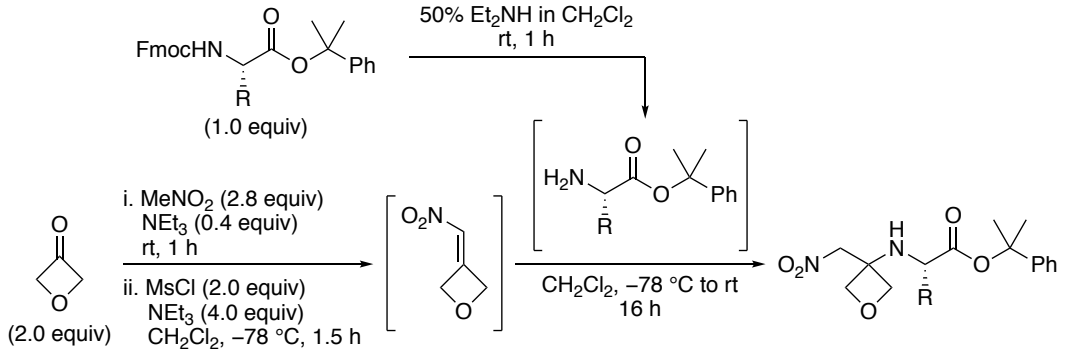

N-Fmoc amino cumyl esters (1.0 equiv) in 50% diethylamine in CH_2Cl_2 (0.5 M) was stirred at room temperature for 1 h. The reaction mixture was concentrated under reduced pressure and the resulting residue repeatedly dissolved in CH_2Cl_2 (3 x 10 mL/mmol) and concentrated under reduced pressure to give the crude amine. Meanwhile, oxetan-3-one (2.0 equiv), nitromethane (2.8 equiv) and triethylamine (0.4 equiv) were stirred at room temperature for 1 h. CH_2Cl_2 (0.25 M) was added and the reaction mixture cooled to −78 °C. Triethylamine (4.0 equiv) was added followed by the dropwise addition of a solution of methanesulfonyl chloride (2.0 equiv) in CH_2Cl_2 (1.0 M). The reaction mixture was stirred at −78 °C for 1.5 h. The crude amine in CH_2Cl_2 (0.25 M) was added to the oxetane mixture *via* syringe at −78 °C. The reaction mixture was allowed to reach room temperature and stirred for 16 h. A saturated solution of NH_4Cl (8 mL/mmol) was added and stirred for 10 min. The layers were separated and the aqueous extracted with CH_2Cl_2 (2 x 10 mL/mmol) and EtOAc (2 x 10 mL/mmol). The combined organics were washed with saturated $NaHCO_3$ (2 x 8 mL/mmol) then brine (4 mL/mmol), dried ($MgSO_4$), filtered and concentrated under reduced pressure, and the products purified by column chromatography.

General procedure 9: *Nitro reduction and Fmoc protection using 2.0 equivalents of FmocOSu*

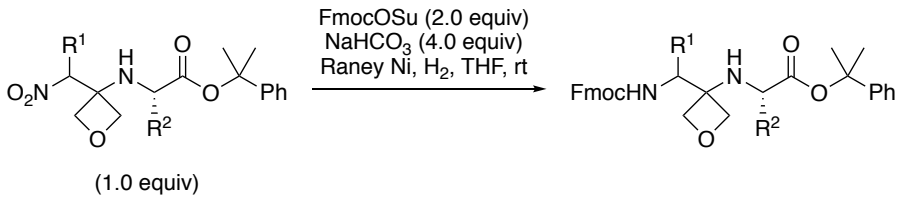

To substrate (1.0 equiv) in THF (0.1 M) was added Fmoc *N*-hydroxysuccinimide ester (2.0 equiv), $NaHCO_3$ (4.0 equiv) and Raney Ni (1 mL/mmol, slurry in H_2O). The reaction mixture was stirred at room temperature under an atmosphere of H_2 (balloon) until consumption of starting material (MS monitoring). The reaction mixture was filtered through a plug of Celite® eluting with EtOAc. The eluent was washed with saturated Na_2CO_3 (3 x 8 mL/mmol) and brine (4 mL/mmol), dried ($MgSO_4$), filtered and concentrated under reduced pressure, and the products purified by column chromatography.

General Procedure 10: *Cumyl ester deprotection*

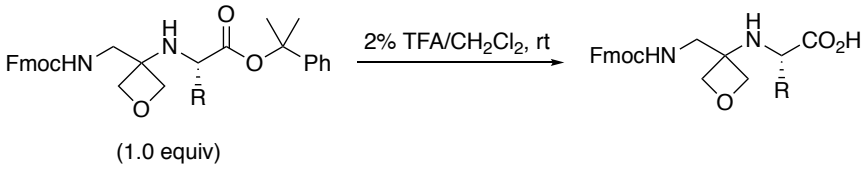

Substrate (1.0 equiv) in 2% TFA/CH_2Cl_2 (0.05 M) was stirred at room temperature until consumption of the starting material (TLC monitoring), The reaction mixture was concentrated under reduced pressure and the resulting residue repeatedly dissolved in CH_2Cl_2 (5 x 20 mL/mmol) and concentrated under reduced pressure to give a crude product that was purified by column chromatography.

General procedure 11: *Cumyl ester deprotection and C-terminal coupling*

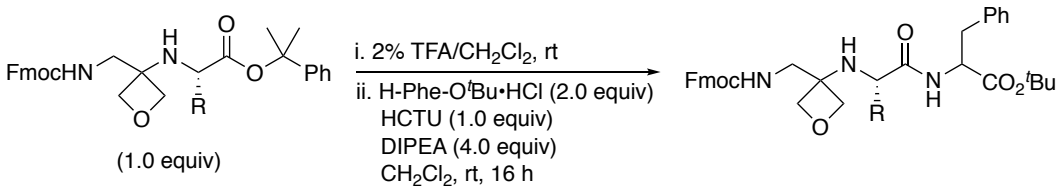

Substrate (1.0 equiv) in 2% TFA/CH_2Cl_2 (0.05 M) was stirred at room temperature until consumption of starting material (TLC monitoring). The reaction mixture was concentrated under reduced pressure and the resulting residue repeatedly dissolved in CH_2Cl_2 (3 x 10 mL/mmol) and concentrated under reduced pressure. To this crude acid in CH_2Cl_2 (0.1 M) was added *D*- or *L*-phenylalanine *tert*-butyl ester hydrochloride (2.0 equiv), DIPEA (4.0 equiv) and HCTU (1.0 equiv). The reaction mixture was stirred at room temperature for 16 h. The mixture was diluted with EtOAc (100 mL/mmol), washed with brine (2 x 50 mL/mmol), 1.0 M HCl (3 x 50 mL/mmol), saturated $NaHCO_3$ (3 x 50 mL/mmol), brine (25 mL/mmol), dried ($MgSO_4$), filtered and concentrated under reduced pressure, and the products purified by column chromatography.

6.3 Experimental Procedures and Characterisation

tert-Butyl [3-(nitromethyl)oxetan-3-yl]-*L*-valinate 111

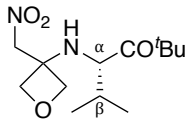

Following general procedure 1, oxetan-3-one (161 μL, 2.51 mmol), nitromethane (189 μL, 3.50 mmol) and *L*-valine *tert*-butyl ester hydrochloride (1.05 g, 5.00 mmol) were combined to give, after column chromatography (10-20% EtOAc in petroleum ether), **111** (410 mg, 1.42 mmol, 57%) as an orange oil. $\mathbf{R_f}$ (15% EtOAc in petroleum ether) 0.27; $[\boldsymbol{\alpha}]_{\mathbf{D}}^{\mathbf{28}}$ –10.9 (*c* 0.10, $CHCl_3$); **^{1}H-NMR** (500 MHz, $CDCl_3$) δ 4.83 (1H, d, *J* = 13.0 Hz, NO_2CHH), 4.76 (1H, d, *J* = 13.0 Hz, NO_2CHH), 4.64 (1H, d, *J* = 7.1 Hz, OC*H*H-Ox), 4.58 (1H, d, *J* = 7.2 Hz, OC*H*H-Ox), 4.52 (1H, d, *J* = 7.1 Hz, OCH*H*-Ox), 4.45 (1H, d, *J* = 7.1 Hz, OCH*H*-Ox), 3.13 (1H, d, *J* = 5.5 Hz, CHα-Val), 2.55-2.19 (1H, bs, NH), 1.97-1.85 (1H, m, CHβ-Val), 1.46 (9H, s, ^{t}Bu), 0.94 (3H, d, *J* = 6.7 Hz, CH_3-Val), 0.86 (3H, d, *J* = 6.9 Hz, CH_3-Val); **^{13}C-NMR** (125 MHz, $CDCl_3$) δ 174.8 (C=O), 82.0 (C, ^{t}Bu), 78.9 (NO_2CH_2 or OCH_2-Ox), 78.8 (NO_2CH_2 or OCH_2-Ox) 78.5 (OCH_2-Ox), 61.8 (CH, α-Val), 59.6 (C, Ox), 32.3 (CH, β-Val), 28.1 (3 x CH_3, ^{t}Bu), 19.4 (CH_3, Val), 17.9 (CH_3, Val); **IR** (film) 3333 (NH), 2966, 2876, 1719 (C=O), 1555, 1146 cm^{-1}; **MS** (ESI$^+$) *m/z* 289 $[M+H]^+$, 311 $[M+Na]^+$; **HRMS** (ESI$^+$) Calcd.. for $C_{13}H_{25}N_2O_5$ $[M+H]^+$: 289.1758, found 289.1754.

Methyl [3-(nitromethyl)oxetan-3-yl]glycinate 113

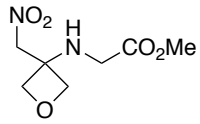

Following general procedure 1, oxetan-3-one (161 μL, 2.51 mmol), nitromethane (189 μL, 3.50 mmol) and glycine methyl ester hydrochloride (628 mg, 5.00 mmol) were combined to give, after column chromatography (30-60% EtOAc in petroleum ether), **113** (282 mg, 1.38 mmol, 55%) as a yellow oil. $\mathbf{R_f}$ (50% EtOAc in petroleum ether) 0.24; **^{1}H-NMR** (500 MHz, $CDCl_3$) δ 4.83 (2H, s, NO_2CH_2), 4.63 (2H, d, *J* = 7.5 Hz, 2 x OC*H*H-Ox), 4.58 (2H, d, *J* = 7.5 Hz, 2 x OCH*H*-Ox), 3.74 (3H, s, CH_3), 3.54 (2H, s, CH_2-Gly), 2.56-2.16 (1H, bs, NH); **^{13}C-NMR** (125 MHz, $CDCl_3$) δ 172.3 (C=O), 78.5 (NO_2CH_2), 78.4 (2 x CH_2-Ox), 59.6 (C, Ox), 52.5 (CH_3), 44.7 (CH_2-Gly); **IR** (film) 3338 (NH), 2957, 2883, 1735 (C=O), 1548, 1208 cm^{-1}; **MS** (ESI$^+$) *m/z* 205 $[M+H]^+$, 227 $[M+Na]^+$, 243 $[M+K]^+$; **HRMS** (ESI$^+$) Calcd. for $C_7H_{13}N_2O_5$ $[M+H]^+$: 205.0819, found 205.0818.

Methyl [3-(nitromethyl)oxetan-3-yl]-*L*-alaninate 114

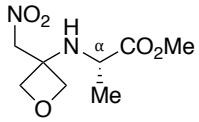

Following general procedure 1, oxetan-3-one (129 μL, 2.01 mmol), nitromethane (151 μL, 2.79 mmol) and *L*-alanine methyl ester hydrochloride (558 mg, 4.00 mmol) were combined to give, after column chromatography (20-40% EtOAc in petroleum ether), **114** (239 mg, 1.10 mmol, 55%) as a yellow oil. $\mathbf{R}_f$ (40% EtOAc in petroleum ether) 0.30; $[\boldsymbol{\alpha}]_{\mathbf{D}}^{\mathbf{29}}$ –2.7 (*c* 0.10, $CHCl_3$); **^{1}H-NMR** (400 MHz, $CDCl_3$) δ 4.89 (1H, d, *J* = 12.8 Hz, NO_2CHH), 4.84 (1H, d, *J* = 12.8 Hz, NO_2CHH), 4.65 (1H, d, *J* = 7.2 Hz, OC*H*H-Ox), 4.62 (1H, d, *J* = 7.1 Hz, OC*H*H-Ox), 4.54 (1H, d, *J* = 7.2 Hz, OCH*H*-Ox), 4.44 (1H, d, *J* = 7.1 Hz, OCH*H*-Ox), 3.73 (3H, s, OCH_3), 3.61 (1H, q, *J* = 7.0 Hz, C*H*α-Ala), 2.87-2.25 (1H, bs, NH), 1.32 (3H, d, *J* = 7.0 Hz, CH_3-Ala); **^{13}C-NMR** (125 MHz, $CDCl_3$) δ 176.0 (C=O), 79.1 (OCH_2-Ox), 79.0 (OCH_2-Ox), 78.2 (NO_2CH_2), 59.7 (C, Ox), 52.6 (OCH_3), 51.4 (CH, α-Ala), 20.4 (CH_3-Ala); **IR** (film) 3337 (NH), 2955, 2880, 1731 (C=O), 1553 cm^{-1}; **MS** (ESI^+) *m/z* 219 $[M+H]^+$, 241 $[M+Na]^+$; **HRMS** (ESI^+) Calcd. for $C_8H_{14}N_2O_5Na$ $[M+Na]^+$: 241.0795, found 241.0797.

Methyl [3-(nitromethyl)oxetan-3-yl]-*L*-serinate 115[1]

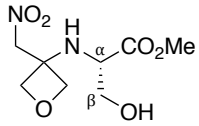

Following general procedure 1, oxetan-3-one (161 μL, 2.51 mmol), nitromethane (189 μL, 3.50 mmol) and *L*-serine methyl ester hydrochloride (778 mg, 5.00 mmol) were combined to give, after column chromatography (50-80% EtOAc in petroleum ether), **115** (321 mg, 1.37 mmol, 55%) as a yellow oil. In this case, due to poor mass recovery, the aqueous layer was further extracted with CH_2Cl_2 (2 x 30 mL) and EtOAc (3 x 30 mL) after initial extraction with CH_2Cl_2 (2 x 30 mL). $\mathbf{R}_f$ (80% EtOAc in petroleum ether) 0.28; **^{1}H-NMR** (300 MHz, $CDCl_3$) δ 4.86 (1H, d, *J* = 13.2 Hz, NO_2CHH), 4.80 (1H, d, *J* = 13.2 Hz, NO_2CHH), 4.66-4.60 (2H, m, 2 x OC*H*H-Ox), 4.54 (2H, d, *J* = 7.2 Hz, 2 x OCH*H*-Ox), 3.84-3.74 (4H, m, CH_3, C*H*Hβ-Ser), 3.68-3.57 (2H, m, CH*H*β-Ser, CHα-Ser), 2.67 (1H, bs, OH), 2.42 (1H, bs, NH); **^{13}C-NMR** (75 MHz, $CDCl_3$) δ 173.4 (C=O), 78.8 (NO_2CH_2 or OCH_2-Ox), 78.6 (NO_2CH_2 or OCH_2-Ox), 78.4 (OCH_2, Ox), 63.8 (CH_2, β-Ser), 59.2 (C, Ox), 57.4 (CH, α-Ser), 52.9 (CH_3); **MS** (ESI^+) *m/z* 235 $[M+H]^+$, 257 $[M+Na]^+$. Data consistent with that reported in literature.[1]

Methyl [3-(nitromethyl)oxetan-3-yl]-*L*-phenylalaninate 116

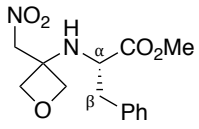

Following general procedure 1, oxetan-3-one (160 μL, 2.50 mmol), nitromethane (187 μL, 3.50 mmol) and *L*-phenylalanine methyl ester hydrochloride (1.08 g, 5.00 mmol) were combined to give, after column chromatography (35% EtOAc in petroleum ether), **116** (399 mg, 1.35 mmol, 54%) as an orange oil. $\mathbf{R}_f$ (35% EtOAc in petroleum ether) 0.30; $[\boldsymbol{\alpha}]_{\mathbf{D}}^{\mathbf{30}}$ +10.5 (*c* 0.10, $CHCl_3$); **^{1}H-NMR** (500 MHz, $CDCl_3$) δ 7.33-7.27 (2H, m, ArH), 7.27-7.22 (1H, m, ArH), 7.18-7.13 (2H, m, ArH), 4.79 (1H, d, *J* = 12.9 Hz, NO_2CHH), 4.73 (1H, d, *J* = 12.9 Hz, NO_2CHH), 4.51 (1H, d, *J* = 7.1 Hz, OC*H*H-Ox), 4.38 (1H, d, *J* = 7.2 Hz, OC*H*H-Ox), 4.35 (m, 2 x OCH*H*-Ox), 3.76-3.65 (4H, m, CH_3 and CHα-Phe), 2.98 (1H, dd, *J* = 13.4 and 6.0 Hz, C*H*Hβ-Phe), 2.86 (1H, dd, *J* = 13.4 and 7.4 Hz, CH*H*β-Phe), 2.36 (1H, bs, NH); **^{13}C-NMR** (125 MHz, $CDCl_3$) δ 175.1 (C=O), 136.7 (C, Ar), 129.5 (2 x CH, Ar), 128.7 (2 x CH, Ar), 127.2 (CH, Ar), 78.9 (OCH_2, Ox), 78.7 (OCH_2, Ox), 78.6 (NO_2CH_2), 59.5 (C, Ox), 57.7 (CH, α-Phe), 52.5 (CH_3), 40.7 (CH_2, β-Phe); **IR** (film) 3333 (NH), 2953, 2879, 1731 (C=O), 1552 cm^{-1}; **MS** (ESI^+) *m/z* 295 $[M+H]^+$, 317 $[M+Na]^+$; **HRMS** (ESI^+) Calcd. for $C_{14}H_{18}N_2O_5Na$ $[M+Na]^+$: 317.1108, found 317.1124.

4-*tert*-Butyl-1-methyl [3-(nitromethyl)oxetan-3-yl]-*L*-aspartate 117

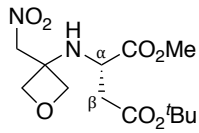

Following general procedure 1, oxetan-3-one (42 μL, 0.66 mmol), nitromethane (49 μL, 0.91 mmol) and *L*-aspartic acid 4-*tert*-butyl-1-methyl ester hydrochloride (314 mg, 1.31 mmol) were combined to give, after column chromatography (30-40% EtOAc in petroleum ether), **117** (112 mg, 0.35 mmol, 54%) as an orange oil. $\mathbf{R}_f$ (30% EtOAc in petroleum ether) 0.22; $[\boldsymbol{\alpha}]_{\mathbf{D}}^{\mathbf{29}}$ –1.4 (*c* 0.10, $CHCl_3$); **^{1}H-NMR** (400 MHz, $CDCl_3$) δ 4.85 (1H, d, *J* = 13.2 Hz, NO_2CHH), 4.78 (1H, d, *J* = 13.2 Hz, NO_2CHH), 4.61 (1H, d, *J* = 7.2 Hz, OC*H*H-Ox), 4.56-4.48 (2H, m, OC*H*H-Ox and OCH*H*-Ox), 4.42 (1H, d, *J* = 7.2 Hz, OCH*H*-Ox), 3.80 (1H, t, *J* = 6.0 Hz, CHα-Asp), 3.68 (3H, s, CH_3), 2.66-2.51 (2H, m, CH_2β-Asp), 1.38 (9H, s, ^{t}Bu), NH not observed; **^{13}C-NMR** (125 MHz, $CDCl_3$) δ 174.4 (C=O), 169.8 (C=O), 81.9 (C, ^{t}Bu), 79.2 (OCH_2, Ox), 78.5 (NO_2CH_2 or OCH_2-Ox), 78.4 (NO_2CH_2 or OCH_2-Ox), 59.6 (C, Ox), 52.9 (CH, α-Asp), 52.7 (OCH_3), 40.4 (CH_2, β-Asp), 28.2 (3 x CH_3, ^{t}Bu); **IR** (film) 3342 (NH), 2977, 2884, 1728 (C=O), 1554, 1149 cm^{-1}; **MS** (ESI^+) *m/z* 341 $[M+Na]^+$, 357 $[M+K]^+$; **HRMS** (ESI^+) Calcd. for $C_{13}H_{22}N_2O_7Na$ $[M+Na]^+$: 341.1319, found 341.1318.

Methyl N^6-(*tert*-butoxycarbonyl)-N^2-[3-(nitromethyl)oxetan-3-yl]-*L*-lysinate 118

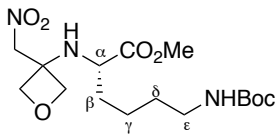

Following general procedure 1, oxetan-3-one (113 μL, 1.76 mmol), nitromethane (131 μL, 2.43 mmol) and N_ε-Boc-*L*-lysine methyl ester hydrochloride (1.03 g, 3.47 mmol) were combined to give, after column chromatography (40-50% EtOAc in petroleum ether), **118** (353 mg, 0.94 mmol, 53%) as a yellow oil. $\mathbf{R_f}$ (50% EtOAc in petroleum ether) 0.32; $[\boldsymbol{\alpha}]_{\mathbf{D}}^{\mathbf{29}}$ +16.0 (*c* 0.10, $CHCl_3$); **^{1}H-NMR** (400 MHz, $CDCl_3$) δ 4.79 (1H, d, *J* = 12.9 Hz, NO_2CHH), 4.74 (1H, d, *J* = 12.9 Hz, NO_2CHH), 4.58 (1H, d, *J* = 7.1 Hz, OC*H*H-Ox), 4.52 (1H, d, *J* = 7.0 Hz, OC*H*H-Ox), 4.50-4.39 (2H, m, OCH*H*-Ox, NH-Boc), 4.35 (1H, d, *J* = 7.0 Hz, OCH*H*-Ox), 3.65 (3H, s, CH_3), 3.43-3.32 (1H, m, CHα-Lys), 3.10-2.94 (2H, m, CH_2ε-Lys), 2.22 (1H, d, *J* = 10.2 Hz, NH-Lys), 1.67-1.10 (15H, m, CH_2β-Lys, CH_2δ-Lys, CH_2γ-Lys, ^{t}Bu); **^{13}C-NMR** (125 MHz, $CDCl_3$) δ 175.9 (C=O, Lys), 156.1 (C=O, Boc), 79.3 (C, ^{t}Bu), 79.2 (OCH_2, Ox), 79.0 (OCH_2, Ox), 78.4 (NO_2CH_2), 59.7 (C, Ox), 55.8 (CH, α-Lys), 52.5 (CH_3), 40.3 (CH_2, ε-Lys), 34.0 (CH_2, β-Lys), 29.9 (CH_2, δ-Lys), 28.6 (3 x CH_3, ^{t}Bu), 22.9 (CH_2, γ-Lys); **IR** (film) 3338 (NH), 2952, 2878, 1731 (C=O), 1695 (C=O), 1554, 1165 cm^{-1}; **MS** (ESI^+) *m/z* 376 $[M+H]^+$, 398 $[M+Na]^+$; **HRMS** (ESI^+) Calcd. for $C_{16}H_{29}N_3O_7Na$ $[M+Na]^+$: 398.1898, found 398.1906.

Methyl [3-(nitromethyl)oxetan-3-yl]-*L*-prolinate 119

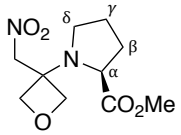

Following general procedure 1, oxetan-3-one (230 μL, 3.59 mmol), nitromethane (269 μL, 4.98 mmol) and *L*-proline methyl ester hydrochloride (1.18 g, 7.11 mmol) were combined to give, after column chromatography (30-40% EtOAc in petroleum ether), **119** (484 mg, 1.98 mmol, 55%) as an orange oil. $\mathbf{R_f}$ (40% EtOAc in petroleum ether) 0.27; $[\boldsymbol{\alpha}]_{\mathbf{D}}^{\mathbf{31}}$ +16.4 (*c* 0.10, $CHCl_3$); **^{1}H-NMR** (500 MHz, $CDCl_3$) δ 4.87 (1H, d, *J* = 12.2 Hz, NO_2CHH), 4.84-4.79 (2H, m, NO_2CHH and OC*H*H-Ox), 4.77 (1H, d, *J* = 7.2 Hz, OC*H*H-Ox), 4.73 (1H, d, *J* = 7.4 Hz, OCH*H*-Ox), 4.37 (1H, d, *J* = 7.2 Hz, OCH*H*-Ox), 3.86 (1H, t, *J* = 5.6 Hz, CHα-Pro), 3.61 (3H, s, OCH_3), 3.23-3.16 (1H, m, NC*H*Hδ-Pro), 2.80 (1H, dd, *J* = 15.3 and 7.5 Hz, NCH*H*δ-Pro), 2.02-1.77 (4H, m, CH_2β-Pro, CH_2γ-Pro); **^{13}C-NMR** (125 MHz, $CDCl_3$) δ 175.0 (C=O), 78.6 (NO_2CH_2), 77.5 (OCH_2, Ox), 76.4 (OCH_2, Ox), 63.0 (C, Ox), 60.0 (CH, α-Pro), 52.2 (CH_3), 47.8 (CH_2, δ-Pro), 30.4 (CH_2, β-Pro), 24.1 (CH_2, γ-Pro); **IR**

(film) 2954, 2875, 1729 (C=O), 1552 cm^{-1}; **MS** (ESI^+) *m/z* 245 $[M+H]^+$, 267 $[M+Na]^+$; **HRMS** (ESI^+) Calcd. for $C_{10}H_{16}N_2O_5Na$ $[M+Na]^+$: 267.0951, found 267.0948.

Methyl (*R*)-2-[[3-(nitromethyl)oxetan-3-yl]amino]-2-phenylacetate 120

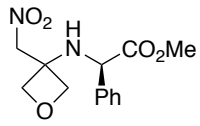

Following general procedure 1, oxetan-3-one (97 μL, 1.51 mmol), nitromethane (113 μL, 2.10 mmol) and (*R*)-(−)-2-phenylglycine methyl ester hydrochloride (605 mg, 3.00 mmol) were combined to give, after column chromatography (0-40% EtOAc in petroleum ether), **120** (218 mg, 0.78 mmol, 52%) as an orange oil. $\mathbf{R_f}$ (40% EtOAc in petroleum ether) 0.29; $[\boldsymbol{\alpha}]_{\mathbf{D}}^{\mathbf{25}}$ –78.3 (*c* 0.24, $CHCl_3$); **^{1}H-NMR** (500 MHz, $CDCl_3$) δ 7.37-7.23 (5H, m, ArH), 4.79 (1H, d, *J* = 13.1 Hz, NO_2CHH), 4.75 (1H, d, *J* = 13.0 Hz, NO_2CHH), 4.64 (1H, s, CHPh), 4.57 (1H, d, *J* = 7.2 Hz, OC*H*H-Ox), 4.46 (1H, d, *J* = 7.2 Hz, OCH*H*-Ox), 4.42 (1H, d, *J* = 7.2 Hz, OC*H*H-Ox), 4.26 (1H, d, *J* = 7.2 Hz, OCH*H*-Ox), 3.64 (3H, s, CH_3), 2.30-1.39 (1H, bs, NH); **^{13}C-NMR** (125 MHz, $CDCl_3$) δ 172.9 (C=O), 138.0 (C, Ar), 129.2 (2 x CH, Ar), 128.9 (CH, Ar), 127.5 (2 x CH, Ar), 78.8 (OCH_2, Ox), 78.7 (OCH_2, Ox), 78.5 (NO_2CH_2), 60.0 (CH_3), 59.5 (C, Ox), 53.1 (CHPh); **IR** (film) 3339 (NH), 2955, 2881, 1731 (C=O), 1551, 1029 cm^{-1}; **MS** (ESI^+) *m/z* 281 $[M+H]^+$, 303 $[M+Na]^+$; **HRMS** (ESI^+) Calcd. for $C_{13}H_{16}N_2O_5Na$ $[M+Na]^+$: 303.0951, found 303.0951.

3-(1-Nitro-2-phenylethylidene)oxetane 31[74]

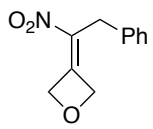

Following general procedure 2, oxetane-3-one (1.04 mL, 16.3 mmol) and (2-nitroethyl)benzene **126**[76] (1.89 g, 12.5 mmol) were combined to give, after column chromatography (20-30% EtOAc in petroleum ether), **31** (1.80 g, 8.75 mmol, 70%) contaminated with its rearrangement product 3-benzylisoxazole-4-carbaldehyde (~19:1 by ^{1}H-NMR) as a yellow solid. $\mathbf{R_f}$ (20% EtOAc in petroleum ether) 0.40; **^{1}H-NMR** (500 MHz, $CDCl_3$) δ 7.39-7.19 (5H, m, ArH), 5.66-5.52 (2H, m, OCH_2), 4.97-4.85 (2H, m, OCH_2), 3.81 (2H, s, CH_2Ph); **^{13}C-NMR** (125 MHz, $CDCl_3$) δ 151.3 (C), 140.0 (C), 134.8 (C, Ar), 129.2 (2 x CH, Ar), 129.0 (2 x CH, Ar), 127.7 (CH, Ar), 80.0 (OCH_2), 75.5 (OCH_2), 34.0 (CH_2Ph). Data consistent with that reported in literature.[74]

3-(1-Nitroethylidene)oxetane 128[75]

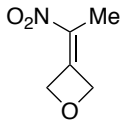

Following general procedure 2, oxetan-3-one (2.08 mL, 32.5 mmol) and nitroethane (1.65 mL, 25.0 mmol) were combined to give, after column chromatography (20-30% EtOAc in petroleum ether), **128** (2.78 g, 21.6 mmol, 86%) as a yellow oil that became a yellow solid upon storage at −20 °C. $\mathbf{R}_f$ (20% EtOAc in petroleum ether) 0.28; **^{1}H-NMR** (500 MHz, $CDCl_3$) δ 5.61-5.53 (2H, m, OCH_2), 5.36-5.28 (2H, m, OCH_2), 2.03 (3H, quint, J = 1.8 Hz, CH_3); **^{13}C-NMR** (125 MHz, $CDCl_3$) δ 149.0 (C), 137.5 (C), 79.8 (OCH_2), 75.7 (OCH_2), 13.1 (CH_3). Data consistent with that reported in literature.[75]

Methyl [3-(1-nitro-2-phenylethyl)oxetan-3-yl]glycinate 91

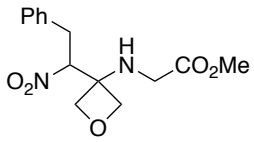

Following general procedure 3, **31** (357 mg, 1.74 mmol) and glycine methyl ester **129**[77] (311 mg, 3.49 mmol) were reacted for 4 h. Purification by recrystallization (EtOH) gave **91** (450 mg, 1.53 mmol, 88%) as white crystals. **^{1}H-NMR** (400 MHz, $CDCl_3$) δ 7.35-7.21 (5H, m, ArH), 5.12 (1H, dd, J = 9.8 and 4.5 Hz, NO_2CH), 4.65 (1H, d, J = 7.5 Hz, OC*H*H-Ox), 4.62 (1H, d, J = 7.5 Hz, OCH*H*-Ox), 4.51 (1H, d, J = 8.0 Hz, OC*H*H-Ox), 4.48 (1H, d, J = 8.0 Hz, OC*H*H-Ox), 3.78 (3H, s, OCH_3), 3.72 (1H, dd, J = 17.3 and 6.0 Hz, C*H*H-Gly), 3.61 (1H, dd, J = 17.3 and 6.0 Hz, CH*H*-Gly), 3.52 (1H, dd, J = 14.6 and 9.8 Hz, CH*H*Ph), 3.29 (1H, dd, J = 14.6 and 4.5 Hz, C*H*HPh), 2.47 (1H, br t, J = 5.9 Hz, NH); **^{13}C-NMR** (100 MHz, $CDCl_3$) δ 172.4 (C=O), 135.3 (C, Ar), 129.0 (2 x CH, Ar), 128.8 (2 x CH, Ar), 127.7 (CH, Ar), 92.8 (NO_2CH), 77.1 (OCH_2-Ox), 76.7 (OCH_2-Ox), 62.1 (C, Ox), 52.4 (OCH_3), 44.4 (CH_2-Gly), 34.6 (CH_2Ph); **MS** (ESI^+) *m/z* 295 $[M+H]^+$, 317 $[M+Na]^+$. Data consistent with that reported in literature.[45]

Methyl [3-(1-nitroethyl)oxetan-3-yl]glycinate 131

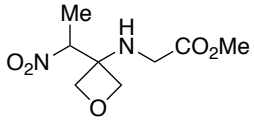

Following general procedure 3, **128** (152 mg, 1.18 mmol) and glycine methyl ester **129**[77] (210 mg, 2.35 mmol) were reacted for 64 h to give, after column chromatography (40-50% EtOAc in petroleum ether), **131** (217 mg, 0.99 mmol, 84%) as a colorless oil. $\mathbf{R}_f$ (50% EtOAc in petroleum ether) 0.38; **^{1}H-NMR** (400 MHz, $CDCl_3$) δ 4.96 (1H, q, J = 6.8 Hz, NO_2CH), 4.66 (1H, d, J = 7.6 Hz, OC*H*H-Ox), 4.64-4.59 (2H, m, OCH_2-Ox), 4.56 (1H, d, J = 7.7

Hz, OCH*H*-Ox), 3.76 (3H, s, OCH_3), 3.67 (1H, d, *J* = 17.2 Hz, C*H*H-Gly), 3.57 (1H, d, *J* = 17.2 Hz, CH*H*-Gly), 2.23 (1H, bs, NH), 1.73 (3H, d, *J* = 6.8 Hz, NO_2CHCH_3); **^{13}C-NMR** (125 MHz, C_6D_6) δ 172.1 (C=O), 85.4 (NO_2CH), 76.9 (CH_2-Ox), 76.2 (CH_2-Ox), 62.1 (C, Ox), 51.5 (OCH_3), 44.4 (CH_2-Gly), 13.3 (NO_2CHCH_3); **IR** (film) 3329 (NH), 2955, 2887, 1737 (C=O), 1548 cm^{-1}; **MS** (ESI^+) *m/z* 219 $[M+H]^+$, 241 $[M+Na]^+$; **HRMS** (ESI^+) Calcd. for $C_8H_{14}N_2O_5Na$ $[M+Na]^+$: 241.0795, found 241.0799.

Methyl [3-((*S*)-1-nitroethyl)oxetan-3-yl]-*L*-valinate and Methyl [3-((*R*)-1-nitroethyl)oxetan-3-yl]-*L*-valinate (50:50 dr) 132

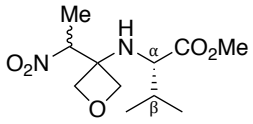

Following general procedure 3, **128** (137 mg, 1.06 mmol) and *L*-valine methyl ester **130**[77] (279 mg, 2.13 mmol) were reacted for 24 h to give a crude product which ^{1}H-NMR showed to consist of a 50:50 mixture of diastereoisomers. Purification by column chromatography (20-30% EtOAc in petroleum ether) gave **132** (246 mg, 0.95 mmol, 89%) as a 50:50 mixture of diastereoisomers and as a colorless oil. $\mathbf{R}_f$ (30% EtOAc in petroleum ether) 0.37, 0.48; **^{1}H-NMR** (500 MHz, $CDCl_3$) δ 4.92 (0.5H, q, *J* = 6.9 Hz, NO_2CHCH_3), 4.87 (0.5H, q, *J* = 6.9 Hz, NO_2CHCH_3), 4.61 (0.5H, d, *J* = 7.6 Hz, OC*H*H-Ox), 4.59 (0.5H, d, *J* = 7.7 Hz, OC*H*H-Ox), 4.53-4.48 (1.5H, m, 3 x OCH*H*-Ox), 4.43 (0.5H, d, *J* = 7.5 Hz, OC*H*H-Ox), 4.40 (0.5H, d, *J* = 7.6 Hz, OCH*H*-Ox), 4.36 (0.5H, d, *J* = 7.6 Hz, OCH*H*-Ox), 3.70-3.65 (3H, m, 2 x OCH_3), 3.41 (0.5H, dd, *J* = 10.2 and 5.2 Hz, CHα-Val), 3.36 (0.5H, dd, *J* = 10.4 and 5.8 Hz, CHα-Val), 2.26 (0.5H, d, *J* = 10.2 Hz, NH), 2.06 (0.5H, d, *J* = 10.3 Hz, NH), 1.98-1.90 (0.5H, m, CHβ-Val), 1.90-1.81 (0.5H, m, CHβ-Val), 1.70-1.60 (3H, m, 2 x NO_2CHCH_3), 0.88 (1.5H, d, *J* = 6.7 Hz, CH_3-Val), 0.84 (1.5H, d, *J* = 6.8 Hz, CH_3-Val), 0.82-0.76 (3H, m, 2 x CH_3-Val); **^{13}C-NMR** (125 MHz, $CDCl_3$) δ 176.3 (C=O), 176.2 (C=O) 87.1 (NO_2CH), 85.0 (NO_2CH), 78.4 (OCH_2-Ox), 77.8 (OCH_2-Ox), 77.7 (OCH_2-Ox), 76.8 (OCH_2-Ox), 62.4 (C, Ox), 62.2 (C, Ox), 60.8 (OCH_3), 60.8 (OCH_3), 52.4 (CH, α-Val), 52.3 (CH, α-Val), 32.2 (CH, β-Val), 32.3 (CH, β-Val), 19.6 (CH_3, Val), 19.4 (CH_3, Val), 18.1 (CH_3, Val), 17.8 (CH_3, Val), 14.3 (NO_2CHCH_3), 13.4 (NO_2CHCH_3); **IR** (film) 3340 (NH), 2959, 2878, 1730 (C=O), 1551 cm^{-1}; **MS** (ESI^+) *m/z* 261 [M+H], 283 $[M+Na]^+$; **HRMS** (ESI^+) Calcd. for $C_{11}H_{20}N_2O_5Na$ $[M+Na]^+$: 283.1264, found 283.1265.

(*S*)-6-Isopropyl-2-oxa-5,8-diazaspiro[3.5]nonan-7-one (*S*)-112

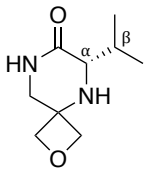

Following general procedure 4, (*S*)-**109**[1] (325 mg, 1.32 mmol) gave, after column chromatography (0-10% MeOH in EtOAc), (*S*)-**112** (197 mg, 1.07 mmol, 81%) as white solid. A crystal suitable for X-ray analysis was grown from $CHCl_3$. $\mathbf{R_f}$ (10% MeOH in EtOAc) 0.31; **mp** 153-158 °C; $[\boldsymbol{\alpha}]_{\mathbf{D}}^{\mathbf{25}}$ –118.1 (*c* 0.10, CH_2Cl_2); **^{1}H-NMR** (300 MHz, $CDCl_3$) δ 6.36 (1H, bs, NHCO), 4.64-4.57 (2H, m, OCH_2-Ox), 4.50 (1H, d, *J* = 7.1 Hz, OC*H*H-Ox), 4.45 (1H, d, *J* = 7.1 Hz, OCH*H*-Ox), 3.65 (1H, dd, *J* = 11.5, 4.6 Hz, NHC*H*H), 3.51-3.40 (2H, m, NHCH*H*, CHα-Val), 2.50-2.34 (1H, m, CHβ-Val), 1.80 (1H, bs, NH-Val), 0.99 (3H, d, *J* = 7.3 Hz, CH_3-Val), 0.91 (3H, d, *J* = 6.8 Hz, CH_3-Val); **^{13}C-NMR** (75 MHz, $CDCl_3$) δ 170.4 (C=O), 81.5 (CH_2, Ox), 79.3 (CH_2, Ox), 59.3 (CH, α-Val), 54.7 (C, Ox), 48.4 ($NHCH_2$), 29.5 (CH, β-Val), 18.5 (CH_3, Val), 15.6 (CH_3, Val); **IR** (film) 3253 (NH), 3106 2965, 2869, 2820, 1649 (C=O), 1321, 980 cm^{-1}; **MS** (ESI^+) *m/z* 185 $[M+H]^+$, 207 $[M+Na]^+$; **HRMS** (ESI^+) Calcd. for $C_9H_{17}N_2O_2$ $[M+H]^+$: 185.1285, found 185.1284.

Crystal Data for $C_9H_{16}N_2O_2$ (*M* =184.24 g/mol): orthorhombic, space group $P2_12_12_1$ (no. 19), *a* = 6.05086(3) Å, *b* = 9.80036(4) Å, *c* = 15.94440(7) Å, *V* = 945.513(7) $Å^3$, *Z* = 4, *T* = 150(2) K, μ(CuKα) = 0.750 mm^{-1}, *Dcalc* = 1.294 g/cm^3, 20278 reflections measured (10.596° ≤ 2Θ ≤ 157.912°), 2044 unique (R_{int} = 0.0318, R_{sigma} = 0.0127) which were used in all calculations. The final R_1 was 0.0347 (I > 2σ(I)) and wR_2 was 0.0883 (all data).

(*R*)-6-Isopropyl-2-oxa-5,8-diazaspiro[3.5]nonan-7-one (*R*)-112

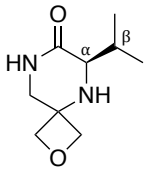

Following general procedure 4, (*R*)-**109**[1] (144 mg, 0.58 mmol) gave, after column chromatography (0-10% MeOH in EtOAc), (*R*)-**112** (84 mg, 0.46 mmol, 78%) as a white solid. **mp** 163-165 ˚C; $[\boldsymbol{\alpha}]_{\mathbf{D}}^{\mathbf{25}}$ +107.5 (*c* 0.10, CH_2Cl_2); other data as described for (*S*)-**112**.

2-Oxa-5,8-diazaspiro[3.5]nonan-7-one 133

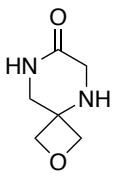

Following general procedure 4, **113** (189 mg, 0.93 mmol) gave **133** (115 mg, 0.81 mmol, 87%) as a white solid, which after work-up required no further purification. **mp** 148-150 °C; **^{1}H-NMR** (400 MHz, DMSO-D_6) δ 7.67 (1H, bs, NHCO), 4.41 (2H, d, *J* = 6.1 Hz, 2 x OC*H*H-Ox), 4.34 (2H, d, *J* = 6.1 Hz, 2 x OCH*H*-Ox), 3.37 (2H, s, C*H*$_2$NHCO), 3.24-3.11 (3H, m, CH_2-Gly and NH-Gly); **^{13}C-**

NMR (125 MHz, DMSO-D_6) δ 168.8 (C=O), 79.2 (2 x OCH_2, Ox), 54.0 (C, Ox), 48.4 (*C*H_2NHCO), 45.5 (CH_2, Gly); **IR** (film) 3261 (NH), 3174, 3102, 3051, 2861, 1672, 1422, 973 cm^{-1}; **MS** (ESI^+) *m/z* 143 $[M+H]^+$, 165 $[M+Na]^+$; **HRMS** (ESI^+) Calcd. for $C_6H_{11}N_2O_2$ $[M+H]^+$: 143.0815, found 143.0814.

(*S*)-6-Methyl-2-oxa-5,8-diazaspiro[3.5]nonan-7-one 134

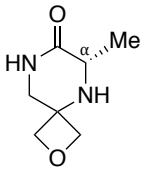

Following general procedure 4, **114** (82 mg, 0.37 mmol) gave, after column chromatography (0-10% MeOH in EtOAc) and recrystallisation (EtOAc/hexane), **134** (47 mg, 0.30 mmol, 80%) as a white solid. $\mathbf{R_f}$ (20% MeOH in EtOAc) 0.22; **mp** 156-158 ˚C; $[\alpha]_D^{26}$ −47.7 (*c* 0.55, $CHCl_3$); **^{1}H-NMR** (400 MHz, $CDCl_3$) δ 6.00 (1H, bs, NHCO), 4.67 (1H, d, *J* = 6.4 Hz, OC*H*H-Ox), 4.63 (1H, d, *J* = 6.4 Hz, OCH*H*-Ox), 4.51 (1H, d, *J* = 7.0 Hz, OC*H*H-Ox), 4.47 (1H, d, *J* = 7.0 Hz, OCH*H*-Ox), 3.72 (1H, dd, *J* = 11.5, 3.1 Hz, NHC*H*H), 3.62 (1H, q, *J* = 6.8 Hz, CHα-Ala), 3.55 (1H, d, *J* = 6.8 Hz, NHCH*H*), 1.95 (1H, bs, NH-Ala), 1.40 (3H, d, *J* = 6.8 Hz, CH_3-Ala); **^{13}C-NMR** (125 MHz, $CDCl_3$) δ 171.6 (C=O), 81.9 (OCH_2, Ox), 80.2 (CH_2, Ox), 55.5 (C, Ox), 51.0 (CH, α-Ala), 49.9 ($NHCH_2$), 18.6 (CH_3-Ala); **IR** (film) 3341 (NH), 3300 (NH), 2993, 2965, 2928, 2871, 1660 (C=O), 1627, 1312, 1081, 971 cm^{-1}; **MS** (ESI^+) *m/z* 157 $[M+H]^+$, 179 $[M+Na]^+$; **HRMS** (ESI^+) Calcd. for $C_7H_{12}N_2O_2Na$ $[M+Na]^+$: 179.0791, found 179.0789.

(*S*)-6-(Hydroxymethyl)-2-oxa-5,8-diazaspiro[3.5]nonan-7-one 135

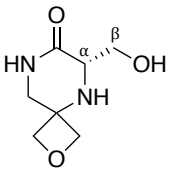

Following general procedure 4, **115** (166 mg, 0.71 mmol) gave, after column chromatography (20% MeOH in EtOAc), **135** (87 mg, 0.51 mmol, 71%) as a beige solid. $\mathbf{R_f}$ (20% MeOH in EtOAc) 0.16; **mp** 109-111 °C; $[\alpha]_D^{24}$ −60.8 (*c* 0.10, MeOH); **^{1}H-NMR** (500 MHz, DMSO-D_6) δ 7.73 (1H, bs, NHCO), 4.67 (1H, dd, *J* = 6.5 and 4.7 Hz, OH), 4.51 (1H, d, *J* = 5.9 Hz, OC*H*H-Ox), 4.43 (1H, d, *J* = 6.3 Hz, OC*H*H-Ox), 4.39 (1H, d, *J* = 5.9 Hz, OCH*H*-Ox), 4.30 (1H, d, *J* = 6.3 Hz, OCH*H*-Ox), 3.66-3.60 (1H, m, C*H*Hβ-Ser), 3.58-3.52 (1H, m CH*H*β-Ser), 3.47 (1H, dd, *J* = 11.7, 3.9 Hz, NHC*H*H), 3.32-3.26 (2H, m, NHCH*H*, CHα-Ser), 3.10 (1H, bs, NH); **^{13}C-NMR** (125 MHz, DMSO-D_6) δ 168.6 (C=O), 80.4 (OCH_2, Ox), 79.2 (CH_2, Ox), 62.3 (CH_2, β-Ser), 56.4 (CH, α-Ser), 54.1 (C, Ox), 48.4 ($NHCH_2$); **IR** (film)

3268 (NH), 2923, 2871, 1649 (C=O), 1320, 970 cm^{-1}; **MS** (ESI^+) *m/z* 173 $[M+H]^+$, 195 $[M+Na]^+$; **HRMS** (ESI^+) Calcd. for $C_7H_{12}N_2O_3Na$ $[M+Na]^+$: 195.0740, found 195.0738.

(*S*)-6-Benzyl-2-oxa-5,8-diazaspiro[3.5]nonan-7-one 136

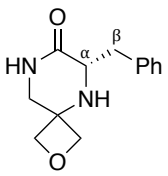

Following general procedure 4, **116** (221 mg, 0.75 mmol) gave, after column chromatography (0-10% MeOH in EtOAc), **136** (140 mg, 0.60 mmol, 80%) as a white solid. $\mathbf{R_f}$ (10% MeOH in EtOAc) 0.32; **^{1}H-NMR** (400 MHz, $CDCl_3$) δ 7.38-7.32 (2H, m, ArH), 7.31-7.24 (3H, m, ArH), 6.55 (1H, s, NHCO), 4.57 (1H, d, *J* = 6.4 Hz, OC*H*H-Ox), 4.49 (1H, d, *J* = 6.4 Hz, OCH*H*-Ox), 4.41 (1H, d, *J* = 7.1 Hz, OC*H*H-Ox), 4.38 (1H, d, *J* = 7.1 Hz, OCH*H*-Ox), 3.76-3.64 (2H, m, CHα-Phe, NHC*H*H), 3.53 (2H, m, NHCH*H*, C*H*Hβ-Phe), 2.80 (1H, dd, *J* = 13.7, 9.9 Hz, CH*H*β-Phe), 1.85 (1H, bs, NH-Phe); **^{13}C-NMR** (100 MHz, $CDCl_3$) δ 170.8 (C=O), 137.7 (C, Ar), 129.4 (2 x CH, Ar), 129.0 (2 x CH, Ar), 127.0 (CH, Ar), 81.8 (OCH_2, Ox), 79.9 (OCH_2, Ox), 56.2 (CH, α-Phe), 55.2 (C, Ox), 49.4 ($NHCH_2$), 38.5 (CH_2, β-Phe); **MS** (ESI^+) *m/z* 233 $[M+H]^+$, 255 $[M+Na]^+$. Data consistent with that reported in literature.[1]

***tert*-Butyl (*S*)-2-(7-oxo-2-oxa-5,8-diazaspiro[3.5]nonan-6-yl)acetate 137**

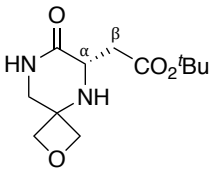

Following general procedure 4, **117** (134 mg, 0.42 mmol) gave, after column chromatography (0-10% MeOH in EtOAc), **137** (74 mg, 0.29 mmol, 69%) as a white solid. $\mathbf{R_f}$ (10% MeOH in EtOAc) 0.32; **mp** 136-138 °C; $\mathbf{[\alpha]_D^{25}}$ −65.0 (*c* 0.19, $CHCl_3$); **^{1}H-NMR** (500 MHz, $CDCl_3$) δ 5.84 (1H, bs, NHCO), 4.66 (1H, d, *J* = 6.2 Hz, OC*H*H-Ox), 4.56 (1H, d, *J* = 6.3 Hz, OCH*H*-Ox), 4.47 (1H, d, *J* = 7.0 Hz, OC*H*H-Ox), 4.37 (1H, d, *J* = 7.0 Hz, OCH*H*-Ox), 3.71 (1H, dd, *J* = 9.1, 2.8 Hz, CHα-Asp), 3.67 (1H, dd, *J* = 11.5, 4.1 Hz, NHC*H*H), 3.49 (1H, d, *J* = 11.5 Hz, NHCH*H*), 2.95 (1H, dd, *J* = 17.5, 2.8 Hz, C*H*Hβ-Asp), 2.55 (1H, dd, *J* = 17.5, 9.1 Hz, CH*H*β-Asp), 1.40 (9H, s, ^{t}Bu), [Note: NH-Asp not observed]; **^{13}C-NMR** (125 MHz, $CDCl_3$) δ 171.6 (C=O), 169.9 (C=O), 81.7 (OCH_2, Ox), 79.8 (OCH_2, Ox), 55.3 (C, Ox), 52.1 (CH, α-Asp), 49.5 ($NHCH_2$), 37.8 (CH_2, β-Asp), 28.3 (3 x CH_3, ^{t}Bu), [Note: C, ^{t}Bu not observed]; **IR** (film) 3230 (NH), 2972, 2857, 1721, 1651 (C=O), 1223 cm^{-1}; **MS** (ESI^+) *m/z* 279 $[M+Na]^+$; **HRMS** (ESI^+) Calcd. for $C_{12}H_{20}N_2O_4Na$ $[M+Na]^+$: 279.1315, found 279.1313.

***tert*-Butyl (*S*)-[4-(7-oxo-2-oxa-5,8-diazaspiro[3.5]nonan-6-yl)butyl]carbamate 138**

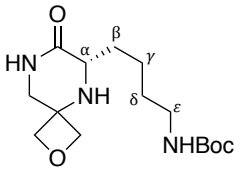

Following general procedure 4, **118** (163 mg, 0.43 mmol) gave, after column chromatography (0-10% MeOH in EtOAc, then 10% MeOH in EtOAc with 0.5% NEt_3), **138** (83 mg, 0.26 mmol, 61%) as a sticky white gum. $\mathbf{R_f}$ (10% MeOH in EtOAc) 0.20; $[\boldsymbol{\alpha}]_{\mathbf{D}}^{\mathbf{26}}$ –41.7 (*c* 0.12, CH_2Cl_2); **^{1}H-NMR** (500 MHz, $CDCl_3$) δ 5.95 (1H, bs, NHCO), 4.63 (1H, d, *J* = 6.5 Hz, OC*H*H-Ox), 4.60 (1H, d, *J* = 6.5 Hz, OCH*H*-Ox), 4.56 (1H, bs, NHBoc), 4.51 (1H, d, *J* = 7.0 Hz, OC*H*H-Ox), 4.45 (1H, d, *J* = 7.0 Hz, OCH*H*-Ox), 3.69 (1H, dd, *J* = 11.5, 4.1 Hz, NHC*H*H), 3.56-3.47 (2H, m, NHCH*H*, CHα-Lys), 3.20-3.02 (2H, m, CH_2ε-Lys), 2.10-1.81 (2H, m, NH-Lys, C*H*Hβ-Lys), 1.78-1.68 (1H, m, CH*H*β-Lys), 1.57-1.35 (13H, m, CH_2δ-Lys, CH_2γ-Lys, ^{t}Bu); **^{13}C-NMR** (125 MHz, $CDCl_3$) δ 171.1 (C=O, Lys), 156.2 (C=O, Boc), 82.0 (OCH_2, Ox), 80.1 (OCH_2, Ox), 55.4 (C, Ox), 55.1 (CH, α-Lys), 49.5 (CH_2), 40.4 (CH_2, ε-Lys) 32.2 (CH_2, β-Lys), 30.2 (CH_2, δ-Lys), 28.6 (3 x CH_3, ^{t}Bu), 22.8 (CH_2, γ-CH_2), [Note: C, ^{t}Bu not observed]; **IR** (film) 3297 (NH), 2932, 2867, 1691 (C=O), 1659 (C=O), 1165, 971 cm^{-1}; **MS** (ESI^+) *m/z* 314 $[M+H]^+$, 336 $[M+Na]^+$; **HRMS** (ESI^+) Calcd. for $C_{15}H_{27}N_3O_4Na$ $[M+Na]^+$: 336.1894, found 336.1903.

(*S*)-Hexahydro-1'H-spiro[oxetane-3,4'-pyrrolo[1,2-a]pyrazin]-1'-one 139

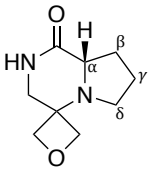

Following general procedure 4, **119** (210 mg, 0.86 mmol) gave, after column chromatography (20% MeOH in EtOAc), **139** (107 mg, 0.59 mmol, 68%) as a white solid. $\mathbf{R_f}$ (20% MeOH in EtOAc) 0.19; **mp** 157-159 °C; $[\boldsymbol{\alpha}]_{\mathbf{D}}^{\mathbf{27}}$ +19.1 (*c* 0.03, $CHCl_3$); **^{1}H-NMR** (400 MHz, $CDCl_3$) δ 6.14 (1H, bs, NH), 4.76-4.70 (2H, m, 2 x OC*H*H-Ox), 4.49 (1H, d, *J* = 6.1 Hz, OCH*H*-Ox), 4.31 (1H, d, *J* = 6.6 Hz, OCH*H*-Ox), 3.80-3.68 (2H, m, NHCH_2), 3.61-3.54 (1H, m, CHα-Pro), 2.99-2.91 (1H, m, C*H*Hδ-Pro), 2.71 (1H, dd, *J* = 16.0, 7.9 Hz, CH*H*δ-Pro), 2.31-2.21 (1H, m, C*H*Hβ-Pro), 2.07-1.96 (1H, m, CH*H*β-Pro), 1.93-1.78 (2H, m, CH_2γ-Pro); **^{13}C-NMR** (125 MHz, $CDCl_3$) δ 172.9 (C=O), 79.3 (OCH_2, Ox), 76.8 (OCH_2, Ox), 58.9 (CH, α-Pro), 57.0 (C, Ox), 46.5 (CH_2, δ-Pro), 45.6 ($NHCH_2$), 28.0 (CH_2, β-Pro), 23.3 (CH_2, γ-Pro); **IR** (film) 3170, 3092, 3049, 2954, 2883, 1651 (C=O), 976 cm^{-1}; **MS** (ESI^+) *m/z* 183 $[M+H]^+$, 205 $[M+Na]^+$; **HRMS** (ESI^+) Calcd. for $C_9H_{15}N_2O_2$ $[M+H]^+$: 183.1128, found 183.1126.

(*R*)-6-Phenyl-2-oxa-5,8-diazaspiro[3.5]nonan-7-one 140

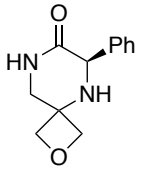

Following general procedure 4, **120** (148 mg, 0.53 mmol) gave, after column chromatography (0-10% MeOH in EtOAc), **140** (98 mg, 0.45 mmol, 85%) as a sticky white gum. $\mathbf{R}_f$ (10% MeOH in EtOAc) 0.36; $[\boldsymbol{\alpha}]_{\mathbf{D}}^{\mathbf{26}}$ −52.2 (*c* 0.11, CH_2Cl_2); **^{1}H-NMR** (400 MHz, $CDCl_3$) δ 7.41-7.21 (5H, m, ArH), 6.33 (1H, s, NHCO), 4.69 (1H, d, *J* = 6.4 Hz, OC*H*H-Ox), 4.62 (1H, d, *J* = 6.4 Hz, OCH*H*-Ox), 4.58 (1H, s, CHPh), 4.44-4.37 (2H, m, OCH_2-Ox), 3.70 (1H, dd, *J* = 11.7 and 3.9 Hz, NHC*H*H), 3.61 (1H, d, *J* = 11.7 Hz, NHCH*H*), 2.97-1.99 (1H, bs, NH); **^{13}C-NMR** (125 MHz, $CDCl_3$) δ 169.6 (C=O), 128.9 (2 x CH, Ar), 128.5 (CH, Ar), 128.4 (2 x CH, Ar) 81.8 (OCH_2, Ox), 80.0 (OCH_2, Ox), 60.6 (CHPh), 55.7 (C, Ox), 49.4 ($NHCH_2$), [Note: C, Ar not observed]; **IR** (film) 3281 (NH), 2941, 2867, 1662 (C=O), 1307, 969 cm^{-1}; **MS** (ESI^+) *m/z* 219 $[M+H]^+$, 241 $[M+Na]^+$; **HRMS** (ESI^+) Calcd. for $C_{12}H_{14}N_2O_2Na$ $[M+Na]^+$: 241.0947, found 241.0948.

9-Benzyl-2-oxa-5,8-diazaspiro[3.5]nonan-7-one 93

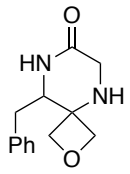

Following general procedure 4, **91** (36 mg, 0.12 mmol) gave, after column chromatography (10% MeOH in EtOAc), **93** (21 mg, 0.09 mmol, 74%) as a white solid. $\mathbf{R}_f$ (10% MeOH in EtOAc) 0.17; **mp** 157-160 °C; **^{1}H-NMR** (400 MHz, $CDCl_3$) δ 7.31-7.26 (2H, m, ArH), 7.24-7.19 (1H, m, ArH), 7.15 (2H, d, *J* = 7.0 Hz, ArH), 5.74 (1H, bs, NHCO), 4.63 (1H, d, *J* = 7.3 H, OC*H*H-Ox), 4.58 (1H, d, *J* = 6.8 Hz, OC*H*H-Ox), 4.52 (1H, d, *J* = 6.8, OCH*H*-Ox), 4.41 (1H, d, *J* = 7.3 Hz, OCH*H*-Ox), 3.75 (1H, dt, *J* = 10.6 and 3.0 Hz, C*H*CH_2Ph), 3.55 (1H, d, *J* = 17.8 Hz, C*H*H-Gly), 3.49 (1H, d, *J* = 17.8 Hz, CH*H*-Gly), 3.03 (1H, dd, *J* = 13.6 and 3.0 Hz, C*H*HPh), 2.70 (1H, dd, *J* =13.6 and 10.6 Hz, CH*H*Ph), 2.17 (1H, bs, NH-Gly); **^{13}C-NMR** (100 MHz, $CDCl_3$) δ 168.4 (C=O), 136.5 (C, Ar), 129.4 (2 x CH, Ar), 129.3 (2 x CH, Ar), 127.4 (CH), 80.1 (OCH_2, Ox), 77.9 (OCH_2, Ox), 58.7 (CH), 58.3 (C, Ox), 45.8 (CH_2, Gly), 38.1 (CH_2Ph); **IR** (film) 3297 (NH), 2948, 2874, 1657 (C=O), 1494, 1454, 1312 cm^{-1}; **MS** (ESI^+) *m/z* 233 $[M+H]^+$, 255 $[M+Na]^+$; **HRMS** (ESI^+) Calcd. for $C_{13}H_{16}N_2O_2$ $[M+H]^+$: 233.1285, found 233.1284.

9-Methyl-2-oxa-5,8-diazaspiro[3.5]nonan-7-one 141

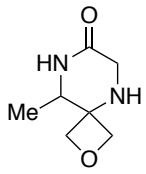

Following general procedure 4, **131** (189 mg, 0.87 mmol) gave, after column chromatography (10-20% MeOH in CH_2Cl_2, 20% MeOH in EtOAc + 1% NEt_3), **141** (109 mg, 0.70 mmol, 81%) as a white solid. $\mathbf{R}_f$ (20% MeOH in EtOAc + 1% NEt_3) 0.25; **mp** 145-147 °C; **^{1}H-NMR** (500 MHz, $CDCl_3$) δ 6.82 (1H, bs, NHCO), 4.60 (1H, d, *J* = 7.0 Hz, OC*H*H-Ox), 4.55 (1H, d, *J* = 6.8 Hz, OC*H*H-Ox), 4.51 (1H, d, *J* = 6.8 Hz, OCH*H*-Ox), 4.43 (1H, d, *J* = 7.0 Hz, OCH*H*-Ox), 3.72 (1H, qd, *J* = 6.6 and 2.3 Hz, CHMe), 3.58 (1H, d, *J* = 17.6 Hz, C*H*H-Gly), 3.51 (1H, d, *J* = 17.6 Hz, CH*H*-Gly), 1.96 (1H, bs, NH-Gly), 1.34 (3H, d, *J* = 6.5 Hz, CH_3); **^{13}C-NMR** (125 MHz, $CDCl_3$) δ 169.2 (C=O), 79.8 (OCH_2, Ox), 77.5 (OCH_2, Ox), 58.1 (C, Ox), 52.9 (CH), 45.8 (CH_2, Gly), 17.5 (CH_3); **IR** (film) 3307 (NH), 3181, 3063, 2955, 2884, 1665 (C=O), 1390, 1307, 974 cm^{-1}; **MS** (ESI$^+$) *m/z* 157 $[M+H]^+$, 179 $[M+Na]^+$; **HRMS** (ESI$^+$) Calcd. for $C_7H_{12}N_2O_2Na$ $[M+Na]^+$: 179.0791, found 179.0791.

(6*S*, 9*S*)- and (6*S*, 9*R*)-6-Isopropyl-9-methyl-2-oxa-5,8-diazaspiro[3.5]nonan-7-one (50:50 dr) 142

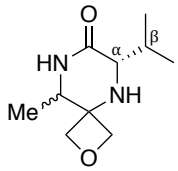

Following general procedure 4, **132** (227 mg, 0.87 mmol) gave, after column chromatography (0-5% MeOH in EtOAc), **142** (133 mg, 0.67 mmol, 77%) as a colourless oil and as a 50:50 mixture of diastereoisomers. $\mathbf{R}_f$ (5% MeOH in EtOAc) 0.34; **^{1}H-NMR** (500 MHz, $CDCl_3$) δ 6.04 (0.5H, bs, NHCO), 5.72 (0.5H, bs, NHCO), 4.70-4.63 (1H, m, OC*H*H-Ox), 4.59-4.52 (1H, m, OCH*H*-Ox), 4.52-4.47 (1H, m, OC*H*H-Ox), 4.45 (0.5H, d, *J* = 7.3 Hz, OCH*H*-Ox), 4.39 (0.5H, d, *J* = 7.3 Hz, OCH*H*-Ox), 3.86-3.77 (0.5H, m, CHMe), 3.55 (0.5H, q, *J* = 6.9 Hz, CHMe), 3.51 (0.5H, d, *J* = 2.8 Hz, CHα-Val), 3.44 (0.5H, d, *J* = 2.8 Hz, CHα-Val), 2.53-2.37 (1H, m, CHβ-Val), 1.84 (1H, bs, NH-Val), 1.45 (1.5H, d, *J* = 6.7 Hz, NHCHC*H*$_3$), 1.23 (1.5H, d, *J* = 6.4 Hz, NHCHC*H*$_3$), 1.05-0.98 (3H, m, CH_3-Val), 0.94 (1.5H, d, *J* = 6.7 Hz, CH_3-Val), 0.92 (1.5H, d, *J* = 6.8 Hz, CH_3-Val); **^{13}C-NMR** (125 MHz, $CDCl_3$) δ 170.9 (C=O), 170.6 (C=O), 82.0 (OCH_2, Ox), 79.4 (OCH_2, Ox), 78.9 (OCH_2, Ox), 77.2 (OCH_2, Ox), 60.1 (CH, α-Val), 59.9 (CH, α-Val), 58.6 (C, Ox), 58.6 (C, Ox), 53.4 (NHCHMe), 52.1 (NHCHMe), 30.2 (CH, β-Val), 29.9 (CH, β-Val), 19.3 (CH_3, Val), 19.2 (CH_3, Val), 18.1 (NHCH*C*H$_3$), 17.0 (NHCH*C*H$_3$), 16.5 (CH_3-Val), 16.4 (CH_3-Val); **IR** (film) 3304 (NH), 2960, 2872, 1654 (C=O), 1310, 973 cm^{-1}; **MS** (ESI$^+$)

m/z 221 $[M+Na]^+$, 419 $[2M+Na]^+$, **HRMS** (ESI^+) Calcd. for $C_{10}H_{18}N_2O_2Na$ $[M+Na]^+$: 221.1260, found 221.1264.

tert-Butyl 3-[(2-methoxy-2-oxoethyl)amino]-3-(nitromethyl)azetidine-1-carboxylate 145

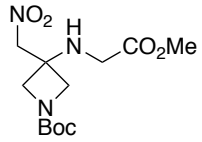

Following general procedure 5, *N*-Boc-azetidin-3-one (428 mg, 2.50 mmol), nitromethane (2.5 mL) and glycine methyl ester hydrochloride (628 mg, 5.00 mmol) were combined to give, after column chromatography (0-40% EtOAc in petroleum ether), **145** (364 mg, 1.20 mmol, 48%) as a yellow solid. $\mathbf{R}_f$ (0-40% EtOAc in petroleum ether) 0.26; **mp** 92-95 °C; **^{1}H-NMR** (500 MHz, $CDCl_3$) δ 4.68 (2H, s, NO_2CH_2), 4.03-3.89 (2H, m, 2 x NC*H*H-Az), 3.87 (2H, d, *J* = 9.4 Hz, 2 x NCH*H*-Az), 3.76 (3H, s, OCH_3), 3.48 (2H, s, CH_2-Gly), 2.31 (1H, bs, NH), 1.44 (9H, s, ^{t}Bu); **^{13}C-NMR** (125 MHz, $CDCl_3$) δ 172.0 (C=O, Gly), 156.2 (C=O, Boc), 80.6 (C, ^{t}Bu), 78.6 (NO_2CH_2), 57.2 (2 x NCH_2, Az), 54.3 (C, Ox), 52.3 (OCH_3), 44.7 (CH_2, Gly), 28.5 (3 x CH_3, ^{t}Bu), [Note: 2 x NCH_2, Az assigned using HSQC]; **IR** (film) 3339 (NH), 3010, 2979, 2955, 1738 (C=O), 1685 (C=O), 1548, 1406, 1120 cm^{-1}; **MS** *m/z* (ESI^+) 326 $[M+Na]^+$, 342 $[M+K]^+$; **HRMS** (ESI^+) Calcd. for $C_{12}H_{21}N_3O_6Na$ $[M+Na]^+$: 326.1323, found 326.1323.

tert-Butyl (*S*)-3-[(1-methoxy-3-methyl-1-oxobutan-2-yl)amino]-3-(nitromethyl) azetidine-1-carboxylate 146

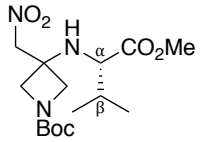

Following general procedure 5, *N*-Boc-azetidin-3-one (384 mg, 2.24 mmol), nitromethane (2.24 mL) and *L*-valine methyl ester hydrochloride (752 mg, 4.49 mmol) were combined to give, after column chromatography (20% EtOAc in petroleum ether), **146** (605 mg, 1.75 mmol, 78%) as a yellow oil. $\mathbf{R}_f$ (20% EtOAc in petroleum ether) 0.29; $[\boldsymbol{\alpha}]_{\mathbf{D}}^{\mathbf{30}}$ –0.4 (*c* 0.18, $CHCl_3$); **^{1}H-NMR** (400 MHz, $CDCl_3$) δ 4.69 (1H, d, *J* = 13.4 Hz, NO_2CHH), 4.59 (1H, d, *J* = 13.4 Hz, NO_2CHH), 4.00-3.88 (1H, m, NC*H*H-Az), 3.92 (2H, s, NCH_2-Az), 3.78-3.68 (4H, m, NCH*H*-Az and OCH_3), 3.14-3.04 (1H, m, CHα-Val), 2.27 (1H, bs, NH), 1.98-1.82 (1H, m, CHβ-Val), 1.44 (9H, s, ^{t}Bu), 0.92 (3H, d, *J* = 6.7 Hz, CH_3-Val), 0.88 (3H, d, *J* = 6.8 Hz, CH_3-Val); **^{13}C-NMR** (125 MHz, $CDCl_3$) δ 175.9 (C=O, Val), 156.3 (C=O, Boc), 80.4 (C, ^{t}Bu), 78.8 (NO_2CH_2), 61.4 (CH, α-Val), 57.7 (NCH_2, Az), 57.4 (NCH_2, Az), 54.3 (C,

Ox), 52.4 (OCH_3), 32.3 (CH, β-Val), 28.5 (3 x CH_3, ^{t}Bu), 19.3 (CH_3, Val), 18.2 (CH_3, Val), [Note: 2 x NCH_2 assigned using HSQC]; **IR** (film) 3339 (NH), 2972, 2884, 1731 (C=O), 1697 (C=O), 1556, 1378, 1163 cm^{-1}; **MS** (ESI^+) *m/z* 346 $[M+H]^+$, 368 $[M+Na]^+$; **HRMS** (ESI^+) Calcd. for $C_{15}H_{27}N_3O_6Na$ $[M+Na]^+$: 368.1792, found 368.1792.

tert-Butyl 7-oxo-2,5,8-triazaspiro[3.5]nonane-2-carboxylate 147

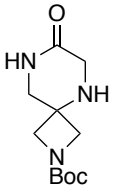

Following general procedure 4, **145** (286 mg, 0.94 mmol) gave **147** (211 mg, 0.87 mmol, 93%) as a white solid which after work up required no further purification. **mp** 156-158 °C; **^{1}H-NMR** (500 MHz, $CDCl_3$) δ 5.94 (1H, bs, NHCO), 3.85 (2H, d, *J* = 9.1 Hz, 2 x NC*H*H-Az), 3.82 (2H, d, *J* = 9.1 Hz, 2 x NCH*H*-Az), 5.59 (2H, s, CH_2-Gly), 3.51 (2H, d, *J* = 1.8 Hz, CH_2NHCO), 1.83 (1H, bs, NH-Gly), 1.45 (9H, s, ^{t}Bu); **^{13}C-NMR** (125 MHz, $CDCl_3$) 168.5 (C=O, Gly), 156.4 (C=O, Boc), 80.3 (C, ^{t}Bu), 58.1 (2 x NCH_2, Az), 50.3 (*C*H_2NHCO), 46.0 (CH_2, Gly), 28.5 (3 x CH_3, ^{t}Bu), [Note: 2 x NCH_2, Az assigned using HSQC and C, Az not assigned]; **IR** (film) 3308 (NH), 3246 (NH) 2976, 2930, 2876, 1699 (C=O), 1680 (C=O), 1445, 1322 cm^{-1}; **MS** (ESI^+) *m/z* 264 $[M+Na]^+$, 483 [2M+H]; **HRMS** (ESI^+) Calcd. for $C_{11}H_{19}N_3O_3Na$ $[M+Na]^+$: 264.1319, found 264.1318.

tert-Butyl (S)-6-isopropyl-7-oxo-2,5,8-triazaspiro[3.5]nonane-2-carboxylate 148

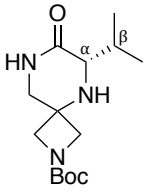

Following general procedure 4, **146** (116 mg, 0.34 mmol) gave, after column chromatography (0-5% MeOH in CH_2Cl_2), **148** (66 mg, 0.23 mmol, 69%) as a white solid. $\mathbf{R_f}$ (5% MeOH in CH_2Cl_2) 0.20; **mp** 162-165 °C; $[\alpha]_D^{26}$ –51.5 (*c* 0.28, $CHCl_3$); **^{1}H-NMR** (400 MHz, $CDCl_3$) δ 6.16 (1H, bs, NHCO), 3.89 (1H, d, *J* = 8.7 Hz, NC*H*H-Az), 3.86-3.78 (2H, m, NCH*H*-Az and NC*H*H-Az), 3.75 (1H, d, *J* = 9.4 Hz, NCH*H*-Az), 3.52-3.42 (2H, m, CHα-Val and NHC*H*H), 3.39 (1H, dd, *J* = 11.4 and 4.2 Hz, NHCH*H*), 2.53-2.37 (1H, m, CHβ-Val), 1.69 (1H, bs, NH), 1.44 (9H, s, ^{t}Bu), 0.99 (3H, d, *J* = 7.1 Hz, CH_3-Val), 0.92 (3H, d, *J* = 6.7 Hz, CH_3-Val); **^{13}C-NMR** (125 MHz, $CDCl_3$) δ 171.1 (C=O, Val), 156.5 (C=O, Boc), 80.2 (C, ^{t}Bu), 60.12 (CH, α-Val), 59.3 (NCH_2, Az), 58.3 (NCH_2, Az) 50.6 (C, Ox), 49.9 ($NHCH_2$), 30.1 (CH, β-Val), 28.5 (3 x CH_3, ^{t}Bu), 19.2 (CH_3, Val), 16.4 (CH_3, Val) [Note: 2 x NCH_2 assigned using HSQC]; **IR** (film) 3283 (NH), 3261 (NH), 2963, 2873, 1691 (C=O), 1652 (C=O),

1403, 1171, 1121 cm^{-1}; **MS** (ESI^+) *m/z* 284 $[M+H]^+$, 306 $[M+Na]^+$; **HRMS** (ESI^+) Calcd. for $C_{14}H_{25}N_3O_3Na$ $[M+Na]^+$: 306.1788, found 306.1791.

(*S*)-5-Benzyl-6-methyl-2-oxa-5,8-diazaspiro[3.5]nonan-7-one 156

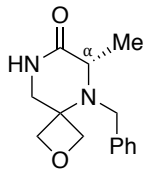

134 (84 mg, 0.54 mmol), Na_2CO_3 (399 mg, 3.76 mmol), NaI (202 mg, 1.35 mmol) and benzyl bromide (161 μL, 1.35 mmol) in MeCN (5 mL) were stirred at reflux for 3 h. On cooling to room temperature, the mixture was poured in water (10 mL) and extracted with EtOAc (3 x 10 mL). The combined organics were washed with brine (1 mL), dried ($MgSO_4$), filtered and concentrated under reduced pressure. Purification by column chromatography (0-5% MeOH in CH_2Cl_2) gave **156** (101 mg, 0.41 mmol, 76%) as a white solid. $\mathbf{R_f}$ (5% MeOH in CH_2Cl_2) 0.38; **mp** 150-152 °C; $[\alpha]_D^{26}$ −31.7 (*c* 0.24, CH_2Cl_2); **^{1}H-NMR** (500 MHz, $CDCl_3$) δ 7.40-7.35 (2H, m, ArH), 7.35-7.30 (2H, m, ArH), 7.29-7.23 (1H, m, ArH), 6.27 (1H, bs, NH), 4.83 (1H, d, *J* = 6.3 Hz, OC*H*H-Ox), 4.74 (1H, d, *J* = 6.3 Hz, OC*H*H-Ox), 4.33 (1H, d, *J* = 6.2 Hz, OCH*H*-Ox), 4.28 (1H, d, *J* = 6.3 Hz, OCH*H*-Ox), 3.95-3.80 (3H, m, NHC*H*$_2$ and C*H*HPh), 3.60 (1H, d, *J* = 14.8 Hz, CH*H*Ph), 3.33 (1H, q, *J* = 7.3 Hz, CH α-Ala), 1.25 (3H, d, *J* = 7.3 Hz, CH_3, Ala); **^{13}C-NMR** (125 MHz, $CDCl_3$) δ 172.7 (C=O), 139.1 (C, Ar), 128.7 (2 x CH, Ar), 128.0 (2 x CH, Ar), 127.5 (CH, Ar), 79.5 (OCH_2, Ox), 78.5 (OCH_2, Ox), 58.6 (C, Ox), 57.2 (CH, α-Ala), 52.9 (CH_2Ph), 47.3 ($NHCH_2$), 19.0 (CH_3, Ala); **IR** (film) 3186 (NH), 3051, 2985, 2947, 2868, 1662 (C=O), 1492, 1363, 1329, 979 cm^{-1}; **MS** (ESI^+) *m/z* 247 $[M+H]^+$, 269 $[M+Na]^+$; **HRMS** (ESI^+) Calcd. for $C_{14}H_{19}N_2O_2$ $[M+H]^+$: 247.1441, found 247.1442.

(*S*)-8-Benzyl-6-methyl-2-oxa-5,8-diazaspiro[3.5]nonan-7-one 157

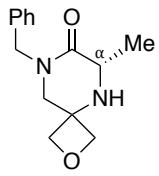

134 (126 mg, 0.81 mmol) was dissolved in DMF (3 mL) and cooled to 0 °C. NaH (60% in mineral oil, 34 mg, 0.85 mmol) was added and the reaction mixture allowed to reach room temperature and stirred for 30 min, whereupon benzyl bromide (101 μL, 0.85 mmol) was added. After stirring for a further 20 h, the mixture was poured into brine (10 mL) and extracted with EtOAc (3 x 20 mL). The combined organic extracts were dried ($MgSO_4$), filtered and concentrated under reduced pressure. Purification by column chromatography (0-5% MeOH in CH_2Cl_2) gave **157** (135 mg, 0.55 mmol, 68%) as a colourless oil. $\mathbf{R_f}$ (5% MeOH

in CH_2Cl_2) 0.27; $[\alpha]_D^{26}$ −56.3 (*c* 0.12, CH_2Cl_2); **^{1}H-NMR** (400 MHz, $CDCl_3$) δ 7.40-7.20 (5H, m, ArH), 4.81 (1H, d, *J* = 14.5 Hz, C*H*HPh), 4.60 (1H, d, *J* = 6.3 Hz, OC*H*H-Ox), 4.44 (1H, d, *J* = 7.0 Hz, OC*H*H-Ox), 4.42-4.31 (3H, m, CH*H*Ph and 2 x OCH*H*-Ox), 3.69 (1H, q, *J* = 6.5 Hz, CHα-Ala), 3.55 (1H, d, *J* = 11.9 Hz, NC*H*H), 3.44 (1H, d, *J* = 11.9 Hz, NCH*H*), 1.97 (1H, bs, NH), 1.45 (3H, d, *J* = 6.7 Hz, CH_3-Ala); **^{13}C-NMR** (125 MHz, $CDCl_3$) δ 169.7 (C=O), 136.6 (C, Ar), 129.0 (2 x CH, Ar), 128.3 (2 x CH, Ar), 127.9 (CH, Ar), 81.9 (OCH_2, Ox), 80.3 (OCH_2, Ox), 55.6 (C, Ox), 53.8 (NCH_2), 51.4 (CH, α-Ala), 50.1 (CH_2Ph), 19.3 (CH_3, Ala); **IR** (film) 3276 (NH), 2933, 2868, 1633 (C=O), 1494, 1452, 1293, 972 cm^{-1}; **MS** (ESI^+) *m/z* 247 $[M+H]^+$, 269 $[M+Na]^+$; **HRMS** (ESI^+) Calcd. for $C_{14}H_{19}N_2O_2$ $[M+H]^+$: 247.1441, found 247.1441.

(*S*)-5-Benzyl-6-methyl-2-oxa-5,8-diazaspiro[3.5]nonane-7-thione 165

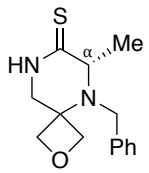

To a solution of **156** (155 mg, 0.63 mmol) in THF (4 mL) was added a suspension of Lawesson's reagent (125 mg, 0.31 mmol) in THF (15 mL). The reaction mixture was stirred at room temperature for 16 h and then at reflux for 4 h. The mixture was allowed to cool to room temperature and concentrated under reduced pressure. Purification by column chromatography (0-5% MeOH in CH_2Cl_2) gave **165** (131 mg, 0.50 mmol, 79%) as a yellow solid. $\mathbf{R}_f$(5% MeOH in CH_2Cl_2) 0.30; **mp** 189-191 ˚C; $[\alpha]_D^{27}$ +2.1 (*c* 0.11, CH_2Cl_2); **^{1}H-NMR** (400 MHz, $CDCl_3$) δ 8.09 (1H, bs, NHCS), 7.33-7.19 (5H, m, ArH), 4.79-7.74 (2H, m, 2 X OC*H*H-Ox), 4.27-4.18 (2H, m, 2 x OCH*H*-Ox), 3.87 (1H, dd, *J* = 13.6 and 1.9 Hz, NHC*H*H), 3.77 (1H, d, *J* = 13.1 Hz, NHCH*H*), 3.73-3.61 (2H, m, CHα-Ala and C*H*HPh), 3.47 (1H, d, *J* = 14.2 Hz, CH*H*Ph), 1.33 (3H, d, *J* = 7.3 Hz, CH_3-Ala); **^{13}C-NMR** (125 MHz, $CDCl_3$) δ 206.5 (C=S), 138.0 (C, Ar), 128.8 (2 x CH, Ar), 128.3 (2 x CH, Ar), 127.8 (CH, Ar), 80.4 (OCH_2, Ox), 79.0 (OCH_2, Ox), 63.1 (CH, α-Ala), 57.5 (C, Ox), 53.1 (CH_2Ph), 48.3 ($NHCH_2$), 22.9 (CH_3, Ala); **IR** (film) 3145 (NH), 3066, 3024, 2981, 2934, 2864, 1568 (C=S), 1336, 980 cm^{-1}; **MS** (ESI^+) *m/z* 263 $[M+H]^+$, 285 $[M+Na]^+$; **HRMS** (ESI^+) Calcd. for $C_{14}H_{18}N_2OSNa$ $[M+Na]^+$: 285.1032, found 285.1033.

(*S*)-5-Benzyl-6-methyl-2-oxa-5,8-diazaspiro[3.5]nonane 166

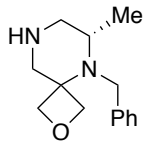

To a suspension of **165** (50 mg, 0.19 mmol) in MeOH (2 mL) was added Raney Ni (slurry in H_2O, 0.5 mL). The reaction mixture was stirred at reflux for 3 h. On cooling to room temperature, the mixture was filtered through a plug of Celite® eluting with EtOAc and the eluent concentrated under reduced pressure. Purification by column chromatography (10-20% MeOH in CH_2Cl_2) gave **166** (29 mg, 0.13 mmol, 68%) as a yellow oil. $\mathbf{R_f}$ (10% MeOH in CH_2Cl_2) 0.28; $[\boldsymbol{\alpha}]_{\mathbf{D}}^{\mathbf{26}}$ +29.3 (*c* 0.03, $CHCl_3$); **^{1}H-NMR** (500 MHz, $CDCl_3$) δ 7.39 (2H, d, *J* = 7.2 Hz, ArH), 7.31 (2H, t, *J* = 7.6 Hz, ArH), 7.25-7.19 (1H, m, ArH), 4.81 (1H, d, *J* = 6.5 Hz, OC*H*H-Ox), 4.60 (1H, d, *J* = 6.8 Hz, OC*H*H-Ox), 4.46 (1H, d, *J* = 6.6 Hz, OCH*H*-Ox), 4.31 (1H, d, *J* = 6.8 Hz, OCH*H*-Ox), 4.18 (1H, d, *J* = 16.4 Hz, C*H*HPh), 3.89 (1H, d, *J* = 16.4 Hz, CH*H*Ph), 3.30 (1H, d, *J* = 12.0 Hz, NHC*H*H), 3.19 (1H, d, *J* = 12.0 Hz, NHCH*H*), 2.90 (1H, dd, *J* = 12.0, 2.9 Hz, C*H*HCHMe), 2.87-2.71 (2H, m, CHMe, NH), 2.67 (1H, dd, *J* = 12.0, 7.5 Hz, CH*H*CHMe), 0.90 (3H, d, *J* = 6.5 Hz, CH_3); **^{13}C-NMR** (125 MHz, $CDCl_3$) δ 142.0 (C, Ar), 128.4 (2 x CH, Ar), 127.2 (2 x CH, Ar), 126.7 (CH, Ar), 78.8 (OCH_2-Ox), 78.6 (OCH_2-Ox), 60.8 (C, Ox), 53.2 ($NHCH_2$), 52.8 (CHMe), 50.8 (CH_2Ph or *C*H_2CHMe), 50.7 (CH_2Ph or *C*H_2CHMe), 16.9 (CH_3); **IR** (film) 3307 (NH), 3059, 3026, 2937, 2872, 2814, 1493, 1452, 973 cm^{-1}; **MS** (ESI^+) *m/z* 233 $[M+H]^+$; **HRMS** (ESI^+) Calcd. for $C_{14}H_{21}N_2O$ $[M+H]^+$: 233.1648, found 233.1650.

Fmoc-G_{Ox}-Phe-OBn 174

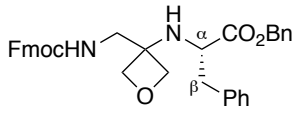

Following general procedure 6, **34**[1] (1.24 g, 3.34 mmol) gave, after column chromatography (5-10% EtOAc in CH_2Cl_2), **174** (1.30 g, 2.32 mmol, 69%) as a sticky white gum. $\mathbf{R_f}$ (5% EtOAc in CH_2Cl_2) 0.21; $[\boldsymbol{\alpha}]_{\boldsymbol{D}}^{\mathbf{29}}$ –3.8 (*c* 0.144, $CHCl_3$) **^{1}H-NMR** (500 MHz, $CDCl_3$) δ 7.78 (2H, d, *J* = 7.5 Hz, ArH-Fmoc), 7.63-7.55 (2H, m, ArH-Fmoc), 7.42 (2H, t, *J* = 7.4 Hz, ArH-Fmoc), 7.39-7.28 (7H, m, ArH) 7.27-7.21 (2H, m, ArH), 7.21-7.11 (3H, m, ArH), 5.15 (1H, d, *J* = 12.1 Hz, OC*H*HPh), 5.11(1H, d, *J* = 12.1 Hz, OCH*H*Ph), 4.80-4.69 (1H, m, NH-G_{Ox}), 4.39 (2H, d, *J* = 6.9 Hz, CH_2-Fmoc), 4.29-4.18 (3H, m, CH-Fmoc and 2 x OC*H*H-Ox), 4.15 (1H, d, *J* = 6.6 Hz, OCH*H*-Ox), 4.10 (1H, d, *J* = 6.4 Hz, OCH*H*-Ox), 3.53 (1H, dd, *J* = 8.9, 4.9 Hz, CHα-Phe), 3.47-3.30 (2H, m, CH_2-G_{Ox}), 13.03 (1H, dd, *J* = 13.4, 4.9 Hz, C*H*Hβ-Phe), 2.75 (1H, dd, *J* = 13.4, 8.9 Hz, CH*H*β-Phe), 2.08 (1H, bs, NH-Phe); **^{13}C-NMR** (125 MHz, $CDCl_3$) δ 175.3 (C=O, Phe), 156.9 (C=O, Fmoc), 144.1

(C, Ar-Fmoc), 144.0 (C, Ar-Fmoc), 141.5 (2 x C, Ar-Fmoc) 137.2 (C, Ar), 135.2 (C, Ar), 129.4 (2 x CH, Ar), 128.84 (CH, Ar), 128.83 (CH, Ar), 128.79 (2 x CH, Ar), 128.76 (CH, Ar), 127.8 (2 x CH, Ar), 127.3 (CH, Ar), 127.2 (2 x CH, Ar), 125.21 (CH, Ar), 125.18 (CH, Ar), 120.1 (2 x CH, Ar), 79.9 (OCH_2, Ox), 79.4 (OCH_2, Ox), 67.5 (CH_2, OCH_2Ph), 66.8 (CH_2, Fmoc), 59.4 (C, Ox), 57.5 (CHα, Phe), 47.4 (CH, Fmoc), 44.9 (CH_2, G_{Ox}), 40.7 (CH_2β, Phe) [Note: 2 x CH, Ar not assigned]; **IR** (film) 3408 (NH), 3332 (NH), 3063, 3030, 2948, 2872, 1719 (C=O), 1512, 1496, 1450, 1224, 1152 cm^{-1}; **MS** (ESI+) *m/z* 563 $[M+H]^+$, 585 $[M+Na]^+$; **HRMS** (ESI+) Calcd. for $C_{35}H_{34}N_2O_5Na$ $[M+Na]^+$: 585.2360, found 585.2361.

Fmoc-G_{Ox}-Gly-OBn 179

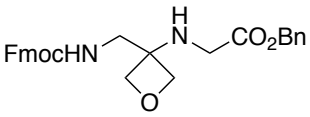

Following general procedure 6, **178**[1] (1.19 g, 4.23 mmol) gave, after column chromatography (30% EtOAc in CH_2Cl_2), **179** (1.50 g, 3.16 mmol, 75%) as a white solid. $\mathbf{R}_f$ (30% EtOAc in CH_2Cl_2) 0.36; **mp** 128-130 °C; **^{1}H-NMR** (500 MHz, $CDCl_3$) δ 7.76 (2H, d, *J* = 7.6 Hz, ArH-Fmoc), 7.60 (2H, d, *J* = 7.4 Hz, ArH-Fmoc), 7.45-7.28 (9H, m, ArH), 5.36-5.24 (1H, m, NH-G_{Ox}), 5.19 (2H, s, CH_2-Bn), 4.55-4.17 (7H, m, C*H*CH_2-Fmoc and 2 x OCH_2-Ox), 3.62-3.35 (4H, m, CH_2-Gly and CH_2-G_{Ox}), 2.10 (1H, bs, NH-Gly); **^{13}C-NMR** (125 MHz, $CDCl_3$) δ 172.5 (C=O, Gly), 157.0 (C=O, Fmoc), 144.0 (2 x C, Ar-Fmoc), 141.5 (2 x C, Ar-Fmoc), 135.3 (C, Ar), 128.9 (2 x CH, Ar), 128.8 (CH, Ar), 128.7 (2 x CH, Ar), 127.8 (2 x CH, Ar), 127.2 (2 x CH, Ar), 125.2 (2 x CH, Ar), 120.1 (2 x CH, Ar), 79.3 (2 x OCH_2, Ox), 67.3 (CH_2, Bn), 67.0 (CH_2, Fmoc), 59.7 (C, Ox), 47.4 (CH, Fmoc), 45.1 (CH_2, Gly), 44.9 (CH_2, G_{Ox}); **IR** (film) 3281 (NH), 3246 (NH), 3063, 2987, 2952, 2887, 1742 (C=O), 1721 (C=O), 1560, 1442, 1394 cm^{-1}; **MS** (ESI^+) *m/z* 473 $[M+H]^+$, 495 $[M+Na]^+$; **HRMS** (ESI^+) Calcd. for $C_{28}H_{29}N_2O_5$ $[M+H]^+$: 473.2071, found 473.2072.

Fmoc-G_{Ox}-Val-OBn 180

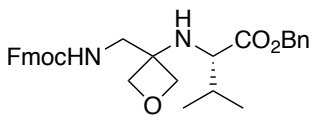

Following general procedure 6, **110**[1] (873 mg, 2.71 mmol) gave, after column chromatography (5-10% EtOAc in CH_2Cl_2), **180** (519 mg, 1.01 mmol, 37%) as a colourless oil. $\mathbf{R}_f$ (5% EtOAc in CH_2Cl_2) 0.25; $[\boldsymbol{\alpha}]_{\mathbf{D}}^{\mathbf{20}}$ −7.4 (*c* 0.45, $CHCl_3$); **^{1}H-NMR** (500 MHz, $CDCl_3$) δ 7.77 (2H, d, *J* = 7.5 Hz, ArH-Fmoc), 7.60 (2H, *J* = 7.5 Hz, ArH-Fmoc), 7.46-7.28 (9H,

m, ArH), 5.24-5.15 (2H, m, NH-G_{Ox} and C*H*H-Bn), 5.13 (1H, d, *J* = 12.0 Hz, CH*H*-Bn), 4.55-4.10 (7H, m, C*H*C*H*$_2$Fmoc and 2 x OCH_2-Ox), 3.66 (1H, dd, *J* = 13.7, 5.6 Hz, C*H*H-G_{Ox}), 3.43 (1H, dd, *J* = 13.7 and 5.0 Hz, CH*H*-G_{Ox}), 3.14 (1H, d, *J* = 5.3 Hz, CHα-Val), 2.15-1.87 (2H, m, NH-Val and CHβ-Val), 0.96 (3H, d, *J* = 6.7 Hz, CH_3-Val), 0.90 (3H, d, *J* = 6.7 Hz, CH_3-Val); **^{13}C-NMR** (125 MHz, $CDCl_3$) δ 176.0 (C=O, Val), 156.9 (C=O, Fmoc), 144.1 (C, Ar-Fmoc), 144.0 (C, Ar-Fmoc), 141.5 (2 x C, Ar-Fmoc), 135.3 (C, Ar), 128.83 (2 x CH, Ar), 128.80 (3 x CH, Ar), 127.8 (2 x CH, Ar), 127.2 (2 x CH, Ar), 125.2 (2 x CH, Ar), 120.1 (2 x CH, Ar), 79.7 (OCH_2, Ox), 79.6 (OCH_2, Ox), 67.3 (CH_2, Bn), 67.0 (CH_2, Fmoc), 61.1 (CH, α-Val), 59.5 (C, Ox), 47.4 (CH, Fmoc), 45.4 (CH_2, G_{Ox}), 32.1 (CH, β-Val), 19.6 (CH_3, Val), 18.1 (CH_3, Val); **IR** (film) 3313 (NH), 2963, 2900, 2879, 1720 (C=O), 1450, 1235, 1145 cm^{-1}; **MS** (ESI$^+$) *m/z* 515 $[M+H]^+$, 537 $[M+Na]^+$; **HRMS** (ESI$^+$) Calcd. for $C_{31}H_{34}N_2O_5Na$ $[M+Na]^+$: 537.2360, found 537.2359.

Fmoc-G_{Ox}-Phe-OMe 186

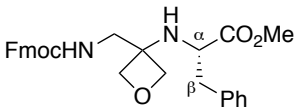

Following general procedure 6, **116** (497 mg, 1.69 mmol) gave, after column chromatography (40% EtOAc in petroleum ether), **186** (717 mg, 1.47 mmol, 87%) as sticky white gum. $\mathbf{R}_f$ (50% EtOAc in petroleum ether) 0.32; $[\boldsymbol{\alpha}]_{\boldsymbol{D}}^{\mathbf{29}}$ –21.3 (*c* 0.075, $CHCl_3$) **^{1}H-NMR** (500 MHz, $CDCl_3$) δ 7.78 (2H, d, *J* = 7.5 Hz, ArH-Fmoc), 7.59 (2H, dd, *J* = 7.2, 3.4 Hz, ArH-Fmoc), 7.42 (2H, t, *J* = 7.4 Hz, ArH-Fmoc), 7.34 (2H, t, *J* = 7.4 Hz, ArH-Fmoc), 7.29-7.23 (2H, m, ArH-Phe), 7.22-7.13 (3H, m, ArH-Phe), 4.90-4.66 (1H, m, NH-G_{Ox}), 4.39 (2H, d, *J* = 6.9 Hz, CH_2-Fmoc), 4.30-4.09 (5H, m, CH-Fmoc and 2 x OCH_2-Ox), 3.72 (3H, s, OCH_3), 3.55-3.32 (3H, m, CHα-Phe and CH_2-G_{Ox}), 3.03 (1H, dd, *J* = 13.4, 4.5 Hz, C*H*Hβ-Phe), 2.74 (1H, dd, *J* = 13.3, 9.3 Hz, CH*H*β-Phe), 2.05 (1H, bs, NH-Phe); **^{13}C-NMR** (125 MHz, $CDCl_3$) δ 175.9 (C=O, Phe), 156.9 (C=O, Fmoc), 144.1 (C, Ar-Fmoc), 144.0 (C, Ar-Fmoc), 141.5 (2 x C, Ar-Fmoc), 137.3 (C, Ar-Phe), 129.4 (2 x CH, Ar), 128.8 (2 x CH, Ar), 127.8 (2 x CH, Ar), 127.3 (CH, Ar), 127.2 (2 x CH, Ar), 125.2 (2 x CH, Ar), 120.1 (2 x CH, Ar), 80.0 (OCH_2, Ox), 79.4 (OCH_2, Ox), 66.8 (CH_2, Fmoc), 59.4 (C, Ox), 57.4 (CH, Fmoc), 52.6 (CH_3), 47.4 (CHα, Phe), 44.9 (CH_2, G_{Ox}), 40.7 (CH_2β-Phe); **IR** (film) 3406 (NH), 3333 (NH), 2949, 2879, 1718 (C=O), 1511, 1449, 1222 cm^{-1}; **MS** (ESI+) *m/z* 487 $[M+H]^+$, 509 $[M+Na]^+$; **HRMS** (ESI+) Calcd. for $C_{29}H_{30}N_2O_5Na$ $[M+Na]^+$: 509.2047, found 509.2045.

Fmoc-Phe-ODmb 189

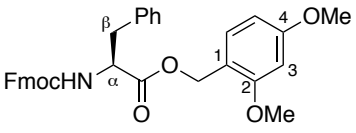

Fmoc-Phe-OH (3.87 g, 10.0 mmol), DCC (2.27 g, 11.0 mmol) and DMAP (122 mg, 1.00 mmol) were combined in CH_2Cl_2 (40 mL). The reaction mixture was cooled to 0 °C and 2,4-dimethoxybenzyl alcohol (2.02 g, 12.0 mmol) was added. The mixture was warmed to room temperature and stirred for 16 h. The reaction mixture was filtered and the eluent washed with saturated $NaHCO_3$ (40 mL) and brine (20 mL), dried ($MgSO_4$), filtered and concentrated under reduced pressure to give a crude product. Purification by flash column chromatography (20% EtOAc in petroleum ether) gave **189** (2.28 g, 7.96 mmol, 80%) as a sticky white gum. $\mathbf{R}_f$(20% EtOAc in petroleum ether) 0.33; $[\boldsymbol{\alpha}]_{\boldsymbol{D}}^{\mathbf{29}}$ –9.4 (*c* 0.168, $CHCl_3$); **^{1}H-NMR** (500 MHz, $CDCl_3$) δ 7.77 (2H, d, *J* = 7.5 Hz, ArH), 7.63-7.50 (2H, m, ArH), 7.44-7.35 (2H, m, ArH), 7.35-7.28 (2H, m, ArH), 7.28-7.11 (4H, m, ArH), 7.09-6.91 (2H, m, ArH), 6.53-6.38 (2H, m, ArH-3, ArH-5), 5.30 (1H, d, *J* = 8.2 Hz, NH), 5.21 (1H, d, *J* = 11.7 Hz, C*H*H-Dmb), 5.12 (1H, d, *J* = 11.7 Hz, CH*H*-Dmb), 4.75-4.65 (1H, m, CHα-Phe), 4.47-4.27 (2H, m, CH_2-Fmoc), 4.20 (0.85H, t, *J* = 7.1 Hz, major rotamer CH-Fmoc), 4.14-4.04 (0.15H, minor rotamer CH-Fmoc), 3.88- 3.70 (6H, m, 2 x OCH_3), 3.15 (0.85H, dd, *J* = 13.9, 5.6 Hz, major rotamer C*H*Hβ-Phe), 3.11 (0.85H, dd, *J* = 13.8, 5.5 Hz, major rotamer CH*H*β-Phe) 2.94-2.81 (0.30H, m, minor rotamer CH_2β-Phe); **^{13}C-NMR** (125 MHz, $CDCl_3$) δ 171.6 (C=O, Phe), 161.7 (C, Ar-4), 159.3 (C, Ar-2), 155.6 (C=O, Fmoc), 144.0 (C, Ar-Fmoc), 143.9 (C, Ar-Fmoc), 141.4 (2 x C, Ar-Fmoc), 135.9 (C, Ar-Phe), 132.1 (CH, Ar-6), 129.6 (2 x CH, Ar), 128.6 (2 x CH, Ar), 127.8 (2 x CH, Ar), 127.2 (2 x CH, Ar), 127.1 (CH, Ar), 125.3 (CH, Ar), 125.2 (CH, Ar), 120.09 (CH, Ar), 120.08 (CH, Ar), 116.0 (C, Ar-1), 104.2 (CH, Ar-3 or Ar-5), 98.7 (CH, Ar-3 or Ar-5), 67.0 (CH_2, Fmoc), 63.1 (CH_2, Dmb), 55.5 (2 x OCH_3), 54.8 (CH, α-Phe), 47.3 (CH, Fmoc), 38.2 (CH_2, β-Phe); **IR** (film): 3320 (NH), 3063, 3003, 2938, 2835, 1720 (C=O), 1688 (C=O), 1524, 1508, 1206 cm^{-1}; **MS** (ESI+) *m/z* 560 $[M+Na]^+$, 576 $[M+K]^+$; **HRMS** (ESI+) Calcd. for $C_{33}H_{31}NO_6Na$ $[M+Na]^+$: 560.2044, found 560.2040.

2,4-Dimethoxybenzyl [3-(nitromethyl)oxetan-3-yl]-*L*-phenylalaninate 193

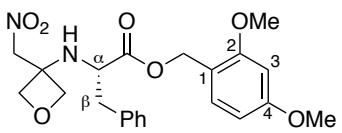

To **189** (702 mg, 1.31 mmol) in CH_2Cl_2 (12 mL) was added diethylamine (2 mL) and the reaction mixture stirred at room temperature for 4 h. The reaction mixture was concentrated under reduced pressure and the resulting residue repeatedly dissolved in CH_2Cl_2 (3 x 10

mL) and concentrated under reduced pressure to give the crude amine. Meanwhile, oxetan-3-one (42 μL, 0.66 mmol), nitromethane (49 μL, 0.92 mmol) and triethylamine (18 μL, 0.13 mmol) were stirred at room temperature for 1 h. CH_2Cl_2 (3 mL) was added and the reaction mixture cooled to −78 °C. Triethylamine (183 μL, 1.32 mmol) was added followed by the dropwise addition of a solution of methanesulfonyl chloride (51 μL, 0.66 mmol) in CH_2Cl_2 (1 ml). The reaction mixture was left to stir at −78 °C for 1.5 h. The crude amine was dissolved in CH_2Cl_2 (6 mL) and added to the oxetane mixture *via* syringe at −78 °C. The reaction mixture was allowed to reach room temperature and stirred for 16 h. A saturated solution of NH_4Cl (6 mL) was added to the reaction mixture and stirred for 10 min. The layers were separated and the aqueous layer extracted with CH_2Cl_2 (2 x 10 mL) and EtOAc (2 x 10 mL). The combined organics were washed with saturated $NaHCO_3$ (6 mL) and brine (4 mL), dried ($MgSO_4$), filtered and concentrated under reduced pressure. The crude product was purified by flash column chromatography (20% EtOAc in petroleum ether) to give **193** (172 mg, 0.40 mmol, 61%) as a yellow oil. $\mathbf{R_f}$ (30% EtOAc in petroleum ether) 0.25; $[\boldsymbol{\alpha}]_{\boldsymbol{D}}^{\mathbf{29}}$ –7.6 (*c* 0.142, $CHCl_3$); **^{1}H-NMR** (500 MHz, $CDCl_3$) δ 7.28-7.19 (3H, m, ArH-Phe), 7.15 (1H, d, *J* = 7.9 Hz, ArH-6), 7.13-7.09 (2H, m, ArH-Phe), 6.50-6.43 (2H, m, ArH-3, ArH-5), 5.11 (1H, d, *J* = 11.6 Hz, C*H*HAr), 5.03 (1H, d, *J* = 11.6 Hz, CH*H*Ar), 4.77 (1H, d, *J* = 12.7 Hz, NO_2CHH), 4.71 (1H, d, *J* = 12.8 Hz, NO_2CHH), 4.50 (1H, d, *J* = 7.1 Hz, OC*H*H-Ox), 4.41-4.34 (2H, m, OCH*H*-Ox and OC*H*H-Ox), 4.25 (1H, d, *J* = 7.1 Hz, OCH*H*-Ox), 3.82 (3H, s, OCH_3), 3.81 (3H, s, OCH_3), 3.73-3.65 (1H, m, CHα-Phe), 2.95 (1H, dd, *J* = 13.3, 6.2 Hz, C*H*Hβ-Phe), 2.85 (1H, dd, *J* = 13.3, 7.1 Hz, CH*H*β-Phe), 2.34 (1H, bs, NH) ppm; **^{13}C-NMR** (125 MHz, $CDCl_3$) δ 174.7 (C=O), 161.8 (C, Ar-4), 159.3 (C, Ar-2), 136.7 (C, Ar-Phe), 132.2 (CH, Ar-6), 129.6 (2 x CH, Ar-Phe), 128.5 (2 x CH, Ar-Phe), 127.0 (CH, Ar-Phe), 115.9 (C, Ar-1), 104.2 (CH, Ar-5), 98.7 (CH, Ar-3), 78.9 (OCH_2, Ox), 78.8 (OCH_2, Ox), 78.4 (NO_2CH_2), 63.0 (CH_2, Dmb), 59.6 (C, Ox), 57.6 (CH, α-Phe), 55.57 (OCH_3), 55.56 (OCH_3), 40.6 (CH_2, β-Phe); **IR** (film): 3326 (NH), 2959, 2884, 2838, 1726 (C=O), 1552, 1207, 1157 cm^{-1}; **MS** (ESI+) *m/z* = 453 $[M+Na]^+$, 883 $[2M+Na]^+$; **HRMS** (ESI+) Calcd. for $C_{22}H_{26}N_2O_7Na$ $[M+Na]^+$: 453.1632, found 453.1633.

Fmoc-G$_{Ox}$-Phe-ODmb 195

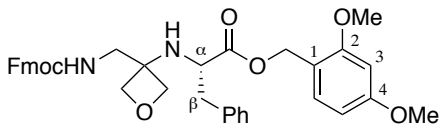

Following general procedure 6, **193** (139 mg, 0.32 mmol) gave, after column chromatography (30-40%

EtOAc in petroleum ether), **195** (125 mg, 0.20 mmol, 63%) as a colourless oil. $\mathbf{R_f}$ (40% EtOAc in petroleum ether) 0.25; $[\boldsymbol{\alpha}]_{\boldsymbol{D}}^{\mathbf{29}}$ –4.7 (*c* 0.143, $CHCl_3$); **^{1}H-NMR** (500 MHz, $CDCl_3$) δ 7.77 (2H, d, *J* = 7.5 Hz, ArH), 7.61-7.54 (2H, m, ArH), 7.41 (2H, t, *J* = 7.4 Hz, ArH), 7.33 (2H, t, *J* = 7.4 Hz, ArH), 7.27-7.11 (6H, m, ArH), 6.50-6.41 (2H, m, ArH-3, ArH-5), 5.17 (1H, d, *J* = 11.6 Hz, C*H*H-Dmb), 5.08 (1H, d, *J* = 11.6 Hz, CH*H*-Dmb), 4.81-4.69 (1H, m, NH-Fmoc), 4.37 (2H, d, *J* = 6.9 Hz, CH_2-Fmoc), 4.25 (1H, d, *J* = 6.6 Hz, OC*H*H-Ox), 4.23-4.17 (2H, m, CH-Fmoc and OC*H*H-Ox), 4.15 (1H, d, *J* = 6.5 Hz, OCH*H*-Ox), 4.11 (1H, d, *J* = 6.3 Hz, OCH*H*-Ox), 3.81 (6H, s, 2 x OCH_3), 3.51-3.26 (3H, m, CH_2-G_{Ox}, CHα-Phe), 3.02 (1H, dd, *J* = 13.4, 4.3 Hz, C*H*Hβ-Phe), 2.72 (1H, dd, *J* = 13.4, 9.2 Hz, CH*H*β-Phe), 2.06 (1H, bs, NH-Phe); **^{13}C-NMR** (125 MHz, $CDCl_3$) δ 175.5 (C=O), 161.8 (C, Ar-4), 159.3 (C, Ar-2), 156.9 (C=O, Fmoc), 144.2 (C, Ar-Fmoc), 144.1 (C, Ar-Fmoc), 141.5 (2 x C, Ar-Fmoc), 137.4 (C, Ar-Phe), 132.1 (CH, Ar-6), 129.5 (2 x CH, Ar), 128.7 (2 x CH, Ar), 127.8 (2 x CH, Ar), 127.2 (2 x CH, Ar), 125.25 (CH, Ar), 125.21 (CH, Ar), 120.1 (2 x CH, Ar), 115.9 (C, Ar-1), 104.2 (CH, Ar-5), 98.7 (CH, Ar-3), 80.0 (OCH_2, Ox), 79.4 (OCH_2, Ox), 66.8 (CH_2, Fmoc), 63.1 (CH_2, Dmb), 59.4 (C, Ox), 57.5 (CH, α-Phe), 55.6 (2 x OCH_3), 47.4 (CH, Fmoc), 44.8 (CH_2, G_{Ox}), 40.6 (CH_2, β-Phe); **IR** (film) 3320 (NH), 2972, 2932, 2890, 1725 (C=O), 1689 (C=O), 1207, 1086, 1044 cm^{-1}; **MS** (ESI+) *m/z* 623 $[M+H]^+$, 645 $[M+Na]^+$; **HRMS** (ESI+) Calcd. for $C_{37}H_{38}N_2O_7Na$ $[M+Na]^+$: 645.2571, found 645.2576.

Fmoc-Phe-OCumyl 192

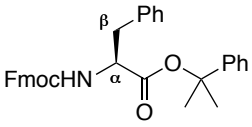

Following general procedure 7, Fmoc-Phe-OH (5.51 g, 40.5 mmol) gave, after column chromatography (0-20% EtOAc in petroleum ether), **192** (9.02 g, 17.8 mmol, 97%) contaminated with traces of 2-phenyl-2-propanol (~19:1 by ^{1}H-NMR) as a white solid. $\mathbf{R_f}$ (15% EtOAc in petroleum ether) 0.29; **mp** 86-90 °C; $[\boldsymbol{\alpha}]_{\boldsymbol{D}}^{\mathbf{25}}$ +3.1 (*c* 0.144, $CHCl_3$); **^{1}H-NMR** (500 MHz, $CDCl_3$) δ 7.76 (2H, d, *J* = 7.6 Hz, ArH-Fmoc), 7.57-7.51 (2H, m, ArH-Fmoc), 7.39 (2H, t, *J* = 7.5 Hz, ArH-Fmoc), 7.33-7.22 (10H, m, ArH), 7.17 (2H, d, *J* = 7.0 Hz, ArH), 5.22 (0.9H, d, *J* = 8.1 Hz, major rotamer NH), 4.96-4.83 (0.1H, m, minor rotamer NH), 4.65 (0.9H, m, major rotamer CHα-Phe), 4.54-4.45 (0.1 H, m, minor rotamer C*H*H-Fmoc), 4.40 (1H, dd, *J* = 10.6, 7.3 Hz, CH*H*-Fmoc), 4.36-4.25 (1H, m, minor rotamer CHα-Phe, major rotamer C*H*H-Fmoc), 4.18 (1H, t, *J* = 7.1 Hz, CH-Fmoc), 3.17 (0.9H, dd, *J* = 13.9, 6.2 Hz, major rotamer C*H*Hβ-Phe), 3.10 (0.9H, dd, *J* = 13.9, 6.2 Hz, major rotamer CH*H*β-Phe), 2.97-

2.80 (0.2H, m, minor rotamer CH_2β-Phe), 1.76 (3H, s, CH_3-cumyl), 1.74 (3H, s, CH_3-cumyl); **^{13}C-NMR** (125 MHz, $CDCl_3$) δ 170.3 (C=O, Phe), 155.7 (C=O, Fmoc), 145.0 (C, Ar-cumyl), 144.0 (C, Ar-Fmoc), 143.9 (C, Ar-Fmoc), 141.4 (2 x C, Ar-Fmoc) 136.1 (C, Ar-Phe), 129.7 (2 x CH, Ar), 128.6 (2 x CH, Ar), 128.5 (2 x CH, Ar), 127.8 (2 x CH, Ar), 127.5 (CH, Ar), 127.2 (3 x CH, Ar), 125.3 (CH, Ar), 125.2 (CH, Ar), 124.5 (2 x CH, Ar), 120.11 (CH, Ar), 120.10 (CH, Ar), 83.7 (C, cumyl), 67.1 (CH_2, Fmoc), 55.2 (CH, α-Phe), 47.3 (CH, Fmoc), 38.5 (CH_2, β-Phe), 28.8 (CH_3, cumyl), 28.0 (CH_3, cumyl); **IR** (film) 3396 (NH), 3241, 3018, 2980, 2924, 1708 (C=O), 1519, 1341, 1239, 985 cm^{-1}; **MS** (ESI$^+$) *m/z* 528 $[M+Na]^+$; **HRMS** (ESI$^+$) Calcd. for $C_{33}H_{31}NO_4Na$ $[M+Na]^+$: 528.2145, found 528.2139.

Fmoc-Val-OCumyl 197

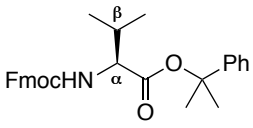

Following general procedure 7, Fmoc-Val-OH (3.39 g, 10.0 mmol) gave, after column chromatography (0-30% EtOAc in petroleum ether), **197** (3.33 g, 7.27 mmol, 73%) as a colourless oil. $\mathbf{R}_f$ (10% EtOAc in petroleum ether) 0.19; $[\boldsymbol{\alpha}]_{\boldsymbol{D}}^{\mathbf{29}}$ –16.8 (*c* 0.076, $CHCl_3$); **^{1}H-NMR** (500 MHz, $CDCl_3$) δ 7.76 (2H, d, *J* = 7.5 Hz, ArH-Fmoc), 7.58 (2H, d, *J* = 7.4 Hz, ArH-Fmoc), 7.45-7.22 (9H, m, ArH), 5.25 (0.9H, d, *J* = 9.0 Hz, major rotamer NH), 5.01-4.82 (0.1H, m, minor rotamer NH), 4.55-4.27 (2.9H, m, major rotamer CHα-Val, C*H*H-Fmoc, major rotamer CH*H*-Fmoc, minor rotamer CH-Fmoc), 4.27-4.17 (1H, m, minor rotamer CH*H*-Fmoc, major rotamer CH-Fmoc) 4.02-3.86 (0.1H, m, minor rotamer CHα-Val), 2.33-2.20 (0.9H, m, major rotamer CHβ-Val), 2.10-1.98 (0.1 H, m, minor rotamer CHβ-Val), 1.82 (3H, s, CH_3-cumyl), 1.81 (3H, s, CH_3-cumyl), 1.00 (2.7H, d, *J* = 6.8 Hz, major rotamer CH_3-Val), 0.90 (3.3H, m, minor rotamer CH_3-Val, CH_3-Val); **^{13}C-NMR** (125 MHz, $CDCl_3$) δ 170.8 (C=O, cumyl), 156.4 (C=O, Fmoc), 145.1 (C, Ar-cumyl), 144.1 (C, Ar-Fmoc), 144.0 (C, Ar-Fmoc), 141.4 (2 x C, Ar-Fmoc), 128.5 (2 x CH, Ar), 127.8 (2 x CH, Ar), 127.5 (CH, Ar), 127.2 (2 x CH, Ar), 125.28 (CH, Ar), 125.25 (CH, Ar), 124.5 (2 x CH, Ar), 120.11 (CH, Ar), 120.10 (CH, Ar), 83.3 (C, cumyl), 67.1 (CH_2, Fmoc), 59.3 (CH, α-Val), 47.3 (CH, Fmoc), 31.5 (CH, β-Val), 28.6 (CH_3, cumyl), 28.4 (CH_3, cumyl), 19.3 (CH_3, Val), 17.4 (CH_3, Val); **IR** (film) 3353 (NH), 3064, 2965, 2874, 1707 (C=O), 1509, 1448, 1202, 1092, 1077, 1029 cm^{-1}; **MS** (ESI$^+$) *m/z* 480 $[M+Na]^+$, 496 $[M+K]^+$; **HRMS** (ESI$^+$) Calcd. for $C_{29}H_{31}NO_4Na$ $[M+Na]^+$: 480.2145, found 480.2140.

Fmoc-Ser(^{t}Bu)-OCumyl 198

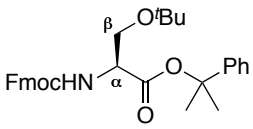

Following general procedure 7, Fmoc-Ser(O^{t}Bu)-OH (2.77 g, 7.23 mmol) gave, after column chromatography (0-15% EtOAc in petroleum ether), **198** (2.79 g, 5.56 mmol, 77%) contaminated with traces of 2-phenyl-2-propanol (~9:1 by ^{1}H-NMR) as a colourless oil. $\mathbf{R}_f$ (10% EtOAc in petroleum ether) 0.30; $[\boldsymbol{\alpha}]_D^{25}$ –5.0 (*c* 0.06, $CHCl_3$); **^{1}H-NMR** (500 MHz, $CDCl_3$) δ 7.76 (2H, d, *J* = 7.6 Hz, ArH), 7.64-7.54 (2H, m, ArH), 7.45-7.20 (9H, m, ArH), 5.63 (0.85H, d, *J* = 8.8 Hz, major rotamer NH), 5.35 (0.15H, d, *J* = 8.6 Hz, minor rotamer NH), 4.56-4.18 (4H, m, CHα-Ser, C*H*C*H*$_2$-Fmoc), 3.93 (0.85H, dd, *J* = 8.8, 2.5 Hz, major rotamer C*H*Hβ-Ser), 3.83-3.76 (0.15H, m, minor rotamer C*H*Hβ-Ser), 3.63 (0.85H, dd, *J* = 8.8, 3.0 Hz, major rotamer CH*H*β-Ser), 3.53-3.43 (0.15H, m, minor rotamer CH*H*β-Ser), 1.84-1.73 (6H, m, 2 x CH_3-cumyl), 1.20 (7.65H, s, major rotamer ^{t}Bu), 1.17 (1.35H, bs, minor rotamer ^{t}Bu); **^{13}C-NMR** (125 MHz, $CDCl_3$) δ 169.2 (C=O, Ser), 156.2 (C=O, Fmoc), 145.4 (C, Ar-cumyl), 144.1 (C, Ar-Fmoc), 144.0 (C, Ar-Fmoc), 141.4 (2 x C, Ar-Fmoc), 128.4 (2 x CH, Ar), 127.8 (2 x CH, Ar), 127.21 (2 x CH, Ar), 127.18 (CH, Ar), 125.3 (2 x CH, Ar), 124.5 (2 x CH, Ar), 120.1 (2 x CH, Ar), 83.4 (C, cumyl), 73.5 (C, ^{t}Bu), 67.2 (CH_2, Fmoc), 62.5 (CH_2, β-Ser), 55.1 (CH, α-Ser), 47.3 (CH, Fmoc), 28.9 (CH_3, cumyl), 28.6 (CH_3, cumyl), 27.6 (3 x CH_3, ^{t}Bu); **IR** (film) 3315 (NH), 3065, 2975, 2934, 2876, 1723 (C=O), 1500, 1199, 1102, 1107, 1060 cm^{-1}; **MS** (ESI+) *m/z* 524 $[M+Na]^+$; **HRMS** (ESI+) Calcd. for $C_{31}H_{35}NO_5Na$ $[M+Na]^+$: 524.2407, found 524.2405.

Fmoc-Asp(^{t}Bu)-OCumyl 199

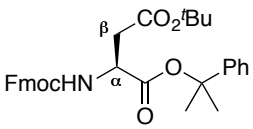

Following general procedure 7, Fmoc-Asp(^{t}Bu)-OH (4.27 g, 10.4 mmol) gave, after column chromatography (10-15% EtOAc in petroleum ether), **199** (4.01 g, 7.56 mmol, 73%) contaminated with traces of 2-phenyl-2-propanol (~9:1 by ^{1}H-NMR) as a colourless oil. $\mathbf{R}_f$ (10% EtOAc in petroleum ether) 0.24; $[\boldsymbol{\alpha}]_D^{25}$ +14.2 (*c* 0.088, $CHCl_3$); **^{1}H-NMR** (500 MHz, $CDCl_3$) δ 7.76 (2H, d, *J* = 7.5 Hz, ArH), 7.59 (2H, d, *J* = 7.5 Hz, ArH), 7.44-7.22 (9H, m, ArH), 5.83 (0.9H, d, *J* = 8.6 Hz, major rotamer NH), 5.46 (0.1H, bs, minor rotamer NH), 4.57 (0.9H, dt, *J* = 8.7, 4.4 Hz, major rotamer CHα-Asp), 4.51-4.29 (2.1H, m, minor rotamer CHα-Asp, CH_2-Fmoc), 4.28-4.18 (1H, m, CH-Fmoc), 2.97 (0.9H, dd, *J* = 17.0, 4.4 Hz, major rotamer C*H*Hβ-Asp), 2.84-2.73 (1H, m, minor rotamer C*H*Hβ-Asp, major rotamer

CH*H*β-Asp), 2.63-2.49 (0.1H, m, CH*H*β-Asp), 1.82 (3H, s, CH_3-cumyl), 1.78 (3H, s, CH_3-cumyl), 1.46 (9H, s, ^{t}Bu); **^{13}C-NMR** (125 MHz, $CDCl_3$) δ 170.3 (C=O, $CO_2{}^t$Bu), 169.5 (C=O, Asp), 156.1 (C=O, Fmoc), 145.2 (C, Ar-cumyl), 144.0 (C, Ar-Fmoc), 143.9 (C, Ar-Fmoc), 141.4 (2 x C, Ar-Fmoc), 128.4 (2 x CH, Ar), 127.8 (2 x CH, Ar), 127.4 (CH, Ar), 127.19 (CH, Ar), 127.16 (CH, Ar), 125.31 (CH, Ar), 125.28 (CH, Ar), 124.4 (2 x CH, Ar), 120.1 (2 x CH, Ar), 83.7 (C, cumyl), 81.9 (C, ^{t}Bu), 67.3 (CH_2, Fmoc), 51.1 (CH, α-Asp), 47.2 (CH, Fmoc), 37.9 (CH_2, β-Asp), 28.8 (CH_3, cumyl), 28.2 (3 x CH_3, ^{t}Bu), 28.1 (CH_3, cumyl); **IR** (film) 3437 (NH), 3064, 2978, 2936, 1721 (C=O), 1498, 1366, 1214, 1136, 1030 cm^{-1}; **MS** (ESI+) *m/z* 552 $[M+Na]^+$, 568 $[M+K]^+$; **HRMS** (ESI+) Calcd. for $C_{32}H_{35}NO_6Na$ $[M+Na]^+$: 552.2357, found 552.2358.

Fmoc-Lys(Boc)-OCumyl 200

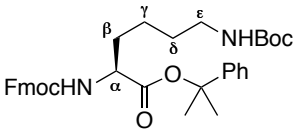

Following general procedure 7, Fmoc-Lys(Boc)-OH (2.53 g, 5.40 mmol) gave, after column chromatography (0-10% EtOAc in CH_2Cl_2), **200** (2.22 g, 3.78 mmol, 70%) as a white solid. **mp** 56-59 °C; $[\boldsymbol{\alpha}]_{\boldsymbol{D}}^{\mathbf{25}}$ +2.0 (*c* 0.15, $CHCl_3$); **^{1}H-NMR** ($CDCl_3$, 500 MHz) δ 7.78 (2H, d, *J* = 7.6, ArH-Fmoc), 7.60 (2H, d, *J* = 7.4 Hz, ArH-Fmoc), 7.46-7.24 (9H, m, ArH), 5.34 (1H, d, *J* = 7.5 Hz, NH-Fmoc), 4.66-4.46 (1H, m, NH-Boc), 4.46-4.28 (3H, m, CH_2-Fmoc and CHα-Lys), 4.27-4.19 (1H, m, CH-Fmoc), 3.23-3.00 (2H, m, CH_2ε-Lys), 1.99-1.89 (1H, m, C*H*Hβ-Lys), 1.83 (3H, s, CH_3-cumyl), 1.82 (3H, s, CH_3-cumyl), 1.78-1.67 (1H, m, CH*H*β-Lys), 1.60-1.29 (13H, m, CH_2γ-Lys, CH_2δ-Lys and ^{t}Bu); **^{13}C-NMR** ($CDCl_3$, 125 MHz) δ 171.1 (C=O, cumyl), 156.2 (C=O), 156.1 (C=O), 145.0 (C, Ar), 144.1 (C, Ar), 143.9 (C, Ar), 141.4 (2 x C, Ar), 128.5 (2 x CH, Ar), 127.8 (2 x CH, Ar), 127.5 (CH, Ar), 127.2 (2 x CH, Ar), 125.3 (2 x CH, Ar), 124.4 (2 x CH, Ar) 120.11 (CH, Ar), 120.10 (CH, Ar), 83.4 (C, cumyl), 79.3 (C, ^{t}Bu), 67.1 (CH_2, Fmoc), 54.2 (CHα, Lys), 47.3 (CH, Fmoc), 40.4 (CH_2ε-Lys), 32.5 (CH_2β, Lys), 29.8 (CH_2δ-Lys), 28.7 (CH_3, cumyl), 28.6 (3 x CH_3, ^{t}Bu), 28.4 (CH_3, cumyl), 22.4 (CH_2γ-Lys); **IR** (film) 3343 (NH), 2976, 2932, 2865, 1689 (C=O), 1511, 1247, 1165, 1136 cm^{-1}; **MS** (ESI+) *m/z* 609 $[M+Na]^+$; **HRMS** (ESI+) Calcd. for $C_{35}H_{42}N_2O_6Na$ $[M+Na]^+$: 609.2935, found 609.2933.

Fmoc-Ala-OCumyl 202

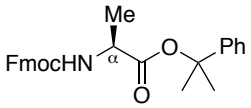

Following general procedure 7, Fmoc-Ala-OH (3.27 g, 10.5 mmol) gave, after repeat column chromatography (10-20% EtOAc in petroleum ether; 10-15% EtOAc in petroleum ether), **202** (3.24 g, 7.55 mmol, 42%) as a colourless oil. $\mathbf{R_f}$ (15% EtOAc in petroleum ether) 0.37; $[\boldsymbol{\alpha}]_{\mathbf{D}}^{\mathbf{22}}$ +10.8 (*c* 0.20, $CHCl_3$); **^{1}H-NMR** (500 MHz, $CDCl_3$) δ 7.75 (2H, d, *J* = 7.5 Hz, ArH-Fmoc), 7.57 (2H, d, *J* = 7.4 Hz, ArH-Fmoc), 7.44-7.22 (9H, m, ArH), 5.33 (0.9 H, d, *J* = 7.3 Hz, major rotamer NH), 5.00 (0.1 H, bs, minor rotamer NH), 4.54-4.29 (3H, m, CH_2-Fmoc, CHα-Ala), 4.28-4.15 (1H, m, CH-Fmoc), 1.82 (3H, s, CH_3-cumyl), 1.78 (3H, s, CH_3-cumyl), 1.46 (2.7H, d, *J* = 7.1 Hz, major diastereoisomer CH_3-Ala), 1.38-1.30 (0.3H, m, minor diastereoisomer CH_3-Ala); **^{13}C-NMR** (125 MHz, $CDCl_3$) δ 171.7 (C=O, Ala), 155.7 (C=O, Fmoc), 145.2 (C, Ar-Ph), 144.1 (C, Ar-Fmoc), 144.0 (C, Ar-Fmoc), 141.3 (2 x C, Ar-Fmoc), 128.5 (2 x CH, Ar), 127.8 (2 x CH, Ar), 127.5 (CH, Ar), 127.2 (2 x CH, Ar), 125.3 (2 x CH, Ar), 124.4 (2 x CH, Ar), 120.1 (2 x CH, Ar), 83.3 (C, cumyl), 67.1 (CH_2, Fmoc), 50.2 (CH, α-Ala), 47.3 (CH, Fmoc), 28.9 (CH_3, cumyl), 28.2 (CH_3, cumyl), 19.0 (CH_3, Ala); **IR** (film) 3332 (NH), 3064, 2981, 2944, 1701 (C=O), 1512, 1448, 1213, 1071 cm^{-1}; **MS** (ESI^+) *m/z* 452 $[M+Na]^+$, 468 $[M+K]^+$; **HRMS** (ESI^+) Calcd. for $C_{27}H_{27}NO_4Na$ $[M+Na]^+$: 452.1832, found 452.1829.

H-Pro-OCumyl 203

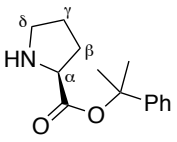

To sodium hydride (60% dispersion in mineral oil, 82 mg, 2.05 mmol) in Et_2O (2 mL) at 0 °C was added 2-phenyl-2-propanol (1.23 g, 4.11 mmol) in Et_2O (2 mL) then stirred at room temperature for 1 h. The reaction mixture was cooled to 0 °C, trichloroacetonitrile (824 µL, 8.22 mmol) added and stirred at room temperature for 3 h. The reaction mixture was concentrated under reduced pressure. Petroleum ether (2 mL) and MeOH (83 µL, 2.05 mmol) were added and stirred at room temperature for 10 min. The reaction mixture was filtered through a plug of Celite® eluting with petroleum ether. The eluent was concentrated under reduced pressure to give the crude imidate. To the crude imidate in CH_2Cl_2 (8 mL) was added Fmoc-Pro-OH (1.39 g, 4.11 mmol) and the reaction mixture stirred at room temperature for 16 h. The mixture was filtered through a plug of Celite® and the eluent concentrated under reduced pressure to give a cream oil. The crude product was stirred in 50% diethylamine in CH_2Cl_2 (8 mL) for 1 h then concentrated under reduced pressure. CH_2Cl_2 was added

and concentrated under reduced pressure (repeated x3, to remove trace diethylamine) to give the crude amine, which was purified by column chromatography (0-7% MeOH in CH_2Cl_2) to give **203** (681 mg, 2.92 mmol, 71%) as a yellow oil. $\mathbf{R_f}$ (10% MeOH in CH_2Cl_2) 0.35; $[\boldsymbol{\alpha}]_D^{25}$ –13.5 (*c* 0.122, $CHCl_3$); **^{1}H-NMR** ($CDCl_3$, 500 MHz) δ 7.40-7.30 (4H, m, ArH), 7.29-7.23 (1H, m, ArH), 3.75 (1H, dd, *J* = 8.5 and 5.8 Hz, CHα-Pro), 3.09-3.00 (1H, m, C*H*Hδ-Pro), 2.92-2.84 (1H, m, CH*H*δ-Pro), 2.41-2.11 (2H, m, NH and C*H*Hβ-Pro), 1.94-1.83 (1H, m, CH*H*β-Pro), 1.83-1.64 (8H, m, 2 x CH_3-cumyl and CH_2γ-Pro); **^{13}C-NMR** ($CDCl_3$, 500 MHz) δ 174.0 (C=O), 145.6 (C, Ar), 128.5 (2 x CH, Ar), 127.3 (CH, Ar), 124.3 (2 x CH, Ar), 82.3 (C, cumyl), 60.5 (CHα, Pro), 47.1 (CH_2δ, Pro), 30.4 (CH_2β, Pro), 28.9 (CH_3, cumyl), 28.4 (CH_3, cumyl), 25.6 (CH_2γ, Pro); **IR** (film) 3335 (NH), 3061, 2977, 2872, 1730 (C=O), 1213, 1199, 1136, 1100 cm^{-1}; **MS** *m/z* (ESI+) 467 $[2M+H]^+$; **HRMS** (ESI+) Calcd. for $C_{14}H_{19}NO_2Na$ $[M+Na]^+$: 256.1308, found 256.1304.

2-Phenylpropan-2-yl [3-(nitromethyl)oxetan-3-yl]-*L*-phenylalaninate 193

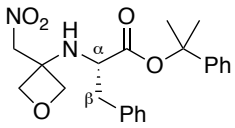

Following general procedure 8, **192** (915 mg, 1.81 mmol), oxetan-3-one (232 μL, 3.62 mmol) and nitromethane (274 μL, 5.07 mmol) were combined to give, after column chromatography (20-30% EtOAc in petroleum ether), **193** (408 mg, 1.02 mmol, 57%) as an orange solid.

Increased scale: **192** (5.85 g, 11.6 mmol) was stirred in 50% diethylamine in CH_2Cl_2 (24 mL) at room temperature for 1 h. The reaction mixture was concentrated under reduced pressure. CH_2Cl_2 (3 x 20 mL) was added and concentrated under reduced pressure (to remove trace diethylamine) to give the crude amine. Meanwhile, to oxetan-3-one (1.48 mL, 23.1 mmol) at 0 °C was added nitromethane (1.75 mL, 32.4 mmol) and triethylamine (0.65 mL, 4.63 mmol). The reaction mixture was stirred at 0 °C for 0.5 h, then at room temperature for 1 h. CH_2Cl_2 (100 mL) was added and the reaction mixture cooled to −78 °C. Triethylamine (6.45 mL, 46.3 mmol) was added followed by the dropwise addition of a solution of methanesulfonyl chloride (1.79 mL, 23.1 mmol) in CH_2Cl_2 (23 mL). The reaction mixture was stirred at −78 °C for 2 h. The crude amine in CH_2Cl_2 (50 mL) was added to the oxetane mixture *via* syringe at −78 °C. The reaction mixture was allowed to reach room temperature and stirred for 16 h. The reaction mixture was poured into a saturated solution of NH_4Cl (100 mL) and stirred at room temperature for 10 min. The layers were separated and the aqueous extracted with CH_2Cl_2 (2 x 125 mL) and EtOAc

(2 x 125 mL). The combined organics were washed with saturated $NaHCO_3$ (2 x 100 mL) and brine (50 mL), dried ($MgSO_4$), filtered and concentrated under reduced pressure. Purification by column chromatography (20-25% EtOAc in petroleum ether) gave **193** (2.75 g, 6.90 mmol, 60%) as an orange solid. $\mathbf{R_f}$ (20% EtOAc in petroleum ether) 0.24; **mp** 76-79 °C; $[\boldsymbol{\alpha}]_{\boldsymbol{D}}^{\mathbf{25}}$ +6.5 (*c* 0.1, $CHCl_3$); **^{1}H-NMR** (500 MHz, $CDCl_3$) δ 7.34-7.27 (4H, m, ArH), 7.27-7.22 (4H, m, ArH), 7.20 (2H, d, *J* = 7.0, ArH), 4.73 (1H, d, *J* = 12.7 Hz, NO_2CHH), 4.66 (1H, d, *J* = 12.7 Hz, NO_2CHH), 4.46 (1H, d, *J* = 7.2 Hz, OC*H*H-Ox), 4.33 (1H, d, *J* = 7.2 Hz, OCH*H*-Ox), 4.29 (1H, d, *J* = 7.2 Hz, OC*H*H-Ox), 4.26 (1H, d, *J* = 7.2 Hz, OCH*H*-Ox), 3.71 (1H, m, CHα-Phe), 2.99 (1H, *J* = 13.4, 6.1 Hz, C*H*Hβ-Phe), 2.83 (1H, *J* = 13.4, 7.6 Hz, CH*H*β-Phe), 2.33 (1H, d, *J* = 9.4 Hz, NH), 1.76 (3H, s, CH_3-cumyl), 1.71 (3H, s, CH_3-cumyl); **^{13}C-NMR** (125 MHz, $CDCl_3$) δ 173.4 (C=O), 144.8 (C, Ar-cumyl), 137.0 (C, Ar-Phe), 129.6 (2 x CH, Ar), 128.6 (2 x CH, Ar), 128.5 (2 x CH, Ar), 127.6 (CH, Ar), 127.1 (CH, Ar), 124.5 (2 x CH, Ar), 83.3 (C, cumyl), 79.0 (NO_2CH_2), 78.8 (OCH_2, Ox), 78.7 (OCH_2, Ox), 59.5 (C, Ox), 58.0 (CH, α-Phe), 40.9 (CH_2, β-Phe), 28.7 (CH_3, cumyl), 27.6 (CH_3, cumyl); **IR** (film) 3348 (NH), 3243, 3067, 3030, 2978, 1727 (C=O), 1694, 1546, 1381, 1233, 1194, 1133, 980 cm^{-1}; **MS** (ESI+) *m/z* 421 $[M+Na]^+$; **HRMS** (ESI+) Calcd. for $C_{22}H_{26}N_2O_5Na$ $[M+Na]^+$: 421.1734, found 421.1736.

2-Phenylpropan-2-yl [3-(nitromethyl)oxetan-3-yl]-*L*-valinate 204

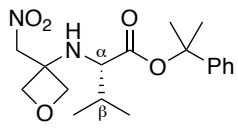

Following general procedure 8, **197** (1.81 g, 3.96 mmol), oxetan-3-one (507 µL, 7.91 mmol) and nitromethane (593 µL, 11.1 mmol) were combined to give, after column chromatography (15-20% EtOAc in petroleum ether), **204** (763 mg, 2.18 mmol, 55%) as a yellow solid. $\mathbf{R_f}$ (20% EtOAc in petroleum ether) 0.32; **mp** 82-85 °C; $[\boldsymbol{\alpha}]_{\boldsymbol{D}}^{\mathbf{25}}$ -21.6 (*c* 0.058, $CHCl_3$); **^{1}H-NMR** (500 MHz, $CDCl_3$) δ 7.41-7.31 (4H, m, ArH), 7.29-7.24 (1H, m, ArH), 4.78 (1H, d, *J* = 12.7 Hz, NO_2CHH), 4.67 (1H, d, *J* = 12.8 Hz, NO_2CHH), 4.57 (1H, d, *J* = 7.2 Hz, OC*H*H-Ox), 4.48 (1H, d, *J* = 7.2 Hz, OC*H*H-Ox), 4.45 (1H, d, *J* = 7.2 Hz, OCH*H*-Ox), 4.43 (1H, d, *J* = 7.2 Hz, OCH*H*-Ox), 3.30 (1H, bs, CHα-Val), 2.22 (1H, bs, NH), 2.12-2.01 (1H, m, CHβ-Val), 1.82 (3H, s, CH_3-cumyl), 1.79 (3H, s, CH_3-cumyl), 0.97 (3H, d, *J* = 6.8 Hz, CH_3-Val), 0.81 (3H, d, *J* = 6.9 Hz, CH_3-Val); **^{13}C-NMR** (125 MHz, $CDCl_3$) δ 174.2 (C=O), 145.0 (C, Ar), 128.5 (2 x CH, Ar), 127.6 (CH, Ar), 124.6 (2 x CH, Ar), 83.0 (C, cumyl), 79.3 (NO_2CH_2), 78.8 (OCH_2), 78.6 (OCH_2), 61.2 (CH, α-Val), 59.6 (C, Ox), 32.1

(CH, β-Val), 28.6 (CH_3, cumyl), 27.9 (CH_3, cumyl), 19.8 (CH_3, Val), 17.3 (CH_3, Val); **IR** (film) 3339 (NH), 2981, 2957, 2932, 2881, 1717 (C=O), 1548, 1312, 1202, 1133, 952 cm^{-1}; **MS** (ESI+) *m/z* 373 $[M+Na]^+$, 389 $[M+K]^+$; **HRMS** (ESI+) Calcd. for $C_{18}H_{26}N_2O_5Na$ $[M+Na]^+$: 373.1734, found 373.1730.

2-Phenylpropan-2-yl *O*-(*tert*-butyl)-*N*-[3-(nitromethyl)oxetan-3-yl]-*L*-serinate 205

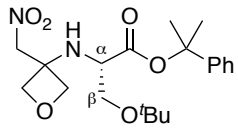

Following general procedure 8, **198** (301 mg, 0.60 mmol), oxetan-3-one (77 µL, 1.20 mmol) and nitromethane (91 µL, 1.68 mmol) were combined to give, after column chromatography (25% EtOAc in petroleum ether), **205** (127 mg, 0.32 mmol, 54%) as a yellow oil. $\mathbf{R_f}$ (25% EtOAc in petroleum ether) 0.30; $[\boldsymbol{\alpha}]_{\boldsymbol{D}}^{\mathbf{25}}$ –7.0 (*c* 0.104, $CHCl_3$); **^{1}H-NMR** (500 MHz, $CDCl_3$) δ 7.44-7.38 (2H, m, ArH), 7.38-7.32 (2H, m, ArH), 7.31-7.23 (1H, m, ArH), 4.84 (2H, s, NO_2CH_2), 4.64 (1H, d, *J* = 7.1 Hz, OC*H*H-Ox), 4.56 (2H, s, OCH_2-Ox), 4.45 (1H, d, *J* = 7.1 Hz, OCH*H*-Ox), 3.67-3.60 (2H, m, CHα-Ser, C*H*Hβ-Ser), 3.54 (1H, dd, *J* = 10.2 and 6.7 Hz, CH*H*β-Ser), 2.59 (1H, bs, NH), 1.82 (3H, s, CH_3-cumyl), 1.80 (3H, s, CH_3-cumyl), 1.20 (9H, s, ^{t}Bu); **^{13}C-NMR** (125 MHz, $CDCl_3$) δ 172.1 (C=O), 145.2 (C, Ar), 128.4 (2 x CH, Ar), 127.4 (CH, Ar), 124.5 (2 x CH, Ar), 83.2 (C, cumyl), 79.4 (OCH_2, Ox), 79.2 (OCH_2, Ox), 78.8 (NO_2CH_2), 73.6 (C, ^{t}Bu), 64.3 (CH_2, β-Ser), 59.6 (C, Ox), 57.1 (CH, α-Ser), 28.7 (CH_3-cumyl), 28.3 (CH_3-cumyl), 27.5 (3 x CH_3, ^{t}Bu); **IR** (film) 3339 (NH), 2979, 2935, 2882, 1724 (C=O), 1554, 1367, 1272, 1133, 1077, 977 cm^{-1}; **MS** (ESI+) *m/z* 417 $[M+Na]^+$; **HRMS** (ESI+) Calcd. for $C_{20}H_{30}N_2O_6Na$ $[M+Na]^+$: 417.1996, found 417.2002.

4-(*tert*-Butyl) 1-(2-phenylpropan-2-yl) [3-(nitromethyl)oxetan-3-yl]-*L*-aspartate 206

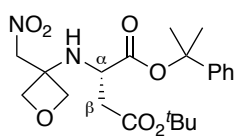

Following general procedure 8, **199** (577 mg, 1.09 mmol), oxetan-3-one (140 µL, 2.18 mmol) and nitromethane (165 µL, 3.05 mmol) were combined to give, after column chromatography (0-30% EtOAc in petroleum ether), **206** (184 mg, 0.43 mmol, 40%) as a yellow oil. $\mathbf{R_f}$ (30% EtOAc in petroleum ether) 0.38; $[\boldsymbol{\alpha}]_{\boldsymbol{D}}^{\mathbf{25}}$ –12.2 (*c* 0.074, $CHCl_3$); **^{1}H-NMR** (500 MHz, $CDCl_3$) δ 7.37-7.31 (4H, m, ArH), 7.29-7.23 (1H, m, ArH), 4.81 (1H, d, *J* = 12.9 Hz, NO_2C*H*H), 4.72 (1H, d, *J* = 12.9 Hz, NO_2CH*H*), 4.65 (1H, d, *J* = 7.2 Hz, OC*H*H-Ox), 4.50 (1H, d, *J* = 7.4 Hz, OC*H*H-Ox), 4.48-4.42 (2H, m, 2 x OCH*H*-Ox), 3.92-3.81 (1H,

m, CHα-Asp), 2.68 (1H, dd, *J* = 15.9 and 4.6 Hz, C*H*Hβ-Asp), 2.59 (1H, bs, NH), 2.54 (1H, dd, *J* = 15.9 and 7.9 Hz, CH*H*β-Asp), 1.79 (3H, s, CH_3-cumyl), 1.78 (3H, s, CH_3-cumyl), 1.45 (9H, s, ^{t}Bu); **^{13}C-NMR** (125 MHz, $CDCl_3$) δ 172.7 (C=O, Asp), 170.0 (C=O, $CO_2{}^t$Bu), 144.9 (C, Ar), 128.5 (2 x CH, Ar), 127.6 (CH, Ar), 124.4 (2 x CH, Ar), 83.5 (C, cumyl), 81.7 (C, ^{t}Bu), 79.1 (NO_2CH_2), 78.9 (OCH_2-Ox), 78.4 (OCH_2-Ox), 59.5 (C, Ox), 53.3 (CH, α-Asp), 40.5 (CH_2, β-Asp), 28.5 (CH_3-cumyl), 28.2 (4 x CH_3, cumyl and ^{t}Bu); **IR** (film) 3300 (NH), 3006, 2985, 2933, 2875, 1733 (C=O), 1716 (C=O), 1549, 1364, 1342, 1135, 942 cm^{-1}; **MS** (ESI+) *m/z* 445 $[M+Na]^+$, 461 $[M+K]^+$; **HRMS** (ESI+) Calcd. for $C_{21}H_{30}N_2O_7Na$ $[M+Na]^+$: 445.1945, found 445.1951.

2-Phenylpropan-2-yl N^6-(*tert*-butoxycarbonyl)-N^2-[3-(nitromethyl)oxetan-3-yl]-*L*-lysinate 207

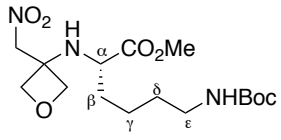

Following general procedure 8, **200** (186 mg, 0.32 mmol), oxetan-3-one (41 μL, 0.64 mmol) and nitromethane (48 μL, 0.90 mmol) were combined to give, after column chromatography (40% EtOAc in petroleum ether), **207** (85 g, 0.18 mmol, 56%) as a yellow oil. $\mathbf{R}_f$ (30% EtOAc in petroleum ether) 0.32; $[\boldsymbol{\alpha}]_{\boldsymbol{D}}^{\mathbf{25}}$ +10.5 (*c* 0.038, $CHCl_3$); **^{1}H-NMR** (500 MHz, $CDCl_3$) δ 7.38-7.32 (4H, m, ArH), 7.30-7.24 (1H, m, ArH), 4.78 (1H, d, *J* = 12.7 Hz, NO_2CHH), 4.73 (1H, d, *J* = 12.7 Hz, NO_2CHH), 4.58-4.48 (3H, m, 2 x OC*H*H-Ox, NH-Boc), 4.45 (1H, d, *J* = 7.2 Hz, OCH*H*-Ox), 4.37 (1H, d, *J* = 6.9 Hz, OCH*H*-Ox), 3.49-3.36 (1H, m, CHα-Lys), 3.18-3.00 (2H, m, CH_2ε-Lys), 2.32-2.19 (1H, m, NH-Lys), 1.80 (3H, s, CH_3-cumyl), 1.79 (3H, s, CH_3-cumyl), 1.75-1.65 (1H, m, C*H*Hβ-Lys), 1.54-1.41 (12H, m, CH*H*β-Lys, CH_2δ-Lys, ^{t}Bu), 1.41-1.28 (2H, m, CH_2γ-Lys); **^{13}C-NMR** (125 MHz, $CDCl_3$) δ 174.2 (C=O, Lys), 156.1 (C=O, Boc), 144.8 (C, Ar), 128.5 (2 x CH, Ar), 127.7 (CH, Ar), 124.5 (2 x CH, Ar), 83.1 (C, cumyl), 79.4 (C, ^{t}Bu) 79.0 (OCH_2-Ox or NO_2CH_2), 78.94 (OCH_2-Ox or NO_2CH_2), 78.86 (CH_2, OCH_2), 59.7 (C, Ox), 56.2 (CH, α-Lys), 40.4 (CH_2, ε-Lys), 34.2 (CH_2, β-Lys), 29.9 (CH_2, δ-Lys), 28.6 (3 x CH_3, ^{t}Bu), 28.5 (CH_3, cumyl), 28.1 (CH_3, cumyl), 22.9 (CH_2, γ-Lys) [NOTE: 79.4 (C, ^{t}Bu) assigned using HMBC]; **IR** (film) 3341 (NH), 2977, 2935, 2876, 1699 (C=O), 1554, 1510, 1365, 1248, 1167, 1133, 979 cm^{-1}; **MS** (ESI+) *m/z* 480 $[M+H]^+$, 502 $[M+Na]^+$; **HRMS** (ESI+) Calcd. for $C_{24}H_{37}N_3O_7Na$ $[M+Na]^+$: 502.2524, found 502.2527.

2-Phenylpropan-2-yl [3-(nitromethyl)oxetan-3-yl]-*L*-prolinate 208

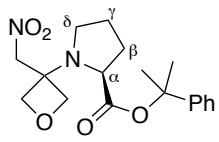

Oxetan-3-one (365 μL, 5.70 mmol), nitromethane (427 μL, 7.98 mmol) and triethylamine (159 μL, 1.14 mmol) were stirred at room temperature for 1 h. CH_2Cl_2 (23 mL) was added and the reaction mixture cooled to −78 °C. Triethylamine (1.59 mL, 11.4 mmol) was added followed by the dropwise addition of a solution of methanesulfonyl chloride (441 μL, 5.70 mmol) in CH_2Cl_2 (6 mL). The reaction mixture was stirred at −78 °C for 1.5 h. H-Pro-Cumyl **203** (665 mg, 2.85 mmol) in CH_2Cl_2 (11 mL) was added to the oxetane mixture *via* syringe at −78 °C. The reaction mixture was allowed to reach room temperature and stirred for 16 h. A saturated solution of NH_4Cl (50 mL) was added and the reaction mixture stirred at room temperature for 10 min. The layers were separated and the aqueous extracted with CH_2Cl_2 (2 x 60 mL) and EtOAc (2 x 60 mL). The combined organics were washed with saturated $NaHCO_3$ (50 mL) and brine (25 mL), dried ($MgSO_4$), filtered and concentrated under reduced pressure. Purification by column chromatography (30-40% EtOAc in petroleum ether) gave **208** (554 mg, 1.59 mmol, 56%) as a yellow oil. $\mathbf{R}_f$(30% EtOAc in petroleum ether) 0.32; $[\boldsymbol{\alpha}]_{\boldsymbol{D}}^{\mathbf{25}}$ –6.8 (*c* 0.112, $CHCl_3$); **^{1}H-NMR** ($CDCl_3$, 500 MHz) δ 7.37-7.30 (4H, m, ArH), 7.28-7.21 (1H, m, ArH), 4.96-4.90 (2H, m, NO_2CHH and $OCHH$), 4.87-4.81 (2H, m, NO_2CHH and $OCHH$), 4.79 (1H, d, J = 7.2 Hz, $OCHH$), 4.32 (1H, d, J = 7.2 Hz, $OCHH$), 3.97 (1H, dd, J = 7.7 and 3.5 Hz, CHα-Pro), 3.26 (1H, td, J = 7.8 and 3.5 Hz, CHHδ-Pro), 2.74 (1H, dd, J = 8.0 and 7.5 Hz, CHHδ-Pro), 2.01-1.82 (4H, m, CH_2β-Pro and CH_2γ-Pro), 1.77 (3H, s, CH_3-cumyl), 1.75 (3H, s, CH_3-cumyl); **^{13}C-NMR** ($CDCl_3$, 125 MHz) δ 173.1 (C=O), 145.4 (C, Ar), 128.5 (2 x CH, Ar), 127.3 (CH, Ar), 124.3 (2 x CH, Ar), 82.3 (C, cumyl), 78.8 (NO_2CH_2 or CH_2, Ox), 78.1 (NO_2CH_2 or CH_2, Ox), 76.3 (CH_2, Ox), 63.1 (C, Ox), 60.8 (CHα, Pro), 47.8 (CH_2δ, Pro), 30.3 (CH_2β, Pro), 28.6 (CH_3, cumyl), 28.3 (CH_3, cumyl), 24.2 (CH_2γ, Pro); **IR** (film) 2978, 2878, 1725 (C=O), 1550, 1348, 1133, 981 cm^{-1}; **MS** *m/z* (ESI+) 371 $[M+Na]^+$, 387 $[M+K]^+$; **HRMS** (ESI+) Calcd. for $C_{18}H_{24}N_2O_5Na$ $[M+Na]^+$: 371.1577, found 371.1578.

2-Phenylpropan-2-yl (3-(nitromethyl)oxetan-3-yl)-*L*-alaninate 209

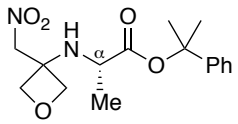

Following general procedure 8, **202** (1.77 g, 4.12 mmol), oxetan-3-one (528 μL, 8.24 mmol) and nitromethane (625 μL, 11.5 mmol) were combined to give, after repeat column chromatography (25-30% EtOAc in petroleum ether; 0-10% EtOAc in CH_2Cl_2), **209** (730 mg, 2.26 mmol,

55%) as a colourless oil. $\mathbf{R_f}$ (5% EtOAc in CH_2Cl_2) 0.40; $[\boldsymbol{\alpha}]_{\mathbf{D}}^{\mathbf{22}}$ +19.4 (*c* 0.10, $CHCl_3$) **^{1}H-NMR** (500 MHz, $CDCl_3$) δ 7.38-7.31 (4H, m, ArH), 7.30-7.24 (1H, m, ArH), 4.81 (1H, d, *J* = 12.6 Hz, NO_2CHH), 4.76 (1H, d, *J* = 12.6 Hz, NO_2CHH), 4.60-4.55 (2H, m, 2 x OC*H*H-Ox), 4.49 (1H, d, *J* = 7.1 Hz, OCH*H*-Ox), 4.38 (1H, d, *J* = 7.0 Hz, OCH*H*-Ox), 3.57 (1H, q, *J* = 7.0 Hz, CHα-Ala), 1.83-1.80 (1H, m, NH), 1.79 (6H, s, 2 x CH_3-cumyl), 1.32 (3H, d, *J* = 7.0 Hz, CH_3-Ala); **^{13}C-NMR** (125 MHz, $CDCl_3$) δ 174.5 (C=O, Ala), 145.0 (C, Ar), 128.5 (2 x CH, Ar), 127.6 (CH, Ar), 124.4 (2 x CH, Ar), 82.9 (C, cumyl), 79.1 (OCH_2, Ox), 79.0 (OCH_2, Ox), 78.8 (NO_2CH_2), 59.8 (C, Ox), 51.9 (CH, α-Ala), 28.39 (CH_3, cumyl), 28.37 (CH_3, cumyl), 20.7 (CH_3, Ala); **IR** (film) 3338 (NH), 2954, 2929, 1717 (C=O), 1550, 1303, 1130, 960 cm^{-1}; **MS** (ESI^+) *m/z* 345 $[M+Na]^+$, 361 $[M+K]^+$; **HRMS** (ESI^+) Calcd. for $C_{16}H_{22}N_2O_5Na$ $[M+Na]^+$: 345.1421, found 345.1423.

Fmoc-G_{Ox}-Phe-OCumyl 196

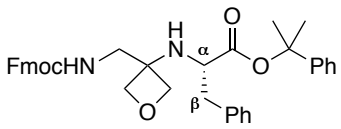

Following general procedure 9, **193** (378 mg, 0.95 mmol) gave, after column chromatography (10% EtOAc in CH_2Cl_2), **196** (324 mg, 0.55 mmol, 58%) as a white solid. $\mathbf{R_f}$ (5% EtOAc in CH_2Cl_2) 0.24; **mp** 55-59 °C; $[\boldsymbol{\alpha}]_{\boldsymbol{D}}^{\mathbf{21}}$ +7.5 (*c* 0.1, $CHCl_3$); **^{1}H-NMR** (500 MHz, $CDCl_3$) δ 7.78 (2H, d, *J* = 7.6 Hz, ArH-Fmoc), 7.57 (2H, t, *J* = 7.4 Hz, ArH-Fmoc), 7.45-7.38 (2H, m, ArH), 7.36-7.14 (12H, m, ArH), 4.76-4.64 (1H, m, NH-G_{Ox}), 4.46-4.30 (2H, m, CH_2-Fmoc), 4.28-4.15 (3H, m, CH-Fmoc and 2 x OC*H*H-Ox), 4.13 (2H, d, *J* = 6.5 Hz, 2 x OCH*H*-Ox), 3.52-3.28 (3H, m, CHα-Phe and CH_2-G_{Ox}), 3.08 (1H, dd, *J* = 13.3, 4.6 Hz, C*H*Hβ-Phe), 2.69 (1H, dd, *J* = 13.2, 9.5 Hz, CH*H*β-Phe), 2.02 (1H, bs, NH-Phe), 1.79 (3H, s, CH_3, cumyl), 1.76 (3H, s, CH_3, cumyl); **^{13}C-NMR** (125 MHz, $CDCl_3$) δ 174.2 (C=O, Phe), 156.9 (C=O, Fmoc), 144.9 (C, Ar-cumyl), 144.12 (C, Ar-Fmoc), 144.07 (C, Ar-Fmoc), 141.47 (C, Ar-Fmoc), 141.46 (C, Ar-Fmoc), 137.5 (C, Ar-Phe), 129.6 (2 x CH, Ar), 128.7 (2 x CH, Ar), 128.5 (2 x CH, Ar), 127.8 (2 x CH, Ar), 127.6 (CH, Ar), 127.23 (CH, Ar), 127.16 (2 x CH, Ar), 125.2 (2 x CH, Ar), 124.5 (2 x CH, Ar), 120.1 (2 x CH, Ar), 83.2 (C, cumyl), 79.9 (OCH_2, Ox), 79.4 (OCH_2, Ox), 66.7 (CH_2, Fmoc), 59.4 (C, Ox), 57.9 (CH, α-Phe), 47.4 (CH, Fmoc), 45.1 (CH_2, G_{Ox}), 40.8 (CH_2, β-Phe), 28.7 (CH_3, cumyl), 27.9 (CH_3, cumyl); **IR** (film) 3335 (NH), 3063, 3026, 2943, 2871, 1717 (C=O), 1218, 1131, 970 cm^{-1}; **MS** (ESI+) *m/z* 613 $[M+Na]^+$; **HRMS** (ESI+) Calcd. for $C_{37}H_{38}N_2O_5Na$ $[M+Na]^+$: 613.2673, found 613.2670.

Fmoc-G_{Ox}-Val-OCumyl 210

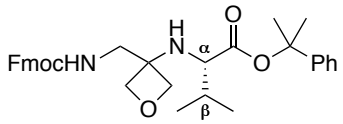

Following general procedure 9, **204** (221 mg, 0.63 mmol) gave, after column chromatography (5-10% EtOAc in CH_2Cl_2), **210** (258 mg, 0.48 mmol, 76%) as a white solid. $\mathbf{R_f}$ (5% EtOAc in CH_2Cl_2) 0.30; **mp** 82-84 °C; $[\boldsymbol{\alpha}]_{\boldsymbol{D}}^{\mathbf{21}}$ +9.4 (*c*, 0.064, $CHCl_3$); **^{1}H-NMR** (500 MHz, $CDCl_3$) δ 7.76 (2H, d, *J* = 7.6 Hz, ArH-Fmoc), 7.66-7.52 (2H, m, ArH-Fmoc), 7.44-7.36 (4H, m, ArH), 7.36-7.27 (4H, m, ArH), 7.27-7.22 (1H, m, ArH), 5.21 (0.9H, bs, major rotamer NH-G_{Ox}), 4.49 (0.1H, bs, minor rotamer NH-G_{Ox}), 4.56-4.04 (7H, m, 2 x OCH_2-Ox, C<u>H</u>C<u>H$_2$</u>-Fmoc), 3.70 (0.9H, dd, *J* = 13.7, 6.3 Hz, major rotamer C*H*H-G_{Ox}), 3.62-3.51 (0.1H, m, minor rotamer C*H*H-G_{Ox}) 3.35 (1H, dd, *J* = 13.7 and 4.7 Hz, CH*H*-G_{Ox}), 3.14 (1H, d, *J* = 4.3 Hz, CHα-Val), 2.15-2.03 (1H, m, CHβ-Val), 2.03-1.88 (1H, m, NH-Val), 1.83 (3H, s, CH_3-cumyl), 1.79 (3H, s, CH_3-cumyl), 1.03 (3H, d, *J* = 6.7, CH_3-Val), 0.86 (3H, d, *J* = 6.8 Hz, CH_3-Val); **^{13}C-NMR** (125 MHz, $CDCl_3$) δ 174.9 (C=O, cumyl), 156.9 (C=O, Fmoc), 145.0 (C, Ar-cumyl), 144.1 (C, Ar-Fmoc), 144.0 (C, Ar-Fmoc), 141.4 (2 x C, Ar-Fmoc), 128.4 (2 x CH, Ar), 127.8 (2 x CH, Ar), 127.6 (CH, Ar), 127.2 (2 x CH, Ar), 125.3 (2 x CH, Ar), 124.6 (2 x CH, Ar), 120.1 (2 x CH, Ar), 82.9 (C, cumyl), 79.7 (OCH_2, Ox), 79.5 (OCH_2, Ox), 67.0 (CH_2, Fmoc), 61.0 (CH, α-Val), 59.5 (C, Ox) 47.4 (CH, Fmoc), 45.8 (CH_2, G_{Ox}), 32.0 (CH, β-Val), 28.7 (CH_3, cumyl), 27.9 (CH_3, cumyl), 20.0 (CH_3, Val), 17.4 (CH_3, Val); **IR** (film) 3339 (NH), 2981, 2958, 2932, 2879, 1717 (C=O), 1548, 1270, 1202, 1160, 985 cm^{-1}; **MS** (ESI+) *m/z* 543 $[M+H]^+$, 565 $[M+Na]^+$; **HRMS** (ESI+) Calcd. for $C_{33}H_{38}N_2O_5Na$ $[M+Na]^+$: 565.2673, found 565.2667.

Fmoc-G_{Ox}-Ser(^{t}Bu)-OCumyl 211

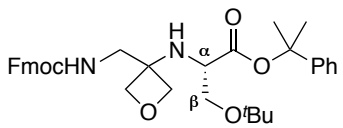

Following general procedure 9, **205** (220 mg, 0.56 mmol) gave, after column chromatography (10-20% EtOAc in CH_2Cl_2), **211** (255 mg, 0.43 mmol, 78%) as a white solid. $\mathbf{R_f}$ (10% EtOAc in CH_2Cl_2) 0.28; **mp** 53-57 °C; $[\boldsymbol{\alpha}]_{\boldsymbol{D}}^{\mathbf{21}}$ +10.0 (*c* 0.1, $CHCl_3$); **^{1}H-NMR** (500 MHz, $CDCl_3$) δ 7.78 (2H, d, *J* = 7.5 Hz, ArH-Fmoc), 7.62-7.60 (2H, m, ArH-Fmoc), 7.47-7.22 (9H, m, ArH), 5.69-5.55 (1H, m, NH-G_{Ox}), 4.53-4.12 (7H, m, C<u>H</u>C<u>H$_2$</u>-Fmoc, 2 x OCH_2-Ox), 3.69-3.48 (4H, m, CH_2-G_{Ox} and CH_2β-Ser), 3.46-3.36 (1H, m, CHα-Ser), 2.35 (1H, bs, NH-Ser), 1.84 (3H, s, CH_3, cumyl), 1.81 (3H, s, CH_3, cumyl), 1.23 (9H, s, ^{t}Bu); **^{13}C-NMR** (125 MHz, $CDCl_3$) δ 172.5 (C=O, Ser), 157.0 (C=O, Fmoc), 145.1 (C,

Ar-cumyl), 144.1 (2 x C, Ar-Fmoc), 141.4 (2 x C, Ar-Fmoc), 128.4 (2 x CH, Ar), 127.7 (2 x CH, Ar), 127.4 (CH, Ar), 127.1 (2 x CH, Fmoc), 125.2 (2 x CH, Ar), 124.4 (2 x CH, Ar), 120.0 (2 x CH, Ar), 83.3 (C, cumyl), 80.5 (OCH_2, Ox), 80.1 (OCH_2, Ox), 73.8 (C, ^{t}Bu), 66.8 (CH_2, Fmoc), 64.1 (CH_2, β-Ser), 59.5 (C, Ox), 57.1 (CH, α-Ser), 47.4 (CH, Fmoc), 45.1 (CH_2, G_{Ox}), 28.8 (CH_3, cumyl), 28.2 (CH_3, cumyl), 27.5 (3 x CH_3, ^{t}Bu); **IR** (film) 3331 (NH), 2974, 2873, 1720 (C=O), 1518, 1449, 1233, 1134, 1077, 972 cm^{-1}; **MS** (ESI+) *m/z* 587 $[M+H]^+$, 609 $[M+Na]^+$; **HRMS** (ESI+) Calcd. for $C_{35}H_{42}N_2O_6Na$ $[M+Na]^+$: 609.2935, found 609.2938.

Fmoc-G_{Ox}-Asp(^{t}Bu)-OCumyl 212

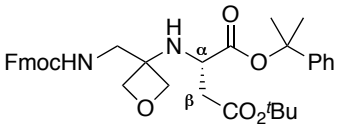

Following general procedure 9, **206** (161 mg, 0.38 mmol) gave, after column chromatography (10% EtOAc in CH_2Cl_2), **212** (180 mg, 0.29 mmol, 77%) as a white solid. $\mathbf{R_f}$ (5% EtOAc in CH_2Cl_2) 0.30; **mp** 52-54 °C; $[\boldsymbol{\alpha}]_{\boldsymbol{D}}^{\mathbf{21}}$ +23.1 (*c* 0.078, $CHCl_3$); **^{1}H-NMR** (500 MHz, $CDCl_3$) δ 7.78 (2H, d, *J* = 7.5 Hz, ArH-Fmoc), 7.66 (1H, d, *J* = 7.4 Hz, ArH-Fmoc), 7.63 (1H, d, *J* = 7.4 Hz, ArH-Fmoc), 7.45-7.39 (2H, m, ArH-Fmoc), 7.39-7.25 (7H, m, ArH), 5.78-5.65 (1H, m, NH-Fmoc), 4.45 (1H, d, *J* = 6.5 Hz, C*H*H-Ox), 4.43-4.28 (4H, m, CH_2-Ox and CH_2-Fmoc), 4.26-4.16 (2H, CH*H*-Ox and CH-Fmoc), 3.82-3.68 (2H, m, C*H*H-G_{Ox} and CHα-Asp), 3.63 (1H, dd, *J* = 14.0 and 4.4 Hz, CH*H*-G_{Ox}), 2.69 (1H, dd, *J* = 15.9 and 3.4 Hz, C*H*Hβ-Asp), 2.48 (1H, dd, *J* = 15.9 and 9.6 Hz, CH*H*β-Asp), 2.21 (1H, bs, NH-Asp), 1.82 (3H, s, CH_3-cumyl), 1.81 (3H, s, CH_3-cumyl), 1.50 (9H, s, ^{t}Bu); **^{13}C-NMR** (125 MHz, $CDCl_3$) δ 173.3 (C=O, Asp), 170.6 (C=O, $CO_2{}^t$Bu), 157.2 (C=O, Fmoc), 144.8 (C, Ar-cumyl), 144.2 (C, Ar-Fmoc), 144.1 (C, Ar-Fmoc), 141.43 (C, Ar-Fmoc), 141.41 (C, Ar-Fmoc), 128.6 (2 x CH, Ar), 127.8 (2 x CH, Ar), 127.6 (CH, Ar), 127.2 (CH, Ar), 125.4 (CH, Ar), 125.3 (CH, Ar), 124.4 (2 x CH, Ar), 120.1 (2 x CH, Ar), 83.4 (C, cumyl), 82.0 (C, ^{t}Bu), 80.2 (OCH_2, Ox), 79.8 (OCH_2, Ox), 67.0 (CH_2, Fmoc), 59.5 (C, Ox), 52.9 (CH, α-Asp), 47.4 (CH, Fmoc), 44.9 (CH_2, G_{Ox}), 40.1 (CH_2, β-Asp), 28.6 (CH_3, cumyl), 28.24 (3 x CH_3, ^{t}Bu), 28.19 (CH_3, cumyl); **IR** (film) 3339 (NH), 2977, 2936, 2873, 1715 (C=O), 1518, 1239, 1132, 971 cm^{-1}; **MS** (ESI+) *m/z* 615 $[M+H]^+$, 637 $[M+Na]^+$; **HRMS** (ESI+) Calcd. for $C_{36}H_{42}N_2O_7Na$ $[M+Na]^+$: 637.2884, found 637.2890.

Fmoc-G_{Ox}-Lys(Boc)-OCumyl 213

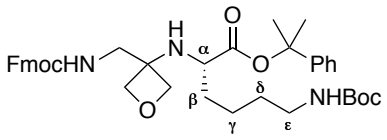

Following general procedure 9, **207** (614 mg, 1.28 mmol) gave, after column chromatography (30-50% EtOAc in CH_2Cl_2), **213** (610 mg, 0.91 mmol, 71%) as a white solid. $\mathbf{R}_f$ (30% EtOAc in CH_2Cl_2) 0.38; **mp** 55-57 °C; $[\boldsymbol{\alpha}]_{\boldsymbol{D}}^{\mathbf{21}}$ +6.7 (*c* 0.09, $CHCl_3$); **^{1}H-NMR** (500 MHz, $CDCl_3$) δ 7.76 (2H, d, *J* = 7.5 Hz, ArH-Fmoc), 7.61-7.54 (2H, m, ArH), 7.43-7.37 (2H, m, ArH), 7.37-7.27 (6H, m, ArH), 7.27-7.22 (1H, m, ArH), 5.43-5.10 (0.85H, m, major rotamer NH-G_{Ox}), 5.06-4.83 (0.15H, m, minor rotamer NH-G_{Ox}), 4.68-4.03 (8H, m, NH-Boc, 2 x OCH_2-Ox, C<u>H</u>C<u>H$_2$</u>-Fmoc), 3.70 (0.85H, dd, *J* = 13.7 and 6.4 Hz, major rotamer C*H*H-G_{Ox}), 3.60 (0.15H, m, minor rotamer C*H*H-G_{Ox}), 3.36 (1H, dd, *J* = 13.8 Hz and 4.6 Hz, CH*H*-G_{Ox}), 3.33-3.22 (1H, m, CHα-Lys), 3.19-3.00 (2H, m, CH_2ε-Lys), 2.04-1.90 (1H, bs, NH-Lys), 1.80 (3H, s, CH_3-cumyl), 1.78 (3H, s, CH_3-cumyl), 1.76-1.67 (1H, m, C*H*Hβ-Lys), 1.63-1.32 (14H, m, CH*H*β-Lys, CH_2γ-Lys, CH_2δ-Lys and ^{t}Bu); **^{13}C-NMR** (125 MHz, $CDCl_3$) δ 175.0 (C=O, cumyl), 157.0 (C=O, Fmoc), 156.1 (C=O, Boc), 144.9 (C, Ar), 144.1 (C, Ar), 144.0 (C, Ar), 141.4 (2 x C, Ar), 128.5 (2 x CH, Ar), 127.8 (2 x CH, Ar), 127.6 (CH, Ar), 127.2 (2 x CH, Ar), 125.3 (2 x CH, Ar), 124.5 (2 x CH, Ar), 120.1 (2 x CH, Ar), 82.9 (C, cumyl), 79.9 (OCH_2, Ox), 79.6 (OCH_2, Ox), 79.3 (C, ^{t}Bu), 67.0 (CH_2, Fmoc), 59.6 (C, Ox), 56.0 (CHα-Lys), 47.4 (CH, Fmoc), 45.7 (CH_2, G_{Ox}), 40.4 (CH_2ε-Lys), 34.2 (CH_2β-Lys), 30.0 (CH_2γ-Lys or CH_2δ-Lys) 28.6 (3 x CH_3, ^{t}Bu), 28.5 (CH_3, cumyl), 28.2 (CH_3, cumyl) 23.1 (CH_2γ-Lys or CH_2δ-Lys); **IR** (film): 3329 (NH), 2973, 2938, 2869, 1702 (C=O), 1511, 1478, 1449, 1365, 1244, 1167, 1132, 1101, 974 cm^{-1}; **MS** (ESI+) *m/z* 672 $[M+H]^+$, 694 $[M+Na]^+$; **HRMS** (ESI+) Calcd. for $C_{39}H_{49}N_3O_7Na$ $[M+Na]^+$: 694.3463, found 694.3457.

Fmoc-G_{Ox}-Ala-OCumyl 215

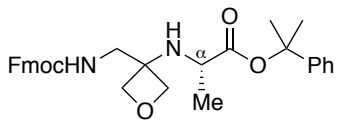

Following general procedure 9, **209** (551 mg, 1.71 mmol) gave, after column chromatography (15-20% EtOAc in CH_2Cl_2), **215** (498 mg, 0.97 mmol, 57%) as a sticky white gum. $\mathbf{R}_f$ (20% EtOAc in CH_2Cl_2) 0.31; $[\boldsymbol{\alpha}]_{\mathbf{D}}^{\mathbf{22}}$ −0.5 (*c* 0.30, $CHCl_3$); **^{1}H-NMR** (500 MHz, $CDCl_3$) δ 7.76 (2H, d, *J* = 7.5 Hz, ArH-Fmoc), 7.64-7.53 (2H, m, ArH-Fmoc), 7.40 (2H, t, *J* = 7.4 Hz, ArH-Fmoc), 7.37-7.27 (6H, m, ArH), 7.27-7.21 (1H, m, ArH), 5.37-5.16 (0.85H, m, major rotamer NH-G_{Ox}), 5.04-4.95 (0.15H, m, minor rotamer NH-G_{Ox}), 4.59-

4.13 (7H, m, 2 x OCH_2-Ox, CH_2CH-Fmoc), 3.71 (0.85H, dd, *J* = 13.7, 6.4 Hz, major rotamer C*H*H-G_{Ox}), 3.61-3.50 (0.15H, m, minor rotamer C*H*H-G_{Ox}), 3.50-3.33 (2H, m, CH*H*-G_{Ox}, CHα-Ala), 2.02 (1H, bs, NH-Ala), 1.79 (3H, s, CH_3-cumyl), 1.78 (3H, s, CH_3-cumyl), 1.35 (3H, d, *J* = 7.0 Hz, CH_3-Ala); **^{13}C-NMR** (125 MHz, $CDCl_3$) δ 175.2 (C=O, Ala), 157.0 (C=O, Fmoc), 145.0 (C, Ar-Ph), 144.1 (C, Ar-Fmoc), 144.0 (C, Ar-Fmoc), 141.4 (2 x C, Ar-Fmoc), 128.5 (2 x CH, Ar), 127.8 (2 x CH, Ar), 127.5 (CH, Ar), 127.2 (2 x CH, Ar), 125.3 (2 x CH, Ar), 124.3 (2 x CH, Ar), 120.1 (2 x CH, Ar), 82.8 (C, cumyl), 80.1 (OCH_2, Ox), 79.8 (OCH_2, Ox), 67.3 (CH_2, Fmoc), 59.5 (C, Ox), 51.7 (CH, α-Ala), 47.4 (CH, Fmoc), 45.4 (CH_2, G_{Ox}), 28.6 (CH_3, cumyl), 28.5 (CH_3, cumyl), 20.9 (CH_3, Ala); **IR** (film) 3327 (NH), 3064, 2977, 2938, 2873, 1717 (C=O), 1517, 1448, 1240, 1130, 972 cm^{-1}; **MS** (ESI^+) *m/z* 515 $[M+H]^+$, 537 $[M+Na]^+$; **HRMS** (ESI^+) Calcd. for $C_{31}H_{34}N_2O_5Na$ $[M+Na]^+$: 537.2360, found 537.2360.

Fmoc-G_{Ox}-Pro-OCumyl 214

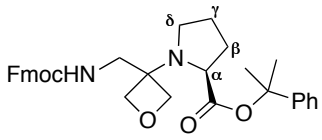

Following general procedure 9, **208** (515 mg, 1.48 mmol) gave, after column chromatography (5-10% EtOAc in CH_2Cl_2), **214** (403 mg, 0.75 mmol, 50%) as a white solid. $\mathbf{R_f}$ (10% EtOAc in CH_2Cl_2) 0.45; **mp** 50-53 °C; $[\boldsymbol{\alpha}]_{\boldsymbol{D}}^{\mathbf{21}}$ +22.4 (*c* 0.078, $CHCl_3$); **^{1}H-NMR** (500 MHz, $CDCl_3$) δ 7.75 (2H, d, *J* = 7.1 Hz, ArH-Fmoc), 7.64-7.55 (2H, m, ArH-Fmoc), 7.42-7.36 (2H, m, ArH-Fmoc), 7.36-7.19 (7H, m, ArH), 5.82-5.71 (0.9H, m, major rotamer NH-G_{Ox}), 5.45-5.32 (0.1H, m, minor rotamer NH-G_{Ox}), 4.72 (1H, d, *J* = 6.7 Hz, OC*H*H-Ox), 4.59 (1H, d, *J* = 6.9 Hz, OC*H*H-Ox), 4.51-4.22 (4H, m, CH_2-Fmoc, 2 x OCH*H*-Ox), 4.22-4.11 (1H, m, CH-Fmoc), 3.79 (1H, dd, *J* = 9.4, 3.9 Hz, CHα-Pro), 3.67 (1H, dd, *J* = 13.3, 4.0 Hz, C*H*H-G_{Ox}), 3.54 (1H, dd, *J* = 13.1, 5.1 Hz, CH*H*-G_{Ox}), 3.23-3.06 (1H, m, C*H*Hδ-Pro), 2.81 (0.9H, q, *J* = 7.9 Hz, major rotamer CH*H*δ-Pro) 2.75-2.61 (0.1 H, m, minor rotamer CH*H*δ-Pro), 2.26-2.10 (1H, m, C*H*Hβ-Pro), 2.09-1.98 (1H, m, CH*H*β-Pro), 1.98-1.83 (2H, m, CH_2γ-Pro), 1.770 (3H, s, CH_3-cumyl), 1.765 (3H, s, CH_3-cumyl); **^{13}C-NMR** (125 MHz, $CDCl_3$) δ 174.1 (C=O, Pro), 145.3 (C, Ar-Ph), 144.2 (2 x C, Ar-Fmoc), 141.1 (2 x C, Ar-Fmoc), 128.5 (2 x CH, Ar), 127.7 (2 x CH, Ar), 127.4 (CH, Ar), 127.2 (2 x CH, Ar), 125.4 (2 x CH, Ar), 124.3 (2 x CH, Ar), 120.0 (2 x CH, Ar), 82.4 (C, cumyl), 77.6 (OCH_2, Ox), 76.9 (OCH_2, Ox), 66.9 (CH_2, Fmoc), 62.2 (C, Ox), 60.5 (CH, α-Pro), 48.4 (CH_2, δ-Pro), 47.4 (CH, Fmoc), 47.0 (CH_2, G_{Ox}), 31.1 (CH_2, β-Pro), 28.6 (CH_3, cumyl), 28.4 (CH_3, cumyl), 24.7 (CH_2, γ-Pro) (NOTE: C=O, Fmoc not

observed); **IR** (film) 3342 (NH), 2947, 2873, 1717 (C=O), 1509, 1465, 1272, 1131, 1100, 979 cm^{-1}; **MS** (ESI+) *m/z* 541 $[M+H]^+$, 563 $[M+Na]^+$; **HRMS** (ESI+) Calcd. for $C_{33}H_{36}N_2O_5Na$ $[M+Na]^+$: 563.2516, found 563.2521.

Fmoc-G_{Ox}-Phe-OH 75

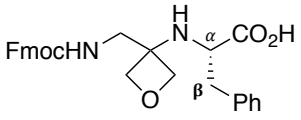

196 (376 mg, 0.62 mmol) in 2% TFA/CH_2Cl_2 (13 mL) was stirred at room temperature until consumption of starting material (TLC monitoring). The reaction mixture was concentrated under reduced pressure and the resulting residue repeatedly dissolved in CH_2Cl_2 (5 x 15 mL) and concentrated under reduced pressure. To the crude acid was added Et_2O (40 mL) and the suspension vigorously stirred at 0 °C for 15 min. The precipitate was collected by vacuum filtration and washed with ice cold Et_2O to give **75** (178 mg, 0.38 mmol, 61%) as a white solid. **mp** 183-186 °C; **^{1}H-NMR** (500 MHz, DMSO-d_6) δ 7.90 (2H, d, *J* = 7.6 Hz, ArH-Fmoc), 7.70 (2H, d, *J* = 7.4 Hz, ArH-Fmoc), 7.42 (2H, t, *J* = 7.4 Hz, ArH-Fmoc), 7.34 (2H, t, *J* = 7.4 Hz, ArH-Fmoc), 7.30-7.10 (6H, m, ArH-Phe and NH-G_{Ox}), 4.40-4.31 (2H, m, CH_2-Fmoc), 4.31-4.18 (4H, m, CH-Fmoc, OCH_2-Ox and OC*H*H-Ox), 4.12 (1H, d, *J* = 6.2 Hz, OCH*H*-Ox), 3.82-3.61 (1H, m, CHα-Phe), 3.53-3.14 (2H, m, CH_2-G_{Ox}, overlapping with H_2O signal), 2.87 (1H, dd, *J* = 13.3, 6.8 Hz, C*H*Hβ-Phe), 2.77 (1H, dd, *J* = 13.0, 7.0 Hz, CH*H*β-Phe) [Note: NH-Phe and CO_2H not assigned]; **^{13}C-NMR** (125 MHz, DMSO-d_6) δ 176.0 (C=O, Phe), 156.9 (C=O, Fmoc), 143.9 (C, Ar-Fmoc), 143.8 (C, Ar-Fmoc), 140.7 (2 x C, Ar-Fmoc), 137.8 (C, Ar-Phe), 129.3 (2 x CH, Ar), 128.0 (2 x CH, Ar), 127.6 (2 x CH, Ar), 127.1 (2 x CH, Ar), 126.3 (CH, Ar), 125.1 (2 x CH, Ar), 120.1 (2 x CH, Ar), 78.08 (OCH_2, Ox), 77.98 (OCH_2, Ox), 65.5 (CH_2, Fmoc), 59.8 (C, Ox), 56.9 (CH, α-Phe), 46.7 (CH, Fmoc), 44.4 (CH_2, G_{Ox}), 39.5 (CH_2, β-Phe) [Note: C=O-Phe assigned using HMBC and CH_2β-Phe assigned using HSQC]; **MS** (ESI^+) *m/z* 473 $[M+H]^+$, 495 $[M+Na]^+$, 511 $[M+K]^+$, 967 $[2M+Na]^+$; **IR** (film): 3410 (NH), 3063, 2884, 1702 (C=O), 1625 (C=O), 1524, 1225, 993 cm^{-1}; **MS** (ESI^-) 471 $[M-H]^-$, 585 $[M+TFA-H]^-$, 943 $[2M-H]^-$; **HRMS** (ESI^+) Calcd. for $C_{28}H_{28}N_2O_5Na$ $[M+Na]^+$: 495.1890, found 495.1891; **HRMS** (ESI^-) Calcd. for $C_{28}H_{27}N_2O_5$ $[M-H]^-$: 471.1925, found 471.1925. NOTE: No optical rotation recorded as compound insoluble in suitable solvents.

Fmoc-G_{Ox}-Val-OH 182

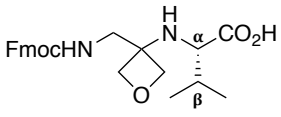

Following general procedure 10, **210** (446 mg, 0.82 mmol) was treated with 2% TFA/CH_2Cl_2 (16 mL) to give, after column chromatography (0-10% MeOH in CH_2Cl_2), **182** (329 mg, 0.77 mmol, 94%) as a white solid. $\mathbf{R}_f$ (10% MeOH in CH_2Cl_2) 0.32; **mp** 103-107 °C; $[\boldsymbol{\alpha}]_{\boldsymbol{D}}^{\mathbf{24}}$ +2.0 (*c* 0.60, $CHCl_3$); **^{1}H-NMR** (500 MHz, MeOD) δ 7.80 (2H, d, *J* = 7.5 Hz, ArH-Fmoc), 7.65 (2H, d, *J* = 7.4 Hz, ArH-Fmoc), 7.39 (2H, t, *J* = 7.4 Hz, ArH-Fmoc), 7.31 (2H, t, *J* = 7.4 Hz, ArH-Fmoc), 4.69 (1H, d, *J* = 7.2 Hz, OC*H*H-Ox), 4.59 (1H, d, *J* = 7.3 Hz, OC*H*H-Ox), 4.48 (1H, d, *J* = 7.3, OCH*H*-Ox), 4.46-4.35 (3H, m, OCH*H*-Ox and CH_2-Fmoc), 4.23 (1H, t, *J* = 6.6 Hz, CH-Fmoc), 3.74 (1H, d, *J* = 4.0 Hz, CHα-Val), 3.70 (1H, d, *J* = 14.9 Hz, C*H*H-G_{Ox}), 3.60 (1H, d, *J* = 14.8 Hz, CH*H*-G_{Ox}), 2.19-2.04 (1H, m, CHβ-Val), 1.06 (3H, d, *J* = 6.9 Hz, CH_3-Val), 1.02 (3H, d, *J* = 6.8 Hz, CH_3-Val); **^{13}C-NMR** (125 MHz, MeOD) δ 174.9 (C=O, Val), 159.7 (C=O, Fmoc), 145.3 (C, Ar-Fmoc), 145.2 (C, Ar-Fmoc), 142.6 (2 x C, Ar-Fmoc), 128.8 (2 x CH, Ar-Fmoc), 128.2 (2 x CH, Ar-Fmoc), 126.13 (CH, Ar-Fmoc), 126.11 (CH, Ar-Fmoc), 121.0 (2 x CH, Ar-Fmoc), 78.03 (OCH_2-Ox), 78.00 (OCH_2-Ox), 68.1 (CH_2-Fmoc), 63.0 (CH, α-Val), 62.7 (C, Ox), 48.4 (CH, Fmoc), 45.1 (CH_2, G_{Ox}), 32.1 (CH, β-Val), 18.9 (CH_3, Val), 18.5 (CH_3, Val); **IR** (film): 3304 (NH), 3040, 2966, 2882, 2882, 1671 (C=O), 1250, 1181, 1134 cm^{-1}; **MS** (ESI^+) *m/z* 447 $[M+Na]^+$, 871 $[2M+Na]^+$; **MS** (ESI^-) *m/z* 423$[M-H]^-$, 847 $[2M-H]^-$; **HRMS** (ESI^+) Calcd. for $C_{24}H_{28}N_2O_5Na$ $[M+Na]^+$: 447.1890, found 447.1879. Compound previously prepared by Carreira and co-workers *via* an alternative route.[46]

Fmoc-G_{Ox}-Ser(^{t}Bu)-OH 216

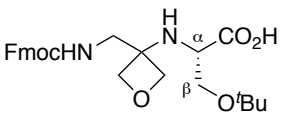

Following general procedure 10, **211** (472 mg, 0.80 mmol) was treated with 2% TFA in CH_2Cl_2 (16 mL) to give, after column chromatography (0-10 % MeOH in CH_2Cl_2), **216** (306 mg, 0.65 mmol, 82%) as a beige solid. $\mathbf{R}_f$ (10% MeOH in CH_2Cl_2) 0.23; **mp** 112-115 °C; $[\boldsymbol{\alpha}]_{\mathbf{D}}^{\mathbf{22}}$ −2.4 (*c* 0.35, $CHCl_3$); **^{1}H-NMR** (500 MHz, $CDCl_3$) δ 7.79 (2H, d, *J* = 7.6 Hz, ArH-Fmoc), 7.65 (2H, d, *J* = 7.5 Hz, ArH-Fmoc), 7.38 (2H, t, *J* = 7.5 Hz, ArH-Fmoc), 7.30 (2H, t, *J* = 7.4 Hz, ArH-Fmoc), 4.69-4.51 (2H, m, 2 x OC*H*H-Ox), 4.51-4.06 (5H, m, 2 x OCH*H*-Ox, $CHCH_2$-Fmoc), 3.88-3.43 (5H, m, CH_2-G_{Ox}, CHα-Ser, CH_2β-Ser), 1.18 (9H, s, ^{t}Bu); **^{13}C-NMR** (125 MHz, MeOD) δ 159.4 (C=O, Fmoc), 145.3 (C, Ar-Fmoc), 145.2 (C, Ar-Fmoc), 142.7 (2 x C, Ar-Fmoc), 128.8 (2 x CH, Ar-Fmoc), 128.2 (2 x CH, Ar-Fmoc),

126.14 (CH, Ar-Fmoc), 126.11 (CH, Ar-Fmoc), 120.9 (2 x CH, Ar-Fmoc), 79.1 (OCH_2, Ox), 78.8 (OCH_2, Ox), 75.0 (C, ^{t}Bu), 67.9 (CH_2, Fmoc), 63.7 (C, Ox), 62.1 (CH_2, β-Ser), 59.6 (CH, α-Ser), 48.5 (CH, Fmoc), 45.0 (CH_2, G_{Ox}), 27.7 (3 x CH_3, ^{t}Bu) [Note: C=O, Ser not observed]; **IR** (film) 3316 (NH), 3036, 2971, 2878, 1716 (C=O), 1642, 1523, 1476, 1239, 1188, 1076 cm^{-1}; **MS** (ESI^+) *m/z* 469 $[M+H]^+$, 491 $[M+Na]^+$, 507 $[M+K]^+$; **HRMS** (ESI^+) Calcd. for $C_{26}H_{32}N_2O_6Na$ $[M+Na]^+$: 491.2153, found 491.2155.

Fmoc-G_{Ox}-Val-Phe-O^{t}Bu (*S*,*S*)-219

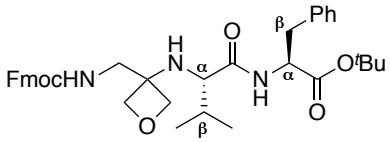

Following general procedure 11, **210** (125 mg, 0.23 mmol) was treated with 2% TFA/CH_2Cl_2 (4.6 mL). The crude acid was coupled with *L*-phenylalanine *tert*-butyl ester hydrochloride (119 mg, 0.46 mmol) to give, after column chromatography (0-3% MeOH in CH_2Cl), (*S*,*S*)-**219** (114 mg, 0.18 mmol, 79%) as a white solid. $\mathbf{R_f}$ (3% MeOH in CH_2Cl_2) 0.24; **mp** 73-77 °C; $[\boldsymbol{\alpha}]_{\boldsymbol{D}}^{\mathbf{25}}$ –12.5 (*c* 0.048, $CHCl_3$); **^{1}H-NMR** (500 MHz, $CDCl_3$) δ 7.76 (2H, d, *J* = 7.5 Hz, ArH), 7.62 (2H, d, *J* = 7.3 Hz, ArH), 7.43-7.36 (2H, m, ArH), 7.36-7.18 (6H, m, ArH, NH-Phe), 7.15 (2H, d, *J* = 7.2 Hz, ArH), 6.06-5.94 (1H, m, NH-G_{Ox}), 4.81-4.71 (1H, m, CHα-Phe) 4.50-4.26 (6H, m, 2 x OCH_2, CH_2-Fmoc), 4.25-4.16 (1H, m, CH-Fmoc), 3.69 (1H, dd, *J* = 14.2, 7.1 Hz, C*H*H-G_{Ox}), 3.32 (1H, dd, *J* = 14.2, 4.6 Hz, CH*H*-G_{Ox}), 3.11 (1H, dd, *J* = 14.0, 5.8 Hz, C*H*Hβ-Phe), 3.04 (1H, d, *J* = 4.1 Hz, CHα-Val), 2.93 (1H, dd, *J* = 13.9 Hz, 8.2 Hz, CH*H*β-Phe), 2.06-1.93 (1H, m, CHβ-Val), 1.86 (1H, bs, NH-Val), 1.41 (9H, s, ^{t}Bu), 0.90 (3H, d, *J* = 6.8 Hz, CH_3-Val), 0.77 (3H, d, *J* = 6.8 Hz, CH_3-Val); **^{13}C-NMR** (125 MHz, $CDCl_3$) δ 174.1 (C=O, Val), 171.9 (C=O, Phe), 157.7 (C=O, Fmoc), 144.1 (C, Ar-Fmoc), 144.0 (C, Ar-Fmoc), 141.4 (2 x C, Ar-Fmoc), 136.3 (C, Ar-Phe), 129.3 (2 x CH, Ar), 128.7 (2 x CH, Ar), 127.8 (2 x CH, Ar), 127.22 (CH, Ar), 127.19 (2 x CH, Ar), 125.3 (2 x CH, Ar), 120.1 (2 x CH, Ar), 82.9 (C, ^{t}Bu), 79.4 (OCH_2, Ox), 79.0 (OCH_2, Ox), 67.2 (CH_2, Fmoc), 62.7 (CH, α-Val), 60.8 (C, Ox), 53.3 (CH, α-Phe), 47.4 (CH, Fmoc), 46.3 (CH_2, G_{Ox}), 38.5 (CH_2, β-Phe), 32.0 (CH, β-Val), 28.1 (3 x CH_3, ^{t}Bu), 19.7 (CH_3, Val), 17.9 (CH_3, Val); **IR** (film) 3325 (NH), 3295 (NH), 2970, 2956, 2940, 2929, 2903, 2868, 1713 (C=O), 1657 (C=O), 1650 (C=O), 1512, 1502, 1240, 1152, 973 cm^{-1}; **MS** (ESI+) *m/z* 628 $[M+H]^+$, 650 $[M+Na]^+$; **HRMS** (ESI+) Calcd. for $C_{37}H_{45}N_3O_6Na$ $[M+Na]^+$: 650.3201, found 650.3201.

Fmoc-G_{Ox}-Val-*D*-Phe-O^{t}Bu (*S,R*)-219

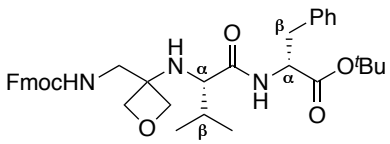

Following general procedure 11, **210** (114 mg, 0.21 mmol) was treated with 2% TFA/CH_2Cl_2 (4.2 mL). The crude acid was coupled with *D*-phenylalanine *tert*-butyl ester hydrochloride (108 mg, 0.42 mmol) to give, after column chromatography (0-3% MeOH in CH_2Cl), (*S*,*R*)-**219** (105 mg, 0.17 mmol, 80%) as a white solid. $\mathbf{R}_f$ (3% MeOH in CH_2Cl_2) 0.15; **mp** 77-81 °C; $[\boldsymbol{\alpha}]_D^{25}$ –9.8 (*c* 0.066, $CHCl_3$); **^{1}H-NMR** ($CDCl_3$) δ 7.77 (2H, d, *J* = 7.5 Hz, ArH-Fmoc), 7.60 (2H, d, *J* = 7.5 Hz, ArH-Fmoc), 7.42-7.37 (2H, m, ArH), 7.34-7.29 (2H, m, ArH), 7.28-7.19 (3H, m, ArH), 7.13 (2H, d, *J* = 7.1 Hz, ArH), 6.72 (1H, d, *J* = 7.5 Hz, NH-Phe), 5.20-5.13 (1H, m, NH-G_{Ox}), 4.79-4.70 (1H, m, CHα-Phe), 4.54-4.31 (3H, m, CH_2-Fmoc, OC*H*H-Ox), 4.31-4.14 (3H, m, OCH*H*-Ox, OC*H*H-Ox, CH-Fmoc), 4.01 (1H, d, *J* = 6.7 Hz, OCH*H*-Ox), 3.56 (1H, dd, *J* = 13.9, 6.3 Hz, C*H*H-G_{Ox}), 3.36 (1H, dd, *J* = 14.0, 5.1 Hz, CH*H*-G_{Ox}), 3.14 (1H, dd, *J* = 14.2, 5.9 Hz, C*H*Hβ-Phe), 3.10-3.02 (1H, m, CHα-Val), 2.96 (1H, dd, *J* = 14.1, 7.8 Hz, CH*H*β-Phe), 2.08-1.85 (2H, m, CHβ-Val, NH-Val), 1.42 (9H, s, ^{t}Bu), 0.90 (3H, d, *J* = 6.7 Hz, CH_3-Val), 0.85 (3H, d, *J* = 6.7 Hz, CH_3-Val); **^{13}C-NMR** (125 MHz, $CDCl_3$) δ 174.5 (C=O, Val), 170.9 (C=O, Phe), 157.2 (C=O, Fmoc), 144.0 (2 x C, Ar-Fmoc), 141.5 (2 x C, Ar-Fmoc), 136.3 (C, Ar-Phe), 129.3 (2 x CH, Ar), 128.7 (2 x CH, Ar), 127.9 (2 x CH, Ar), 127.2 (3 x CH, Ar), 125.2 (2 x CH, Ar), 120.2 (2 x CH, Ar), 82.6 (C, ^{t}Bu), 78.9 (OCH_2, Ox), 78.7 (OCH_2, Ox), 67.1 (CH_2, Fmoc), 62.0 (CH, α-Val), 60.0 (C, Ox), 53.4 (CH, α-Phe), 47.4 (CH, Fmoc), 46.4 (CH_2, G_{Ox}), 38.1 (CH_2, β-Phe), 32.1 (CH, β-Val), 28.1 (3 x CH_3, ^{t}Bu), 19.8 (CH_3, Val), 17.7 (CH_3, Val); **IR** (film) 3325 (NH), 2959, 2876, 1720 (C=O), 1651 (C=O), 1513, 1239, 1150, 975 cm^{-1}; **MS** (ESI+) *m/z* 628 $[M+H]^+$, 650 $[M+Na]^+$; **HRMS** (ESI+) Calcd. for $C_{37}H_{45}N_3O_6$ Na $[M+Na]^+$: 650.3201, found 650.3199.

Fmoc-G_{Ox}-Lys(Boc)-Phe-O^{t}Bu 220

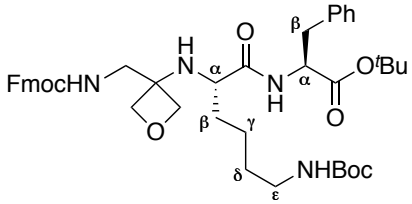

Following general procedure 11, **213** (104 mg, 0.15 mmol) was treated with 2% TFA/CH_2Cl_2 (3 mL). The crude acid was coupled with *L*-phenylalanine *tert*-butyl ester hydrochloride (80 mg, 0.31 mmol) to give, after column chromatography (0-3% MeOH in CH_2Cl_2), **220** (93 mg, 0.12 mmol, 79%) as a white solid. $\mathbf{R}_f$ (3% MeOH in CH_2Cl_2); 0.20; **mp** 72-75 °C; $[\boldsymbol{\alpha}]_D^{25}$ +9.2 (*c* 0.06, $CHCl_3$);

^{1}H-NMR (500 MHz, $CDCl_3$) δ 7.76 (2H, d, *J* = 7.5 Hz, ArH), 7.63 (2H, d, *J* = 7.4 Hz, ArH), 7.55-7.46 (1H, m, NH-Phe), 7.42-7.37 (2H, m, ArH), 7.36-7.18 (5H, m, ArH), 7.15 (2H, d, *J* = 7.0 Hz, ArH), 6.12 (1H, bs, NH-G_{Ox}), 4.76 (1H, dt, *J* = 8.3 and 5.9, CHα-Phe), 4.58 (1H, bs, NH-Boc), 4.50-4.25 (6H, m, 2 x OCH_2-Ox, CH_2-Fmoc), 4.25-4.17 (1H, m, CH-Fmoc), 3.70 (1H, dd, *J* = 14.2 and 7.1 Hz, C*H*H-G_{Ox}), 3.29 (1H, dd, *J* = 14.1 and 4.2 Hz, CH*H*-G_{Ox}), 3.20-2.98 (4H, m, CHα-Lys, CH_2ε-Lys and C*H*Hβ-Phe), 2.93 (1H, dd, *J* = 13.9 and 8.2 Hz, CH*H*β-Phe), 1.92 (1H, bs, NH-Lys), 1.59-1.35 (21H, m, CH_2β-Lys, C*H*Hδ-Lys and 2 x ^{t}Bu), 1.31-1.13 (3H, m, CH*H*δ-Lys and CH_2γ-Lys); **^{13}C-NMR** (125 MHz, $CDCl_3$) δ 174.5 (C=O, Lys), 171.8 (C=O, Phe), 157.7 (C=O, Fmoc), 156.3 (C=O, Boc), 144.2 (C, Ar-Fmoc), 144.0 (C, Ar-Fmoc), 141.4 (2 x C, Ar-Fmoc), 136.3 (C, Ar-Phe), 129.4 (2 x CH, Ar), 128.6 (2 x CH, Ar), 127.8 (2 x CH, Ar), 127.21 (CH, Ar), 127.16 (2 x CH, Ar), 125.4 (CH, Ar), 125.3 (CH, Ar), 120.1 (2 x CH, Ar), 82.9 (C, ^{t}Bu), 79.4 (overlapping signals: OCH_2, Ox and C, ^{t}Bu), 79.2 (OCH_2, Ox), 67.2 (CH_2, Fmoc), 60.9 (C, Ox), 57.4 (CH, α-Lys), 53.1 (CH, α-Phe), 47.4 (CH, Fmoc), 45.9 (CH_2, G_{Ox}), 39.8 (CH_2, ε-Lys), 38.4 (CH_2, β-Phe), 34.1 (CH_2, β-Lys), 30.0 (CH_2, δ-Lys), 28.6 (3 x CH_3, ^{t}Bu), 28.1 (3 x CH_3, ^{t}Bu), 22.6 (CH_2, γ-Lys); **IR** (film) 3322 (NH), 2973, 2930, 2865, 1881, 1706 (C=O), 1513, 1244, 1153 cm^{-1}; **MS** (ESI+) *m/z* 757 $[M+H]^+$, 779 $[M+Na]^+$; **HRMS** (ESI+) Calcd. for $C_{43}H_{56}N_4O_8Na$ $[M+Na]^+$: 779.3990, found 779.3987.

Boc-Gly-G_{Ox}-Phe-OCumyl 221

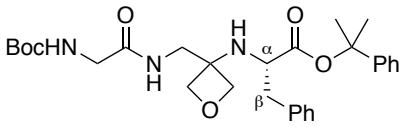

196 (234 mg, 0.40 mmol) in 50% diethylamine in CH_2Cl_2 (2 mL) was stirred at room temperature for 1 h. The reaction mixture was concentrated under reduced pressure and the resulting residue repeatedly dissolved in CH_2Cl_2 (3 x 5 mL) and concentrated under reduced pressure to give the crude amine. The crude amine was dissolved in CH_2Cl_2 (4 mL) and Boc-Gly-OH (277 mg, 1.58 mmol), DIPEA (552 µL, 3.17 mmol) and HCTU (654 mg, 1.58 mmol) added. The reaction mixture was stirred at room temperature for 16 h. The reaction mixture was concentrated under reduced pressure and dissolved in EtOAc (50 mL). The organics were washed with brine (3 x 10 mL), saturated $NaHCO_3$ (2 x 10 mL) and brine (5 mL), dried ($MgSO_4$), filtered and concentrated under reduced pressure. The crude material was purified by flash column chromatography (40-67% EtOAc in CH_2Cl_2) to give **221** (137 mg, 0.26 mmol, 65%) as a colourless oil. $\mathbf{R_f}$ (40% EtOAc in CH_2Cl_2) 0.31; $[\boldsymbol{\alpha}]_{\boldsymbol{D}}^{\mathbf{29}}$ –3.5 (*c* 0.092, $CHCl_3$); **^{1}H-NMR**

(500 MHz, $CDCl_3$) δ 7.39-7.29 (7H, m, ArH), 7.29-7.22 (3H, m, ArH), 5.75-5.63 (1H, m, NH-G_{Ox}), 4.85 (1H, bs, NH-Gly), 4.19 (1H, d, *J* = 6.5 Hz, OC*H*H-Ox), 4.16 (1H, d, *J* = 6.5 Hz, OC*H*H-Ox), 4.09 (1H, d, *J* = 6.6 Hz, OCH*H*), 4.07 (1H, d, *J* = 6.7 Hz, OCH*H*), 3.57-3.36 (5H, m, CH_2-G_{Ox}, CH_2-Gly, CHα-Phe), 3.08 (1H, dd, *J* = 10.7, 3.6 Hz, C*H*Hβ-Phe), 2.65 (1H, dd, *J* = 10.7, 7.7 Hz, CH*H*β-Phe), 2.02 (1H, bs, NH-Phe), 1.80 (3H, s, CH_3-cumyl), 1.74 (3H, s, CH_3-cumyl), 1.42 (9H, s, ^{t}Bu); **^{13}C-NMR** (125 MHz, $CDCl_3$) δ 174.2 (C=O, Phe), 169.5 (C=O, Gly), 144.7 (C, Ar-cumyl), 137.6 (C, Ar-Phe), 129.6 (2 x CH, Ar), 128.7 (2 x CH, Ar), 128.4 (2 x CH, Ar), 127.5 (CH, Ar), 127.1 (CH, Ar), 124.4 (2 x CH, Ar), 83.3 (C, cumyl), 79.9 (overlapping signals OCH_2, Ox and C, ^{t}Bu), 79.5 (OCH_2, Ox), 59.0 (C, Ox), 57.7 (CH, α-Phe), 43.8 (CH_2, Gly), 42.8 (CH_2, G_{Ox}), 40.6 (CH_2, β-Phe), 28.9 (CH_3, cumyl), 28.3 (3 x CH_3, ^{t}Bu), 27.4 (CH_3, cumyl) [NOTE: C=O, Boc not observed]; **IR** (film) 3321 (NH), 2978, 2932, 2873, 1716 (C=O), 1674 (C=O), 1496, 1366, 1272, 1248, 1165, 1134, 1101, 974 cm^{-1}; **MS** (ESI^+) *m/z* 526 $[M+H]^+$, 548 $[M+Na]^+$, 564 $[M+K]^+$; **HRMS** (ESI^+) Calcd. for $C_{29}H_{39}N_3O_6Na$ [M+Na]: 548.2731, found 548.2735.

2-Phenylpropan-2-yl [3-((*S*)-1-nitroethyl)oxetan-3-yl]-*L*-alaninate and 2-Phenylpropan-2-yl [3-((*R*)-1-nitroethyl)oxetan-3-yl]-*L*-alaninate (dr 55:45) 257

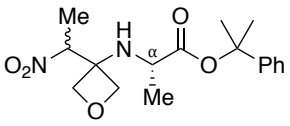

202 (976 mg, 2.27 mmol) in 50% diethylamine in CH_2Cl_2 (5 mL) was stirred at room temperature for 1 h. The reaction mixture was concentrated under reduced pressure and the resulting residue repeatedly dissolved in CH_2Cl_2 (3 x 20 mL) and concentrated under reduced pressure to give the crude amine. To the crude amine in CH_2Cl_2 (7.5 mL) was added **128** (196 mg, 1.51 mmol) in CH_2Cl_2 (7.5 mL). The reaction mixture was stirred at room temperature until consumption of the nitroalkene (^{1}H-NMR monitoring, 8 h) and then concentrated under reduced pressure to give a crude product which ^{1}H-NMR showed to consist of a 50:50 mixture of diastereoisomers. Purification by column chromatography (10-20% EtOAc in petroleum ether) gave **257** (436 mg, 1.30 mmol, 86%) as a 55:45 mixture of diastereoisomers and as a colourless oil. $\mathbf{R}_f$ (20% EtOAc in petroleum ether) 0.29; **^{1}H-NMR** (500 MHz, $CDCl_3$) δ 7.40-7.30 (4H, m, ArH), 7.30-7.22 (1H, m, ArH), 4.97-4.86 (1H, m, NO_2CH), 4.61-4.57 (1.55H, m, 2 x major diastereoisomer OC*H*H-Ox and minor diastereoisomer OC*H*H-Ox), 4.55 (1H, d, *J* = 7.5 Hz, OCH*H*-Ox), 4.48 (0.45H, d, *J* = 7.6 Hz, minor diastereoisomer OC*H*H-Ox), 4.45 (0.45H, d, *J* = 7.6 Hz, minor

diastereoisomer OCH*H*-Ox), 4.41 (0.55 H, d, *J* = 7.8 Hz, major diastereoisomer OCH*H*-Ox), 3.79-3.69 (0.45H, m, minor diastereoisomer CHα-Ala), 3.68-3.57 (0.55H, m, major diastereoisomer CHα-Ala), 2.36 (0.45H, bs, minor diastereoisomer NH), 2.19 (0.55H, bs, major diastereoisomer NH), 1.81-1.77 (6H, m, 2 x CH_3-cumyl), 1.68 (1.35H, d, *J* = 7.1 Hz, minor diastereoisomer $NO_2CHC\mathit{H_3}$), 1.67 (1.65H, d, *J* = 7.0 Hz, major diastereoisomer $NO_2CHC\mathit{H_3}$), 1.34 (1.35H, d, *J* = 7.1 Hz, minor diastereoisomer CH_3-Ala), 1.32 (1.65H, d, *J* = 7.1 Hz, major diastereoisomer CH_3-Ala); **^{13}C-NMR** (125 MHz, $CDCl_3$) δ 174.9 (C=O), 174.7 (C=O), 145.1 (C, Ar), 128.52 (2 x CH, Ar), 128.5 (2 x CH, Ar), 127.53 (CH, Ar), 127.48 (CH, Ar), 124.39 (2 x CH, Ar), 124.37 (2 x CH, Ar), 86.9 (NO_2CH), 85.3 (NO_2CH), 82.83 (C, cumyl), 82.78 (C, cumyl), 78.2 (OCH_2, Ox), 77.9 (OCH_2, Ox), 77.8 (OCH_2, Ox), 76.9 (OCH_2, Ox), 62.6 (C, Ox), 62.2 (C, Ox), 51.9 (CH, α-Ala), 51.7 (CH, α-Ala), 28.52 (CH_3, cumyl), 28.47 (CH_3, cumyl), 28.45 (CH_3, cumyl), 28.3 (CH_3, cumyl), 21.3 (CH_3, $NO_2CHC\mathit{H_3}$), 21.0 (CH_3, $NO_2CHC\mathit{H_3}$), 14.0 (CH_3, Ala), 13.5 (CH_3, Ala); **IR** (film) 3342 (NH), 2981, 2937, 2883, 1730 (C=O), 1549, 1448, 1366, 1271, 1132, 1101 cm^{-1}; **MS** (ESI^+) *m/z* 359 $[M+Na]^+$; **HRMS** (ESI^+) Calcd. for $C_{17}H_{24}N_2O_5Na$ $[M+Na]^+$: 359.1577, found 359.1571.

Fmoc-*L*-A_{Ox}-Ala-OCumyl and Fmoc-*D*-A_{Ox}-Ala-OCumyl (dr 58:42) (±,*S*)-255

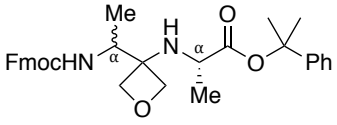

Following general procedure 9, **257** (377 mg, 1.12 mmol, dr 55:45) gave, after column chromatography (5-20% EtOAc in CH_2Cl_2), (±,*S*)-**255** (467 mg, 0.88 mmol, 79%) as a white solid which HPLC analysis showed to consist of a 58:42 mixture of diastereoisomers. **R_f** (15% EtOAc in CH_2Cl_2) 0.47; **^{1}H-NMR** (500 MHz, $CDCl_3$) δ 7.76 (2H, d, *J* = 7.6 Hz, ArH-Fmoc), 7.63-7.54 (2H, m, ArH-Fmoc), 7.45-7.20 (9H, m, ArH), 5.69-4.91 (1H, m, NH-A_{Ox}), 4.78-4.02 (8H, m, $CHCH_2$-Fmoc, CHα-A_{Ox}, 2 x OCH_2-Ox), 4.01-3.63 (1H, m, CHα-Ala), 1.82 (3H, s, CH_3-cumyl), 1.79 (1.8H, s, major diastereoisomer CH_3-cumyl), 1.78 (1.2H, s, minor diastereoisomer CH_3-cumyl), 1.38 (3H, d, *J* = 6.9 Hz, CH_3-Ala), 1.23-0.90 (3H, m, CH_3-A_{Ox}); **^{13}C-NMR** (125 MHz, $CDCl_3$) δ 175.6 (2 x C=O, Ala), 156.5 (C=O, Fmoc), 156.3 (C=O, Fmoc), 145.17 (C, Ar-cumyl), 145.15 (C, Ar-cumyl), 144.12 (C, Ar-Fmoc), 144.09 (C, Ar-Fmoc), 144.06 (C, Ar-Fmoc), 141.5 (C, Ar-Fmoc), 128.53 (CH, Ar), 128.48 (CH, Ar), 127.82 (CH, Ar), 127.79 (CH, Ar), 127.49 (CH, Ar), 127.47 (CH, Ar), 127.2 (CH, Ar), 125.36 (CH, Ar), 125.27 (CH, Ar), 125.19 (CH, Ar), 124.4 (CH, Ar), 124.3 (CH, Ar), 120.12 (CH, Ar), 120.08 (CH, Ar), 82.80 (C, cumyl), 82.78

(C, cumyl), 79.1 (OCH_2, Ox), 79.0 (OCH_2, Ox), 78.9 (OCH_2, Ox), 77.9 (OCH_2, Ox), 66.8 (CH_2, Fmoc), 66.7 (CH_2, Fmoc), 62.5 (C, Ox), 62.4 (C, Ox), 52.1 (CH, α-Ala), 52.0 (CH, Fmoc or α-A_{Ox}), 51.2 (CH, α-Ala), 47.5 (CH, Fmoc or α-A_{Ox}), 47.4 (CH, Fmoc), 28.8 (CH_3, cumyl), 28.2 (CH_3, cumyl), 28.1 (CH_3, cumyl), 21.7 (CH_3, Ala), 20.8 (CH_3, Ala), 14.9 (CH_3, A_{Ox}), 14.6 (CH_3, A_{Ox}); **IR** (film) 3330 (NH), 2976, 2940, 2875, 1718 (C=O), 1496, 1448, 1241, 1132, 1101 cm^{-1}; **MS** (ESI^+) *m/z* 529 $[M+H]^+$, 551 $[M+Na]^+$; **HRMS** (ESI^+) Calcd. for $C_{32}H_{36}N_2O_5Na$ $[M+Na]^+$: 551.2516, found 551.2515; **HPLC** (Chiralcel OD-H (0.46 cm x 25 cm, 5 μm), 20% isopropanol in hexane, 25 °C, 1.0 mL/min, λ = 254 nm) t_R = 54 min (major), 93 min (minor).

3-((*R*)-1-Nitroethyl)-*N*-((*S*)-1-phenylethyl)oxetan-3-amine (*R*,*S*)-277

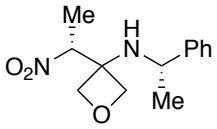

To **128** (100 mg, 0.77 mmol) in CH_2Cl_2 (8.0 mL) was added (*S*)-(−)-α-methylbenzylamine (120 μL, 0.93 mmol) and the reaction mixture stirred at room temperature for 16 h. The reaction mixture was concentrated under reduced pressure to give a crude product which ^{1}H-NMR showed to consist of 60:40 mixture of diastereoisomers. Purification by column chromatography (12.5% EtOAc in petroleum ether) gave the major diastereoisomer (*R*,*S*)-**277** (108 mg, 0.43 mmol, 56%, dr >95:5) as a white solid. $\mathbf{R_f}$ (20% EtOAc in petroleum ether) 0.29; **mp** 76-79 °C; $[\boldsymbol{\alpha}]_{\boldsymbol{D}}^{\mathbf{18}}$ −10.3 (*c* 0.60, $CHCl_3$); **^{1}H-NMR** (500 MHz, $CDCl_3$) δ 7.39-7.29 (4H, m, ArH), 7.28-7.21 (1H, m, ArH), 5.05 (1H, q, *J* = 6.9 Hz, NO_2CH), 4.53 (1H, d, *J* = 7.2 Hz, OC*H*H-Ox), 4.43 (1H, d, *J* = 7.6 Hz, OC*H*H-Ox), 4.41 (1H, d, *J* = 7.6 Hz, OCH*H*-Ox), 4.30-4.22 (2H, m, OCH*H*-Ox and NHC*H*), 1.84 (1H, bs, NH), 1.73 (3H, d, *J* = 6.9 Hz, NO_2CHCH_3), 1.37 (3H, d, *J* = 6.7 Hz, $NHCHCH_3$); **^{13}C-NMR** (125 MHz, $CDCl_3$) δ 146.7 (C, Ar), 128.9 (2 x CH, Ar), 127.4 (CH, Ar), 126.3 (2 x CH, Ar), 86.2 (CH, NO_2CH), 77.8 (OCH_2, Ox), 76.9 (OCH_2, Ox), 62.4 (C, Ox), 52.7 (CH, NHCH), 26.3 (CH_3, NO_2CHCH_3), 14.4 (CH_3, $NHCHCH_3$); **IR** (film) 3330 (NH), 2977, 2968, 2925, 2881, 1546, 1389, 1289, 974 cm^{-1}; **MS** (ESI^+) *m/z* 251 [M+H], 273 $[M+Na]^+$, 289 $[M+K]^+$; **HRMS** (ESI^+) Calcd. for $C_{13}H_{19}N_2O_3$ $[M+H]^+$: 251.1390, found 251.1397.

3-((*S*)-1-Nitroethyl)-*N*-((*R*)-1-phenylethyl)oxetan-3-amine (*S,R*)-277

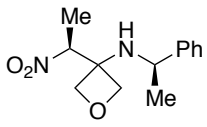

To **128** (1.06 g, 8.17 mmol) in CH_2Cl_2 (82 mL) was added (*R*)-(+)-α-methylbenzylamine (1.25 mL, 9.81 mmol) and the reaction mixture stirred at room temperature for 16 h. The reaction mixture was concentrated under reduced pressure to give a crude product which ^{1}H-NMR showed to consist of 60:40 mixture of diastereoisomers. Purification by column chromatography (10-15% EtOAc in petroleum ether) gave the major diastereoisomer (*S,R*)-**277** (1.03 g, 4.12 mmol, 50%, dr >95:5) as a white solid. **mp** 71-74 °C; $[\alpha]_D^{19}$ +7.9 (*c* 0.19, $CHCl_3$); other data as described for (*R,S*)-**277**.

3-(1-nitropropylidene)oxetane 289[75]

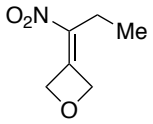

Following general procedure 2, oxetan-3-one (883 μL, 13 mmol) and 1-nitropropane (893 μL, 10 mmol) were combined to give, after column chromatography (15-20% EtOAc in petroleum ether), **289** (679 mg, 4.74 mmol, 47%) as a colourless oil. $\mathbf{R}_f$ (20% EtOAc in petroleum ether) 0.24; **^{1}H-NMR** (500 MHz, $CDCl_3$) δ 5.62-5.54 (2H, m, OCH_2-Ox), 5.39-5.32 (2H, m, OCH_2-Ox), 2.45 (2H, q, *J* = 7.4 Hz, CH_2CH_3), 1.15 (3H, t, *J* = 7.4 Hz, CH_2CH_3); **^{13}C-NMR** (125 MHz, $CDCl_3$) δ 148.7 (C), 142.7 (C), 79.9 (OCH_2-Ox), 75.7 (OCH_2-Ox), 21.3 (CH_2), 11.7 (CH_3). Data consistent with that reported in literature.[75]

3-(2-Methyl-1-nitropropyl)oxetan-3-ol 292

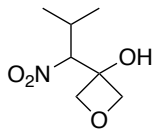

1-Iodo-2-methylpropane (2.30 mL, 20.0 mmol) in Et_2O (50 mL) was added dropwise *via* an addition funnel to a suspension of silver nitrite (4.00 g, 26.0 mmol) in Et_2O (50 mL) at 0 °C. The reaction flask was wrapped in aluminium foil to protect the reaction from light. The reaction mixture was allowed to reach room temperature and stirred for 3 d. A further amount of silver nitrite (1.54 g, 10.0 mmol) was added and the reaction mixture stirred at room temperature for 3 d. The reaction mixture was filtered through Celite® eluting with Et_2O and the eluent concentrated under reduced pressure (Note: rotary evaporator water bath cooled to 0 °C) to give crude 2-methyl-1-nitropropane which was used immediately without further purification.

To crude 2-methyl-1-nitropropane was added oxetan-3-one (4.0 mL, 5.0 M) and triethylamine (558 μL, 4.00 mmol) and the reaction mixture stirred at 60 °C for 4 d. The reaction mixture was concentrated under reduced pressure and the crude material purified by column chromatography (20% EtOAc in petroleum ether) to give **292** (680 mg, 3.88 mmol, 19%) as a white solid. $\mathbf{R}_f$ (20% EtOAc in petroleum ether) 0.29; **mp** 74-77 °C; **^{1}H-NMR** (500 MHz $CDCl_3$) δ 4.75 (1H, d, *J* = 9.9 Hz, NO_2CH), 4.67 (1H, d, *J* = 7.2 Hz, OC*H*H-Ox), 4.58 (1H, d, *J* = 7.2 Hz, OC*H*H-Ox), 4.54 (1H, d, *J* = 7.2 Hz, OCH*H*-Ox), 4.51 (1H, d, *J* = 7.2 Hz, OCH*H*-Ox), 3.48 (1H, s, OH), 2.55-2.42 (1H, m, CH-^{i}Pr), 1.05 (3H, d, *J* = 6.6 Hz, CH_3), 0.99 (3H, d, *J* = 6.9 Hz, CH_3); **^{13}C-NMR** (125 MHz, $CDCl_3$) δ 97.7 (CH, NO_2CH), 82.6 (OCH_2, Ox), 82.1 (OCH_2, Ox), 74.2 (C, Ox), 30.1 (CH, ^{i}Pr), 19.8 (CH_3), 18.9 (CH_3); **IR** (film) 3346 (OH), 2978, 2962, 2923, 2890, 2854, 1545, 1536, 1299, 1246, 981 cm^{-1}; **HRMS** (ESI^+) Calcd. for $C_7H_{13}NO_4Na$ $[M+Na]^+$: 198.0737, found 198.0736.

3-(2-Methyl-1-nitropropylidene)oxetane 293

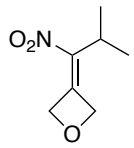

292 (580 mg, 3.31 mmol) in CH_2Cl_2 (33 mL) was cooled to −78 °C. Triethylamine (969 μL, 6.95 mmol) was added followed by the dropwise addition of a solution of methanesulfonyl chloride (282 μL, 3.64 mmol) in CH_2Cl_2 (4 mL). The reaction mixture was stirred at −78 °C for 90 min, after which the dry-ice bath was removed, and the reaction mixture stirred for 60 min. The reaction mixture was filtered through a plug of silica eluting with 25% EtOAc in petroleum ether and the eluent concentrated under reduced pressure. Purification by column chromatography (15-20% EtOAc in petroleum ether) gave **293** (188 mg, 1.20 mmol, 36%) as a yellow oil. $\mathbf{R}_f$ (20% EtOAc in petroleum ether) 0.41; **^{1}H-NMR** (500 MHz, $CDCl_3$) δ 5.58 (2H, t, *J* = 3.7 Hz, OCH_2-Ox), 5.44 (2H, t, *J* = 3.7 Hz, OCH_2-Ox), 3.10 (1H, sep, *J* = 7.0 Hz, CH), 1.17 (6H, d, *J* = 7.0 Hz, 2 x CH_3); **^{13}C-NMR** (125 MHz, $CDCl_3$) δ 148.3 (C), 146.5 (C), 80.6 (OCH_2, Ox), 75.8 (OCH_2, Ox), 28.9 (CH), 20.0 (2 x CH_3). Data consistent with that reported in literature.[75]

3-((*R*)-2-Methyl-1-nitropropyl)-*N*-((*S*)-1-phenylethyl)oxetan-3-amine 299

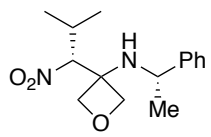

293 (57 mg, 0.36 mmol) in *n*-hexane (4.0 mL) was cooled to −20 °C. (*S*)-(−)-α-Methylbenzylamine (56 μL, 0.43 mmol) was added and the

reaction mixture stirred for 16 h by which time the cooling bath had reached room temperature. The reaction mixture was concentrated under reduced pressure to give a crude product which ^{1}H-NMR showed to consist of a 85:15 mixture of diastereoisomers. Purification by column chromatography (10% EtOAc in petroleum ether) gave the major diastereoisomer **299** (71 mg, 0.26 mmol, 71%, dr >95:5) as a colourless oil. $\mathbf{R_f}$ (10% EtOAc in petroleum ether) 0.34; $[\boldsymbol{\alpha}]_{\mathbf{D}}^{\mathbf{25}}$ −16.7 (*c* 0.46, $CHCl_3$); **^{1}H-NMR** (500 MHz, $CDCl_3$) δ 7.46 (2H, d, *J* = 7.6 Hz, ArH), 7.35-7.29 (2H, m, ArH), 7.23 (1H, t, *J* = 7.3 Hz, ArH), 4.83 (1H, d, *J* = 7.2 Hz, OC*H*H-Ox), 4.74 (1H, d, *J* = 10.1 Hz, NO_2CH), 4.55-4.47 (2H, m, OCH*H*-Ox, NHC*H*), 4.38 (1H, d, *J* = 7.6 Hz, OC*H*H-Ox), 4.19 (1H, d, *J* = 7.6 Hz, OCH*H*-Ox), 2.73 (1H, dsep, *J* = 10.1, 6.7 Hz, CH-^{i}Pr), 2.36 (1H, bs, NH), 1.42 (3H, d, *J* = 6.8 Hz, NHCHC*H*$_3$), 1.02 (3H, d, *J* = 6.6 Hz, CH_3-^{i}Pr), 0.84 (3H, d, *J* = 6.8 Hz, CH_3-^{i}Pr); **^{13}C-NMR** (125 MHz, $CDCl_3$) δ 148.2 (C, Ar), 128.7 (2 x CH, Ar), 127.0 (CH, Ar), 126.4 (2 x CH, Ar), 100.2 (CH, NO_2CH), 78.4 (OCH_2, Ox), 77.6 (OCH_2, Ox), 61.9 (C, Ox), 52.3 (CH, NHCH), 29.5 (CH, ^{i}Pr), 27.3 (CH_3, NHCH*C*H$_3$), 20.0 (CH_3, ^{i}Pr), 18.9 (CH_3, ^{i}Pr); **IR** (film) 3361 (NH), 3029, 2966, 2877, 1547, 1466, 1370, 992 cm^{-1}; **MS** (ESI$^+$) *m/z* 301 $[M+Na]^+$; **HRMS** (ESI$^+$) Calcd. for $C_{15}H_{22}N_2O_3Na$ $[M+Na]^+$: 301.1523, found 301.1517.

Fmoc-*D*-A_{Ox}-NH_2 (*R*)-282

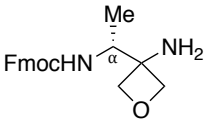

To (*R,S*)-**277** (531 mg, 2.12 mmol) in MeOH (21 mL) was added 20% $Pd(OH)_2$/C (212 mg). The reaction mixture was stirred under an atmosphere of H_2 (balloon) at room temperature for 4 d. The reaction mixture was filtered through a plug of Celite® eluting with MeOH and the eluent concentrated under reduced pressure to give the crude diamine. To the crude diamine was added CH_2Cl_2 (10 mL), $NaHCO_3$ (356 mg, 4.24 mmol) and Fmoc *N*-hydroxysuccinimide ester (715 mg, 2.21 mmol) and stirred at room temperature for 2 h. The reaction mixture was diluted with EtOAc and washed with saturated Na_2CO_3 (2 x 20 mL) and brine (10 mL), dried ($MgSO_4$), filtered and concentrated under reduced pressure. Purification by column chromatography (100% EtOAc; then 0-5% MeOH in CH_2Cl_2) gave (*R*)-**282** (415 mg, 1.23 mmol, 58%) as a sticky white gum. $\mathbf{R_f}$ (10% MeOH in CH_2Cl_2) 0.44; $[\boldsymbol{\alpha}]_{\mathbf{D}}^{\mathbf{18}}$ – 9.6 (*c* 0.45, $CHCl_3$); **^{1}H-NMR** (500 MHz, $CDCl_3$) δ 7.77 (2H, d, *J* = 7.5 Hz, ArH), 7.59 (2H, d, *J* = 7.4 Hz, ArH), 7.40 (2H, t, *J* = 7.4 Hz, ArH), 7.32 (2H, t, *J* = 7.4 Hz, ArH), 5.13 (0.85H, d, *J* = 8.2 Hz, major rotamer NH-A_{Ox}), 5.04-4.85 (0.15H, m, minor rotamer

NH-A_{Ox}), 4.57 (1H, d, *J* = 6.6 Hz, OC*H*H-Ox), 4.54 (1H, d, *J* = 6.3 Hz, OC*H*H-Ox), 4.49-4.37 (2H, m, CH_2-Fmoc), 4.36-4.26 (2H, m, 2 x OCH*H*-Ox), 4.26-4.15 (1.85H, m, CH-Fmoc, major rotamer CHα-A_{Ox}), 4.04-3.81 (0.15H, m, minor rotamer CHα-A_{Ox}), 1.57 (2H, s, NH_2-overlapping with H_2O signal), 1.11 (2.55 H, d, *J* = 6.5 Hz, major rotamer CH_3-A_{Ox}), 1.03-0.90 (0.45H, m, minor rotamer CH_3-A_{Ox}); **^{13}C-NMR** (125 MHz, $CDCl_3$) δ 156.3 (C=O), 144.1 (C, Ar), 144.0 (C, Ar), 141.5 (2 x C, Ar), 127.8 (2 x CH, Ar), 127.2 (2 x CH, Ar), 125.2 (CH, Ar), 125.1 (CH, Ar), 120.14 (CH, Ar), 120.1 (CH, Ar), 83.0 (OCH_2, Ox), 82.4 (OCH_2, Ox), 66.7 (CH_2, Fmoc), 58.9 (C, Ox), 51.5 (CHα, A_{Ox}), 47.5 (CH, Fmoc), 14.8 (CH_3, A_{Ox}); **IR** (film) 3298 (NH), 2946, 2868, 1700 (C=O), 1529, 1448, 1242, 1050, 970 cm^{-1}; **MS** (ESI^+) *m/z* 339 $[M+H]^+$, 361 $[M+Na]^+$; **HRMS** (ESI^+) Calcd. for $C_{18}H_{20}N_5O_2Na$ $[M+Na]^+$: 361.1509, found 361.1511.

Fmoc-*L*-A_{Ox}-NH_2 (*S*)-282

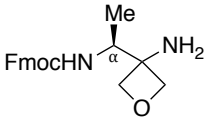

To (*S,R*)-**277** (605 mg, 2.42 mmol) in MeOH (24 mL) was added 20% $Pd(OH)_2$/C (242 mg). The reaction mixture was stirred under an atmosphere of H_2 (balloon) at room temperature for 4 d. The reaction mixture was filtered through a plug of Celite® eluting with MeOH and the eluent concentrated under reduced pressure to give the crude diamine. To the crude diamine was added CH_2Cl_2 (10 mL), $NaHCO_3$ (407 mg, 4.84 mmol) and Fmoc *N*-hydroxysuccinimide (816 mg, 2.42 mmol) and stirred at room temperature for 2 h. The reaction mixture was diluted with EtOAc and washed with saturated Na_2CO_3 (2 x 20 mL) and brine (10 mL), dried ($MgSO_4$), filtered and concentrated under reduced pressure. Purification by column chromatography (100% EtOAc; then 0-5% MeOH in CH_2Cl_2) gave (*S*)-**282** (407 mg, 1.20 mmol, 50%) as a sticky white gum. $[\alpha]_D^{22}$ +7.1 (*c* 0.47, $CHCl_3$); other data as described for (*R*)-**282**.

(9*H*-Fluoren-9-yl)methyl (*R*)-(1-(3-(4-bromobenzamido)oxetan-3-yl)ethyl)carbamate 304

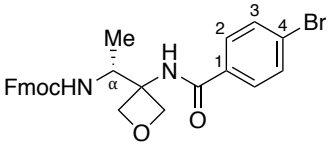

To (*R*)-**282** (289 mg, 0.85 mmol) in CH_2Cl_2 (9.0 mL) was added DIPEA (297 µL, 1.71 mmol) and 4-bromobenzoyl chloride (375 mg, 1.71 mmol). The reaction mixture was stirred at room temperature for 16 h. The reaction mixture was diluted with CH_2Cl_2 (20

mL), washed with a saturated solution of $NaHCO_3$ (20 mL) and brine (10 mL), dried ($MgSO_4$), filtered and concentrated under reduced pressure. Purification by column chromatography (60% EtOAc in petroleum ether) gave **304** (384 mg, 0.74 mmol, 87%) as a white solid. A crystal suitable for X-ray analysis was grown from PhMe. $\mathbf{R_f}$ (60% EtOAc in petroleum ether) 0.43; **mp** 164-167 °C; $[\boldsymbol{\alpha}]_{\mathbf{D}}^{\mathbf{22}}$ +23.5 (*c* 0.50, $CHCl_3$); **^{1}H-NMR** (500 MHz, $CDCl_3$) δ 7.76 (2H, d, *J* = 7.6 Hz, ArH-Fmoc), 7.67 (2H, d, *J* = 8.0 Hz, ArH-2), 7.61-7.53 (4H, m, ArH-Fmoc and ArH-3), 7.44-7.36 (2H, m, ArH-Fmoc), 7.33-7.25 (2H, m, ArH-Fmoc), 6.91 (1H, s, NHCOAr), 5.93 (1H, d, *J* = 7.1 Hz, NH-A_{Ox}), 4.98 (1H, d, *J* = 6.6 Hz, OC*H*H-Ox), 4.92 (1H, d, *J* = 6.4 Hz, OC*H*H-Ox), 4.67 (1H, d, *J* = 6.7 Hz, OCH*H*-Ox), 4.57 (1H, d, *J* = 6.6 Hz, OCH*H*-Ox), 4.46-4.27 (3H, m, CH_2-Fmoc and CH-A_{Ox}), 4.23-4.16 (1H, m, CH-Fmoc), 1.36 (3H, d, *J* = 6.4 Hz, CH_3-A_{Ox}); **^{13}C-NMR** (125 MHz, $CDCl_3$) δ 167.1 (C=O, COAr), 157.0 (C=O, Fmoc), 143.94 (C, Ar-Fmoc), 143.89 (C, Ar-Fmoc), 141.5 (C, Ar-Fmoc), 141.4 (C, Ar-Fmoc), 132.6 (C, Ar-1), 132.1 (2 x CH, Ar-3), 128.8 (2 x CH, Ar-2), 127.9 (2 x CH, Ar-Fmoc), 127.2 (2 x CH, Ar-Fmoc), 127.1 (C, Ar-4), 125.2 (2 x CH, Ar-Fmoc), 120.1 (2x CH, Ar-Fmoc), 78.0 (OCH_2, Ox), 77.5 (OCH_2, Ox), 67.1 (CH_2, Fmoc), 60.7 (C, Ox), 52.6 (CH, A_{Ox}), 47.3 (CH, Fmoc), 15.5 (CH_3, A_{Ox}); **IR** (film) 3371 (NH), 3352 (NH), 2967, 2893, 1693 (C=O), 1643 (C=O), 1516, 1248, 989 cm^{-1}; **MS** (ESI^+) *m/z* 543 [M(^{79}Br)+Na]$^+$, 545 [M(^{81}Br)+Na]$^+$; **HRMS** (ESI^+) Calcd. for $C_{27}H_{25}BrN_2O_4Na$ [M+Na]$^+$: 543.0890 (^{79}Br) and 545.0874 (^{81}Br), found 543.0890 (^{79}Br) and 545.0873 (^{81}Br).

Crystal Data for $C_{28.75}H_{27}BrN_2O_4$ (*M* =544.43 g/mol): monoclinic, space group C2 (no. 5), *a* = 25.7843(4) Å, *b* = 5.30700(10) Å, *c* = 18.5521(3) Å, *β* = 95.2280(10)°, *V* = 2528.06(7) Å^3, *Z* = 4, *T* = 100(2) K, μ(CuKα) = 2.526 mm^{-1}, *Dcalc* = 1.430 g/cm^3, 22540 reflections measured (6.884° ≤ 2Θ ≤ 136.32°), 4460 unique (R_{int} = 0.0686, R_{sigma} = 0.0454) which were used in all calculations. The final R_1 was 0.0722 (I > 2σ(I)) and wR_2 was 0.2005 (all data).

2-Phenylpropan-2-yl (*S*)-2-hydroxypropanoate (*S*)-307

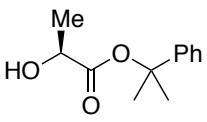

Following general procedure 7, *L*-lactic acid (1.05 g, 25.6 mmol) gave, after column chromatography (10-15% EtOAc in petroleum ether), (*S*)-**307** (1.47 g, 7.07 mmol, 61%) contaminated with traces of 2-phenyl-2-propanol (~19:1 by ^{1}H-NMR) as a colourless oil. $\mathbf{R_f}$ (15% EtOAc in petroleum ether) 0.30; $[\boldsymbol{\alpha}]_{\mathbf{D}}^{\mathbf{22}}$ −3.5 (*c* 0.50, $CHCl_3$); **^{1}H-NMR** (500 MHz, $CDCl_3$) δ 7.39-7.32 (4H, m, ArH),

7.31-7.24 (1H, m, ArH), 4.24 (1H, q, J = 6.9 Hz, CH), 2.76 (1H, bs, OH), 1.82 (3H, s, CH_3-cumyl), 1.80 (3H, s, CH_3-cumyl), 1.45 (3H, d, J = 6.9 Hz, CHC*H*$_3$); **^{13}C-NMR** (125 MHz, $CDCl_3$) δ 174.6 (C=O), 145.1 (C, Ar), 128.5 (2 x CH, Ar), 127.5 (CH, Ar), 124.3 (2 x CH, Ar), 83.5 (C, cumyl), 67.0 (CH), 28.8 (CH_3, cumyl), 28.4 (CH_3, cumyl), 20.6 (CH*C*H$_3$); **IR** (film) 3358 (OH), 3058, 2977, 2937, 1721 (C=O), 1446, 1368, 1219, 1123, 1042 cm^{-1}; **MS** (ESI$^+$) *m/z* 231 $[M+Na]^+$, 439 $[2M+Na]^+$; **HRMS** (ESI$^+$) Calcd. for $C_{12}H_{16}O_3Na$ $[M+Na]^+$: 231.0992, found 231.0994.

(*R*)-1-Oxo-1-[(2-phenylpropan-2-yl)oxy]propan-2-yl 4-nitrobenzoate 308

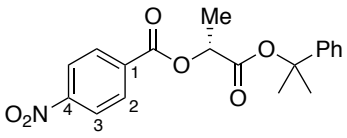

To (*S*)-**307** (1.27 g, 6.08 mmol) in CH_2Cl_2 (61 mL) was added triphenylphosphine (2.39 g, 9.12 mmol) and 4-nitrobenzoic acid (1.52 g, 9.12 mmol) and the reaction mixture cooled to 0 °C. Diethyl azodicarboxylate (1.44 mL, 9.12 mmol) was added dropwise and the reaction mixture stirred at room temperature for 16 h. The reaction mixture was concentrated under reduced pressure and the crude mixture dissolved in EtOAc (150 mL). The organics were washed with a saturated solution of $NaHCO_3$ (3 x 50 mL) and brine (25 mL), dried ($MgSO_4$), filtered and concentrated under reduced pressure. Purification by column chromatography (10% EtOAc in petroleum ether) gave **308** (2.06 g, 5.77 mmol, 95%) as a yellow oil. $\mathbf{R_f}$ (10% EtOAc in petroleum ether) 0.30; $[\boldsymbol{\alpha}]_{\mathbf{D}}^{\mathbf{22}}$ +6.9 (*c* 1.60, $CHCl_3$); **^{1}H-NMR** (500 MHz, $CDCl_3$) δ 8.30-8.26 (2H, m, ArH-3), 8.26-8.21 (2H, m, ArH-2), 7.39-7.29 (4H, m, ArH), 7.28-7.22 (1H, m, ArH), 5.35 (1H, q, J = 7.1 Hz, CH), 1.82 (3H, s, CH_3-cumyl), 1.80 (3H, s, CH_3-cumyl), 1.67 (3H, d, J = 7.1 Hz, CHC*H*$_3$); **^{13}C-NMR** (125 MHz, $CDCl_3$) δ 168.7 (C=O, cumyl), 164.2 (C=O, Bz), 150.8 (C, Ar-1 or Ar-4), 145.0 (C, Ar-cumyl), 135.2 (C, Ar-1 or Ar-4), 131.1 (2 x CH, Ar-3), 128.5 (2 x CH, Ar), 127.5 (CH, Ar), 124.3 (2 x CH, Ar), 123.6 (2 x CH, Ar-2), 83.7 (C, cumyl), 70.3 (CH), 28.8 (CH_3, cumyl), 28.3 (CH_3, cumyl), 17.0 (CH_3, CH*C*H$_3$); **IR** (film) 3112, 3058, 2985, 2940, 2877, 1753 (C=O), 1726 (C=O), 1525, 1346, 1268, 1213, 1098 cm^{-1}; **MS** (ESI$^+$) *m/z* 380 $[M+Na]^+$, 396 $[M+K]^+$; **HRMS** (ESI$^+$) Calcd. for $C_{19}H_{19}NO_6Na$ $[M+Na]^+$: 380.1105, found 380.1110.

2-Phenylpropan-2-yl (*R*)-2-hydroxypropanoate (*R*)-307

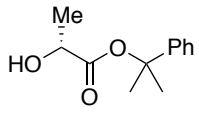

To **308** (3.12 g, 8.74 mmol) in MeOH (87 mL) was added K_2CO_3 (1.27 g, 9.17 mmol) and the reaction mixture stirred at room temperature for 5 min before it was quenched with a saturated solution of NH_4Cl (150 mL). The resulting mixture was extracted with EtOAc (3 x 150 mL) and the combined organics washed with brine (50 mL), dried ($MgSO_4$), filtered and concentrated under reduced pressure. The crude product was purified by column chromatography (10-15% EtOAc in petroleum ether) to give (*R*)-**307** (1.52 g, 7.32 mmol, 84%) as a colourless oil that became a white solid upon storage at −20 °C. **mp** 58-60 °C; $[\boldsymbol{\alpha}]_{\mathbf{D}}^{\mathbf{21}}$ +1.0 (*c* 0.70, $CHCl_3$); **^{1}H-NMR** (500 MHz, $CDCl_3$) δ 7.38-7.32 (4H, m, ArH), 7.31-7.24 (1H, m, ArH), 4.23 (1H, qd, *J* = 6.8, 5.5 Hz, CH), 2.76 (1H, d, *J* = 5.2 Hz, OH), 1.82 (3H, s, CH_3-cumyl), 1.80 (3H, s, CH_3-cumyl), 1.45 (3H, d, *J* = 6.9 Hz, CH*C*H_3); other data as described for (*S*)-**307**.

Fmoc-*D*-A_{Ox}-Ala-OCumyl (*R*,*S*)-255

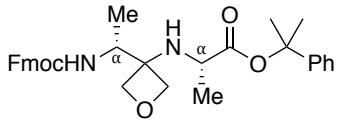

The synthesis of (*R*,*S*)-**255** was adapted from a procedure originally published by Carreira and co-workers.[47]

To (*R*)-**307** (459 mg, 2.20 mmol) in CH_2Cl_2 (10 mL) at −20 °C was added DIPEA (825 µL, 4.74 mmol) followed by the dropwise addition of a solution of triflic anhydride (408 µL, 2.42 mmol) in CH_2Cl_2 (2.5 mL). The reaction mixture was allowed to reach room temperature and stirred for 1 h. Petroleum ether (12.5 mL) was added and the reaction mixture filtered through a plug of silica gel eluting with 50% CH_2Cl_2 in petroleum ether. The eluent was concentrated under reduced pressure to give triflate **283** (629 mg, 1.85 mmol, 84%) which was used immediately without further purification.

To triflate **283** in MeCN (4.0 mL) was added a solution of (*R*)-**282** (377 mg, 1.12 mmol) and DIPEA (322 µL, 1.85 mmol) in MeCN (4.0 mL). The reaction mixture was stirred at 30 °C for 20 h and then concentrated under reduced pressure. The crude material was purified by repeat column chromatography (30-40% EtOAc in petroleum ether; 10-20% EtOAc in CH_2Cl_2) to give (*R*,*S*)-**255** (340 mg, 0.64 mmol, 57%, dr 98:2) as a white solid. $\mathbf{R}_f$ (30% EtOAc in petroleum ether) 0.21; **mp** 63-65 °C; $[\boldsymbol{\alpha}]_{\mathbf{D}}^{\mathbf{22}}$ −18.4 (*c* 0.38, $CHCl_3$); **^{1}H-NMR** (500 MHz, $CDCl_3$) δ 7.76 (2H, d, *J* = 7.5 Hz, ArH-Fmoc), 7.58 (2H, d, *J* = 7.4 Hz, ArH-Fmoc), 7.43-7.23 (9H, m, ArH), 5.20 (0.85H, d, *J* = 8.3 Hz, major rotamer NH-A_{Ox}),

5.03 (0.15H, bs, minor rotamer NH-A_{Ox}), 4.61-4.40 (8H, m, $CHCH_2$-Fmoc, CHα-A_{Ox}, 2 x OCH_2-Ox), 3.88-3.76 (1H, m, CHα-Ala), 2.07 (1H, bs, NH-Ala), 1.82 (3H, s, CH_3-cumyl), 1.79 (3H, s, CH_3-cumyl), 1.38 (3H, d, J = 6.9 Hz, CH_3-Ala), 1.12 (2.55H, d, J = 6.4 Hz, major rotamer, CH_3-A_{Ox}), 1.04-0.91 (0.45H, m, minor rotamer, CH_3-A_{Ox}); **^{13}C-NMR** (125 MHz, $CDCl_3$) δ 175.6 (C=O, Ala), 156.3 (C=O, Fmoc), 145.2 (C, Ar-cumyl), 144.1 (2 x C, Ar-Fmoc), 141.5 (2 x C, Ar-Fmoc), 128.5 (2 x CH, Ar), 127.8 (2 x CH, Ar), 127.5 (CH, Ar), 127.2 (2 x CH, Ar), 125.18 (CH, Ar), 125.2 (CH, Ar), 124.3 (2 x CH, Ar), 120.1 (2 x CH, Ar), 82.8 (C, Ox), 79.0 (OCH_2, Ox), 77.9 (OCH_2, Ox), 66.7 (CH_2, Fmoc), 62.5 (C, Ox), 52.0 (CH, Fmoc or α-A_{Ox}), 51.2 (CH, α-Ala), 47.5 (CH, Fmoc or α-A_{Ox}), 28.8 (CH_3, cumyl), 28.2 (CH_3, cumyl), 21.7 (CH_3, Ala), 14.6 (CH_3, A_{Ox}); **IR** (film) 3332 (NH), 2977, 2942, 2875, 1719 (C=O), 1496, 1447, 1270, 1131 cm^{-1}; **MS** (ESI^+) *m/z* 529 $[M+H]^+$, 551 $[M+Na]^+$; **HRMS** (ESI^+) Calcd. for $C_{32}H_{36}N_2O_5Na$ $[M+Na]^+$: 551.2516, found 551.2520; **HPLC** (Chiralcel OD-H (0.46 cm x 25 cm, 5 μm), 20% isopropanol in hexane, 25 °C, 1.0 mL/min, λ = 254 nm) t_R = 55 min (major), 97 (minor).

Fmoc-*L*-A_{Ox}-Ala-OCumyl (*S,S*)-255

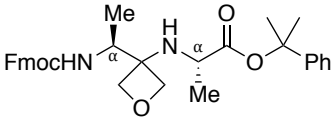

The synthesis of (*S*,*S*)-**255** was adapted from a procedure originally published by Carreira and co-workers.[47]

To (*R*)-**307** (458 mg, 2.20 mmol) in CH_2Cl_2 (10 mL) at −20 °C was added DIPEA (824 μL, 4.73 mmol) followed by the dropwise addition of a solution of triflic anhydride (407 μL, 2.42 mmol) in CH_2Cl_2 (2.5 mL). The reaction mixture was allowed to reach room temperature and stirred for 1 h. Petroleum ether (12.5 mL) was added and the reaction mixture filtered through a plug of silica gel eluting with 50% CH_2Cl_2 in petroleum ether. The eluent was concentrated under reduced pressure to give triflate **283** (734 mg, 2.16 mmol, 98%) which was used immediately without further purification.

To triflate **283** in MeCN (4.0 mL) was added a solution of (*S*)-**282** (338 mg, 1.00 mmol) and DIPEA (376 μL, 2.16 mmol) in MeCN (4.0 mL). The reaction mixture was stirred at 30 °C for 20 h and then concentrated under reduced pressure. The crude material was purified by repeat column chromatography (30-40% EtOAc in petroleum ether; 10-20% EtOAc in CH_2Cl_2) to give (*S*,*S*)-**255** (264 mg, 0.50 mmol, 50%, dr >98:2) as a white solid. $\mathbf{R_f}$ (30% EtOAc in petroleum ether) 0.21; **mp** 73-76 °C; $[\boldsymbol{\alpha}]_{\mathbf{D}}^{\mathbf{18}}$ −13.4 (*c* 0.25, $CHCl_3$); **^{1}H-**

NMR (500 MHz, $CDCl_3$) δ 7.76 (2H, d, *J* = 7.5 Hz, ArH-Fmoc), 7.59 (2H, d, *J* = 7.5 Hz, ArH-Fmoc), 7.44-7.21 (9H, m, ArH), 5.57 (0.9 H, d, *J* = 7.1 Hz, major rotamer NH-A_{Ox}), 5.28-5.08 (0.1H, m, minor rotamer NH-A_{Ox}), 4.67-3.81 (8H, m, 2 x OCH_2-Ox, CH_2CH-Fmoc, CHα-A_{Ox}), 3.79-3.64 (0.9H, m, major rotamer CHα-Ala), 3.63-3.51 (0.1H, m, minor rotamer CHα-Ala), 1.82 (3H, s, CH_3-cumyl), 1.80-1.70 (4H, m, CH_3-cumyl, NH-Ala), 1.38 (3H, d, *J* = 6.8 Hz, CH_3-Ala), 1.16 (2.7H, d, *J* = 5.9 Hz, major rotamer CH_3-A_{Ox}), 1.07-0.96 (0.3H, m, minor rotamer CH_3-A_{Ox}); **^{13}C-NMR** (125 MHz, $CDCl_3$) δ 175.5 (C=O, Ala), 156.5 (C=O, Fmoc), 145.2 (C, Ar-cumyl), 144.12 (C, Ar-Fmoc), 144.10 (C, Ar-Fmoc), 141.5 (2 x C, Ar-Fmoc), 128.5 (2 x CH, Ar), 127.8 (2 x CH, Ar), 127.5 (CH, Ar), 127.2 (2 x CH, Ar), 125.4 (CH, Ar), 125.3 (CH, Ar), 124.4 (2 x CH, Ar), 120.1 (2 x CH, Ar), 82.8 (C, cumyl), 79.1 (OCH_2, Ox), 78.9 (OCH_2, Ox), 66.8 (CH_2, Fmoc), 62.4 (C, Ox), 52.1 (CH, α-Ala), 52.0 (CH, α-A_{Ox}), 47.4 (CH, Fmoc), 28.9 (CH_3, cumyl), 28.1 (CH_3, cumyl), 20.8 (CH_3, Ala), 14.9 (CH_3, A_{Ox}); **IR** (film) 3329 (NH), 2976, 2937, 2876, 1718 (C=O), 1497, 1448, 1242, 1132, 1077 cm^{-1}; **MS** (ESI^+) *m/z* 529 $[M+H]^+$, 551 $[M+Na]^+$, 567 $[M+K]^+$; **HRMS** (ESI^+) Calcd. for $C_{32}H_{36}N_2O_5Na$ $[M+Na]^+$: 551.2516, found 551.2512; **HPLC** (Chiralcel OD-H (0.46 cm x 25 cm, 5 μm), 20% isopropanol in hexane, 25 °C, 1.0 mL/min, λ = 254 nm) t_R = 56 min (minor), 87 min (major).

6.4 Chiral NMR Analysis of (*S*)-112 Using Pirkle's Alcohol

(*S*)-**112** (6.7 mg, 0.036 mmol) and (*S*)-Pirkle's alcohol (10.0 mg, 0.03 mmol) were added to $CDCl_3$ (0.8 mL). ^{1}H-NMR (700 MHz, $CDCl_3$) analysis gave spectra A. Then (*R*)-**112** (2.2 mg, 0.012 mmol) and (*S*)-Pirkle's alcohol (3.3 mg, 0.012 mmol) were added to the solution to give spectrum B. Integration of the signals at 0.89 (d, J = 6.8 Hz) and 0.88 (d, J = 6.8 Hz) ppm in spectra B relative to those in spectra A confirmed >95% ee (*S*)-**112**

A. Expanded ^{1}H-NMR (700 MHz, $CDCl_3$) spectra of (*S*)-**112** with (*S*)-Pirkle's alcohol:

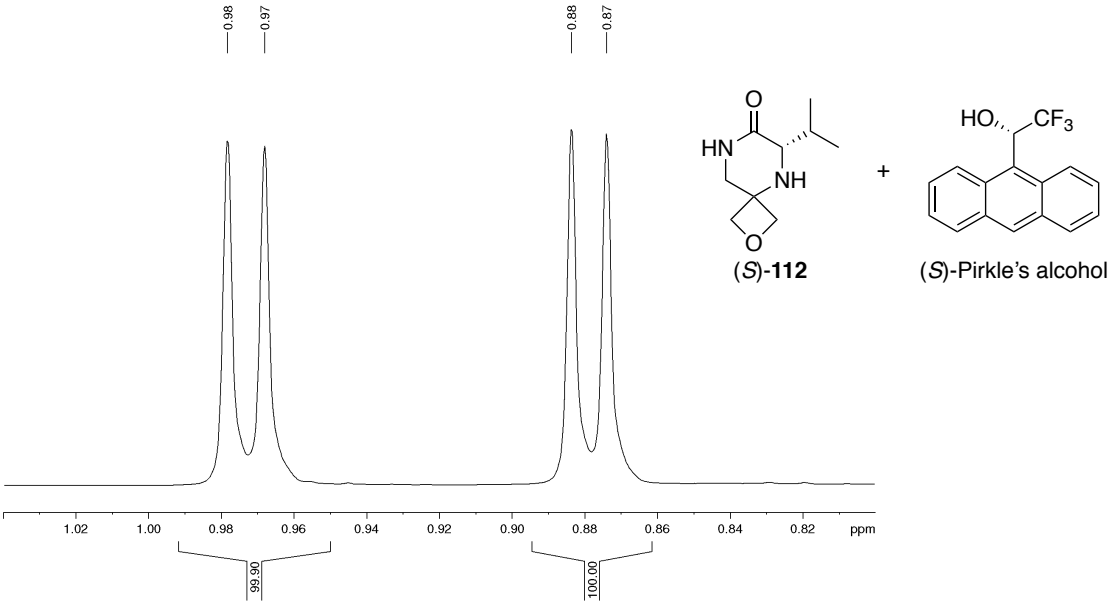

B. Expanded ^{1}H-NMR (700 MHz, $CDCl_3$) spectra of *(S)*-**112**:(*R*)-**112** (3:1) with (*S*)-Pirkle's alcohol:

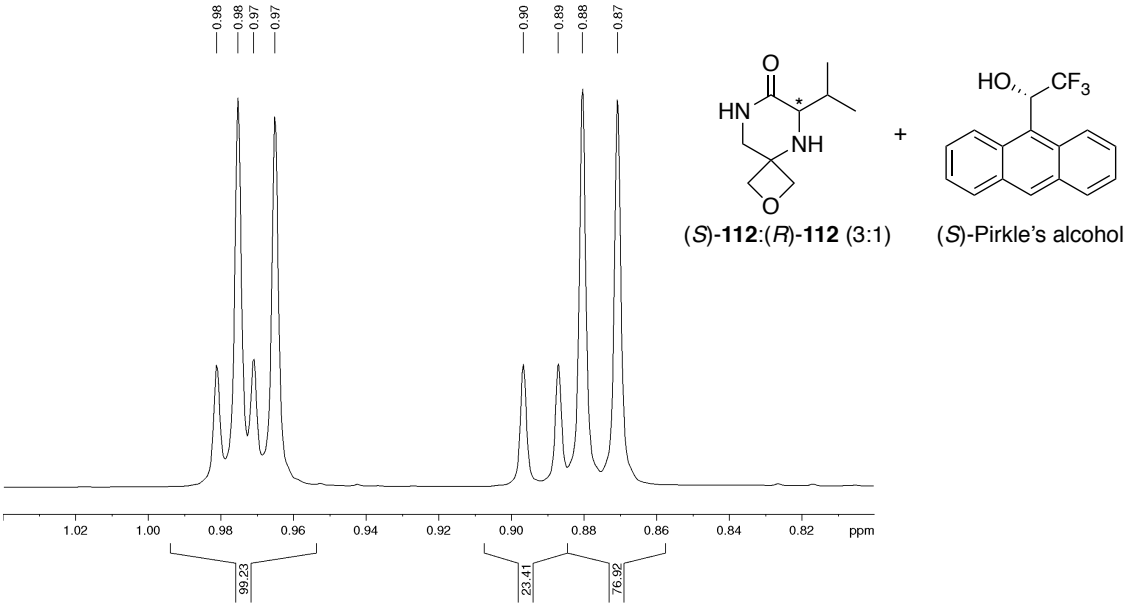

A. ^{1}H-NMR (700 MHz, $CDCl_3$) spectra of (*S*)-**112** with Pirkle's alcohol:

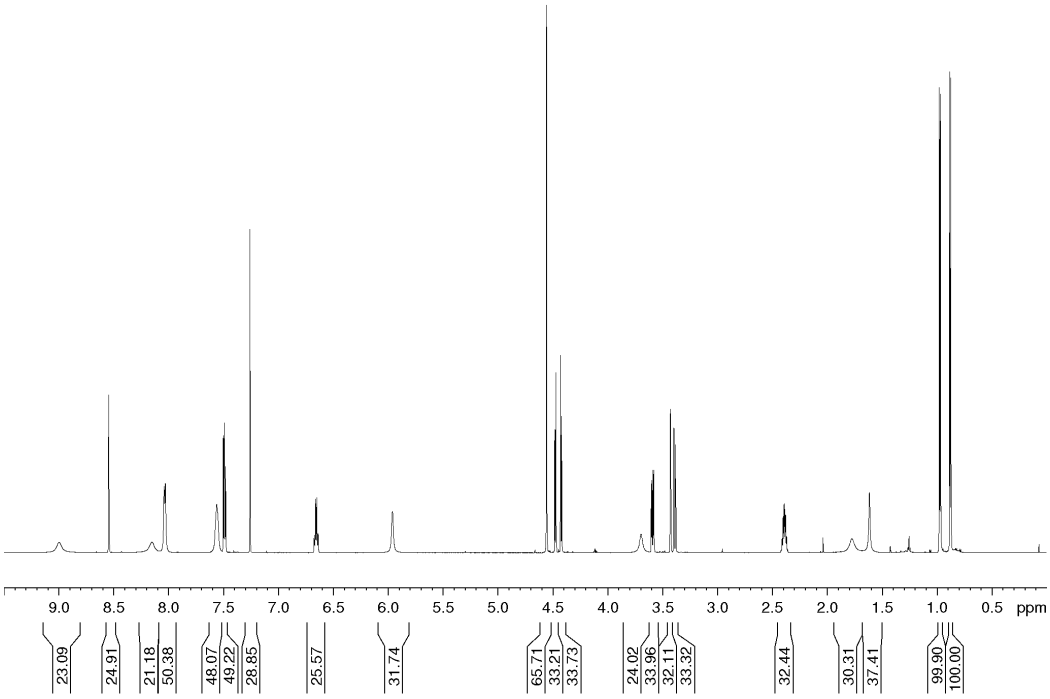

B. ^{1}H-NMR (700 MHz, $CDCl_3$) of (*S*)-**112**:(*R*)-**112** (3:1) with Pirkle's alcohol:

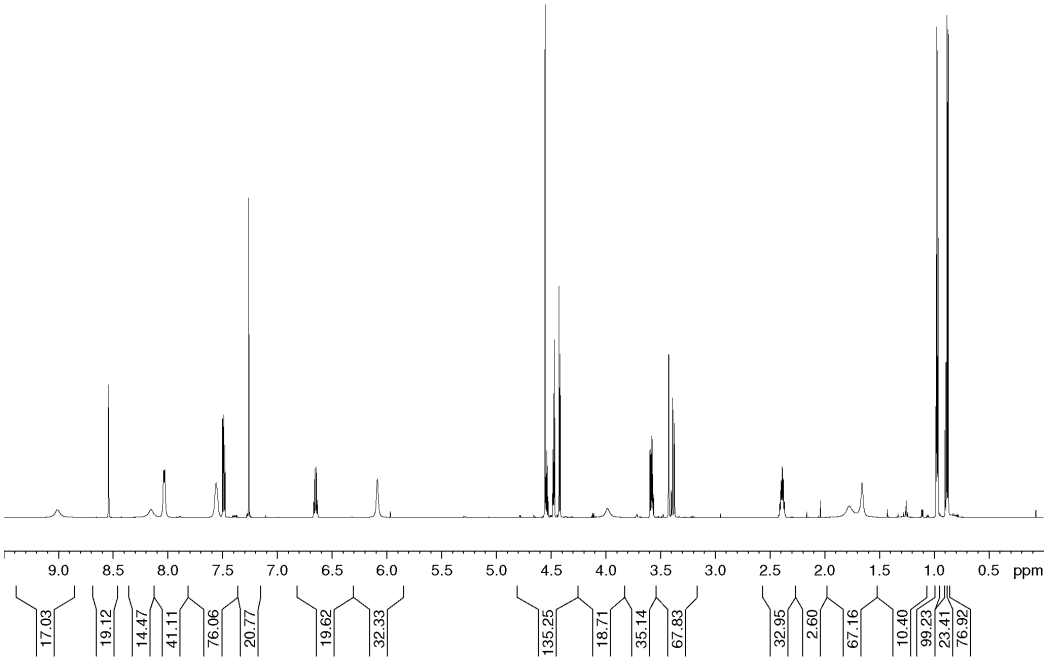

6.5 Configurational Integrity of (*S,S*)-219 and (*S,R*)-219

The configurational integrity of the *C*-terminal amino acid residue during the synthesis and application of *N*-Fmoc-G_{Ox}-dipeptides was confirmed by the solution-phase synthesis of (*S,S*)-**219** and (*S,R*)-**219**. Reaction of **210** with 2% TFA in CH_2Cl_2, followed by coupling with *L*- and *D*-phenylalanine *tert*-butyl ester with HCTU gave (*S,S*)-**219** and (*S,R*)-**219** respectively (Scheme 6.1). The diastereotopic purity of (*S,S*)-**219** and (*S,R*)-**219** was determined by comparison of the CH_3-Val region (0.96-0.66 ppm) in the crude ^{1}H-NMR (500 MHz, $CDCl_3$) spectra. Integration of the signal at 0.77 (J = 6.8 Hz) ppm in spectrum A relative to that in spectrum B confirmed dr >95:5 indicating that no detectable epimerization arises during coupling.

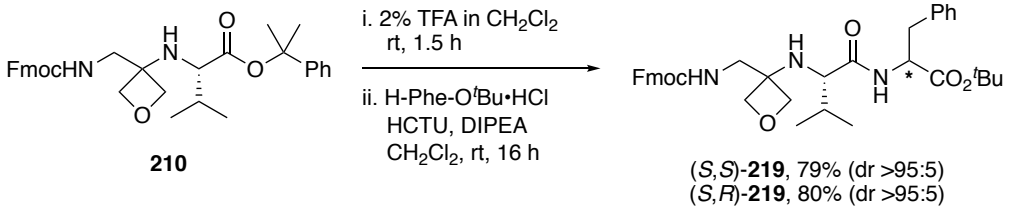

Scheme 6.1 *C*-Terminal couplings of oxetane containing dipeptides proceed with no detectable epimerisation. [a] Coupling conditions: H-Phe-O^{t}Bu · HCl (2.0 equiv), HCTU (1.0 equiv), DIPEA (4.0 equiv), CH_2Cl_2, rt.

A. Expanded ^{1}H-NMR (500 MHz, $CDCl_3$) of crude (*S,S*)-**219**

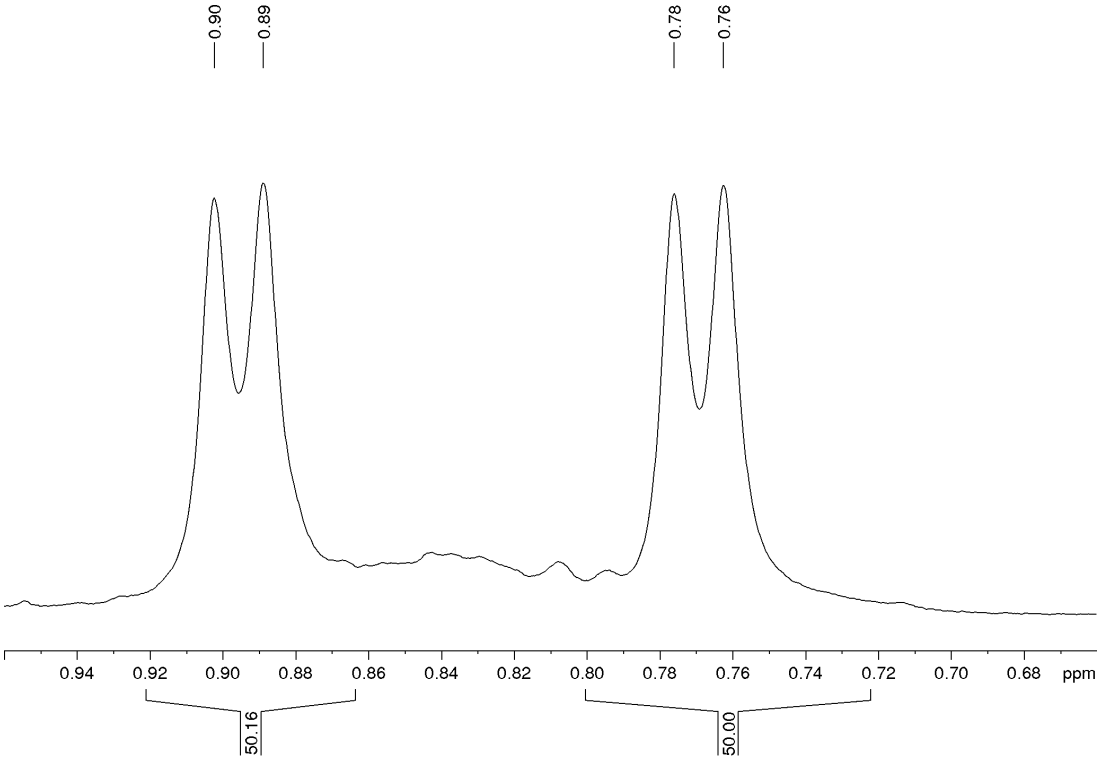

B. Expanded ^{1}H-NMR (500 MHz, $CDCl_3$) of crude (*S,R*)-**219**

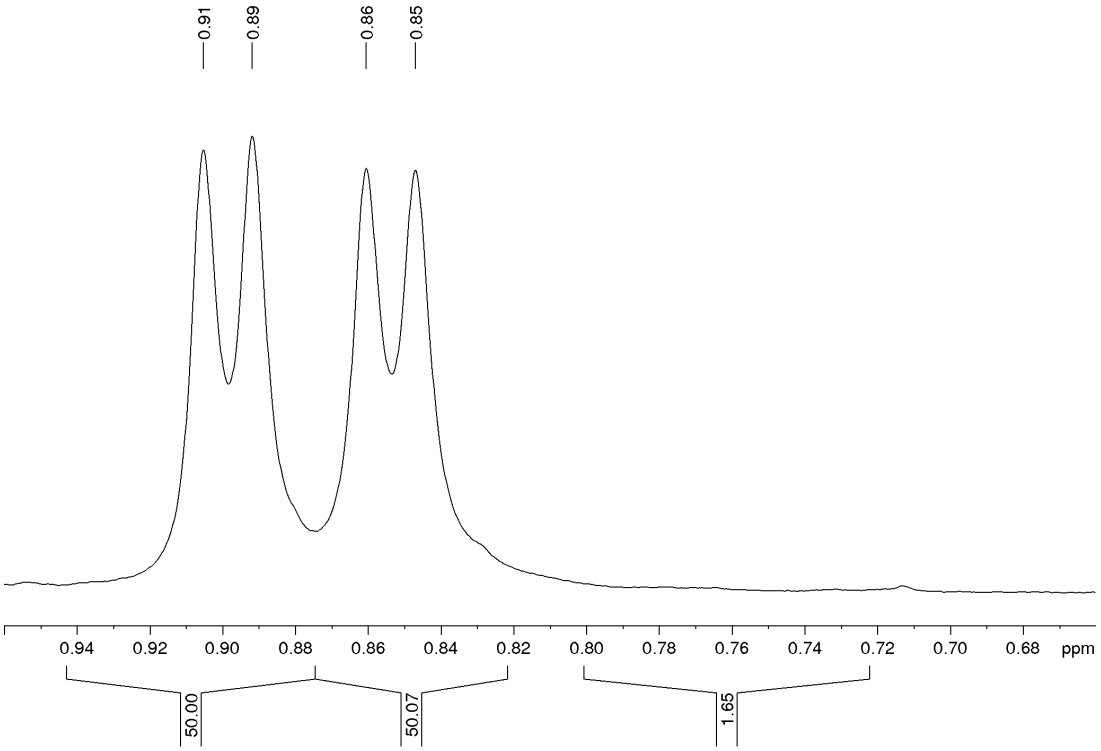

A. ^{1}H-NMR (500 MHz, $CDCl_3$) of crude (*S,S*)-**219**

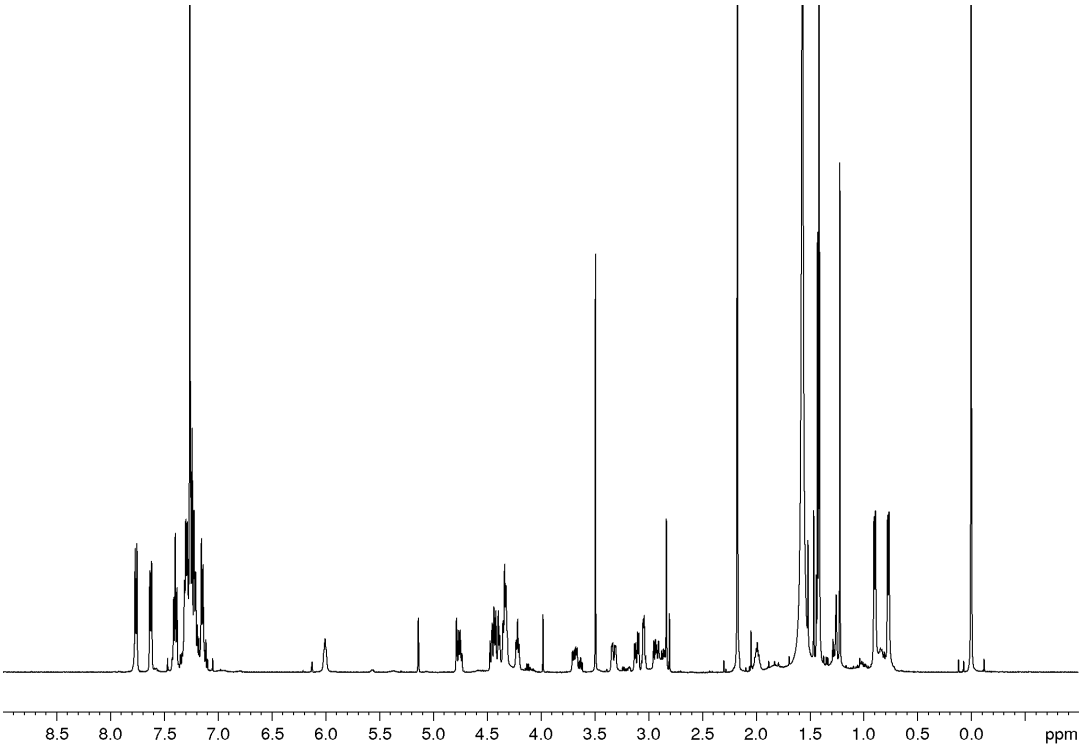

B. ^{1}H-NMR (500 MHz, $CDCl_3$) of crude (*S,R*)-**219**

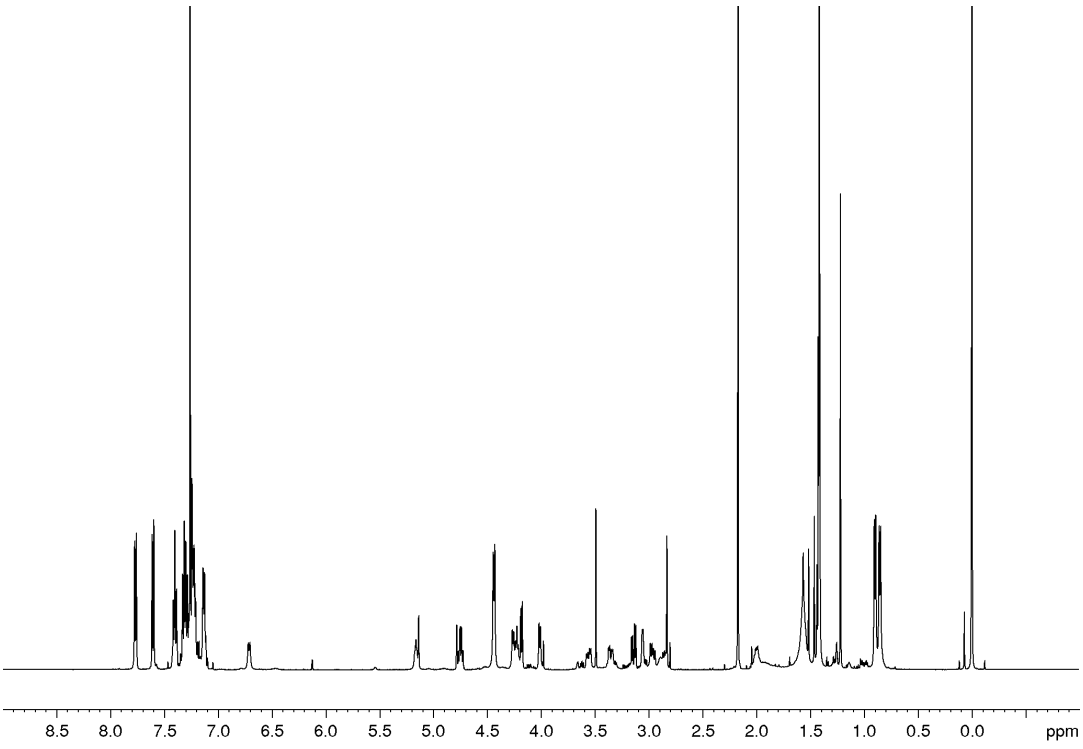

6.6 Microwave Assisted Solid-Phase Synthesis of Peptides

Synthesis and Analysis of Ac-Ala-G_{Ox}-Phe-Ala-NH_2 176

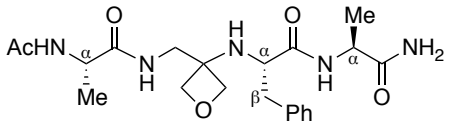

176 was synthesised at the University of Leicester on a CEM Liberty1 automated microwave-assisted solid-phase peptide synthesiser (CEM Corporation) using an Fmoc/^{t}Bu protecting group strategy on a 0.1 mmol synthetic scale using Rink amide resin.

Deprotection was carried out using 20% piperidine in DMF at 75 °C for 30 s and then 3 min followed by washing. *N*-α-Fmoc protected amino acids (3 equiv) were coupled using HCTU (3 equiv) and DIPEA (6 equiv) at 75 °C for 5 min followed by washing.

Oxetane containing dipeptide building block **175** (3 equiv) was dissolved in DMF (0.066 M) followed by addition of HCTU (3 equiv) and DIPEA (6 equiv). The resulting solution was allowed to activate for 5 min before addition to the resin.

N-terminal acetylation was carried out manually using Ac_2O (3 equiv) and DIPEA (3 equiv) in DMF at room temperature.

The peptide was cleaved from the resin using a cleavage cocktail of 95% TFA, 2.5% H_2O and 2.5% triisopropylsilane (TIS) for 1 h at room temperature before being drained and the cleavage cocktail blown off using a stream of nitrogen. The peptide was precipitated and washed three times in cold Et_2O and spun down to a pellet before the Et_2O was removed and the peptide dried under a steady stream of nitrogen.

The crude peptide was purified by reverse-phase HPLC using a Dionex Ultimate 3000 system with a Phenomenex Gemini-NX 5 µm C18 110 Å packed column with dimensions 250 x 21.20 mm and collected fractions were lyophilized on a FreeZone Benchtop Freeze Dry System. Purity was determined by analytical reverse-phase HPLC using a Dionex Ultimate 3000 system with a Phenomenex Gemini-NX 5 µm C18 110 Å packed column with dimensions 150 x 4.60 mm. Retention times (t_R) are reported in minutes.

Characterisation Data: **HPLC** Purity 98% (t_R = 8.8 [5-100% MeCN+ 0.1% TFA in water + 0.1% TFA over 15 min], t_R = 10.6 [5-50% MeCN+ 0.1% TFA in water + 0.1% TFA over 15 min]). **HRMS** (ESI^+) Calcd. For $C_{21}H_{31}N_5O_5Na$ $[M+Na]^+$: 456.2217, found 456.2219. **^{1}H-NMR** (400 MHz, $CDCl_3$) δ 7.38-7.31 (1H, m, NH), 7.12-7.04 (6H, NH and ArH), 6.80-6.73 (1H, m, NH), 5.99 (1H, s, NH), 5.67 (1H, s, NH), 4.16 (1H, d, *J* = 6.4 Hz, OC*H*H-Ox), 4.11-3.99 (5H, m, OCH*H*-Ox, OCH_2-Ox, 2 x CHα-Ala), 3.67-3.54 (2H,

m, CHα-Phe and C*H*H-G_{Ox}), 3.28-3.20 (1H, m, CH*H*-G_{Ox}), 2.86 (1H, dd, *J* = 13.6, 6.5 Hz, C*H*Hβ-Phe), 2.76 (1H, dd, *J* = 13.4, 7.1 Hz, CH*H*β-Phe), 1.72 (3H, s, Ac), 1.09-1.05 (6H, m, 2 x CH_3-Ala).

Synthesis and Analysis of Peptides 225-233

Synthesis and analysis of oxetane-modified peptides **225-233** was carried out by Dr Astrid Knuhtsen, Dr Alex Hoose and Dr Andrew Jamieson at the University of Glasgow. Experimental procedures and characterisation data is included in the supporting information of the Organic Letters publication and is available free of charge on the ACS Publications website.[124]

https://pubs.acs.org/doi/suppl/10.1021/acs.orglett.7b01466

6.7 Determination of Diastereomeric Ratio

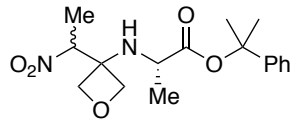

257

The diastereomeric ratio of **257** was determined by integration of the CHα-Ala signals at 3.85-3.66 ppm (1H, m, diastereoisomer 1) and 3.66-3.47 ppm (1H, m, diastereoisomer 2) in the crude ^{1}H-NMR (300 MHz, $CDCl_3$) spectrum.

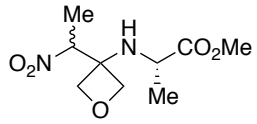

263

The diastereomeric ratio of **263** was determined by integration of the CH_3-Ala signals at 1.68 ppm (3H, d, J = 6.8 Hz, diastereoisomer 1) and 1.64 ppm (3H, d, J = 6.9 Hz, diastereoisomer 2) in the crude ^{1}H-NMR (400 MHz, $CDCl_3$) spectrum.

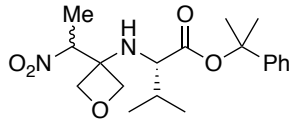

264

The diastereomeric ratio of **264** was determined by integration of the CHα-Val signals at 3.46 ppm (1H, dd, J = 10.3, 4.3 Hz, diastereoisomer 1) and 3.40 ppm (1H, dd, J = 10.3, 4.4 Hz, diastereoisomer 2) in the crude ^{1}H-NMR (400 MHz, $CDCl_3$) spectrum.

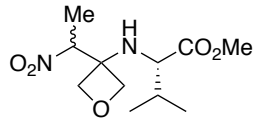

132

The diastereomeric ratio of **132** was determined by integration of the NO_2CH signals at 4.92 ppm (1H, q, J = 6.8 Hz, diastereoisomer 1) and 4.87 ppm (1H, q, J = 6.9 Hz, diastereoisomer 2) in the crude ^{1}H-NMR (500 MHz, $CDCl_3$) spectrum.

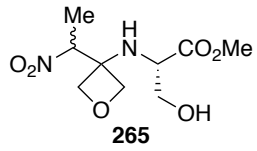

265

The diastereomeric ratio of **265** was determined by integration of the OC*H*H-Ox signals at 4.45 ppm (1H, d, J = 7.7 Hz, diastereoisomer 1) and 4.39 ppm (1H, d, J = 7.8 Hz, diastereoisomer 2) in the crude ^{1}H-NMR (400 MHz, $CDCl_3$) spectrum.

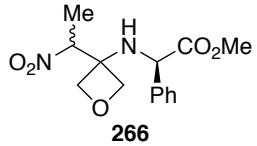

266

The diastereomeric ratio of **266** was determined by integration of the CHPh signals at 4.87 (1H, bs, diastereoisomer 1) and 4.82 ppm (1H, bs, diastereoisomer 2) in the crude ^{1}H-NMR (400 MHz, $CDCl_3$) spectrum.

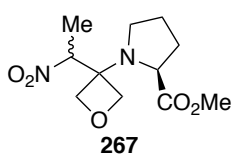

267

The diastereomeric ratio of **267** was determined by integration of the OC*H*H-Ox signals at 4.59 (1H, d, J = 7.8 Hz, diastereoisomer 1) and

4.48 ppm (1H, d, J = 7.4 Hz, diastereoisomer 2) in the crude ^{1}H-NMR (300 MHz, $CDCl_3$) spectrum.

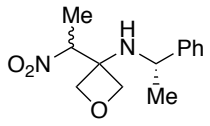

277

The diastereomeric ratio of **277** was determined by integration of the NO_2CH signals at 5.05 ppm (1H, q, J = 6.9 Hz, diastereoisomer 1) and at 4.86 ppm (1H, q, J = 6.9 Hz, diastereoisomer 2) in the crude ^{1}H-NMR (300 MHz, $CDCl_3$) spectrum.

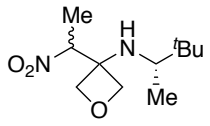

278

The diastereomeric ratio of **278** was determined by integration of the OC*H*H-Ox signals at 4.59 ppm (1H, d, J = 7.1 Hz, diastereoisomer 1) and at 4.48 ppm (1H, d, J = 7.0 Hz, diastereoisomer 2) in the crude ^{1}H-NMR (400 MHz, $CDCl_3$) spectrum.

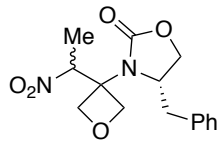

280

The diastereomeric ratio of **280** was determined by integration of the NO_2CH signals at 5.54 ppm (1H, q, J = 7.1 Hz, diastereoisomer 1) and at 5.39 ppm (1H, q, J = 6.9 Hz, diastereoisomer 2) in the crude ^{1}H-NMR (300 MHz, $CDCl_3$) spectrum.

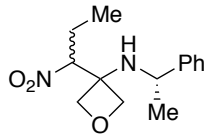

297

The diastereomeric ratio of **297** was determined by integration of the NO_2CH signals at 4.80 ppm (1H, dd, J = 11.0, 3.1 Hz, diastereoisomer 1) and at 4.71 ppm (1H, dd, J = 11.3, 2.9 Hz, diastereoisomer 2) in the crude ^{1}H-NMR (400 MHz, $CDCl_3$) spectrum.

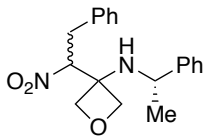

298

The diastereomeric ratio of **298** was determined by integration of the C*H*HPh signals at 3.30 ppm (1H, dd, J = 14.8, 4.1 Hz, diastereoisomer 1) and at 3.20 ppm (1H, dd, J = 14.8, 3.4 Hz, diastereoisomer 2) in the crude ^{1}H-NMR (400 MHz, $CDCl_3$) spectrum.

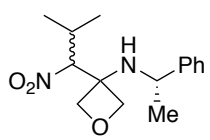

299

The diastereomeric ratio of **299** was determined by integration of the OC*H*H-Ox signals at 4.26 ppm (1H, d, J = 7.1 Hz, diastereoisomer 1) and at 4.19 ppm (1H, d, J = 7.6 Hz, diastereoisomer 2) in the crude ^{1}H-NMR (400 MHz, $CDCl_3$) spectrum.

6.8 Diastereomeric Purity of (*R,S*)-277 and (*S,R*)-277

Confirmation that (*R,S*)-**277** was isolated as a single diastereoisomer (dr >95:5) was demonstrated by comparison of the NO_2CH signals in the crude ^{1}H-NMR (300 MHz, $CDCl_3$) spectrum with the same region in the ^{1}H-NMR (500 MHz, $CDCl_3$) spectrum after column chromatography. Integration of the signals at 5.05 (q, J = 6.8 Hz) ppm and 4.86 (q, J = 6.9 Hz) ppm in spectrum A relative to that in spectrum B confirmed dr >95:5. ^{1}H-NMR analysis of (*S,R*)-**277** was identical and also confirmed dr >95:5.

A. Expanded ^{1}H-NMR (300 MHz, $CDCl_3$) of crude (*R,S*)-**277**

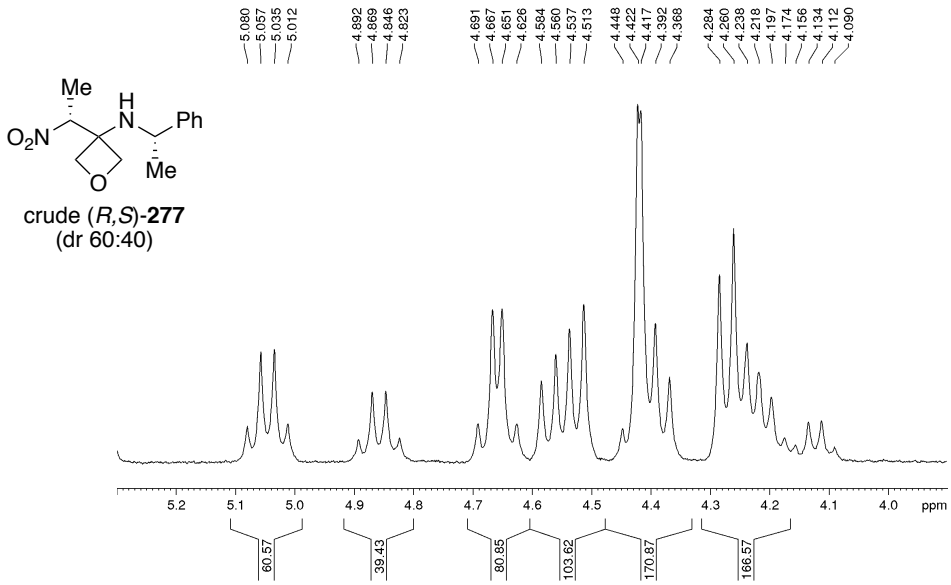

B. Expanded ^{1}H-NMR (500 MHz, $CDCl_3$) of (*R,S*)-**277** after column chromatography

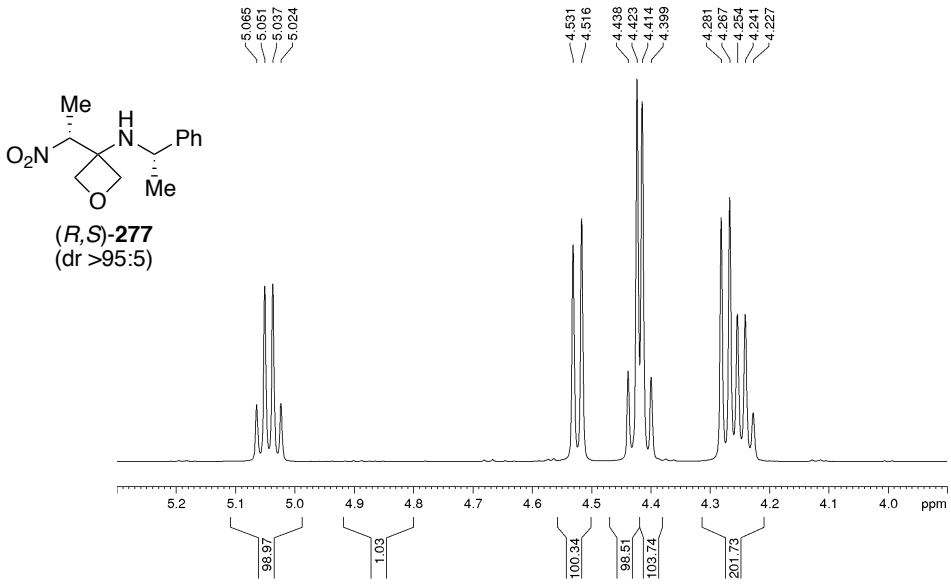

6.9 HPLC Analysis of (±,*S*)-255, (*R*,*S*)-255 and (*S*,*S*)-255

HPLC analysis was conducted on an Agilent Technologies 1200 Series HPLC, using Chiralcel OD-H column (0.46 cm x 25 cm, 5 µm) at 25 °C, with detection by UV at 254 nm. Samples were eluted at a flow rate of 1.0 mL/min with a mobile phase system composed of 20% isopropanol in hexane. Retention times (t_R) are reported in minutes.

(±,*S*)-**255**

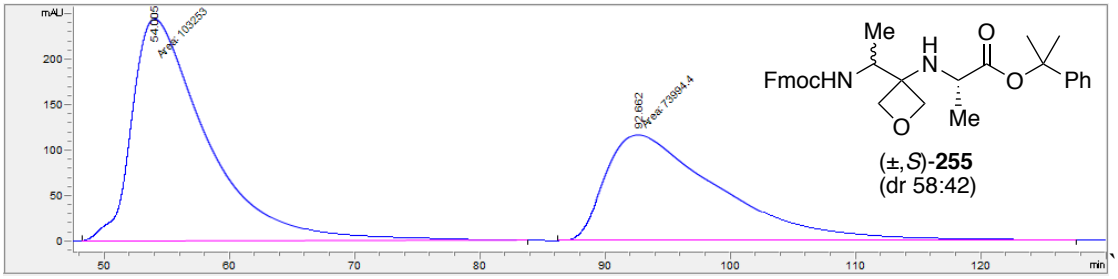

#	Time	Area	Height	Width	Area%	Symmetry
1	54.005	103252.9	245.4	7.0114	58.254	0.423
2	92.662	73994.4	116.8	10.5588	41.746	0.391

(*R*,*S*)-**255**

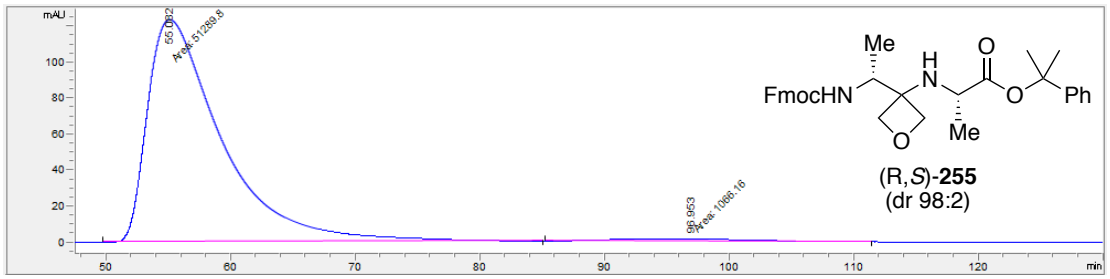

#	Time	Area	Height	Width	Area%	Symmetry
1	55.082	51289.8	123.4	6.929	97.964	0.41
2	96.953	1066.2	1.3	13.2996	2.036	1.216

(*S*,*S*)-**255**

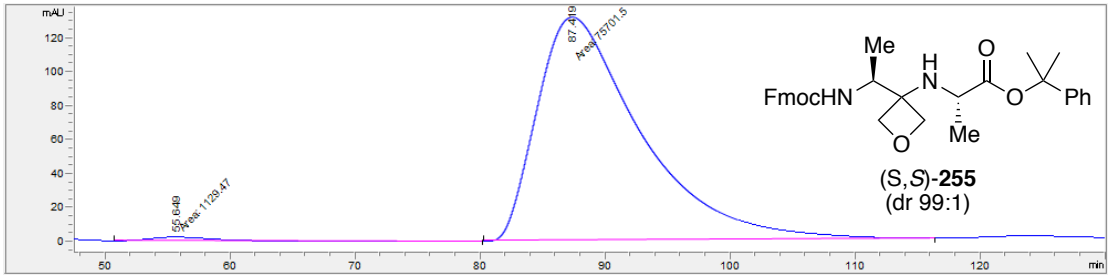

#	Time	Area	Height	Width	Area%	Symmetry
1	55.649	1129.5	2.3	8.1607	1.470	0.399
2	87.419	75701.5	131.1	9.6274	98.530	0.498

6.10 Solid-Phase Synthesis of KAAAA Peptides

Synthesis of peptides **246**, **248**, **252** and **254** was carried out by Dr Ina Wilkening at the University of Warwick.

Peptides were synthesised on a Prelude peptide synthesiser (ProteinTechnologies Inc.) using an Fmoc/^{t}Bu protecting group strategy on a 0.025 mmol synthetic scale using NovaSyn® TGR R resin (Novabiochem).

The resin was manually loaded with Fmoc-Tyr(^{t}Bu)-OH as follows; resin (0.025 mmol), was pre-swollen in DMF for 1 h and washed with DMF. Fmoc-Tyr(^{t}Bu)-OH (115 mg, 0.25 mmol), PyBOP (130 mg, 0.25 mmol) and DIPEA (87 μL, 0.50 mmol) in DMF (0.67 M) were added to the resin and the mixture agitated at room temperature for 1 h. The solvent was removed and the resin washed several times with DMF. Loading was repeated in case of a positive TNBS-test.

Deprotection was carried out in 20% piperidine in DMF at room temperature for 20 min followed by washing. *N*-α-Fmoc protected amino acids (10 equiv) were coupled using HATU activation with DIPEA or HCTU activation with NMM at room temperature for 45 min followed by washing.

Oxetane-containing dipeptide building blocks were first deprotected as follows; (*S*,*S*)-**255** or **215** (2.0 equivalents) in 2% TFA/CH_2Cl_2 (0.05 M) was stirred at room temperature until consumption of starting material. The reaction mixture was concentrated under reduced pressure and the resulting residue dissolved in CH_2Cl_2 and concentrated under reduced pressure (3x) to give the crude acid. The crude acid was manually double coupled using HATU (1.9 equiv) and DIPEA (6.0 equiv) at room temperature for 2-12 h until a negative TNBS test was observed.

Peptide **248** was synthesised using HCTU activation with NMM. The first 12 amino acids were attached by double coupling at room temperature for 45 min whereas the last 5 amino acids were attached by triple coupling at room temperature for 45 min. After each amino acid, the peptide was capped with Ac_2O:NMM:DMF (5:5:90; v/v/v) at room temperature for 2 x 15 min. After the last amino acid, the Fmoc group was cleaved manually with 20% piperidine in DMF at room temperature for 20 min and the *N*-terminus was capped with Ac_2O:NMM:DMF (5:5:90; v/v/v) at room temperature for 2 x 20 min.

Oxetane-modified peptides **246**, **252** and **254** were synthesised using HATU activation with DIPEA. Amino acids were attached by triple couplings at room temperature for 45 min. Incorporation of the deprotected oxetane-containing dipeptide building block was achieved as described above. In case of the *N*-terminal oxetane-modified peptides **252** and **252** the last two coupling steps with alanine and lysine were also done manually under standard conditions.

Peptide cleavage was performed using a cleavage cocktail of 95% TFA, 2.5% triisopropylsilane (TIS) and 2.5% water and the resin agitated at room temperature under nitrogen for 1 h. The cleavage cocktail was evaporated using a stream of nitrogen and the peptide was precipitated from solution with ice cold Et_2O. Crude peptides were purified by preparative HPLC (Agilent Infinity 1260) using an Agilent PLRP-S column (100 Å, 8 µm, 150 x 25 mm). Gradients were run using a solvent system consisting of A (H_2O + 0.1% TFA) and B (MeCN + 0.1% TFA), collected fractions were lyophilised on a ScanVac CoolSafe freeze dryer.

Pure peptides were analysed on an Agilent Technologies 1200 Series RP-HPLC, using an Agilent Eclipse Plus C18 (5 µm, 4.6 x 150 mm) at 25 °C, with detection by UV at 214 and 280 nm. Gradients were run using a solvent system consisting of solution A (5% MeCN in H_2O + 0.1% TFA) and B (5% H_2O in MeCN + 0.1% TFA). Two gradients were used to characterise each peptide; a gradient from 5-95% solution B over 20 min and a gradient from 5-50% solution B over 20 min. Analytical RP-HPLC data is recorded as column retention time (t_R) in minutes (min). High-resolution mass spectra were recorded using a Bruker MaXis Impact.

Entry	Peptide Sequence	t_R (min)[a]	Purity (%)[b,c]
1	Ac-KAAAA-KAAAA-KAAAA-KGY-NH_2, **248** parent	8.75 + 10.46	92
2	Ac-KAAAA-KA**A_{Ox}**AA-KAAAA-KGY-NH_2, **246** Central A_{Ox}	7.83 + 8.61	90
3	Ac-KA**A_{Ox}**AA-KAAAA-KAAAA-KGY-NH_2, **252** *N*-Terminal A_{Ox}	9.39 + 11.47	76
4	Ac-KA**G_{Ox}**AA-KAAAA-KAAAA-KGY-NH_2, **254** *N*-Terminal G_{Ox}	9.35 + 11.38	90

Peptide Characterisation Data – Table 1 [a] First t_R is the gradient from 5-95% solution B over 20 min; second number is the gradient from 5-50% over 20 min. [b] At 214 nm. [c] Lowest purity of the two gradients run.

Entry	Peptide Sequence	HRMS		ΔMW (ppm)
		Calculated	Observed	
1	Ac-KAAAA-KAAAA-KAAAA-KGY-NH_2, **248** parent	822.9808 $[M+2H]^{2+}$	822.9808 $[M+2H]^{2+}$	0.0
2	Ac-KAAAA-KA**A_{Ox}**AA-KAAAA-KGY-NH_2, **246** Central A_{Ox}	858.9784 $[M+2Na]^{2+}$	858.9766 $[M+2Na]^{2+}$	2.1
3	Ac-KA**A_{Ox}**AA-KAAAA-KAAAA-KGY-NH_2, **252** *N*-Terminal A_{Ox}	558.3334 $[M+3H]^{3+}$	558.3331 $[M+3H]^{+}$	-0.5
4	Ac-KA**G_{Ox}**AA-KAAAA-KAAAA-KGY-NH_2, **254** *N*-Terminal G_{Ox}	851.9706 $[M+2Na]^{2+}$	851.9701 $[M+2Na]^{2+}$	-0.6

Peptide Characterisation Data – Table 2

6.11 Circular Dichroism

Concentration Determination

Peptide samples were dissolved in 10 mM potassium phosphate buffer pH 7.0, 10 mM potassium phosphate buffer pH 7.0 + 1.0 NaCl, MeOH and 80% MeOH in water. Concentrations of peptides were determined spectroscopically using the extinction coefficient for tyrosine (ε_{275} = 1450 M^{-1} cm^{-1}). Final concentrations ranged from 34 to 100 μM in 10 mM potassium phosphate buffer pH 7.0, 43 to 165 μM in 10 mM potassium phosphate buffer pH 7.0 + 1.0 M NaCl, 153 to 192 μL in MeOH and 47 to 178 μM in 80% MeOH in water.

CD Measurements

CD experiments were performed on a Jasco J-815 spectropolarimeter with temperature control which was routinely calibrated with (1*S*)-(+)-10-camphorsulfonic acid. Spectra were recorded in a 0.1 cm cuvette between 250 and 180 nm using a 1.0 nm pitch with a 1.0 nm band width. Response time was set at 1 s with scanning speed at 100 nm/min and temperature of 0 or 5 °C. Each spectrum represents the average of 10 scans.

CD Data Analysis

The raw CD data was processed by subtraction of the solvent signal and converted to mean residue ellipticity $[\theta]_{\mathrm{MRW}}$ using the equation:

$$[\theta]_{\mathrm{MRW}} = \theta/(10 \times C \times N_P \times l) \qquad \text{(eq 4)}$$

where θ is the ellipticity in millidegrees, C, is the peptide molar concentration (M), l is the cell path length (cm), and N_p is the number of peptide units (oxetane-modified peptides N_p = 18; parent peptide **248** N_p = 19).

CD data was analysed for secondary structure using equations 1-3 (**Method 1**) described in Chapter 4 and DichroWeb (Selcon3, Ref. set 4, **Method 2**).[142,143]

References

1. Powell, N. H.; Clarkson, G. J.; Notman, R.; Raubo, P.; Martin, N. G.; Shipman, M. *Chem. Commun,* **2014**, *50*, 8797.
2. Bailey, P. D. *An introduction to peptide chemistry*; Wiley: Chichester, UK, **1990**.
3. Berg, J. M.; Tymoczko, J. L.; Stryer, L. *Biochemistry*, Sixth Edit.; W.H. Freeman and Company: New York, **2006**.
4. Avan, I.; Hall, C. D.; Katritzky, A. R. *Chem. Soc. Rev.* **2014**, *43*, 3575.
5. Fosgerau, K.; Hoffmann, T. *Drug Discov. Today* **2015**, *20*, 122.
6. Lee, S.; Xie, J.; Chen, X. *Chem. Rev.* **2010**, *110*, 3087.
7. Dasgupta, A.; Mondal, J. H.; Das, D. *RSC Adv.* **2013**, *3*, 9117.
8. Giannis, A.; Kolter, T. *Angew. Chemie Int. Ed. Engl.* **1993**, *32*, 1244.
9. Trabocchi, A.; Guarna, A. *Peptidomimetics in Organic and Medicinal Chemistry*; John Wiley & Sons, Ltd: Chichester, UK, **2014**.
10. Liskamp, R. M. J.; Rijkers, D. T. S.; Kruijtzer, J. A. W.; Kemmink, J. *ChemBioChem* **2011**, *12* , 1626.
11. Grauer, A.; König, B. *Eur. J. Org. Chem.* **2009**, 5099.
12. Vagner, J.; Qu, H.; Hruby, V. J. *Curr. Opin. Chem. Biol.* **2008**, *12*, 292.
13. Melendez, R. E.; Lubell, W. D. *J. Am. Chem. Soc.* **2004**, *126*, 6759.
14. Boeglin, D.; Lubell, W. D. *J. Comb. Chem.* **2005**, *7*, 864.
15. Zhang, R.; Durkin, J. P.; Windsor, W. T. *Bioorg. Med. Chem. Lett.* **2002**, *12*, 1005.
16. Fässler, A.; Bold, G.; Capraro, H. G.; Cozens, R.; Mestan, J; Poncioni, B.; Rösel, J.; Tintelnot-Blomley, M; Lang, M. *J. Med. Chem.* **1996**, *39*, 3203.
17. Von Hentig, N. *Drugs Today*, **2008**, *44*, 103.
18. Liebman, J. F.; Greenberg, A. *Biophys. Chem.* **1974**, *1*, 222.
19. Sarabia, F.; Chammaa, S.; Ruiz, A.; Ortiz, L.; Herrera, F. *Curr. Med. Chem*. **2004**, *11*, 1309.
20. Stawikowski, M.; Cudic, P. *Methods Mol. Biol.* **2007**, *386*, 321.
21. VanderMolen, K. M.; McCulloch, W.; Pearce, C. J.; Oberlies, N. H. *J. Antibiot.* **2011**, *64*, 525.
22. Mukherjee, S.; Verma, H.; Chatterjee, J. *Org. Lett.* **2015**, *17,* 3150.
23. Culik, R. M.; Jo, H.; DeGrado, W. F.; Gai, F. *J. Am. Chem. Soc.* **2012**, *134*, 8026.
24. Reiner, A.; Wildemann, D.; Fischer, G.; Kiefhaber, T. *J. Am. Chem. Soc.* **2008**, *130*, 8079.
25. Zacharie, B.; Lagraoui, M.; Dimarco, M.; Penney, C. L.; Gagnon, L. *J. Med. Chem.*

1999, *42*, 2046.

26. Bach, A.; Eildal, J. N. N.; Stuhr-Hansen, N.; Deeskamp, R.; Gottschalk, M.; Pedersen, S. W.; Kristensen, A. S.; Strømgaard, K. *J. Med. Chem.* **2011**, *54*, 1333.
27. Bull, J. A.; Croft, R. A.; Davis, O. A.; Doran, R.; Morgan, K. F. *Chem. Rev.* **2016**, *116*, 12150.
28. Ahmad, S.; Yousaf, M.; Mansha, A.; Rasool, N.; Zahoor, A. F.; Hafeez, F.; Rizvi, S. M. A. *Synth. Commun.* **2016**, *46*, 1397.
29. Burkhard, J. A.; Wuitschik, G.; Rogers-Evans, M.; Müller, K.; Carreira, E. M. *Angew. Chem. Int. Ed.* **2010**, *49*, 9052.
30. Wuitschik, G.; Carreira, E. M.; Wagner, B.; Fischer, H.; Parrilla, I.; Schuler, F.; Rogers-Evans, M.; Müller, K. *J. Med. Chem.* **2010**, *53*, 3227.
31. Carreira, E. M.; Fessard, T. C. *Chem. Rev.* **2014**, *114*, 8257.
32. Luger, P.; Buschmann, J. *J. Am. Chem. Soc.* **1984**, *106*, 7118.
33. Wani, M. C.; Taylor, H. L.; Wall, M. E.; Coggon, P.; McPhail, A. T. *J. Am. Chem. Soc.* **1971**, *93*, 2325.
34. Omura, S.; Murata, M.; Imamura, N.; Iwai, Y.; Tanaka, H.; Furusaki, A.; Matsumoto, T. *J. Antibiot.* **1984**, *37*, 1324.
35. Bridwell-Rabb, J.; Zhong, A.; Sun, H. G.; Drennan, C. L.; Liu, H. *Nature* **2017**, *544*, 322.
36. Pullaiah, K. C.; Surapaneni, R. K.; Rao, C. B.; Albizati, K. F.; Sullivan, B. W.; Faulkner, D. J.; He, C. H.; Clardy, J. *J. Org. Chem.* **1985**, *50*, 3666.
37. Wuitschik, G.; Rogers-Evans, M.; Müller, K.; Fischer, H.; Wagner, B.; Schuler, F.; Polonchuk, L.; Carreira, E. M. *Angew. Chem. Int. Ed.* **2006**, *45*, 7736.
38. Wuitschik, G.; Rogers-Evans, M.; Buckl, A.; Bernasconi, M.; Märki, M.; Godel, T.; Fischer, H.; Wagner, B.; Parrilla, I.; Schuler, F.; Schneider, J.; Alker, A.; Schweizer, W. B.; Müller, K.; Carreira, E. M. *Angew. Chem. Int. Ed.* **2008**, *47*, 4512.
39. Burkhard, J. A.; Wuitschik, G.; Plancher, J.-M.; Rogers-Evans, M.; Carreira, E. M. *Org. Lett.* **2013**, *15*, 4312.
40. Lassalas, P.; Oukoloff, K.; Makani, V.; James, M.; Tran, V.; Yao, Y.; Huang, L.; Vijayendran, K.; Monti, L.; Trojanowski, J. Q.; Lee, V. M.-Y.; Kozlowski, M. C.; Smith, A. B.; Brunden, K. R.; Ballatore, C. *ACS Med. Chem. Lett.* **2017**, *8*, 864.
41. Burkhard, J. A.; Guérot, C.; Knust, H.; Rogers-Evans, M.; Carreira, E. M. *Org. Lett.* **2010**, *12*, 1944.

42. Ragab, S. S.; Kassir, A. F.; Guillot, R.; Scherrmann, M.-C.; Boddaert, T.; Aitken, D. J. *Chem. Commun.* **2018**, *54*, 1968.
43. Barker, S. F.; Angus, D.; Taillefumier, C.; Probert, M. R.; Watkin, D. J.; Watterson, M. P.; Claridge, T. D. W.; Hungerford, N. L.; Fleet, G. W. J. *Tetrahedron Lett.* **2001**, *42*, 4247.
44. Claridge, T. D.; Goodman, J. M.; Moreno, A.; Angus, D.; Barker, S. F.; Taillefumier, C.; Watterson, M. P.; Fleet, G. W. *Tetrahedron Lett.* **2001**, *42*, 4251.
45. Powell, N. H. Novel Oxetane-Containing Spirocycles and Peptidomimetics, PhD Thesis, University of Warwick, 2014.
46. McLaughlin, M.; Yazaki, R.; Fessard, T. C.; Carreira, E. M. *Org. Lett.* **2014**, *16*, 4070.
47. Möller, G. P.; Müller, S.; Wolfstädter, B. T.; Wolfrum, S.; Schepmann, D.; Wünsch, B.; Carreira, E. M. *Org. Lett.* **2017**, *19*, 2510.
48. Effenberger, F.; Burkard, U.; Willfahrt, J. *Angew. Chemie* **1983**, *95*, 50.
49. Boutureira, O.; Martínez-Sáez, N.; Brindle, K. M.; Neves, A. A.; Corzana, F.; Bernardes, G. J. L. *Chem. Eur. J.* **2017**, *23*, 6483.
50. Martínez-Sáez, N.; Sun, S.; Oldrini, D.; Sormanni, P.; Boutureira, O.; Carboni, F.; Compañón, I.; Deery, M. J.; Vendruscolo, M.; Corzana, F.; Adamo, R.; Bernardes, G. J. L. *Angew. Chem. Int. Ed.* **2017**, *56*, 14963.
51. Zheng, Y.; Tice, C. M.; Singh, S. B. *Bioorg. Med. Chem. Lett.* **2014**, *24*, 367.
52. Zheng, Y. J.; Tice, C. M. *Expert Opin. Drug Discov*. **2016**, *11,* 831.
53. Borthwick, A. D. *Chem. Rev.* **2012**, *112*, 3641.
54. Dinsmore, C. J.; Beshore, D. C. *Tetrahedron* **2002**, *58*, 3297.
55. Ben Ameur Mehdi, R.; Shaaban, K. A.; Rebai, I. K.; Smaoui, S.; Bejar, S.; Mellouli, L. *Nat. Prod. Res.* **2009**, *23*, 1095.
56. Miyoshi, T.; Miyairi, N.; Aoki, H.; Kohsaka, M.; Sakai, H.; Imanaka, H. *J. Antibiot.* **1972**, *25*, 569.
57. Edmondson, S.; Danishefsky, S. J.; Sepp-Lorenzino, L.; Rosen, N. *J. Am. Chem. Soc.* **1999**, *121*, 2147.
58. Daugan, A.; Grondin, P.; Ruault, C.; Le Monnier de Gouville, A.-C.; Coste, H.; Kirilovsky, J.; Hyafil, F.; Labaudinière, R. *J. Med. Chem.* **2003**, *46*, 4525.
59. Daugan, A.; Grondin, P.; Ruault, C.; Le Monnier de Gouville, A.-C.; Coste, H.; Kirilovsky, J.; Hyafil, F.; Labaudinière, R. *J. Med. Chem.* **2003**, *46*, 4533.
60. Liddle, J.; Allen, M. J.; Borthwick, A. D.; Brooks, D. P.; Davies, D. E.; Edwards,

R. M.; Exall, A. M.; Hamlett, C.; Irving, W. R.; Mason, A. M.; McCafferty, G. P.; Nerozzi, F.; Peace, S.; Philp, J.; Pollard, D.; Pullen, M. A.; Shabbir, S. S.; Sollis, S. L.; Westfall, T. D.; Woollard, P. M.; Wu, C.; Hickey, D. M. B. *Bioorg. Med. Chem. Lett.* **2008**, *18*, 90.

61. Borthwick, A. D.; Liddle, J. *Med. Res. Rev.* **2011**, *31*, 576.
62. Nicholson, B.; Lloyd, G. K.; Miller, B. R.; Palladino, M. A.; Kiso, Y.; Hayashi, Y.; Neuteboom, S. T. C. *Anticancer. Drugs* **2006**, *17*, 25.
63. Assessment of Docetaxel + Plinabulin Compared to Docetaxel + Placebo in Patients With Advanced NSCLC With at Least One Measurable Lung Lesion - Full Text View - ClinicalTrials.gov https://clinicaltrials.gov/show/NCT02504489. (accessed Mar 13, 2018).
64. Ressurreição, A. S. M.; Bordessa, A.; Civera, M.; Belvisi, L.; Gennari, C.; Piarulli, U. *J. Org. Chem.* **2008**, *73*, 652.
65. Basarab, G. S.; Doig, P.; Galullo, V.; Kern, G.; Kimzey, A.; Kutschke, A.; Newman, J. P.; Morningstar, M.; Mueller, J.; Otterson, L.; Vishwanathan, K.; Zhou, F.; Gowravaram, M. *J. Med. Chem.* **2015**, *58*, 6264.
66. Dineen, T. A.; Chen, K.; Cheng, A. C.; Derakhchan, K.; Epstein, O.; Esmay, J.; Hickman, D.; Kreiman, C. E.; Marx, I. E.; Wahl, R. C.; Wen, P. H.; Weiss, M. M.; Whittington, D. A.; Wood, S.; Fremeau, R. T.; White, R. D.; Patel, V. F. *J. Med. Chem.* **2014**, *57*, 9811.
67. Irbesartan: medicine to treat high blood pressure – NHS, UK https://beta.nhs.uk/medicines/irbesartan/ (accessed Mar 13, 2018).
68. Du, J.; Chun, B. K.; Mosley, R. T.; Bansal, S.; Bao, H.; Espiritu, C.; Lam, A. M.; Murakami, E.; Niu, C.; Micolochick Steuer, H. M.; Furman, P. A.; Sofia, M. J. *J. Med. Chem.* **2014**, *57*, 1826.
69. Xiong, H.; Foulk, M.; Aschenbrenner, L.; Fan, J.; Tiong-Yip, C. L.; Johnson, K. D.; Moustakas, D.; Fleming, P. R.; Brown, D. G.; Zhang, M.; Ferguson, D.; Wu, D.; Yu, Q. *Bioorganic Med. Chem. Lett.* **2013**, *23*, 6789.
70. Johansson, A.; Löfberg, C.; Antonsson, M.; Von Unge, S.; Hayes, M. A.; Judkins, R.; Ploj, K.; Benthem, L.; Lindén, D.; Brodin, P.; Wennerberg, M.; Fredenwall, M.; Li, L.; Persson, J.; Bergman, R.; Pettersen, A.; Gennemark, P.; Hogner, A. *J. Med. Chem.* **2016**, *59*, 2497.
71. Zhu, Q.; Lu, Y. *Org. Lett.* **2009**, *11*, 1721.
72. Chittari, P.; Thomas, A.; Rajappa, S. *Tetrahedron Lett.* **1994**, *35*, 3793.

73. Singh, V.; Kanojiya, S.; Batra, S. *Tetrahedron* **2006**, *62*, 10100.
74. Burkhard, J. A.; Tchitchanov, B. H.; Carreira, E. M. *Angew. Chem. Int. Ed.* **2011**, *50*, 5379.
75. Phelan, J. P.; Patel, E. J.; Ellman, J. A. *Angew. Chem. Int. Ed.* **2014**, *53*, 11329.
76. Astolfi, P.; Charles, L.; Gigmes, D.; Greci, L.; Rizzoli, C.; Sorana, F.; Stipa, P. *Org. Biomol. Chem.* **2013**, *11*, 1399.
77. McKerrow, J. D.; Al-Rawi, J. M. A.; Brooks, P. *Synth. Commun.* **2010**, *40*, 1161.
78. Stoermer, D.; Dellaria, J. F.; Amos, D. T.; Zimmermann, B. M.; Dressel, L. T.; Bonk, J. D.; Radmer, M. R. Substituted Imidazoquinolines, Imidazopyridines, and Imidazonaphthyridines. International Patent 2006028545 A2, Jul 5, 2007.
79. Kisanga, P. B.; Verkade, J. G.; Schwesinger, R. *J. Org. Chem.* **2000**, *65*, 5431.
80. Monleõn, A.; Glaus, F.; Vergura, S.; Jørgensen, K. A. *Angew. Chem. Int. Ed.* **2016**, *55*, 2478.
81. Horton, D. A.; Bourne, G. T.; Smythe, M. L. *Chem. Rev.* **2003**, *103*, 893.
82. Siau, W. Y.; Bode, J. W. *J. Am. Chem. Soc.* **2014**, *136*, 17726.
83. Beadle, J. D.; Powell, N. H.; Raubo, P.; Clarkson, G. J.; Shipman, M. *Synlett* **2016**, *27*, 169.
84. Bodanszky, M.; Bodanszky, A. *The Practice of Peptide Synthesis*; Springer Berlin Heidelberg: Berlin, Heidelberg, 1994.
85. Merrifield, R. B. *J. Am. Chem. Soc.* **1963**, *85*, 2149.
86. The Nobel Prize in Chemistry 1984 https://www.nobelprize.org/nobel_prizes/chemistry/laureates/1984/ (accessed Mar 31, 2018).
87. Sewald, N.; Jakubke, H.-D. *Peptides: Chemistry and Biology*; Wiley-VCH: Weinheim, Germany, **2009**.
88. El-Faham, A.; Albericio, F. *Chem. Rev.* **2011**, *111*, 6557.
89. Chan, W. C.; White, P. D. *Fmoc Solid Phase Peptide Synthesis : A Practical Approach*; Oxford University Press, **2000**.
90. Vanier, G. S. In: Jensen, K. J.; Shelton, P. T.; Pedersen, S. L. (eds) *Peptide Synthesis and Applications*. **2013**, 235.
91. Biron, E.; Chatterjee, J.; Kessler, H. *Org. Lett.* **2006**, *8*, 2417.
92. Boeijen, A.; Ameijde, J. Liskamp, R. M. J. *J. Org. Chem.* **2001**, *66*, 8454.
93. Nadon, J.-F.; Rochon, K.; Grastilleur, S.; Langlois, G.; Dao, T. T. H.; Blais, V.; Guérin, B.; Gendron, L.; Dory, Y. L. *ACS Chem. Neurosci.* **2017**, *8*, 40.

94. Lee, K. J.; Lee, W. S.; Yun, H.; Hyun, Y.-J.; Seo, C. D.; Lee, C. W.; Lim, H.-S. *Org. Lett.* **2016**, *18*, 3678.
95. Traoré, M.; Doan, N.-D.; Lubell, W. D. *Org. Lett.* **2014**, *16*, 3588.
96. Wu, H.; Teng, P.; Cai, J. *Eur. J. Org. Chem.* **2014**, 1760.
97. Maegawa, T.; Fujiwara, Y.; Ikawa, T.; Hisashi, H.; Monguchi, Y.; Sajiki, H. *Amino Acids* **2009**, *36*, 493.
98. Isidro-Llobet, A.; Álvarez, M.; Albericio, F. *Chem. Rev.* **2009**, *109*, 2455.
99. Nicolaou, K. C.; Estrada, A. A.; Zak, M.; Lee, S. H.; Safina, B. S. *Angew. Chem. Int. Ed.* **2005**, *44*, 1378.
100. Pascal, R.; Sola, R. *Tetrahedron Lett.* **1998**, *39*, 5031.
101. Charette, A. D; Barbay, J. K.; He, W. *Encycl. Reagents Org. Synth.* **2016**.
102. McMurray, J. S. *Tetrahedron Lett.* **1991**, *32*, 7679.
103. Yue, C.; Thierry, J.; Potier, P. *Tetrahedron Lett.* **1993**, *34*, 323.
104. Respondek, T.; Cueny, E.; Kodanko, J. J. *Org. Lett.* **2012**, *14*, 150.
105. Bach, T.; Schröder, J. *Tetrahedron Lett.* **1997**, *38*, 3707.
106. Subirós-Funosas, R.; El-Faham, A.; Albericio, F. *Biopolymers* **2012**, *98*, 89.
107. Janecka, A.; Fichna, J.; Janecki, T. *Curr. Top. Med. Chem.* **2004**, *4*, 1.
108. Aubry, A.; Birlirakis, N.; Sakarellos-Daitsiotis, M.; Sakarellos, C.; Marraud, M. *Biopolymers* **1989**, *28*, 27.
109. Blomberg, D.; Kreye, P.; Fowler, C.; Brickmann, K.; Kihlberg, J. *Org. Biomol. Chem.* **2006**, *4*, 416.
110. Johansson, A.; Kollman, P.; Rothenberg, S.; McKelvey, J. *J. Am. Chem. Soc.* **1974**, *96*, 3794.
111. Mosnaim, A. D.; Puente, J.; Saavedra, R.; Diamond, S.; Wolf, M. E. *Pharmacology* **2003**, *67*, 6.
112. Hambrook, J. M.; Morgan, B. A.; Rance, M. J.; Smith, C. F. C. *Nature* **1976**, *262*, 782.
113. Roscetti, G.; Possenti, R.; Bassano, E.; Roda, L. G. *Neurochem. Res.* **1985**, *10*, 1393.
114. Du, X.; Zhou, J.; Shi, J.; Xu, B. *Chem. Rev.* **2015**, *115*, 13165.
115. Weiss, R. G. *J. Am. Chem. Soc.* **2014**, *136*, 7519.
116. Draper, E. R.; Adams, D. J. *Chem.* **2017**, *3*, 390.
117. Fleming, S.; Ulijn, R. V. *Chem. Soc. Rev.* **2014**, *43*, 8150.
118. Mahler, A.; Reches, M.; Rechter, M.; Cohen, S.; Gazit, E. *Adv. Mater.* **2006**, *18*,

1365.

119. Truong, W. T.; Su, Y.; Gloria, D.; Braet, F.; Thordarson, P. *Biomater. Sci.* **2015**, *3*, 298.
120. Adams, D. J.; Butler, M. F.; Frith, W. J.; Kirkland, M.; Mullen, L.; Sanderson, P. *Soft Matter* **2009**, *5*, 1856.
121. Adams, D. J.; Mullen, L. M.; Berta, M.; Chen, L.; Frith, W. J. *Soft Matter* **2010**, *6*, 1971.
122. Jayawarna, V.; Ali, M.; Jowitt, T. A.; Miller, A. F.; Saiani, A.; Gough, J. E.; Ulijn, R. V. *Adv. Mater.* **2006**, *18*, 611.
123. McDougall, L.; Draper, E. R.; Beadle, J. D.; Shipman, M.; Raubo, P.; Jamieson, A. G.; Adams, D. J. *Chem. Commun.* **2018**, *54*, 1793.
124. Beadle, J. D.; Knuhtsen, A.; Hoose, A.; Raubo, P.; Jamieson, A. G.; Shipman, M. *Org. Lett.* **2017**, *19*, 3303.
125. Ruan, F.; Chen, Y.; Hopkins, P. B. *J. Am. Chem. Soc.* **1990**, *112*, 9403.
126. Marqusee, S.; Robbins, V. H.; Baldwin, R. L. *Proc. Natl. Acad. Sci. USA.* **1989**, *86*, 5286.
127. Chakrabartty, A.; Schellman, J. A.; Baldwin, R. L. *Nature* **1991**, *351*, 586.
128. Chakrabartty, A.; Kortemme, T.; Baldwin, R. L. *Protein Sci.* **1994**, *3*, 843.
129. Pauling, L.; Corey, R. B.; Branson, H. R. *Proc. Natl. Acad. Sci. USA.* **1951**, *37*, 205.
130. Yin, H.; Lee, G.-I.; Hamilton, A. D. *Drug Discovery Res.* **2007**, 281.
131. Liskamp, R. M. J. *Recl. Trav. Chim. Pays-Bas* **2010**, *113*, 1.
132. Fustero, S.; Chiva, G.; Piera, J.; Volonterio, A.; Zanda, M.; González, J.; Ramallal, A. M. *Chem. Eur. J.* **2007**, *13*, 8530.
133. Kida, T.; Sato, S.; Yoshida, H.; Teragaki, A.; Akashi, M. *Chem. Commun.* **2014**, *50*, 14245.
134. Hong, L.; Sun, W.; Yang, D.; Li, G.; Wang, R. *Chem. Rev.* **2016**, *116*, 4006.
135. Wendt, J. A.; Aubé, J. *Tetrahedron Lett.* **1996**, *37*, 1531.
136. Phelan, J. P.; Ellman, J. A. *Adv. Synth. Catal.* **2016**, *358*, 1713.
137. Yin, H.; Lee, G.-I.; Hamilton, A. D. *Drug Discovery Res.* **2007**, 281.
138. Anderson, J. E. *J. Chem. Soc. Perkin Trans. 2* **1974**, *0*, 10.
139. Jensen, F. R.; Bushweller, C. H.; Beck, B. H. *J. Am. Chem. Soc.* **1969**, *91*, 344.
140. Das, C.; Raghothama, S.; Balaram, P. *J. Am. Chem. Soc.* **1998**, *120*, 5812.
141. Luo, P.; Baldwin, R. L. *Biochemistry* **1997**, *36*, 8413.

142. Whitmore, L.; Wallace, B. A. *Biopolymers* **2008**, *89*, 392.
143. Sreerama, N.; Venyaminov, S. Y. U.; Woody, R. W. *Protein Sci.* **2008**, *8*, 370.
144. Hirota, N.; Goto, Y.; Mizuno, K. *Protein Sci.* **2008**, *6*, 416.
145. Toniolo, C.; Polese, A.; Formaggio, F.; Crisma, M.; Kamphuis, J. *J. Am. Chem. Soc.* **1996**, *118*, 2744.
146. Millhauser, G. L. *Biochemistry* **1995**, *34*, 3873.
147. Armen, R.; Alonso, D. O. V; Daggett, V. *Protein Sci.* **2003**, *12*, 1145.
148. Miltschitzky, S.; Koenig, B. *Org. Prep. Proced. Int.* **2005**, *37*, 307.
149. Panteleev, P. V; Bolosov, I. A.; Balandin, S. V; Ovchinnikova, T. V. *Acta Naturae* **2015**, *7*, 37.
150. Geden, J. V.; Beasley, B. O.; Clarkson, G. J.; Shipman, M. *J. Org. Chem.* **2013**, *78*, 12243.
151. Pancholi, A. K.; Geden, J. V.; Clarkson, G. J.; Shipman, M. *J. Org. Chem.* **2016**, *81*, 7984.
152. Hamzik, P. J.; Brubaker, J. D. *Org. Lett.* **2010**, *12*, 1116.
153. Noble, A.; Anderson, J. C. *Chem. Rev.* **2013**, *113*, 2887.
154. García-Muñoz, M. J.; Dema, H. K.; Foubelo, F.; Yus, M. *Tetrahedron: Asymmetry* **2014**, *25*, 362.
155. Haque, T. S; Little, J. C.; Gellman, S. H. *J. Am. Chem. Soc.* **1996**, *118*, 6975.
156. Maynard, A. J.; Sharman, G. J.; Searle, M. S. *J. Am. Chem. Soc.* **1998***, 120*, 199.